UNIVERSIDADE DE SÃO PAULO
INSTITUTO DE BIOCIÊNCIAS
DEPARTAMENTO DE FISIOLOGIA
PROGRAMA DE PÓS-GRADUAÇÃO EM
CIÊNCIAS (FISIOLOGIA GERAL)

Mecanismos de modulação de genes de relógio por radiação UVA e luz visível em melanócitos normais (Melan-a) e transformados (melanoma B16-F10)

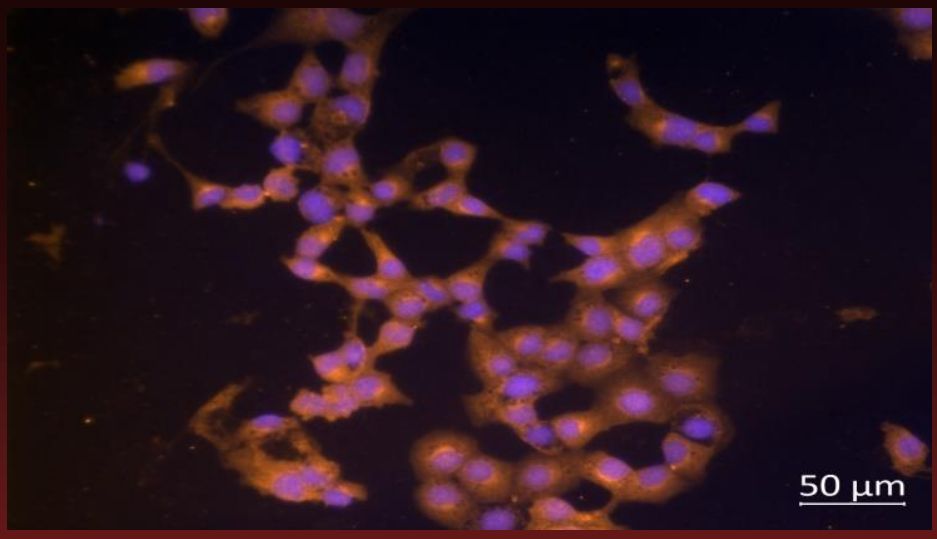

Mechanisms of clock gene modulation by UVA radiation and visible light in normal (Melan-a) and transformed (B16-F10) melanocytes

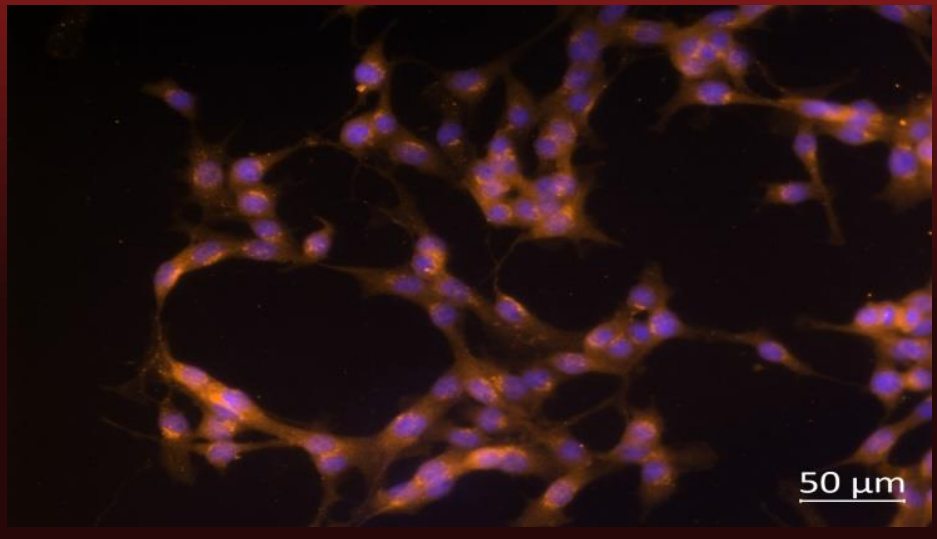

Leonardo Vinícius Monteiro de Assis

São Paulo
2019

Leonardo Vinícius Monteiro de Assis

Mecanismos de modulação de genes de relógio por radiação UVA e luz visível em melanócitos normais (Melan-a) e transformados (melanoma B16-F10)

Mechanisms of clock gene modulation by UVA radiation and visible light in normal (Melan-a) and transformed (B16-F10) melanocytes

Doctoral Dissertation presented at the University of São Paulo, Institute of Biosciences to obtain the title of Doctor in Sciences in the field of General Physiology

Advisor: Professor Ana Maria de Lauro Castrucci

São Paulo

2019

Ficha catalográfica elaborada pelo Serviço de Biblioteca do Instituto de Biociências da USP,
com os dados fornecidos pelo autor no formulário:
http://www.ib.usp.br/biblioteca/ficha-catalografica/ficha.php

Leonardo Vinícius Monteiro , de Assis
Mecanismos de modulação de genes de relógio por radiação UVA e luz visível em melanócitos normais (Melan-a) e transformados (melanoma B16-F10) / de Assis Leonardo Vinícius Monteiro ; orientador Ana Maria de Lauro Castrucci. -- São Paulo, 2019.

181 f.

Tese (Doutorado) - Instituto de Biociências da Universidade de São Paulo, Departamento de Fisiologia.

1. Radiação ultravioleta A (UVA), luz visível e temperatura. 2. melanopsina e rodopsina. 3. genes de relógio. 4. melanócito normais e melanócito maligno. 5. Mus musculus e Homo sapiens . I. Castrucci, Ana Maria de Lauro, orient. II. Título.

Bibliotecária responsável pela estrutura da catalogação da publicação:
Elisabete da Cruz Neves – CRB – 8/6228

LEONARDO VINÍCIUS MONTEIRO DE ASSIS

Mecanismos de modulação de genes de relógio por radiação UVA e luz visível em melanócitos normais (Melan-a) e transformados (melanoma B16-F10)

Mechanisms of clock gene modulation by UVA radiation and visible light in normal (Melan-a) and transformed (B16-F10) melanocytes

JUDGING COMMITTEE:

Prof. Dr.

Prof. Dr.

Prof. Dr.

Prof. Dr. Advisor Ana Maria de Lauro Castrucci

São Paulo, ___/___/___

DEDICATION

I dedicate this Ph. D. thesis to my parents – Suzana and Tadeu –
who never spared efforts and with great
personal sacrifice invested –
even in the most challenging and adverse scenarios –
in my education; thus, shaping my future.

EPIGRAPH

The mind of the prudent [always]
acquires knowledge, And the ear of the
wise [always] seeks knowledge.

Proverbs 18:15
Amplified Bible (AMP)

ACKNOWLEDGMENTS

I thank God in the figure of Jesus Christ that through his sacrifice life and freedom were freely given to me; thus, providing me a sense of purpose for my life. I thank my mother, Suzana, for being such a strong and faithful woman that never lost the vision and invested everything in my education. I thank my father, Tadeu, for his strength, faith, and character. Thanks mom and dad for providing all the physical, financial, and emotional support. I am very grateful for my aunt Nésia for being such an important figure in my life. I also thank my brother, Gustavo, for always being there and to be a great example to be followed. I thank Aline for being a good friend – thank you for your heart.

I am deeply grateful to my mentor and advisor, Prof. Ana Castrucci, for believing in my work and for investing her time and resources in my training. She has impacted and shaped my life; she has a great portion in the scientist that I am today. I will carry on your teachings for my entire life. I cannot forget to thank Nathália Moraes for being an excellent coworker, and for being such a good partner in lab – I thank you for your work, teachings, and friendship. I am grateful to Prof. Carlos Menck for being an excellent mentor and collaborator, and for providing the resources and structures that were key in the development of this Ph. D. I express my gratitude to the coworkers that along the years participated in the development of my project. I thank Nathana, Jennifer, Bruno, Rodrigo, Daniela, Neto, and Cris. Thank you, Márcio, for providing the necessary technical assistance. I especially thank the undergraduate students that participated in this project: Thainá, Keila, Giovanna, Glenda, and Isabella. Thank you for being part of this project and for being patient with me – you have taught me so much. I thank the funding agencies FAPESP

(Project 2013/24337-4), CAPES, and CNPq for providing the financial resources that were essential in this Ph.D. project.

In the last section I thank the people that were important as they have supported me along these five years. I thank my friend Brian Blevins for being such an excellent mentor. I am so grateful for our weekly talks in which I learnt so much with you – thank you for being there for me. I thank Scott Barnet for being such an excellent and inspiring leader for me – thank you so much for the provocative and hard questions. I thank Mauro Isoldi, my first mentor, for his mentoring along these years. I also thank Daniel Deeds for his friendship and mentoring. I express gratitude to Felippe, Alliny, Vinicius, and Ingrid for being great friends and for the support in the hardest moments.

I am so in debt and grateful to the Mount Zion Church and its leaders. I thank: Pr. Teófilo Hayashi for his inspiring words and leadership; Pr. César Bianco for his heart and encouragement and for being a bright light in the hardest moments; and Pr. Eduardo Nunes for being a carrier of healing and hope at the VOX's services. I thank Marcello Danelli and Ivan Bonilla for their leadership and the friends from VOX Connections – thank you all for the friendship and encouragement! I also thank Lehon and Marcia, and Ivan and Alexandra for their friendship and mentoring. I thank my friend, Estevão, for his amazing heart and patience – thank you very much for being such a great friend. I express my gratitude to Letícia Mendes and for her sincere friendship. I cannot forget to say a huge thank to my friends from the "The Squad": Gabriel Takahashi, Guilherme Assis, Henrique Oliveira, Lucas Pinheiro, Matheus Murata, Matheus Dionisio, Fábio Vieira, and Murillo Augusto – thank you all very much!

I thank my beautiful and lovely companion, Mariana, for joining my life, and thus, making it so much more colorful, brighter, and funnier – I

love you and your heart. And again, I thank God for providing all the pieces together at the correct time, and thus, making an amazing story.

ABSTRACT

The skin has a system that can detect light in a fashion similar to the retina. Although its presence was initially reported almost 20 years ago, only in 2011 functional studies started to be reported. The biological clock of the skin has also been reported in the beginning of the century, but its function and relevance still remain unexplored. Thus, this Ph.D. project was designed to explore the functionality of both systems in melanocytes, and whether the disruption of these systems is associated with the development of melanoma cancer. Using *in vitro, in vivo,* and bioinformatics approaches, we have shown that: 1) the biological clock of malignant melanocytes is more responsive to visible light, UVA radiation, estradiol, and temperature compared to normal cells; 2) UVA radiation is detected by melanopsin (OPN4) and rhodopsin (OPN2), which triggers a cGMP related cascade that leads to immediate pigment darkening (IPD) in normal and malignant melanocytes; 3) in addition to detecting UVA radiation, OPN4 also senses thermal energy, which activates the biological clock of both normal and malignant melanocytes; 4) regarding the biological clock, we have provided several layers of evidence that proves that in melanoma a chronodisruption scenario is established compared to healthy skin and/or normal pigment cells; 5) *in vivo* tumor samples display a low amplitude circadian rhythm of clock gene expression and an ultradian oscillatory profile in melanin content; 6) a non-metastatic melanoma leads to a systemic chronodisruption, which we suggest that could favor the metastatic process; 7) in human melanoma, we demonstrated the role of *BMAL1* as a prognostic marker and a putative marker of immune therapy success. Taken altogether, these results significantly contributed to the literature as it brought to light new and interesting targets and processes, which will be explored in future projects.

Keywords: Ultraviolet A (UVA) radiation; visible light; temperature; melanopsin; rhodopsin; clock genes, melanocyte; malignant melanocyte; melanoma; *Mus musculus*; *Homo sapiens*

RESUMO

A pele possui um sistema que pode detectar luz de forma análoga à retina. Embora a presença deste sistema tenha sido inicialmente descrita quase há 20 anos, apenas no ano de 2011 estudos funcionais começaram a ser relatados. Sabe-se que o relógio biológico da pele também foi identificado no início do século, mas sua função e relevância ainda continuam pouco exploradas. Diante deste cenário, este projeto de doutorado foi desenhado para investigar a funcionalidade de ambos os sistemas em melanócitos e se perturbação dos mesmos estaria associada com o desenvolvimento de melanoma. Através do uso de abordagens *in vitro*, *in vivo* e de bioinformática, nós demonstramos que: 1) o relógio biológico de melanócitos malignos é mais responsivo à luz visível, radiação UVA, estradiol e temperatura comparado ao de células normais; 2) a radiação UVA é detectada por melanopsina (OPN4) e rodopsina (OPN2), que ativam uma via de sinalização dependente de GMPc, levando ao processo de pigmentação imediata (IPD) em melanócitos normais e malignos; 3) além de detecção de radiação UVA, a OPN4 também detecta energia térmica que, por sua vez, ativa o relógio biológico de melanócitos normais e malignos; 4) relativo ao relógio biológico, provamos por diferentes abordagens que, no melanoma, um cenário de cronoruputura está estabelecido em comparação a pele saudável e/ou melanócitos; 5) tumores *in vivo* apresentam um ritmo circadiano de baixa amplitude na expressão dos genes de relógio e um ritmo ultradiano oscilatório no conteúdo de melanina; 6) um melanoma não metastático leva a um quadro sistêmico de cronoruptura, o qual sugerimos favorecer o processo de metástase; 7) em melanoma humano, demonstramos o papel do gene *BMAL11* como marcador de prognóstico e um possível indicador de sucesso de imunoterapias. Portanto, este projeto contribuiu de forma significante para

a literatura científica uma vez que trouxe à luz novos e interessantes alvos terapêuticos e processos, os quais serão explorados em projetos futuros.

Palavras Chaves: Radiação ultravioleta A (UVA); luz visível; temperatura; melanopsina; rodopsina; genes de relógio; melanócito; melanócito maligno; melanoma; *Mus musculus*; *Homo sapiens*

SUMMARY

INTRODUCTION

The Importance of Timing in Science

The statement “timing is everything” holds a great meaning in several areas of science – specially in Biological and Biomedical fields. In fact, the number of studies that evaluate the influence of time on physiological responses from less complex organisms to man has increased considerably over the past decades (reviewed in Green et al., 2008). The temporalization and temporal segregation of physiological events are important to keep the homeostasis from the cellular to the organismic level. Since environmental alterations occur in a predictable fashion along 24 hours, the presence of a biological system able to interpret time and, based on this information, to anticipate and regulate several physiological and behavioral processes – even in the absence of environmental cues – is key for the survival of all beings and maintenance of the species (Hogenesch and Ueda, 2011).

It is known that before the awakening process in humans, heartbeat rate and blood pressure, for instance, increase in anticipation of the locomotor activity onset (reviewed in Kovac et al., 2009); the same anticipatory profile is observed in hepatic and adipose cells as well as in skeletal muscle, which maximizes the efficiency of metabolism, storage, and energy usage (reviewed in Green et al., 2008; Hogenesch and Ueda, 2011). It has been shown that other functions such as memory, learning, and awareness also oscillate throughout the day (reviewed in Froy, 2010; Gerstner and Yin, 2010; Kyriacou and Hastings, 2010).

Within this line, a biological system able to exert such role must have the following features: 1) an afferent pathway sensitive to rhythmic environmental variation such as the presence and absence of light; 2) a

central clock (oscillator) able to interpret the incoming signals, as mentioned above, but also, through cellular and biochemical mechanisms, able to keep track of time; 3) an efferent pathway that leaves the central clock and transmits this temporal information, through neuronal and/or humoral paths, to the whole organism. Based on this complex system, the whole organism may then display a single time zone that is shared by all organs.

The above-described system is also known as the biological clock system. In mammals, this system is primarily synchronized by the light-dark (LD) cycle, which is due to the rotation of Earth on its own axis. Interestingly, all circadian rhythms, i.e., rhythms that take 24 h to complete, persist even in the absence of synchronizing factors. We classify this scenario as free running since the biological rhythms display periods slightly different from 24 hours; however, these rhythms can be entrained by a cyclic environmental cue (*zeitgeber*), and then the period of these rhythms is exactly 24 h (Golombek and Rosenstein, 2010).

In mammals, these signals allow the organism to be under a single time zone (reviewed in West and Bechtol, 2015; Brown and Azzi, 2013). In fact, one may say that a stable relationship between the central and the peripheral clocks is one of the main functions of the circadian system; this internal coherence is key for the survival of the organism and maintenance of the species (Baron and Reid, 2014; West and Bechtol, 2015; Potter et al., 2016; Roenneberg and Merrow, 2016; Smolensky et al., 2016). Not surprisingly, the loss of internal coherence, i.e., chronodisruption, has been extensively observed in jetlagged people as well as in shift workers, in which acute and chronic loss of phase between central and peripheral oscillators is found, respectively (Baron and Reid, 2014; Boivin and Boudreau, 2014). Several lines of evidence have associated the scenario of chronodisruption with onset of several diseases, including cancer

(Savvidis and Koutsilieris, 2012; Lengyel et al., 2013; Baron and Reid, 2014; Kelleher et al., 2014).

Taken altogether, the temporalization and the anticipatory mechanisms of the organism are crucial so that all physiological processes take place in appropriate moments and in synchrony with the environment. The environmental temporal information and its respective interpretation by the animals allow them to be prepared to face the challenges posed by the environment. Consequently, failures in this temporal system and/or integration of the temporal information with the physiological systems have been shown to contribute to the onset of diseases and syndromes. Therefore, understanding how the biological clock controls our physiology and how it is altered in diseases is an important and exciting field with predictable clinical implications.

Clock Machinery at the Molecular Level

In mammals, the LD cycle is the main environmental cue responsible for entraining the central clock. The retina exerts a fundamental role in this process. Initial studies carried out in *Xenopus laevis* melanophores showed that upon white light exposure melanosome dispersion was observed, a process mediated by a new light sensor, an opsin named melanopsin (Provencio et al., 1998). Some years later, melanopsin was identified in mammals, being expressed in a subset of intrinsically photosensitive retinal ganglion cells found in the outer layer of the retina (Provencio et al., 2002). In that same year, Professor Provencio's group elegantly showed that melanopsin is responsible for entraining the biological clock in response to the LD cycle (Panda et al., 2002; 2003).

The retinohypothalamic tract brings light information from the retina to the SCN through the release of glutamate and pituitary adenylyl cyclase activating polypeptide (PACAP) (Hannibal, 2006). In addition, indirect pathways can modify the response of the SCN to light stimulus, such as: the intergeniculate leaflet route through the release of neuropeptide Y and GABA; and the pathway arising from the median and dorsal raphe nucleus, in which serotonin is the main neurotransmitter. Nevertheless, the retinohypothalamic tract seems to be enough to adjust the central clock to LD cycle (Crosio et al., 2000).

Once the photic signal reaches the SCN, several events take place, ultimately dependent on the moment of light exposure. In fact, it is long known the effect of light pulses upon the locomotor activity of mice: animals exposed to light in the beginning of the dark phase show delays of the clock; while light exposure during the late dark phase advances the clock; but the same lighting stimulus during the subjective day causes no effect on the phase of the clock (Pittendrigh and Daan, 1976).

It has been established that exposure to light at the subjective night leads to rapid transcription of several immediate genes such as *c-Fos* and *Per1* having cAMP binding protein (CREB) as the central player (Ginty et al., 1993; Kornhauser et al., 1996; Obrietan et al., 1998; Golombek and Rosenstein, 2010). However, the cascade linking light stimulus and CREB activation remains elusive. At the center of this autonomously generated rhythm lie the clock genes, which are the biological tools capable of keeping track of time through a complex biochemical mechanism. The molecular clockwork mechanism in mammals is currently well-known and comprises feedback loops of transcription and translation of several genes, as described below (Buhr and Takahashi, 2013; Takahashi, 2017).

Bmal1 and *Clock* genes encode proteins which constitute the positive loop of the core circuit. In the cytoplasm, BMAL1 and CLOCK

proteins form a heterodimer (BMAL1/CLOCK) that migrates to the nucleus where it binds to E-box sequences present in the promoters of its target genes. The expression of *Per* (*1*, *2*, and *3)* and *Cry* (*1* and *2*) genes, which correspond to the negative loop of regulation, is activated by BMAL1/CLOCK. Subsequently, PER and CRY proteins form a heterodimer (PER/CRY) that migrates to the nucleus where it inhibits the activity of BMAL1/CLOCK. The stability of PER/CRY is critical for the repressing phase of this molecular mechanism. In fact, the stability is mainly carried out by kinases 1ε and 1δ (CK1ε/CK1δ); when only PER is phosphorylated, it is tagged to degradation (Takahashi, 2017). Interestingly, the first mammal identified as a circadian mutant – the tau hamster – exhibits a 20 h free-stage locomotor activity due to a CK1ε mutation (Ralph and Menaker, 1988). On the other hand, CRY proteins are phosphorylated and then marked for degradation by AMPK1 and DYRK1A/GSK-3β kinases (reviewed in Buhr and Takahashi, 2013; Takahashi, 2017).

In addition to the main circuit, another interlaced loop comprises the activation of *Rev-Erbα/β* and *Rorα/β* genes by CLOCK/BMAL1, through E-box sequences present in their promoter regions. REV-ERBα/β and RORα/β compete for the RORE sequence that lies in the promoter region of *Bmal1:* REV-ERBα/β inhibits while RORα/β activates *Bmal1* transcription. A third circuit is based on the presence of D-box sequences in the promoter regions of some other genes, such as *Hlf*, *Dbp*, *Tef*, and *Nfil3*, which is considered a third level of regulation. Although this loop has not been shown to be essential for the clock, its players provide robustness and precision to the clock machinery (reviewed in Buhr and Takahashi, 2013; Takahashi, 2017). It is of importance to highlight that CLOCK/BMAL1 also activates the transcription of a variety of clock-controlled genes (CCGs) in a tissue-specific manner, which ultimately

contributes to the temporal control of biological processes in the organism. Based on these, clock genes have received increasing interest due to their key role in regulating the body homeostasis (Potter et al., 2016; Roenneberg and Merrow, 2016; Takahashi, 2017).

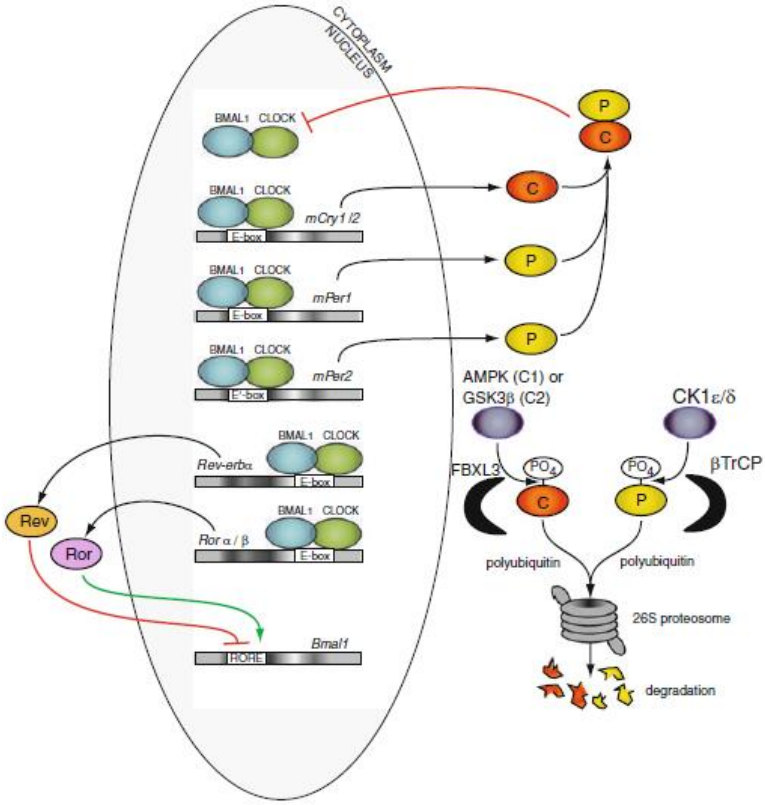

Figure 1. Regulation of clock genes in mammals. Taken from Buhr and Takahashi, 2013.

Per1 and *Per2* seem to share complementary and non-redundant roles in the SCN response to light. It has been suggested that PER1 would interact with other clock proteins – at post-transcriptional level – while PER2 would participate as a positive regulator of clock gene expression (Bae et al., 2001; Zheng et al., 2001). Interestingly, the phenomenon of paralogue compensation is elegantly described in SCN: a reduction on *Per1* or *Cry1* levels results in high levels of *Per2* or *Cry2*, respectively, but

the same effect does not occur when *Per2* or *Cry2* are reduced (Baggs et al., 2009). The last member of the *Per* family – *Per3* does not seem to play an important role in the regulation of other clock genes in the SCN (Shearman et al., 2000; Bae et al., 2001); however, it has been shown that *Per3* may play a role in response to chronic light stimulus (Pereira et al., 2014). Still, the role of *Per3* in the SCN can be considered minor as mice harboring deletions on both *Per1* and *Per2* are not entrained by LD cycle (Bae et al., 2001; Zheng et al., 2001). In fact, double knockout mice *Per1/Per2* or *Cry1/Cry2* show no intrinsic rhythmicity (Van der Horst et al., 1999, Vitaterna et al., 1999; Bae et al., 2001). Specific SCN *Clock* removal does not lead to loss of locomotor activity since another clock gene, *Npas2,* is able to assume the role of *Clock* (Debruyne et al., 2007a). *Bmal1* seems to be the only clock gene whose removal results in loss of locomotor rhythmicity, and arrhythmic profiles in clock gene expression (Bunger et al., 2000; Mieda and Sakurai, 2011; Husse et al., 2011; 2014).

Relationship Between Central and Peripheral Clocks

The temporal information from the LD cycle is interpreted by a complex biochemical mechanism that involves several genes and proteins, as mentioned above. Such system is well-comprehended; however, the mechanisms through which the SCN shares this temporal information with the whole organism is less understood.

Thus far, clock genes have been shown to be expressed in almost every mammalian cell, demonstrating the presence of single cell temporal controlling system. It is known that the central clock is resistant to genetic perturbations such as mutations and/or gene deletion. For example, *Clock* deletion does not affect the rhythm of locomotor activity (Debruyne et al., 2007b) while the deletion of this gene in peripheral tissues results in an

arrhythmic profile (DeBruyne et al., 2007b). Another difference between central and peripheral clocks lies on the neuronal coupling that only exists in the SCN. In cell culture, the expression of clock genes of peripheral tissue is rapidly lost, a process known as damping effect, while SCN explants in culture still exhibit rhythmic gene expression and electrical activity for weeks (Welsh et al., 2004; Brown and Azzi, 2013). A third difference that must be stressed is the responsiveness found only in peripheral tissues to synchronizing signals arisen from the SCN. For example, glucocorticoid and temperature are important signals for peripheral tissues but the SCN is insensitive to such stimuli. In fact, the LD cycle is the most significant cue for the SCN while the peripheral clocks respond to a complex and many times redundant myriad of factors such as neurotransmitters, hormones, body temperature, and feeding time (reviewed in Brown and Azzi, 2013).

During many years the relationship between central and peripheral clocks was and still is highly debatable. Initially, the "slave-master" model was set forth. In this model, the synchronization of the peripheral clocks was only and exclusively attributed to the SCN. In this view, the peripheral tissues are insensitive or unaffected by internal and/or external stimuli (Dibner et al., 2010; Richards and Gumz, 2012). The second proposed model was the "orchestra", in which the SCN is seen as the "conductor", and the peripheral tissues are seen as "performers of the orchestra". Within this line, each clock is able to play its own "instrument", but the conduction of the music is given to the "conductor" – the SCN –, which ultimately allows an efficient and harmonic melody. Therefore, each peripheral clock may adapt to several internal and external stimuli, but they are conducted by the LD cycle that is perceived by the SCN (Kowalska and Brown, 2007; Dibner et al., 2010; Richards and Gumz, 2012).

In fact, the orchestra model of organization represents a hierarchy in which the SCN influence the peripheral clocks; however, new and exciting evidence has recently questioned this model. For example, it was shown that feeding time can reset the clock gene machinery of peripheral tissues without affecting the SCN (Buijs et al., 2013). Pioneering studies carried out by Oster and Takahashi groups have shed light into a new model of organization – the Federated model (Izumo et al., 2014; Husse et al., 2015), which is detailed below.

The idea of an organizational system composed by different *zeitgebers* that act in independent fashions in peripheral tissues is highly interesting. Based on the organ specific deletion of *Bmal1* in the SCN, a new interpretation has been created (Husse et al., 2011; Husse et al., 2014). When these mice were kept in constant dark (DD), no locomotor activity rhythm was observed, but when the animals were kept in LD cycle a locomotor activity rhythm was found, an event that does not take place in traditionally SCN-lesioned mice (Ralph et al., 1990). In addition, the level of glucocorticoids oscillated in LD while in DD the oscillatory profile was lost (Husse et al., 2011). Surprisingly, rhythmic clock gene expression in peripheral tissues was lost in DD but was kept, although with some phase advance or delay, in LD cycle, another feature not seen in traditionally SCN-lesioned mice (Tanioka et al., 2009). Based on these findings, it has been suggested that the SCN is necessary for the synchronization of peripheral tissues when the organism is deprived of environmental cues (Husse et al., 2014; Husse et al., 2015). It should be acknowledged that the role of SCN is not diminished in the Federated System of organization since SCN is still important for the proper sustainability of the entire clock network. On the other hand, this new model argues in favor of more flexibility and influence of peripheral tissues on the regulation of the clock network.

In another study in which *Bmal1* was selectively deleted in the entire forebrain (Izumo et al., 2014), the results are in line with the above-mentioned ones. Clock gene expression of peripheral tissues were rhythmic in mice kept in LD cycle while in DD the amplitude of expression was reduced, and the phases were dispersed. Interested in understanding the role of feeding in the regulation of peripheral clocks, the authors used a feeding restriction regime in mice kept in DD. Curiously, the feeding cues were able to synchronize the clock in the liver and kidney while the ones from heart, lungs, and spleen were less sensitive. These findings suggest that, in the absence of a central working clock, the rhythms are lost but they can be rescued by an external *zeitgeber*, such as LD cycle or feeding time (Izumo et al., 2014).

The studies favoring the Federated model of organization suggest that an external *zeitgeber* may be tissue-specific. Each physiological process is synchronized by a specific set of *zeitgebers* which are more relevant to that particular process, which ultimately confers an increased plasticity to the system. However, in the absence of environmental cues, the peripheral clocks rely on the coordinating signals provided by the SCN. But, in the absence of the SCN, these rhythms can be rescued by an external *zeitgeber*, that suggests the existence of secondary pathways through which peripheral clocks are synchronized in a SCN-independent fashion (Husse et al., 2015). The identity of these structures is still unknown and is a matter of intense research.

Taken altogether, the Federated model of organization provides a horizontal organizing perspective while the orchestra model provides a top-to-bottom view. It is still in debate whether the Federated system is more realistic and physiological in comparison to the Orchestra model.

The Biological Clock of the Skin

The skin represents the first barrier between the body and the external environment, thus it is not surprising that this organ is under the influence of environmental oscillatory factors such as light – in its several wavelengths – and temperature. A strong set of evidence show that the skin has a circadian system that is responsible for controlling several cellular functions (Sandu et al., 2012; Luber et al., 2014). Furthermore, oscillatory profiles are found in skin protection barrier (Yosipovitch et al., 2004), trans-epidermal water loss (Yosipovitch et al., 1998), sebum secretion, temperature, pH (Le Fur et al., 2001), DNA repair (Gaddameedhi et al., 2011) as well as in cellular proliferation (Luber et al., 2014).

Nonetheless, many important questions still remain answered: does the current evidence of circadian function in the skin indicates a local temporal controlling system? Could these functions be generated within the skin and its cells? If yes, is this system under the control of SCN?

In 2000, the presence of *CLOCK* and *PER1* was reported in human skin (Zanello et al., 2000). Subsequently, *CLOCK*, *TIM*, *PER1*, *CRY1*, and *BMAL1* cyclic expression was shown in human mucosa and skin. In addition, *PER1* peak was found to take place concomitantly with thymidylate synthetase's, thus suggesting a link between clock gene machinery and cell cycle (Bjarnason et al., 2001). In 2002, a study demonstrated that UVB radiation initially downregulated clock genes in human keratinocytes, which were then upregulated hours after radiation (Kawara et al., 2002). Similar phenomenon was reported years later: UV radiation leads to a reduction of CLOCK protein. This, in turn, resulted in reduced TIMP3 levels (metallopeptidase inhibitor 3), a protein that regulates several inflammatory processes (Park et al., 2018).

Unfortunately, the literature is scarce in studies addressing the effects of light and UV radiation on clock gene expression of skin cells.

An elegant study provided great contribution to our current understanding regarding the role of light as a synchronizing factor in skin, and the influence of SCN on that organ. The authors showed that mouse skin from various body regions displayed rhythmic expression of clock genes when the animals were kept either in LD cycle or DD (Tanioka et al., 2009). The same study provided the only available evidence regarding the role of SCN in the skin. Upon SCN lesion, the rhythmic expression of clock genes in the skin was lost as well as the rhythmic locomotor activity (Tanioka et al., 2009). Light exposure was not able to synchronize the clock gene machinery of the skin, a fact that shows the importance of the SCN control; however, these data should be carefully analyzed since although SCN lesion has brought out most of the pioneering findings, it has been shown not to be the best strategy. Thus far, it is still obscure relationship between the SCN and the skin clock in view of the Federated model (Husse et al., 2014).

In human keratinocytes, there is a functional clock gene machinery, which may be modulated by dexamethasone. Pharmacological manipulation of some components of the clock machinery resulted in loss of oscillatory profile. It was shown that low temperature is an important environmental cue since cold pulse (33ºC during 2 h) entrained these cells; in addition, temperature shock also affected CCGs associated with cholesterol homeostasis and differentiation (Sporl et al., 2011).

It should be emphasized that there are few literature reports that address the clock gene machinery and the processes regulated by it in the skin. It is known that fibroblasts, keratinocytes, and melanocytes possess a functional clock machinery that displays cell-specific phase and period of gene expression after synchronization with dexamethasone. This,

therefore, indicates a particular regulatory mechanism within each cell type (Sandu et al., 2012), thus suggesting the presence of multi-oscillatory circadian system in the skin, responsible for the fine tuning of skin physiology to external factors such as light, UV radiation, temperature as well to SCN-controlled internal signals (Sandu et al., 2012; 2015).

Still in this line, an elegant study has pointed a significant role for the clock within the skin: Upon *BMAL1* or *PER1* silencing in human hair follicle melanocytes, an increase on melanin content, tyrosinase expression, and dendricity was found. Additionally, clock gene silencing increased melanosome quantity and their transfer to neighboring keratinocytes (Hardman et al., 2015). The multi-oscillatory circadian system of the skin also regulates the hydration of *stratum corneum* in humans (Yosipovitch et al., 1998; Luber et al., 2014), but the underlying mechanism was until recently unknown. In 2014, it was shown that mice harboring *Clock* deletion showed reduced *stratum corneum* hydration, which was associated with reduced expression of aquaporin 3, a protein that shows a circadian oscillatory profile in wild type mice (Matsunaga et al., 2014).

Another feature controlled by the skin local timing system is DNA repair: an important DNA repair enzyme, xeroderma pigmentosum, complementation group a, XPA, exhibits an oscillatory profile in protein and activity levels (Gaddameedhi et al., 2011). Interestingly, mice exposed to UV radiation in the early morning, when the levels are low, display higher incidence of skin tumors when compared to mice exposed to UV radiation when XPA expression is high (Gaddameedhi et al., 2011).

Taken altogether, murine melanocyte as well as its malignant counterpart are excellent models to understand the role of light and UV radiation in the modulation of clock gene machinery.

The Photosensitive System of Skin

The classical system of photoreception that leads to image and non-image forming processes is well described in the eyes (Solomon and Lennie, 2007; Musio and Santillo, 2012). At the core of this system lie opsins, the biological sensors able to detect the solar energy ranging from ultraviolet radiation to red light (Solomon and Lennie, 2007). Mammalian opsins are G-protein coupled receptors which require the chromophore retinal, an analogue of vitamin A, for their proper functioning. Upon light stimulation by a photon in a specific wavelength, 11-*cis* retinal bound to the opsins is photo-isomerized to *all-trans* retinal. This event triggers the activation of specific signaling pathways that evoke biological responses (Leung and Montell, 2017). Interestingly, a similar photosensitive system is also expressed in the skin.

In 2001, the expression of rhodopsin (OPN2) was first shown in skin cells (mouse, Miyashita et al., 2001). Since then, several groups have demonstrated the presence of cone opsins (OPN1SW and OPN1MW) (Tsutsumi et al., 2009; Haltaufderhyde et al., 2015;Castellano-Pellicena et al., 2018), rhodopsin (OPN2) (Tsutsumi et al., 2009; Lopes et al., 2010; Wicks et al., 2011; Haltaufderhyde et al., 2015;Buscone et al., 2017) as well as encephalopsin (OPN3) (Haltaufderhyde et al., 2015; Buscone et al., 2017; Regazzetti et al., 2018; Castellano-Pellicena et al., 2018), peropsin (Toh et al., 2016), and neuropsin (OPN5) (Kojima et al., 2011; Haltaufderhyde et al., 2015; Castellano-Pellicena et al., 2018). Taken together, the above-mentioned studies provide strong indication that human and murine skin possess an elegant mechanism that is able to capture light. Unfortunately, the physiology of this system and the biological processes it regulates are poorly understood.

Since 2011, several groups around the world focused to better understand this photosensitive system. The pioneering study by Wicks and colleagues was an important boost to the field. The authors showed that UVR (90% UVA e 10% UVB, 40 kJ/m^2) leads to immediate pigment darkening (IPD) of human skin, a process dependent on OPN2, G protein, phospholipase C (PLC), and calcium (Wicks et al., 2011). In the same year, another group demonstrated the presence of OPN5 in mouse skin and reported that UVA radiation (0.0198 kJ/m^2) does not affect the local molecular clock. In 2013, a study demonstrated that UVA radiation (10 or 100 kJ/m^2), but mainly violet light (100 or 500 kJ/m^2) increases the level of *OPN2* and reduces mRNA of proliferation markers in human keratinocytes (Kim et al., 2013). Oancea's group also reported the expression of several opsins in human keratinocytes and melanocytes, and that UVR radiation (90% UVA e 10% UVB, 5 kJ/m^2) does not affect mRNA levels of *OPN1SW*, *OPN2*, *OPN3*, and *OPN5* in these cells (Haltaufderhyde et al., 2015).).

More recently, peropsin mRNA and protein were detected in human keratinocytes, and its functionality was demonstrated since violet light-induced calcium influx was lost upon gene silencing by RNAi (Toh et al., 2016). Buscone and colleagues detected the protein expression of OPN2 and OPN3, but not OPN1SW, OPN1MW, OPN4, and OPN5 in the basal layer of epidermis, in dermal fibroblasts, and in hair follicles of humans (Buscone et al., 2017). In the same study, blue light stimulation (32 kJ/m^2) increased hair follicle proliferation, a process dependent on OPN3. The role of OPN2 in this process was not investigated by the authors (Buscone et al., 2017). Using *ex vivo* model of human skin, the expression of several opsins was evaluated but only *OPN3* was detected by qPCR (Regazzetti et al., 2018. Interestingly, blue light exposure (500 kJ/m^2) did not affect *OPN3* levels; however, the blue light-induced pigmentary process was lost

upon *OPN3* silencing (Regazzetti et al., 2018). In a recent study, OPN1SW, OPN3, and OPN5 were detected in the epidermis of human facial and abdominal skin *in situ*. *OPN3* gene silencing in keratinocytes did not affect DNA synthesis, but the level of differentiation was reduced after blue light stimulation (Castellano-Pellicena et al., 2018).

Solar Radiation and its Physiological and Pathological Effects

The majority of all beings requires solar radiation to perform its metabolic activities. The electromagnetic spectrum of solar radiation that reaches Earth comprises several types of radiation: infrared (780 nm – 1100 nm), visible light (400 – 780 nm), and UV radiation (200 – 400 nm). It should be highlighted that infrared radiation, even though it displays important roles in several important processes (Dupont et al., 2013; Sklar et al., 2013), will not be discussed here. The focus of this study is UV radiation and visible light.

The solar radiation in the UV wavelength that reaches Earth represents 5% of all solar spectrum, in which UVA (320 – 400 nm) and (UVB 280 – 320) constitute approximately 90-95% and 5-10%, respectively (Dupont et al., 2013; Sklar et al., 2013; Wicks et al., 2011). UVA radiation penetrates deeper the skin when compared to UVB radiation, and UVC radiation (200 – 280 nm), fortunately, is almost completely filtrated by the stratosphere. The presence of UVC is detrimental to life itself since the wavelength of UVC coincides with the maximal absorption of DNA and other organic molecules. Therefore, the deleterious effects of UVC, if were present on Earth, would be catastrophic to life (Matsumi and Kawasaki, 2003; Ridley et al., 2009; Dupont et al., 2013).

Visible light, on the other hand, comprises approximately 50% of the solar spectrum and it is known to deeply penetrate the skin (Dupont et al., 2013; Sklar et al., 2013). Visible light as well as UVA radiation are routinely seen as innocuous; however, an increasing number of studies has shown their deleterious effects on biological systems. Both visible light and UVA radiation lead to increased formation of reactive oxygen species (ROS) (Zastrow et al., 2009), increased levels of inflammatory cytokines (Mahmoud et al., 2008), and DNA damage (Cadet et al., 1997; Mahmoud et al., 2008). In the next lines, we will describe the deleterious effects of UVB and UVA radiation, and visible light.

The molecule of DNA is susceptible to damages caused by several factors such as, but not limited to, smoking, pollution, drugs, medication, and endogenous metabolism products – especially reactive oxygen species (ROS) (Menck and Munford, 2014). UVB radiation is the best studied deleterious agent of the skin: It induces to the formation of cyclobutane pyrimidine dimers (CPP) and photic products (6-4 PP), which lead to C-T transition known to occur in UV-induced skin cancer. In fact, due to the high frequency of C-T transition in damage caused by UV, these mutations are known as UV signature (Wikonkal and Brash, 1999).

UVB radiation penetrates less in the skin when compared to UVA radiation, being only able to affect the basal layer of epidermis. Thus far, the deleterious effects of ROS and reactive nitrogen species (RNS) are known to promote inflammation, burning, and early aging. In fact, the high energy found in UVB radiation photons can be absorbed by DNA bases, which can be repaired by DNA repairing systems. It is widely known that failures in DNA repair are directly associated with oncogenic processes (Dupont et al., 2013). Among the beneficial effects of UVB radiation is its key role in the pathway for Vitamin D synthesis. Upon UVB radiation, 7-dehydrocholesterol is converted into pre-vitamin D3 in the skin (Desotelle

et al., 2012). UVB radiation is also known to cause delayed tanning (DT), which involves the *de novo* production of tyrosinase (Mahmoud et al., 2008; Dupont et al., 2013).

UVA radiation, on the other hand, is less energetic than UVB radiation, but it is present in higher quantities and it can penetrate deeper, reaching the dermis. UVA radiation can be subdivided into: UVA2 (315 – 340 nm) and UVA1 (340 – 400 nm). Even though UVA radiation penetrates deeper in the skin, its deleterious effects are less marked (Ridley et al., 2009). In fact, it is long known the role of UVA in the immediate pigment darkening (IPD) (Rosen et al., 1987), associated with the concept that UVA radiation does not pose a threat to the skin, what led to dissemination of artificial tanning (Dupont et al., 2013). Nevertheless, it is currently accepted that UVA radiation, in fact, exerts deleterious effects, with the formation of ROS and RNS. These players modify proteins, lipids, and DNA, which ultimately results in oxidative damage linked to early aging and skin cancer (Miyamura et al., 2011; Pfeifer and Besaratinia, 2012; Svobodova et al., 2012).

As mentioned above, a well-known effect of UVA radiation is the IPD which takes place in response to low dosage of UVA (1 – 5 J/cm^2), an effect that fades away within minutes to hours. It was believed that IPD was due to the oxidation and redistribution of pre-existing melanin (Mahmoud et al., 2008); however, this traditional view was questioned since in human melanocytes IPD results from a fast melanin synthesis, in a process dependent on rhodopsin (Wicks et al., 2011), which will be discussed in depth in Chapter 5.

Contrary to UVB, UVA radiation has a low potential of interacting with DNA bases as its deleterious effects are mainly due to oxidative stress caused by ROS, i.e., its effects are indirect. UVA-driven ROS interact with DNA bases generating mutagenic bases, mainly 8-oxoguanine (Fortini et

al., 2003). Since DNA absorbs weakly in UVA wavelength, the generation of CPD and 6-4 PP is not expected (Ridley et al., 2009), as confirmed by early studies. However, with the advances of detection techniques, it was later shown that CPD and 6-4 PP are generated by UVA radiation (Matsunaga et al., 2014), and that UVA-induced CPD and 6-4 PP seem to persist longer than UVB-generated similar products (Mouret et al., 2006). Nonetheless, UVA radiation is less effective in generating DNA photoproducts when compared to UVB by a factor of 10^5 - fold (Runger and Kappes, 2008). In addition to DNA, other chromophores absorb energy and can transfer it to DNA, in a process known as type I photosensitizing reaction, or to oxygen leading to ROS formation known as type II reaction, generating DNA damage. The latter is the main form through which UVA elicits DNA damage (Runger and Kappes, 2008; Sklar et al., 2013).

As to the deleterious effects of white light, there have been few reports in the literature. Although few, these studies have clearly shown that white light is able to generate ROS (Zastrow et al., 2009). Interestingly, it was shown that UVB, UVA, and white light are responsible for 4%, 46%, and 50% of ROS production in an *in vitro* model (Runger and Kappes, 2008). In addition, white light increases the levels of inflammatory cytokines (IL-1, IL-6 e IL-8) as well as matrix metalloproteinases (Liebel et al., 2012). It is also known that white light generates DNA damage upon oxidation, but not by generating dimers (Cadet et al., 1997; Liebel et al., 2012). Furthermore, white light is also known to induce IPD (Mahmoud et al., 2008). When compared to the effects of UV radiation, the effects of visible light are less understood and, therefore, need further investigation.

The spectrum of blue light is near UVA radiation's and, therefore, it is believed that either deleterious or beneficial effects of both

wavelengths will overlap. Interestingly, blue light therapy is used for the treatment of neonates with jaundice, and its therapeutic efficacy is extremely high (Olah et al., 2013). On the other hand, long term deleterious effects such as oxidative stress, DNA damage, and asthma have been reported (Gathwala and Sharma, 2002; Aspberg et al., 2010). It was also shown that blue light exerts deleterious effects on murine cone cells through increased ROS production, altered protein synthesis, and aggregation of shortwave opsins, leading to severe cellular damage, all of which could be prevented by the antioxidant N-acetyl-cysteine (Kuse et al., 2014). Moreover, a blue light pulse (10 J/cm^2) has been shown to rapidly reduce the viability of murine melanoma cells (Sparsa et al., 2010). The same protocol was used in a patient with cutaneous melanoma, which decreased the hemorrhagic process, cellular growth, and necrosis of the tumoral tissue (Sparsa et al., 2010).

Within this therapeutic line, blue light has also been used to counterbalance circadian perturbation found in patients suffering from seasonal affective disorder (SAD) (Roecklein et al., 2009), a syndrome associated with the shortening of the day light length. Since it is highly likely that a perturbation of the circadian system takes place in this syndrome, several studies have shown blue as well as white light as a therapeutic approach with promising results (Strong et al., 2009; Gordijn et al., 2012).

Taken altogether and considering the broad biological effects of solar radiation that can be deleterious or beneficial, it is essential the existence of a complex biological system in the skin that is able to, within a short time interval, perceive light, activate repair mechanisms, and/or synthesize protective substances, as well as to anticipate the solar radiation, a role performed by the cutaneous opsin system and biological clock.

Protective Photopigments that Absorb and Dissipate the Energy from UV Radiation and Visible Light

Due to continuous exposure to harmful agents that leads to DNA damage, the skin is under constant threat and, therefore, it displays protective mechanisms against such events (Krutmann et al., 2017). In the following lines, a visible light/UV radiation-induced pigmentary mechanism will be presented, which is related to DNA protection.

It is widely accepted that UV-induced DNA damage and/or repair trigger biochemical signals that ultimately increase melanogenesis (Gilchrest and Eller, 1999). The melanogenic pathway, in general lines, can be described as follows: the amino acid tyrosine is oxidized by a complex comprising two enzymes: Tyrosine- and dopa-oxidases. This first step is common for the synthesis of either eumelanin or pheomelanin, in which tyrosine is transformed into dopaquinone. In the presence of cysteine or other compounds that have thiol groups (ex. glutathione), the biochemical reaction between thiol groups and dopaquinone is fast, and thus, the pheomelanin pathway is favored. Cysteine may be added to several positions at the dopaquinone ring, but the 5-S-cysteinyldopa or 5-S-glutathionyldopa are the predominant isomers. Then, the mixture of cysteine-dopaquinone undergoes several biochemical reactions until benzothiazines, and finally, to pheomelanin (Figure 2, right side) (Solano, 2014).

On the other hand, in the absence of cysteine or glutathione, dopaquinone undergoes a spontaneous intracellular cyclization into leukodopachrome (cyclodopa), which is a potent reducing agent. Cyclodopa reacts with non-cyclic dopaquinone and generates dopa and dopachrome. It is known that the former, through a not well-known pathway, leads to a mixture of 5,6-dihydroxyindole (DHI) and 5,6-

dihydroxyindole-2-carboxylic acid (DHICA). In the final step, both DHI and DHICA are oxidized by tyrosinase into 5,6-dihydroxyindoles. Then, subsequent cross-linking reaction between the reduced (5,6-dihydroxyindoles) and the oxidized forms (5,6-indolequinones) gives rise to the final eumelanin pigment (Figure 2, left side).

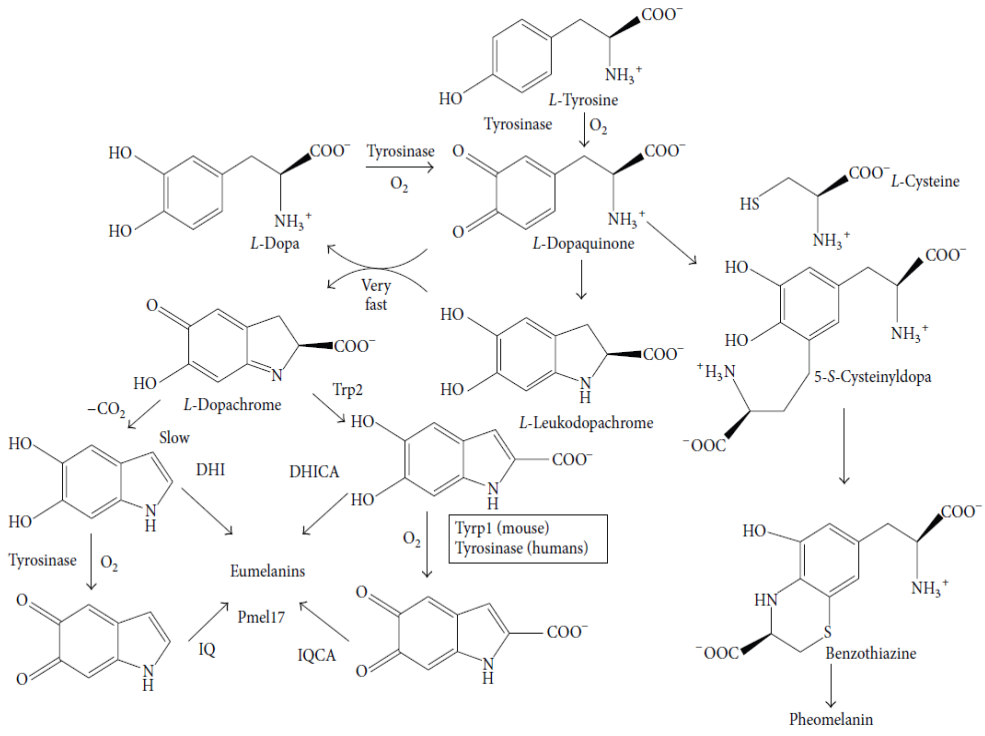

Figure 2: Biochemical synthetic pathways of pheomelanin and eumelanin synthesis. Taken from Solano, 2014.

The synthesis of melanin takes place in specific organelles named melanosomes found in melanocytes. This cell type represents 1% of the total epidermis cell population. Once produced, the melanosome transfer from melanocytes to keratinocytes is crucial for the protective effect exerted by melanin. In keratinocytes, the pigment migrates to regions near the nucleus where it acts as “shield” against UV radiation and visible light (Thody et al., 1991; Brenner and Hearing, 2008). In fact, it is estimated that melanin absorbs approximately 50 to 75 % of UV radiation that reaches the skin (Brenner and Hearing, 2008).

Interestingly, it has been demonstrated that enhancing DNA repair process after UV exposure, through the usage of an excision enzyme, leads to increased melanin synthesis (Gilchrest et al., 1993). In another classic study, the introduction of small thymidine dinucleotide like fragments, similar to those sequences that are removed during DNA repair, also leads to increased melanin levels (Eller et al., 1994). Similarly, agents which break one DNA strand also stimulate melanogenesis *in vitro* (Eller et al., 1996). However, in opposition to the protection against UV radiation, melanin may also exert toxic effects – especially after UV exposure. It is known that melanin can interact with DNA, thus acting as a photosensitizer that produces ROS after visible light or UVA radiation exposure (Korytowski et al., 1987; Kvam and Tyrrell, 1999; Chiarelli-Neto et al., 2014). Interestingly, it has been demonstrated that pheomelanin is more susceptible to photodegradation compared to eumelanin, due to increased generation of hydrogen peroxide and superoxide anion after UV exposure (Brenner and Hearing, 2008). Nevertheless, the clinical relevance of the deleterious effects of melanin in pathological process is still not fully understood, and further studies are required (Takeuchi et al., 2004; Brenner and Hearing, 2008).

OBJECTIVES

Taken the literature described above, the aims of this thesis were to characterize the presence of the photosensitive system in melanocytes and to explore the functionality of this system by analyzing how visible light and UVA radiation interact with and are perceived by opsins. In a concurrent approach, we also investigated how both photosensitive and temporal controlling systems are dysregulated and contribute to the carcinogenic process of melanoma. The results and conclusions of this project are described in the following chapters. At the end of these chapters, a summary of our findings in the light of the current literature, the questions that were answered, the frontiers that have been opened, and future perspective for the field will be provided.

CHAPTERS

Chapter 1: The Effect of White Light on Normal and Malignant Murine Melanocytes: A Link between Opsins, Clock Genes, and Melanogenesis

The content provided in this chapter has been published in BBA Molecular Cell Research, 2016 1863(6PtA):1119-33. DOI: 10.1016/j.bbamcr.2016.03.001.

Authors' names: de Assis LVM, Moraes MN, da Silveira Cruz-Machado S, Castrucci AML.

Biochimica et Biophysica Acta 1863 (2016) 1119–1133

Contents lists available at ScienceDirect

Biochimica et Biophysica Acta

journal homepage: www.elsevier.com/locate/bbamcr

The effect of white light on normal and malignant murine melanocytes: A link between opsins, clock genes, and melanogenesis

L.V.M. de Assis [a], M.N. Moraes [a], S. da Silveira Cruz-Machado [b], A.M.L. Castrucci [a,*]

[a] Laboratory of Comparative Physiology of Pigmentation, Department of Physiology, Institute of Biosciences, University of São Paulo, São Paulo, Brazil
[b] Laboratory of Chronopharmacology, Department of Physiology, Institute of Biosciences, University of São Paulo, São Paulo, Brazil

ARTICLE INFO

Article history:
Received 2 February 2016
Received in revised form 29 February 2016
Accepted 2 March 2016
Available online 3 March 2016

Keywords:
Mouse
Melanocytes
Melanoma
Clock genes
Opsins
Cancer

ABSTRACT

The skin possesses a photosensitive system comprised of opsins whose function is not fully understood, and clock genes which exert an important regulatory role in skin biology. Here, we evaluated the presence of opsins in normal (Melan-a cells) and malignant (B16–F10 cells) murine melanocytes. Both cell lines express *Opn2*, *Opn4* – for the first time reported in these cell types – as well as *S-opsin*. OPN4 protein was found in a small area capping the cell nuclei of B16–F10 cells kept in constant dark (DD); twenty-four hours after the white light pulse (WLP), OPN4 was found in the cell membrane. Despite the fact that B16–F10 cells expressed less *Opn2* and *Opn4* than Melan-a cells, our data indicate that the malignant melanocytes exhibited increased photoresponsiveness. The clock gene machinery is also severely downregulated in B16–F10 cells as compared to Melan-a cells. *Per1*, *Per2*, and *Bmal1* expression increased in B16–F10 cells in response to WLP. Although no response in clock gene expression to WLP was observed in Melan-a cells, gene correlational data suggest a minor effect of WLP. In contrast to opsins and clock genes, melanogenesis is significantly upregulated in malignant melanocytes in comparison to Melan-a cells. *Tyrosinase* expression increased after WLP only in B16–F10 cells; however no increase in melanin content after WLP was seen in either cell line. Our findings may prove useful in the treatment and the development of new pharmacological approaches of depigmentation diseases and skin cancer.

1. Introduction

The skin is the first barrier between the organism and the external environment and it is subject to frequent daily oscillation of environmental temperature and light. These two factors represent an important source of possible damage to skin cells [13,15,17,19,70]. Since oscillation in the amplitude of these factors can be predicted, a system able to anticipate these cyclic oscillations is crucial for the organism homeostasis.

At the core of this temporal system lies the molecular clock gene machinery [11,12,18,59,65]. *Clock* (*Circadian Locomotor Output Cycles Kaput*) and *Bmal1* (*Aryl hydrocarbon receptor nuclear translocator-like protein 1*) represent a positive component while *Per* (*Period*) and *Cry* (*Cryptochrome*) compose the negative limb of a system of interlaced feedback loops. The oscillation in clock gene expression and subsequently the protein levels are crucial to keep track of time through a well-described auto-regulatory feedback loop of transcription factors. BMAL1 forms a heterodimer with CLOCK or NPAS2 (in the suprachiasmatic nucleus, SCN), which activates the transcription of *Per1*, *Per2*, and *Per3*, and *Cry1* and *Cry2* by binding to a specific DNA element named E-box in the promoter of the target genes. Once PERs are in the cytoplasm they dimerize with CRY1 and CRY2 which, after being phosphorylated by casein kinase 1δ (CK1δ) or CK1ε, are targeted toward the nucleus to inhibit the transcriptional activity of BMAL1/CLOCK heterodimer. Another loop of regulation is also exerted through E-box activation: CLOCK/BMAL1 activates *nuclear receptor subfamily 1, group D, member 1/2* (*Rev-Erbα/β*) and *RAR-related orphan receptor alpha/beta* (*RORα/β*) expression. After being translated, REV-ERBα/β competes with RORα/β for the orphan receptor response element (RORE) sequence present in *Bmal1* promoter: REV-ERBα/β inhibits while RORα/β stimulates *Bmal1* expression. To terminate the repression phase and to restart a new cycle of transcription, the degradation of PER and CRY is required. Such event is carried out by CK1δ or CK1ε that target PER for ubiquination whereas CRY is phosphorylated by 5′-AMP-activated protein kinase catalytic subunit alpha-1 (AMPK1) and dual specificity tyrosine-phosphorylation-regulated kinase 1 A (DYRK1A) (for review see [11,12,18,59,65]).

In mammals, the SCN is the central oscillator [71] responsible for controlling the temporal expression of clock genes and clock-controlled genes (CCG) in peripheral tissues, and ultimately align the

* Corresponding author at: Departamento de Fisiologia, Instituto de Biociências, Universidade de São Paulo, R. do Matão, trav. 14, no. 101, São Paulo 05508-900, Brazil.
E-mail address: amdlcast@ib.usp.br (A.M.L. Castrucci).

http://dx.doi.org/10.1016/j.bbamcr.2016.03.001
0167-4889/

entire organism under a single timing [11,59]. The light and dark cycle (LD) is the most important environmental timing clue, *Zeitgeber*, in mammals; this information is interpreted by a subset of retinal ganglion cells – that express melanopsin, OPN4 – into electrical stimuli that reach the SCN through the retinohypothalamic tract, which then entrain the SCN [63,64].

The presence of clock genes in peripheral tissues was first reported in 1998 in isolated mammalian fibroblasts [1], and two years later in the skin [95]. In 2001, the expression of clock genes in human oral mucosa and skin was reported to be cyclic, and an association between *Per1* and cell cycle was reported [9]. Since then few studies have investigated the effect of several stimuli [75,83], among them the white light [84], on the regulation of clock gene expression in murine and human skin cells. Recently, the important role of clock genes in the regulation of skin pigmentation response was reported [28], and currently it has been proposed that the skin cells – keratinocytes, melanocytes, and fibroblasts – display distinct clock gene machineries that comprise a local multioscillatory circadian system [75].

Several features have been reported to oscillate in a circadian manner in the skin such as: blood flow, protection barrier [92], transepidermal water loss, surface pH, and temperature [93]. For instance, DNA repair has been shown to oscillate in murine skin with a maximal activity in afternoon/evening, which coincides with the onset of mouse locomotor activity [22]. Recently, mice harboring mutation on *Clock* showed decreased hydration of the stratum corneum, what was linked to reduced aquaporin 3 expression (*Ap3*) in the epidermis [55].

In addition to clock gene machinery, murine and human skin [43,85], as well as cultured melanocytes [24,37,51,58,85], display an interesting photosensitive system comprised of opsins; however, the role and functionality of this photosensitive system in regulating local physiological processes are still poorly understood but it began to be recently addressed [3,4,87].

Melanocytes are specialized cutaneous cells which produce and store melanin, a pigment produced in lysosome-like structures named melanosomes. Shortly, tyrosine is oxidized by an enzymatic complex formed by tyrosinase and dopa oxidase, resulting in dopaquinone. In the presence of high concentration of thiol groups pheomelanin formation is favored; on the contrary, dopaquinone is transformed in leucodopachrome, which then generates a mixture of 5,6-dihidroxyindol (DHI) e 5,6-dihidroxyindol-2-carboxylic acid (DHICA). The last reactions catalyzed again by tyrosinase produce eumelanin [82], which may be transferred to adjacent keratinocytes where it forms a perinuclear shield protecting the cells against the deleterious effect of ultraviolet (UV) radiation and white light. Even though the classical and well-known protective role of melanin is well established [81], emerging evidence is showing that melanin may participate in DNA damage through reactive oxygen (ROS) and nitrogen species (RNS) in response to UVA radiation and white light [14,67]. Whether melanin has as protective and/or a carcinogenic role in skin cancer has yet to be established. Despite this open question, it has been demonstrated that melanocytes respond to white light pulse (WLP) with increased melanin content through immediate pigment darkening (IPD), persistent pigment darkening (PPD), and delayed tanning (DT) [54,73,80].

Based on the above-mentioned literature, we hypothesized that the malignant transformation alters the melanocyte photosensitive system. To test this hypothesis we investigated the response of opsins, clock genes, and melanogenic machinery evoked by WLP in normal, Melan-a, and malignant, B16–F10, murine melanocytes.

2. Material & methods

2.1. Cell culture

Melan-a or B16–F10 cells were cultured in 75 cm^2 flasks with RPMI 1640 medium containing phenol red (Atená, Campinas, SP, Brazil), supplemented with 14.3 mM $NaHCO_3$, 15 mM HEPES, 10% fetal bovine serum (FBS) (Atená, Campinas, SP, Brazil), and 1% antibiotic/antimycotic solution (10,000 U/mL penicillin, 10,000 μg/mL streptomycin, and 25 μg/mL amphotericin B, Life Technologies, Carlsbad, CA, USA). The pH was adjusted to 7.2, and the cells were kept at 37 °C with 5% CO_2. The maintenance of the cell cultures and the experiment setup were carried under ambient lighting. The cells were kept during six days in complete darkness in order to free run.

During the experiments the cells were maintained in RPMI 1640 without phenol red (Atená, Campinas, SP, Brazil or Life Technologies, Carlsbad, CA, USA) in 25 cm^2 flasks at 37 °C with 5% CO_2. FBS was reduced to 2%, and the medium was supplemented with 10^{-7} M retinal (*all-trans* Sigma-Aldrich, St. Louis, MO, USA). Phorbol 12-myristate 13-acetate (TPA, Sigma-Aldrich, St. Louis, MO, USA) at 200 nM was always present in Melan-a cell media, as it is required for proper cell growth [5]. Cell manipulation during the experiments was carried out under red dim light (7 W Konex bulb and Safe-Light filter GBX-2, Kodak, Rochester, NY, USA). During the experiments no cell handling or feeding was carried out.

2.2. White light stimulation

Melan-a or B16–F10 cells were seeded at the initial density of 10^6 and 10^5 cells, respectively. The cells were divided into 2 groups: (1) control group, kept in DD throughout experiment and (2) experimental group kept in DD for six days, exposed to a 15 min WLP at the beginning of the 7th day (420 to 750 nm, 95.18 μW/cm^2, 650 lx), and returned to DD until the end of the experiment. No UVA or UVB radiation was detected in the white light spectrum (UV Detector, Vilver Lourmat, Marne-la-Vallée, France). Total RNA was extracted 24 h after the WLP, and then every 6 h for 18 h. For melanin quantification assay, cells were kept as above, but the extraction took place 24 (ZT 24) and 36 (ZT 36) hours after the WLP.

2.3. Total RNA extraction and reverse transcriptase PCR (RT-PCR)

The medium was removed and Tri-Reagent (Ambion, Grand Island, NY, USA) was added directly to the cells. The lysate was subject to the manufacturer's suggested procedure. In order to remove genomic DNA contamination, the samples were treated with DNAse I (turbo-DNase, Life Technologies, Carlsbad, CA, USA) according to the manufacturer's instructions. RNA concentration and quality (OD_{260}/OD_{280}) were determined in a NanoDrop spectrophotometer (NanoDrop, Wilmington, DE, USA). One to four μg of total RNA was subject to reverse transcriptase reaction using random primers and Superscript III, in addition to the reagents recommended by the enzyme manufacturer (Life Technologies, Carlsbad, CA, USA).

2.4. Quantitative PCR (qPCR)

Quantitative PCR was performed with the products of reverse transcription using oligopeptides spanning introns, designed and synthesized by IDT (Coralville, IA, USA) or Life Technologies (Carlsbad, CA, USA), based on sequences obtained from GenBank (http://www.ncbi.nlm.nih.gov/genbank). All primers exhibited efficiency between 86% and 120%. The access number of each gene, the respective primer sequences and the concentrations are shown in Table 1.

The qPCR reactions were performed through two different protocols: multiplex for simultaneous analysis (*TaqMan*®) and *SYBR® GreenER™*. The *TaqMan*® solutions contained *Per1* and *Clock*, or *Opn2* and *Bmal1*, primers and fluorescent probes (Table 1), Supermix 2× (Bio-Rad Laboratories, Hercules, CA, USA, or Life Technologies, Carlsbad, CA, USA), supplemented to final concentrations of 400 μM dNTPs, 6 mM $MgCl_2$, and 0.1 U/μL Platinum Taq DNA polymerase (Life Technologies, USA). Each experimental cDNA was run in triplicates in 96 well plates. The assays were performed using i5

Table 1
Sequences and concentrations of primers and probes, and gene access numbers.

Templates	Primers and probes	Final concentration
RNA 18S	For: 5′-CGGCTACCACATCCAAGGAA-3′ Rev: 5′-GCTGGAATTACCGCG GCT-3′	50 nM 50 nM
mBmal1 (NM_001243048)	For: 5′-AAGCTTCTGCACAATCCACAGCAC -3′ Rev: 5′-TGTCTGGCTCATTGTCTTCGTCCA-3′ Probe: 5′-/5HEX/-AAAGCTGGCCACCCACGA AGATGGG/3BHQ_1/-3′	300 nM 300 nM 200 nM
mPer1 (NM_0011065.3)	For: 5′-AGCAGGTTCAGGCTAACCAGGAAT-3′ Rev: 5′-AGGTGTCCTGGTTTCGAAGTGTGT-3′ Probe: 5′-/6FAM/-AGCCTTGTGCCATGGACA TGTCTACT/3BHQ_1/-3′	300 nM 300 nM 200 nM
mClock (NM_007715.6)	For: 5′-CTCTGCTGCCTTTCCACTACAA-3′ Rev: 5′-TGCTGAGGCTGGTGTTGCT-3′ Probe: 5′-/5HEX/AGAGCACTTTCCCTCCTTCG CACC A/3BHQ_1/-3′	300 nM 300 nM 200 nM
mPer2 (NM_011066)	For: 5′-TTCCTACAGCATGGAGCAGGTTGAT-3′ Rev: 5′-ATGAGGAGCCAGGAACTCCACAAA-3′	300 nM 300 nM
mCry1 (NM_009963.4)	For: 5′-AGCAGACACCATCACATCAG-3′ Rev: 5′-CAGGGGAAGGAACGCCATATT-3′	300 nM 300 nM
mTyrosinase (NM_011661.4)	For: 5′-TCCTCCTGGCAGATCATTTGT-3′ Rev: 5′-TGGTCCCTCAGGTGTTCCA-3′	300 nM 300 nM
mS-Opsin (NM_007538.3)	For: 5′-TGGGCACCAAGTATCGAAGC-3′ Rev: 5′-ATCTCCAGAATGCAAGCCCG-3′	300 nM 300 nM
mOpsin (NM_008106.2)	For: 5′-TCTTGTGGCCTCCCTACCAT-3′ Rev: 5′-TGCAGGTGACACTGAAGAGAC-3′	300 nM 300 nM
mOpn4 (NM_001128599.1)	For: 5′-ACATCTTCATCTTCAGGGCCA-3′ Rev: 5′-ACTCACCGCAGCCCTCAC-3′	300 nM 300 nM
mOpn2 (NM_145383.1)	For: 5′-TGCCACACTTGGAGGTGAAA-3′ Rev: 5′-ACCACGTAGCGCTCAATGG-3′ Probe: 5′-/6-FAM/-CGCCCTGTGGTCCCTGGTGG/3BHQ_1′	300 nM 300 nM 200 nM

thermocycler (Bio-Rad Laboratories, Hercules, CA, USA) in the following conditions: 7 min at 95 °C, followed by 45 cycles of 30 s at 95 °C and 30 s at 55 °C.

The analysis assays for *Per2*, *Cry1*, *Tyrosinase*, *Opn1-SW*, *Opn1-MW*, *Opn4*, and 18S RNA were carried out by *SYBR® GreenER™* technology. The solutions contained the primers (Table 1) and Kapa *SYBR®* Fast qPCR Master Mix 2× (Kapa Biosystems, Wilmington, MA, USA). Each experimental cDNA was run in duplicates in 96-well plates. This assay was performed in iCycler thermocycler (Bio-Rad Laboratories, Hercules, CA, USA) in the following conditions: 10 min at 95 °C, followed by 45 cycles of 15 s at 95 °C, 1 min at 60 °C, and 80 cycles of 10 s at 55 °C, with a gradual increase of 0.5 °C.

Ribosomal 18S RNA, which did not vary along time under our experimental conditions (data not shown), was chosen as a reference gene in all gene expression reactions in both *TaqMan®* and *SYBR® GreenER™* methodologies.

2.5. Immunocytochemistry

A peptide consisting of the 15 N-terminal amino acid sequence of mouse OPN4 (GenBank accession NP_038915) with an appended C-terminal cysteine (MDSPSGPRVLSSLTQC) was synthesized (Uniformed Services University of the Health Biomedical Instrumentation Center, Bethesda, MD, USA), conjugated to keyhole limpet hemocyanin, and used to immunize rabbits (Covance Labs, Denver, PA, USA). Specificity of this antiserum was confirmed in previous studies showing a dose-dependent loss of immunoreactivity by preadsorption with increasing concentrations of the antigenic peptide, and by the lack of immunoreactivity in retinas of OPN4-null mice [64]. The primary antibody of rhodopsin is a rabbit polyclonal antibody acquired from Santa Cruz Biotechnology (Dallas, TX, USA).

Melan-a or B16–F10 cells were seeded (10^4/well) into 8-chamber-slides in the experimental medium as described above. The cells were kept in DD for 3 days and at the beginning of the 4th day they were divided into 2 groups: the control remained in DD while the experimental group was exposed to a 15 min WLP (420 to 750 nm, 95.18 μW/cm^2, 650 lx). Twenty-four hours later the medium was removed and the cells were fixed in 4% paraformaldehyde (Electron Microscopy Sciences, Hatfield, PA, USA) in phosphate-buffered saline (PBS) at 4 °C for 30 min. After blockade of non-specific sites with 6% normal goat serum containing 22.52 mg/mL of glycine (Sigma-Aldrich, St. Louis, MO, USA) in PBS at 4 °C for 1 h, the cells were incubated overnight at 4 °C with primary anti-OPN4 (1:500 and 1:1000) or anti-OPN2 (1:50 to 1:400). A Cy3-labeled anti-rabbit secondary antibody at 1:500 was applied for 1 h at room temperature, to reveal the primary antibody binding.

Primary and secondary antibodies were diluted in incubation buffer containing 1% bovine serum albumin (Calbiochem, San Diego, CA, USA), 0.25% carrageenan lambda and 0.3% Triton X-100 (both from Sigma-Aldrich, St. Louis, MO, USA). The material was mounted with DAPI-Vectashield Hard aqueous medium (Vector Laboratories, Burlingame, CA, USA) and coverslipped. Images were obtained in an inverted fluorescence microscope Axiovert 40CFL (Zeiss, Oberkochen, Germany) with a mercury lamp of 50 W, and DAPI (excitation 358 and emission 463 nm) and Cy3 (excitation 549 and emission 562 nm) filters.

2.6. Imaging flow cytometry (Amnis)

The protein expression and the percentage of cells expressing OPN2 and OPN4 were assessed in Melan-a and B16–F10 cells by imaging flow cytometry (FlowSight system, Amnis, EMD-Millipore, Seattle, WA, USA). This technique combines the sensitivity of microscopic single cell staining with the advantage of high cell counts for analysis as made possible by flow cytometry assays. Melan-a or B16–F10 cells were seeded in 75 cm^2 flasks, kept in DD for 3 days, and collected in the 4th day by resuspending the cells in Tyrode/EDTA solution. After centrifugation and extensive washes, 2×10^6 cells were used in each staining. For antibody staining, similar procedures as described in the immunocytochemistry section were followed. Briefly, after fixation and permeabilization, OPN2 or OPN4 polyclonal antibodies were incubated at 1:50 and 1:500 dilutions, respectively, followed by incubation with a sheep FITC-conjugated anti-rabbit antibody at 1:200 dilution (Sigma-Aldrich, St. Louis, MO, USA).

Results were collected at 50,000 cell counts per sample by FlowSight using a 488 nm laser. In order to compare OPN2 or OPN4 positive over negative cells, isotype controls were performed by the omission of the primary antibody and the incubation with FITC-conjugated anti-rabbit antibody. The data analysis was performed by IDEAS software (Amnis, EMD-Millipore, Seattle, WA, USA) based on scatter plot of bright field area versus aspect ratio. Putative single cells were selected by gating only the area consistent with single cells in the absence of doublets or debris-like dots based on cell imaging of each dot. The expression and the percentage of OPN2- or OPN4-FITC positive cells were determined based on the frequency of the counts over isotype controls.

2.7. Melanin quantification

Melan-a and B16–F10 cells were harvested with Tyrode/EDTA solution, and after cell counting, the cell suspension was centrifuged at 100 ×*g* for 5 min, the supernatant was discarded, and 1 M NaOH in 10% DMSO was added to the cell pellet. The lysate was heated at 80 °C for 2 h, centrifuged at 1050 ×*g* for 15 min, and 200 μL of each sample supernatant were added in duplicates to wells of a flat-bottom plate. Melanin was quantified by absolute absorbance at 475 nm in a plate reader (SpectraMax 250, Molecular Devices, Sunnyvale, CA, USA), and the values plotted against a standard curve of synthetic melanin

(Sigma-Aldrich, St. Louis, MO, USA) ranging from 3.125 to 200 μg/mL. Melanin concentration was expressed as μg of melanin per 10^6 cells.

2.8. Data and statistical analysis

All data were checked for Gaussian distribution through D'Agostino-Pearson omnibus and Shapiro–Wilk test. Cycle threshold (C_T) for each reaction was determined as the number of cycles corresponding to the points of the geometric portions of the amplification curves crossed by the threshold line. ΔC_T was then determined subtracting the C_Ts for 18S RNA from the C_T for each gene at the same time point (both corresponding to the average of triplicate or duplicate wells of the same cDNA). The highest Δ_{CT} was then subtracted from each Δ_{CT} value to obtain $\Delta\Delta_{CT}$, which was used as the negative exponential of base 2 ($2^{-\Delta\Delta CT}$, [50]). The average of the log values ($n = 4$ flasks from at least two independent experiments) was graphed as mean ± SEM relative to the minimal value in control group (DD condition). The temporal gene expression and melanin content of each group were analyzed by One-way ANOVA followed by Tukey post-test. The differences in both gene expression and melanin content assays between cells exposed to WLP and those in DD at the same time point were analyzed by Two-way ANOVA followed by Bonferroni post-test.

To compare gene expression and melanin content between Melan-a and B16–F10 cells in DD group, unpaired Student's *t* test was used; samples that displayed Gaussian distribution were analyzed by *t* test with Welch correction while those that did not show normal distribution were analyzed by Mann–Whitney test. Significance was set for $p < 0.05$. All analyses were carried out in GraphPad Prism Version 6.0 (La Jolla, CA, USA).

3. Results

3.1. Cell morphology and cell culture analysis

In this study we used two murine cellular models: normal melanocytes namely Melan-a cells and malignant melanocytes, B16–F10 cells, both derived from C57BL/6J mouse. It is interesting to note the different morphology of these cells: Melan-a cells possess few dendrites whereas a single B16–F10 cell displays several ones (Fig. 1). Such a feature would allow B16–F10 cells to form a communication network with neighboring and distant cells, in contrast with Melan-a cells.

3.2. Screening of opsins in Melan-a and B16–F10 cells

Interested in investigating the effects of light on peripheral tissue of mammals – more specifically on melanocytes – we evaluated the presence of light sensitive systems in Melan-a and B16–F10 cells, assessing gene expression of retinal opsins in these lines. Our results show that both cell lines express *Opn2*, the classical opsin rhodopsin and one of the three types of cone opsins, *Opn1-SW* (Table 2) similar to what has been demonstrated in human melanocytes [24]. Melanopsin, *Opn4*, expressed in mammalian intrinsically photosensitive retinal ganglion cells, and responsible for the entrainment of the circadian system [63], is here demonstrated for the first time to be expressed in both Melan-a and B16–F10 cell lines (Table 2).

3.3. Effect of white light pulse in the expression of Opn4 and Opn2

Since *Opn2* and *Opn4* were the most expressed opsins in both Melan-a and B16–F10 cells, we decided to evaluate their temporal profile in control and experimental groups, and whether WLP would affect their expression. In both cell lines in DD condition no time-dependent oscillation was observed in the expression of *Opn2* and *Opn4* (One-way ANOVA, Fig. 2A–D).

After WLP only B16–F10 cells showed changes in the expression of both opsins: a reduction in *Opn2* expression at ZT 24 in comparison to its respective control (Two-way ANOVA, $p \leq 0.01$) (Fig. 2C), and a marked increase in *Opn4* expression at ZT 36 and ZT 42 in comparison to their respective controls (Two-way ANOVA, $p \leq 0.01$ and $p \leq 0.05$,

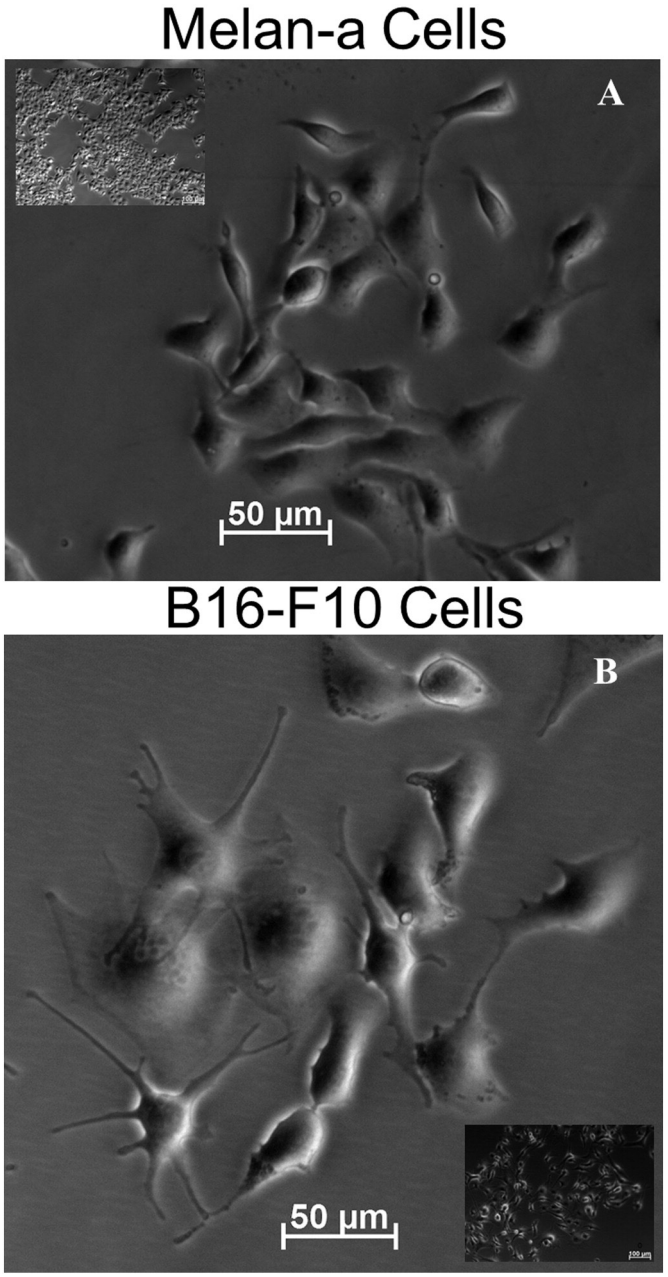

Fig. 1. Representative photomicrographies of Melan-a and B16–F10 cells. Melan-a and B16–F10 cells were seeded (10^6 and 10^5 cells/25 cm^2, respectively), and kept at least three days in DD. A) Melan-a cells at 200× magnification. Note the absence of dendrites and connections to distant cells. Inset: Melan-a cell population at 100× magnification; B) B16–F10 cells at 200× magnification. Note the neuron-like shape of B16–F10 cells and several dendrites extended by each cell, allowing connection with neighboring and distant cells. Inset: B16–F10 cell population at 100× magnification.

Table 2
Screening of opsins in Melan-a and B16–F10 cells through qPCR assay. C_T values in between parentheses. mRNAs were considered not to be expressed when C_T values were higher than 35.

Gene	Melan-a (C_T value)	B16–F10 (C_T value)
Opn2	Expressed (27)	Expressed (29)
Opn4	Expressed (29)	Expressed (27)
S-opsin	Expressed (32)	Expressed (32)
M-opsin	Not expressed (36)	Not expressed (35)

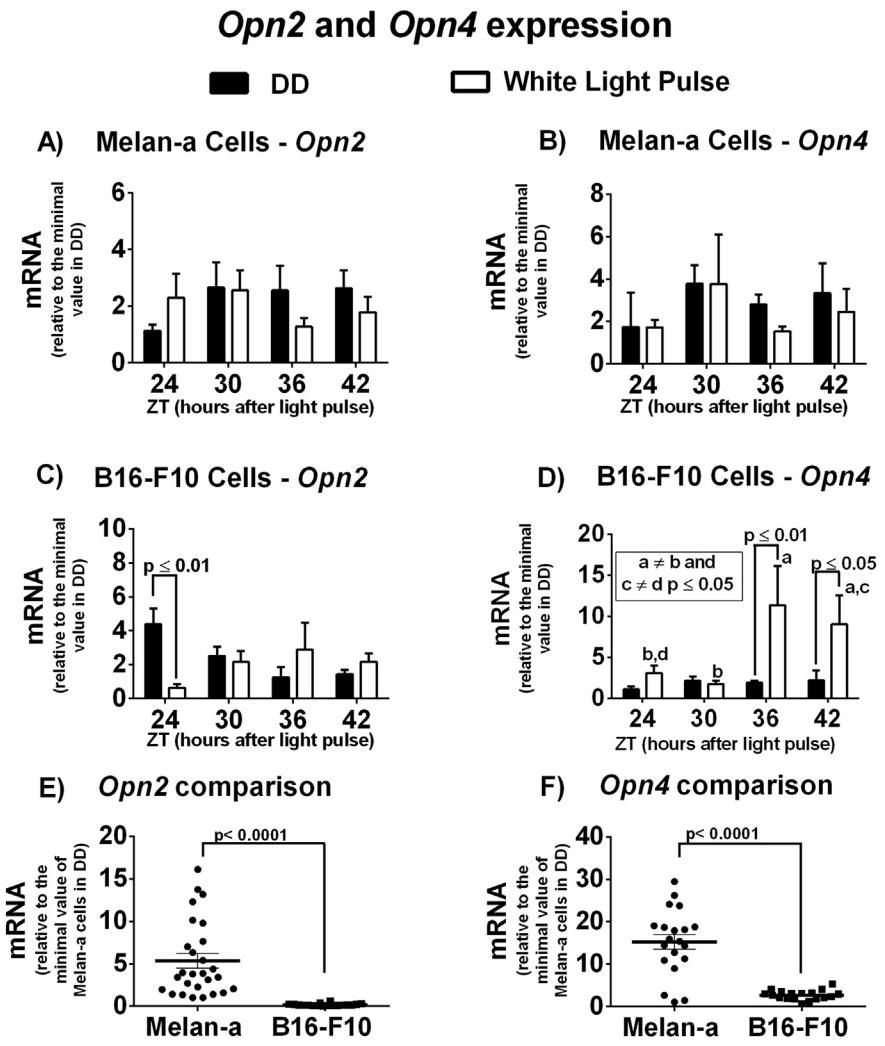

Fig. 2. Expression of *Opn2* and *Opn4* in Melan-a and B16–F10 cells. A) Melan-a *Opn2* n = 4–8; B) Melan-a *Opn4* n = 3–7; C) B16–F10 *Opn2* n = 3–6; D) B16–F10 *Opn4* n = 3–5; E) *Opn2* n = 28 and 18 for Melan-a and B16–F10 cells, respectively; F) *Opn4* n = 20 and 18 for Melan-a and B16–F10 cells, respectively. Gene expression was normalized by 18S RNA transcript and expressed relative to the minimal value of each cell line in DD (A–D) or to the minimal value of Melan-a cells in DD (E and F). In this and in the following figures of gene expression values are shown as mean ± SEM; temporal variation in each group was analyzed by One-way ANOVA followed by Tukey post-test; the difference between the groups was analyzed by Two-way ANOVA followed by Bonferroni post-test; mRNA levels between the two cells lines were compared by Student's *t* test. p values are shown in the graphs.

respectively); in addition, we observed that after WLP *Opn4* expression showed a temporal oscillation with higher expression at ZT 36 and 42 in comparison to ZT 24 and 30 (One-way ANOVA $p \leq 0.05$). Therefore, our data show that Melan-a cell *Opn4* and *Opn2* are not responsive to WLP whereas in B16–F10 these genes are affected in opposite way by WLP. Surprisingly, B16–F10 cells express 30-fold and 6-fold less *Opn2* and *Opn4* respectively than Melan-a cells (Fig. 2E and F, Student's *t* test, $p < 0.0001$).

3.4. Immunocytochemistry of OPN2and OPN4

Next we evaluated the presence and localization of OPN2 and OPN4 proteins in Melan-a and B16–F10. Polyclonal rabbit anti-OPN2 was tested ranging from 1:50 to 1:400 dilutions; representative immunostaining of OPN2 at 1:100 dilution is shown in Fig. 3. Polyclonal rabbit anti-OPN4 was tested at 1:500 and 1:1000 dilutions and in both concentrations positive labeling was detected. Fig. 4 shows representative immunostaining of OPN4 at 1:500 dilution. No immunostaining was observed when the secondary antibody (1:500) was incubated in the absence of the primary one (Fig. S1).

OPN2 has been previously detected in murine melanocytes [58]; however, the finding of OPN4 in both cell lines is intriguing since this opsin has been implicated with circadian system and regulation of clock genes in the SCN. OPN2 and OPN4 were localized diffusely in the cytoplasm and in the cell membrane in Melan-a cells kept in DD or after the WLP (Figs. 3 and 4). B16–F10 cells showed a strong staining of OPN2 in the cell membrane which was stronger after the WLP, but no difference in protein localization was found (Fig. 3). On the other hand, OPN4 in B16–F10 cells in DD showed a diffuse staining in the cytoplasm and a strong labeling in a cap region near the nuclei membrane; twenty-four hours after the WLP OPN4 migrated from the regions near the nuclei to the cell membrane (Fig. 4).

3.5. Imaging flow cytometry

The flow cytometry imaging assay showed that approximately 81.8% and 92.06% of Melan-a cells were OPN2- and OPN4-positive, respectively. Regarding B16–F10 cells approximately 98% and 74.37% of the cells were positive for OPN2 and OPN4, respectively (Fig. 5). These data show that majority of Melan-a and B16–F10 cells express

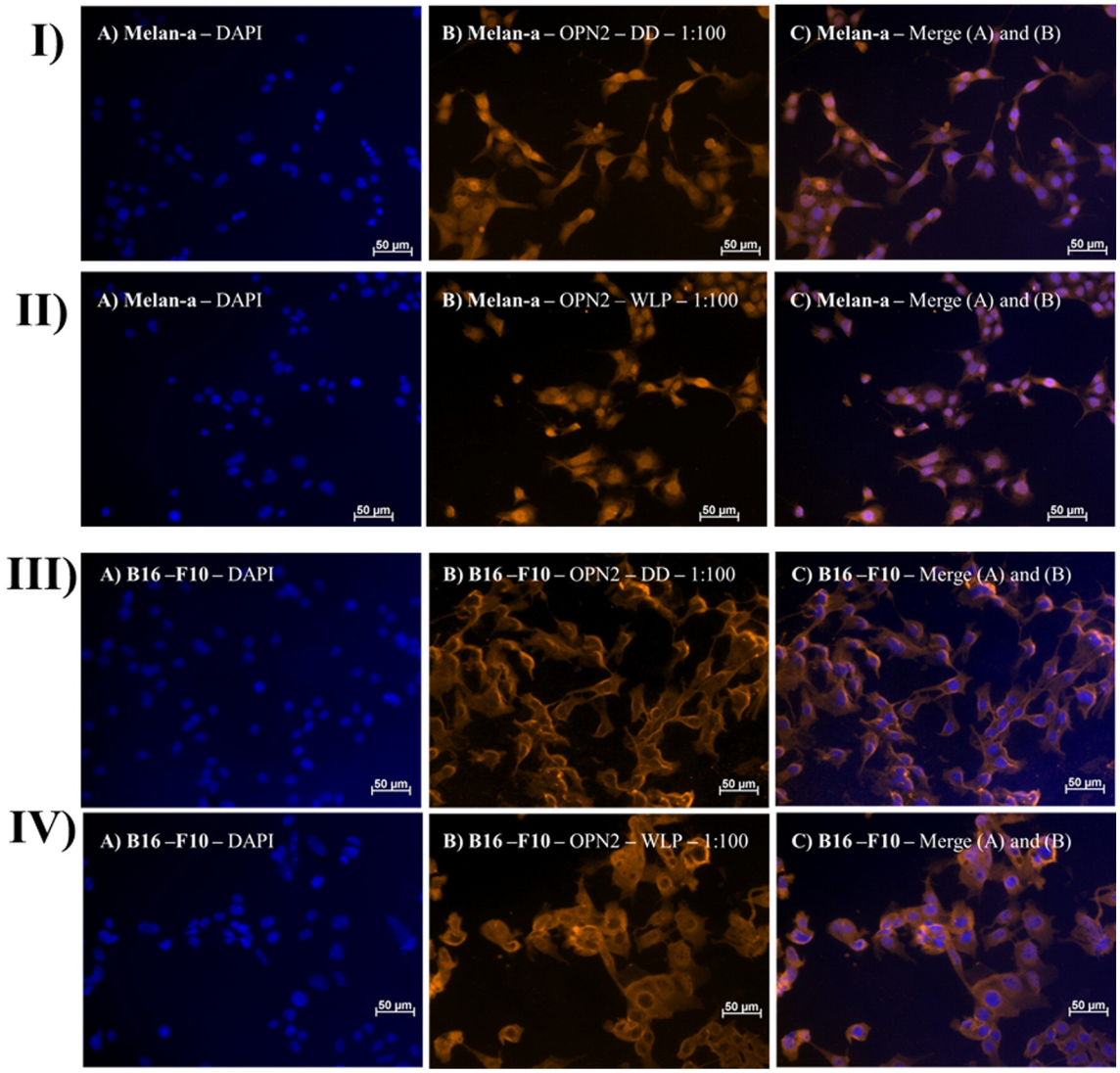

Fig. 3. Representative fields of OPN2 immunostaining in Melan-a and B16–F10 cells. I) OPN2 in Melan-a cells kept in DD; II) OPN2 in Melan-a cells 24 h after the WLP; III) OPN2 in B16–F10 cells kept in DD; IV) OPN2 in B16–F10 cells 24 h after the WLP. A) DAPI stained nuclei in blue; B) immunopositivity of OPN2 with 1:100 antiserum revealed by Cy3-labeled secondary antibody in orange; C) merged A and B images. Photomicrographies were taken with Axiocam MRm camera (Zeiss) and pseudocolored with Axiovision software (Zeiss). Scale bar 50 µm (200× magnification).

both proteins – OPN2 and OPN4 – thus indicating that both cell lines are equipped to respond to light stimuli.

3.6. Clock gene expression after white light pulse

Next, we investigated the role of this photosensitive system in regulating the physiological processes of melanocytes, and whether WLP could affect clock gene expression in Melan-a and B16–F10 cells.

No time-dependent oscillation of *Per1*, *Per2*, *Bmal1*, *Clock*, or *Cry1* expression was seen in DD or in white light-exposed (One-way ANOVA) Melan-a cells. The clock gene machinery in Melan-a cells seemed to be completely unresponsive to WLP since no difference in clock gene expression was found between DD and white light exposed groups (Two-way ANOVA) (Fig. 6A–E).

Unlike normal melanocytes, the clock gene machinery in B16–F10 cells was affected by WLP. *Per1* expression increased 24 and 30 h after the WLP in comparison to the respective DD controls ($p \leq 0.05$ and $p \leq 0.001$, respectively, Two-way ANOVA followed by Bonferroni post-test) (Fig. 7A); however, no temporal oscillation of *Per1* was seen in either group (One-way ANOVA, Fig. 7A).

Per2 transcripts showed no temporal variation in B16–F10 cells kept in DD (One-way ANOVA) while in the white light stimulated group a peak of expression was observed at ZT 30. At this ZT, a marked increase in gene expression was found in the white light exposed cells in comparison to their respective control ($p \leq 0.01$, Two-way ANOVA followed by Bonferroni post-test, Fig. 7B), and in comparison to the other time points of light-exposed cells (ZT 24, ZT 36, and ZT 42, $p \leq 0.01$, $p \leq 0.01$, and $p \leq 0.05$, respectively, One-way ANOVA followed by Tukey post-test).

Bmal1 (Fig. 7C) and *Cry1* (Fig. 7E) expression did not oscillate in DD or in the white light exposed group (One-way ANOVA); and no statistical difference was found between groups (Two-way ANOVA) (Fig. 7C and E). Similar to the other genes, *Clock* expression did not oscillate in the DD group (One-way ANOVA) but a temporal increase of *Clock* expression in the white light group was also observed at ZT 30 as compared to ZT 24 ($p \leq 0.01$, One-way ANOVA followed by Tukey post-test), and at ZT 42 in comparison to ZT 24 and ZT36 ($p \leq 0.001$ and $p \leq 0.01$, One-way ANOVA followed by Tukey post-test) (Fig. 7D), suggesting an ultradian oscillatory profile. An increase of transcripts was found at ZT 30 and ZT 42 in comparison to

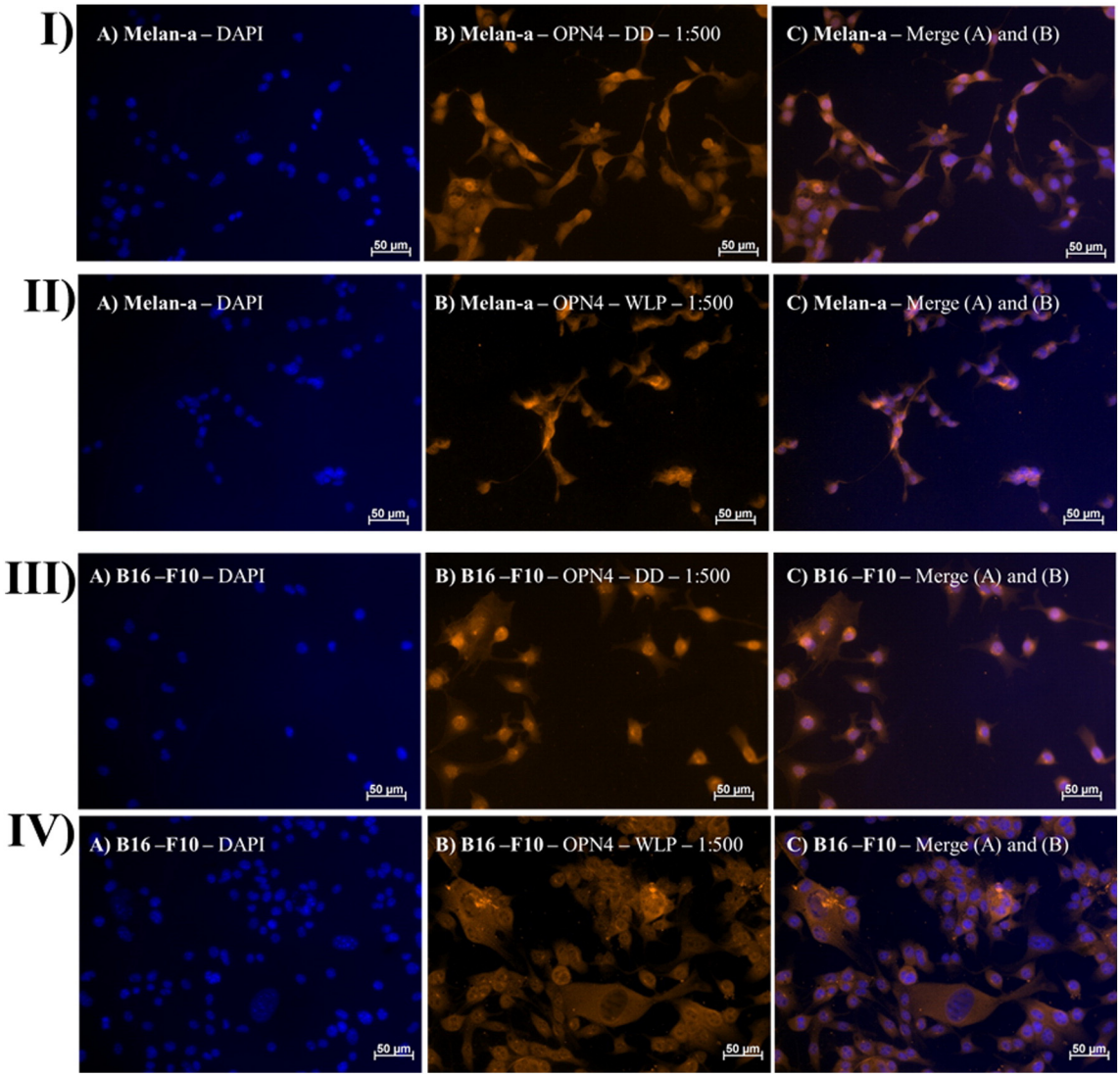

Fig. 4. Representative fields of OPN4 immunostaining in Melan-a and B16–F10 cells. I) OPN4 in Melan-a cells kept in DD; II) OPN4 in Melan-a cells 24 h after the WLP; III) OPN4 in B16–F10 cells kept in DD; IV) OPN4 in B16–F10 cells 24 h after the WLP. A) DAPI stained nuclei in blue; B) immunopositivity of OPN4 with 1:500 antiserum revealed by Cy3-labeled secondary antibody in orange; C) merged A and B images. Photomicrographies were taken with Axiocam MRm camera (Zeiss) and pseudocolored with Axiovision Software (Zeiss). Scale bar 50 μm (200× magnification).

each respective control ($p \leq 0.001$ and $p \leq 0.05$, Two-way ANOVA followed by Bonferroni post-test).

Considering the striking difference in light response between normal and malignant melanocytes, we compared the levels of gene expression of both cell lines. All clock genes, but *Per1* (Fig. 8A), were highly expressed in Melan-a cells as compared to B16–F10 cells (Student's *t* test) (Fig. 8B–E). *Per2* and *Clock* expression was 9-fold ($p < 0.0001$, Fig. 8B and D), *Bmal1* expression was 1.5-fold ($p = 0.0352$, Fig. 8C), and *Cry1* expression was 1.6-fold ($p = 0.0151$, Fig. 8E) higher in Melan-a cells than in B16–F10 cells. Thus, our data show that clock gene expression is severely downregulated in B16–F10 cells as compared to Melan-a cells.

3.7. Melanin synthesis

Bearing in mind the remarkable difference between normal and malignant melanocytes regarding their response to white light, we investigated whether that same stimulus would also differentially affect melanogenesis in Melan-a cells as compared to B16–F10 cells. Melanin synthesis depends on tyrosinase — the limiting enzyme for melanin production ([81,82]). It is known that *Tyrosinase* gene possesses a highly conserved E-box element in its promoter [6,62,81], rendering it a CCG. In fact, melanin synthesis was recently shown to be a clock regulated event [28].

In DD, *Tyrosinase* expression did not oscillate in Melan-a or B16–F10 cells (One-way ANOVA) (Fig. 9A, B). After the light pulse, the normal cell line still did not show any *Tyrosinase* alteration; B16–F10 cells, however, exhibited a significant increase of the enzyme transcripts (Fig. 9B): The expression at ZT 24 and ZT 30 was 3 and 4-fold higher after light stimulus than their respective DD control groups ($p \leq 0.05$ and $p \leq 0.01$, Two-way ANOVA followed by Bonferroni post-test). The expression of *Tyrosinase* in the light-exposed group was higher at ZT 24, ZT 30, and ZT 42 than at ZT 36 ($p \leq 0.05$, $p \leq 0.01$, and $p \leq 0.01$, respectively, One-way ANOVA followed by Tukey post-test), suggesting an ultradian oscillatory pattern (Fig. 9B). In addition, we have found that, in DD, B16–F10 cells express 3.5-fold more *Tyrosinase* than Melan-a cells ($p < 0.0001$, Student's *t* test) (Fig. 9C).

After assessing *Tyrosinase* expression we quantitated the final product, melanin, after exposure to WLP. In both cell types, melanin levels did not temporally vary in DD or in light-exposed groups

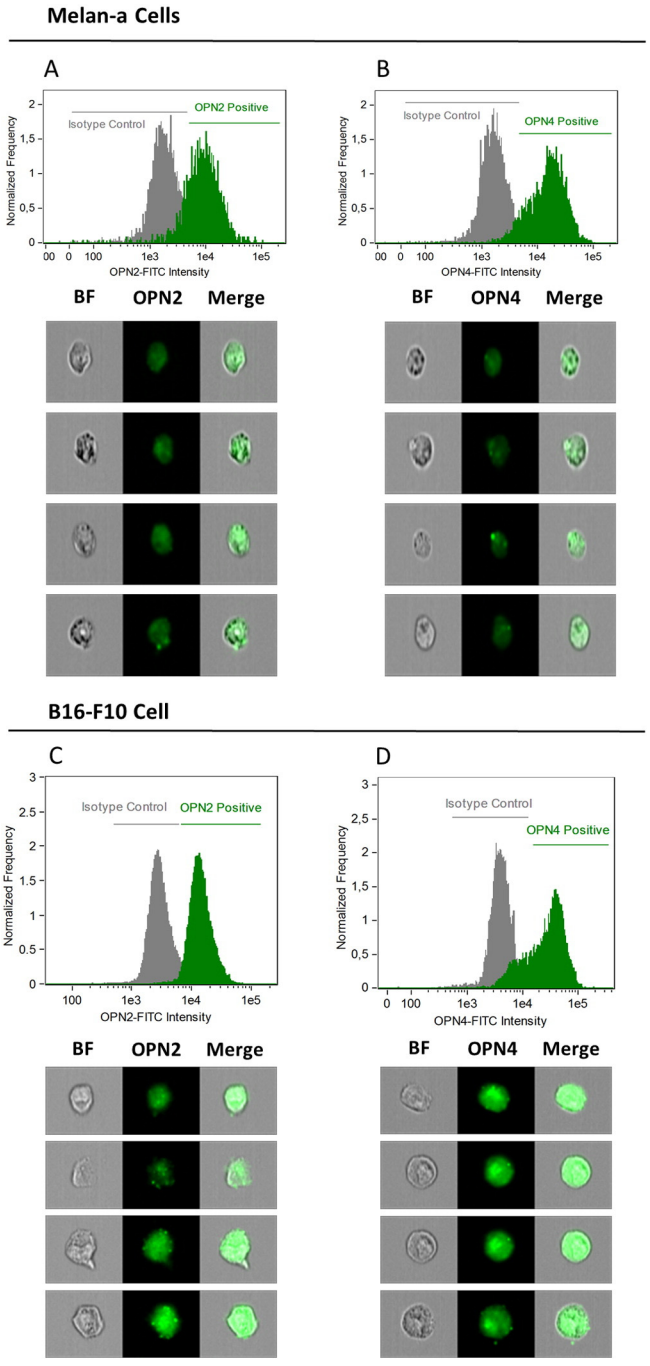

Fig. 5. Imaging flow cytometry. Melan-a and B16–F10 cells stained for OPN2 and OPN4. Note the displacement of fluorescence intensity to the right in comparison to the isotype control after cells were incubated with OPN2 (A and C) and OPN4 (B and D) antibodies, what demonstrates that both Melan-a and B16–F10 cells express OPN2 and OPN4 proteins. Each cell is represented by a row of three images, from left to right: representative images of bright field (BF), FITC fluorescence (green) of OPN2 or OPN4 antibodies, and the merged image.

(One-way ANOVA), nor was any increase in melanin content found after the light stimulus as compared to the respective control (Two-way ANOVA) (Fig. 10A and B). Accordingly to *Tyrosinase* expression, melanin content in B16–F10 cells in DD was about 3-fold higher than in Melan-a cells ($p = 0.0021$, Student's *t* test) (Fig. 10C). Even though an increase in *Tyrosinase* expression was found in B16–F10 cells after WLP, melanin content was not altered. Our data show that the melanogenesis machinery – here comprised of *Tyrosinase* expression and melanin content – is upregulated in B16–F10 cells in comparison to Melan-a cells ($p = 0.0021$, Student's *t* test).

4. Discussion

Human and murine melanocytes express several opsins which may comprise a photosensitive system [24,37,51,58,85]. Since light perception that leads to SCN entrainment is considered to be restricted to the retina in mammals, the role of a photosensitive system in the skin as well as which physiological processes it may regulate [3,4,87] is still obscure.

Our data show that both Melan-a and B16–F10 cell lines express short wavelength cone opsin (*Opn1-SW*), *rhodopsin* (*Opn2*), and *melanopsin* (*Opn4*). The expression of *Opn1-SW* had been previously detected in human melanocytes [24] and of its protein OPN1-SW in human and murine skin [85], although its function has yet to be elucidated. The expression of *Opn2* and OPN2 has also been demonstrated and quantified in human and murine skin and melanocytes [51,58,85]. Curiously, OPN2 was reported to mediate an early melanin synthesis triggered by UVA radiation, thus acting as a UV sensor [87].

We show here that *Opn2* expression was irresponsive to WLP in Melan-a cells whereas in B16–F10 cells the expression of *Opn2* was reduced 24 h after the light stimulus. Violet light and UVA radiation have been shown to increase *Opn2* expression in human keratinocytes, in which this opsin regulates the expression of proliferation markers [42]; however, UVA radiation did not affect *Opn2* expression in human melanocytes [24].

Our data show that B16–F10 cells express significantly less *Opn2* in comparison to Melan-a. In both cell lines OPN2 is located in the cytoplasm and cell membrane; although the WLP did not alter the opsin localization in either cell type, membrane staining in B16–F10 cells seemed to be stronger after light stimulus. The fact that OPN2 is present in the membrane is suggestive of its functionality in both cell lines; however, functionality assays are needed to confirm this hypothesis. This is the first report showing that WLP does reduce *Opn2* expression in malignant melanocytes, whereas it does not affect the opsin transcripts in normal melanocytes.

OPN4 was originally discovered in *Xenopus laevis* melanophores [68] where it mediates melanin pigment dispersion in response to blue light [36,60]. Since OPN4 has been shown to be expressed in the mammalian retina and to participate in mammalian photo-entrainment of the circadian system [63], the expression of *Opn4* and OPN4 in our models is intriguing. In the mammalian retina, OPN4 is classically localized in the membrane of a subpopulation of ganglion cells [69], rendering them photosensitive [7]. It has been previously reported that human skin cells do not express *Opn4* [24,87]; this is the first report of *Opn4* and OPN4 expression in mammalian skin cells.

We have found that *Opn4* in Melan-a is unresponsive to WLP; however, B16–F10 cells respond with an increase in *Opn4* expression 36 and 42 h after the light pulse. Similarly to *Opn2* the expression of *Opn4* is lower in B16–F10 cells when compared to Melan-a cells. One might think that the reduced expression of both *Opn2* and *Opn4* could lead to an impairment of the photosensitive system in B16–F10; however, as shown in the results, that was not the case.

Moreover, in Melan-a cells OPN4 is located in the cytoplasm and membrane in both DD and after the light pulse. Interestingly, OPN4 was found in the cytoplasm near the cell nucleus, possibly Golgi complex, in B16–F10 cells kept in DD, but it translocates to cytoplasm and membrane after the light pulse. This suggests that OPN4 may act as a white light photoreceptor in B16–F10 cells. In fact, the migration of OPN4 to the cell membrane took place 24 h after the light stimulus while an increase in *Opn4* gene expression was found later at ZT 36 and ZT 42, what indicates an immediate response of protein migration followed by the increase of opsin transcripts in B16–F10 cells.

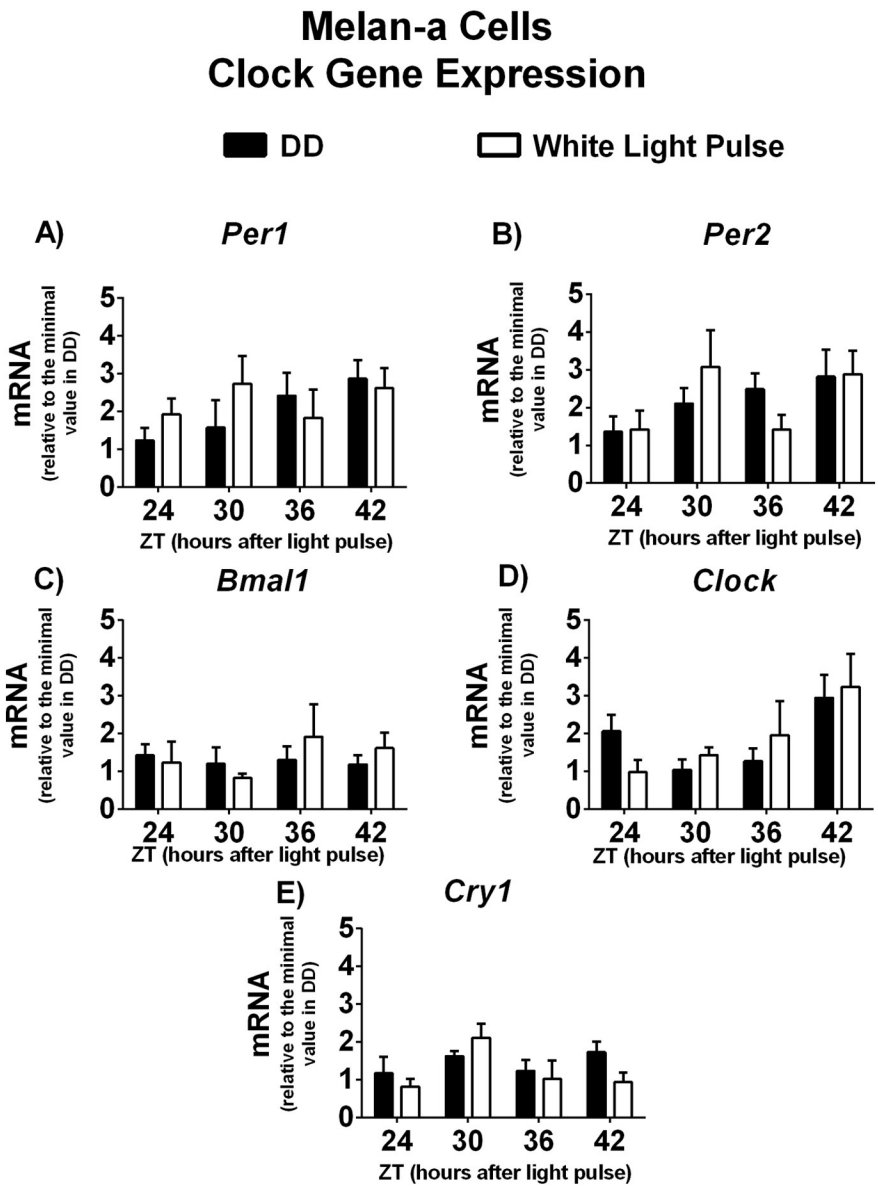

Fig. 6. Clock gene expression in Melan-a cells. A) *Per1* n = 3–7; B) *Per2* n = 3–8; C) *Bmal1* n = 4–8; D) *Clock* n = 3–6; E) *Cry1* n = 3–4. Gene expression was normalized by 18S RNA transcript and expressed relative to the minimal value in DD.

The carcinogenic process in B16–F10 cells, as discussed above, has likely led to reduced *Opn2* and *Opn4* expression, which could result in an impairment of the photosensitive system in malignant melanocytes; however, our findings point to the opposite direction. In fact, B16–F10 cells are responsive to the WLP by increasing *Opn4* expression and OPN4 migration, a feature not shared by the normal melanocytes. Based on this, we speculate that the carcinogenic process could have augmented the sensitivity of the photosensitive system – despite the reduced expression of the analyzed genes – rendering B16–F10 cells photoresponsive to white light in comparison to the normal melanocytes. Our data further reinforce the intriguing role of this opsin in peripheral tissues since OPN4 has been detected in blood vessels mediating blue light-dependent relaxation [79].

It has been shown that WLP at different intensities resets the clock machinery in the SCN [8,45,46,64,66,74,77]. In fact, blue wavelength is the major responsible for resetting clock gene machinery in the SCN through OPN4 activation [64]. A previous report from our laboratory has shown that a 15 min pulse of 20.82×10^2 μW/cm^2 white light leads to 50% of pigment dispersion as compared to α-MSH – a potent melanosome-dispersing hormone – in *Xenopus* melanophores, the typical melanopsin bearing model [36]. In addition, we have also demonstrated that a 10 min pulse of either 87.95 μW/cm^2 white light or 87.85–95.17 μW/cm^2 blue light, a much lower irradiance, is enough to evoke melanin granule dispersion [60], and that light–dark cycle and blue light pulse increase clock gene expression in *X. laevis* melanophores [61]. Thus, these studies place OPN4 as the strongest candidate to convey light information to the amphibian melanophore clock. How far in evolution has this system been conserved in skin pigment cells has yet to be established.

Our data thus far show that in Melan-a cells the WLP does not affect clock gene machinery; this response is in line with an elegant in vivo study showing that clock gene oscillation in murine skin is lost when the SCN is removed, and it is not recovered by external light [84]. A limitation of this study and many others in which the results were based on SCN ablation is that the surgical removal of SCN carried all the connections to and from the surrounding areas [32–34].

To address this limitation, a selective SCN driven *Bmal1* knockout has been created with interesting results [33,34]. When the

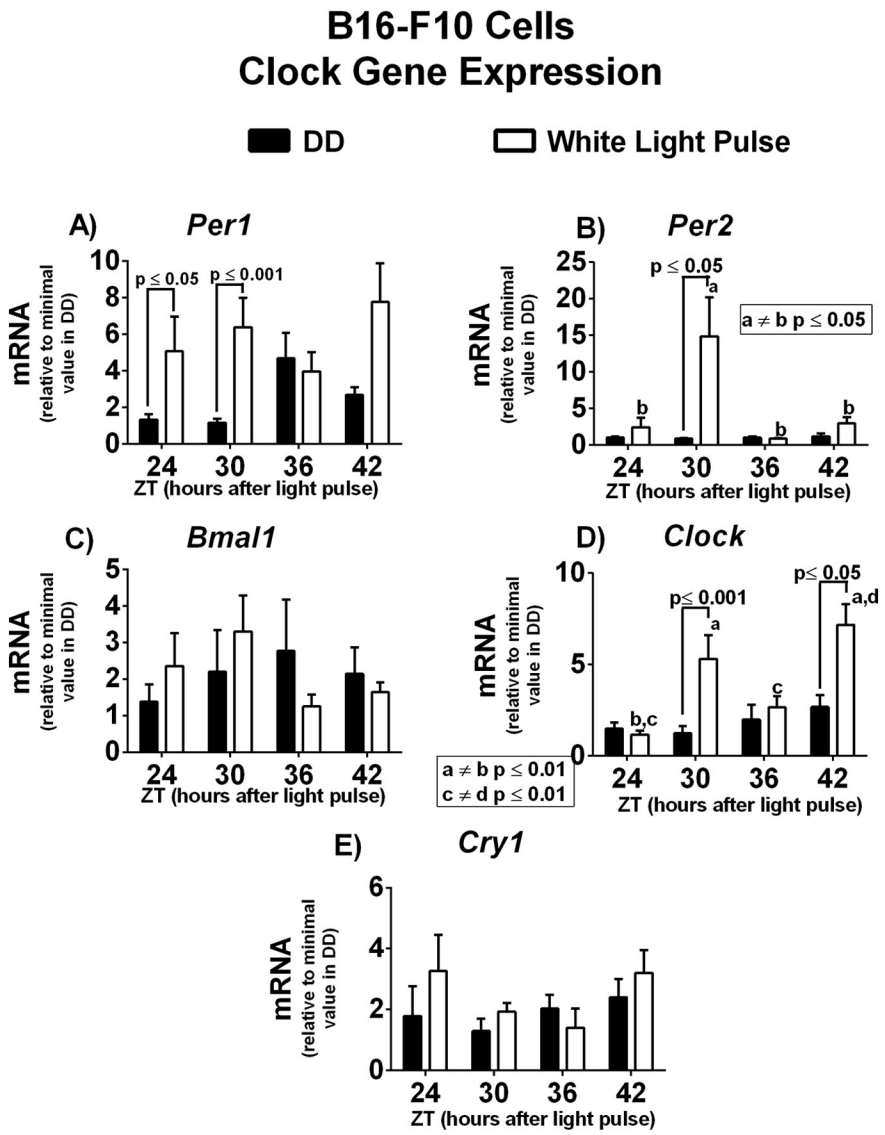

Fig. 7. Clock gene expression in B16–F10 cells. A) *Per1* n = 4–6; B) *Per2* n = 4–7; C) *Bmal1* n = 4–6; D) *Clock* n = 3–6; E) *Cry1* n = 4–6. Gene expression was normalized by 18S RNA transcript and expressed relative to the minimal value in DD.

knockout animals were kept in free running conditions no locomotor activity rhythm was observed; however, in the presence of LD cycle the locomotor activity rhythm was restored [33] — an effect not observed in classical SCN-lesioned animals [71]. Similar findings were obtained with forebrain/SCN-specific *Bmal1* knockout mice: rhythmic clock gene expression in peripheral tissues was observed in mice kept in LD cycle but it was lost in free-running conditions [38]. Based on these studies a new model to explain the role of SCN in regulating peripheral clocks has been set forth [32] in which the SCN is required to sustain the rhythms in free running conditions but it is dispensable to sustain rhythms when LD cycle is imposed. This new model has been coined as the federated system (for review [32]).

Unexpectedly, the WLP affected the clock gene machinery in malignant melanocytes — the B16–F10 cells. To our knowledge this is the first report showing that the clock gene machinery of malignant melanocytes responds to WLP. We found a marked increase in *Per1*, *Per2* and *Clock* expression after the WLP while *Cry1* and *Bmal1* expression was not affected. It is widely accepted that *Per* and *Cry* genes display antiphase relationship with *Clock* and *Bmal1* in a synchronized clock gene machinery [11,12]. These data, therefore, are suggestive that the clock gene machinery activation in B16–F10 cells in response to WLP is not a canonical activation of clock gene machinery.

In view of these findings, in the next paragraphs we will discuss possible hypotheses to explain our results:

I) The clock response displayed by B16–F10 cells could be related to the severe level of downregulation of the clock gene expression – *Per2*, *Bmal1*, *Clock*, and *Cry1* – in comparison to the transcript levels found in Melan-a cells. Since B16–F10 cells have reduced clock gene machinery expression they might respond to a lower light intensity than the one that supposedly would stimulate these genes in Melan-a cells.
Cancer cells are known to display several mutations on key genes that ultimately lead to uncontrolled cellular growth, resistance to apoptosis, induced angiogenesis, deregulated cellular energetics, genome instability, tumor induced inflammation, and immune system avoidance [26,27]. In addition, the expression of clock genes and proteins in human skin tumors [48] has been associated with clock gene machinery disruption what contributes to cancer development [41]. Over the past decade several studies have

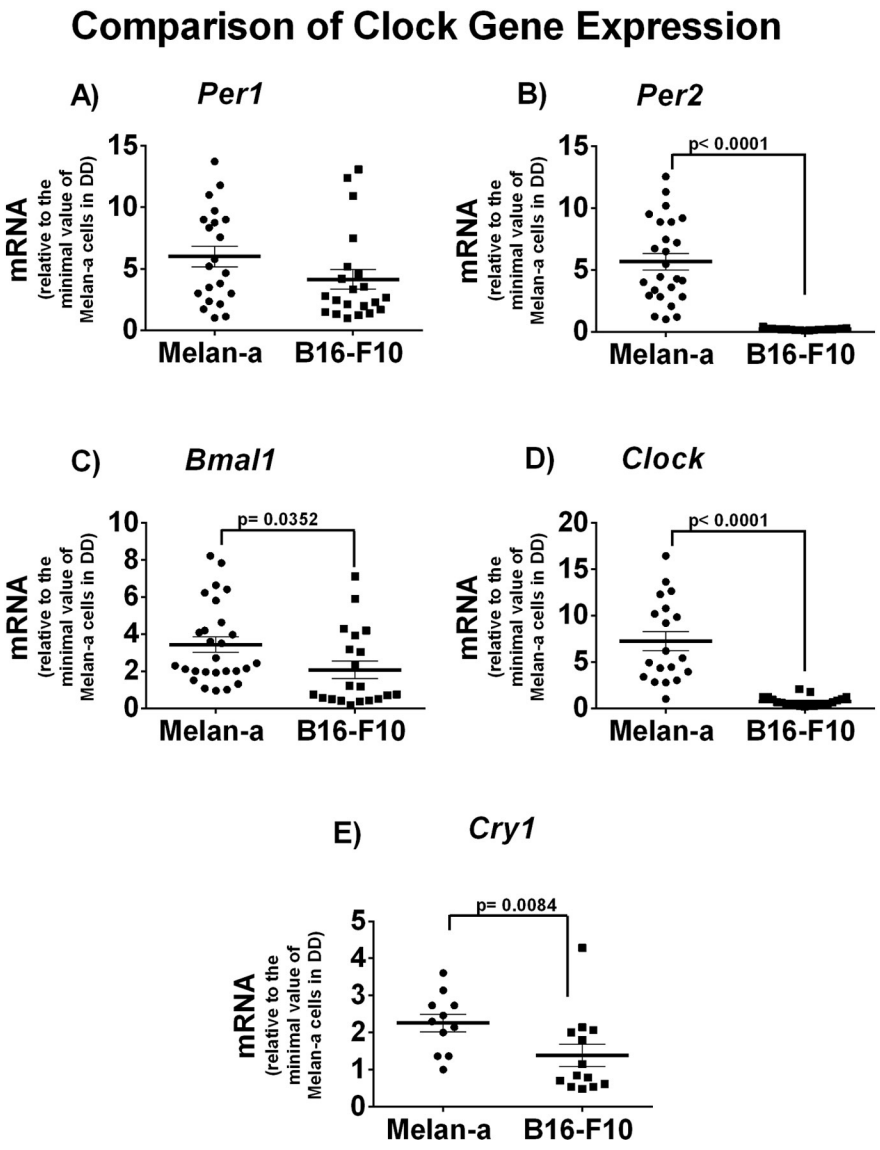

Fig. 8. Clock gene expression comparison between Melan-a and B16–F10 cells in DD. A) *Per1* n = 21 for both cell lines; B) *Per2* n = 25 and 19 for Melan-a and B16–F10 cells, respectively; C) *Bmal1* n = 25 and 20 for Melan-a and B16–F10 cells, respectively; D) *Clock* n = 18 and 21 for Melan-a and B16–F10 cells, respectively; E) *Cry1* n = 11 and 13 for Melan-a and B16–F10 cells, respectively. Gene expression was normalized by 18S RNA transcript and expressed relative to the minimal value of Melan-a in DD.

increased our knowledge regarding the role of clock genes in cancer. These genes have been shown to regulate key physiological processes such as DNA repair, cell cycle, metastasis, angiogenesis among others (For review [41,76]). The temporal organization of physiological processes is crucial to the organism homeostasis, a feature that is controlled by the clock gene machinery. Following this line, *Per* family genes and *Bmal1* have been reported as tumor suppressor genes [21,40,88,91]. Therefore, it is not surprising that clock genes are downregulated in cancer cells [20,41,76,89].

II) It is also tempting to speculate the role of the photosensitive system in Melan-a and B16–F10 cells. The presence of such a system is somehow an important feature for melanocytes because it qualifies these cells to perceive external lighting. In fact, white light leads to increased melanogenesis in the skin [54,80], and the same is also true for UV radiation, which leads to IPD (only UVA radiation) and DT process (both UVA and UVB radiation) [30,35,44,80,94].

Recently, it has been shown that UVA-induced increase of human melanocyte melanogenesis requires retinal, G protein, intracellular and extracellular Ca^{2+} [87], resembling the canonical opsin-mediated phenomenon [31]: OPN2 and transient receptor potential channel A1 (TRPA1) have been reported to mediate this UV-induced early melanin synthesis in human melanocytes [3,87]. Interestingly, the signaling pathway activated in this response involves Gαq/11 [4], similarly to OPN4 cascade in the mammalian retina [31] and *Xenopus* melanophores [36].

Accordingly, our data show that B16–F10 cells possess a more sensitive photoresponsive system, which is likely related to the carcinogenic process. Since these cells are more sensitive to WLP, this then may be responsible for clock gene activation in these cells. However, it is also important to state that the carcinogenic process could have led to increased photoresponsiveness independently of clock gene activation in these cells. Unfortunately, we cannot establish a cause–effect relationship, but it is clear that these findings may prove useful in the treatment of melanomas.

III) The lack of response by Melan-a cells could also be related to a non-functional photosensitive system; however, it is unlikely that Melan-a cells opsin system is not functional, since it is known that murine and human melanocytes respond to visible light and UV radiation by increasing melanin content [37,52,54,73,80]. It is

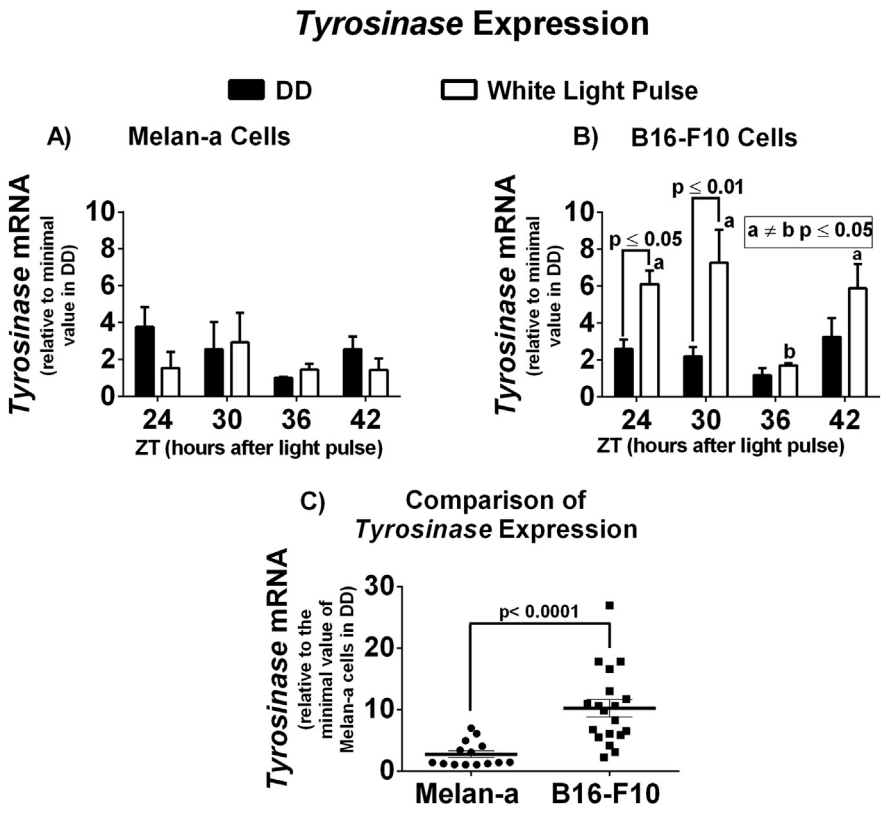

Fig. 9. *Tyrosinase* expression in Melan-a and B16–F10 cells. A) Melan-a cells n = 3–4; B) B16–F10 cells n = 3–6; C) *Tyrosinase* in Melan-a compared to B16–F10 cells in DD n = 14 and 20, respectively. Gene expression was normalized by 18S RNA transcript and expressed relative to the respective minimal value in DD in A and B, and to the minimal value of Melan-a cells in DD in C.

important to mention that the light intensity used in our study is much lower than the ones reported in the literature to increase melanogenesis [54,80], what will be further discussed in details.

Another possibility to explain this lack of response is the fact that Melan-a cells in culture require constant PKC activation with phorbol esters to prevent senescence [5]; however, PKC signaling pathway has

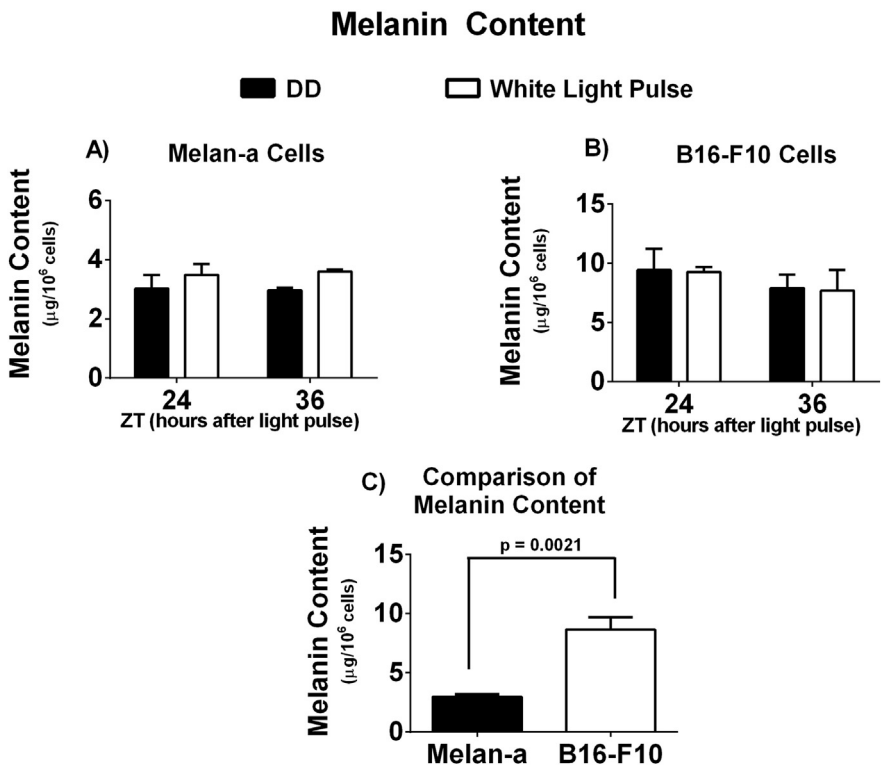

Fig. 10. Melanin content in Melan-a and B16–F10 cells. A) Melan-a cells n = 3; B) B16–F10 cells n = 3; C) melanin content in Melan-a compared to B16–F10 cells in DD n = 6. Values are shown as mean ± SEM. p value is shown in the graph.

been shown to play an important role in clock gene activation in peripheral tissue of mammalian and non-mammalian vertebrates [36,60,72,78]. If light-induced clock gene activation in mammalian pigment cells is also exerted through PKC signaling then no response would be observed, as the system would be maximally activated. And that may also explain the much higher expression of clock genes in Melan-a cells as compared to the malignant cells.

To better understand this issue we evaluated the effect of white light on clock gene expression by analyzing gene correlation profile in the normal melanocyte cell line. Interestingly, this tool indicated a positive correlation between *Per1* and *Clock*, and *Bmal1* and *Clock* expression in both DD and in light-exposed groups. On the other hand, no correlation was observed between *Per2* and *Clock* in DD group but in the white light-treated cells a positive correlation was seen (Fig. S2). This piece of evidence suggests that, despite the lack of alteration in gene expression along the time and after light exposure, WLP does exert an effect on the clock gene machinery of Melan-a cells. *Per1* does not correlate with *Tyrosinase* in DD, but a positive correlation appears after the light pulse. Remarkably, *Per2* showed a negative correlation with *Tyrosinase* in DD, shifting to a positive one after the light stimulus. *Bmal1* and *Clock* showed a positive correlation with *Tyrosinase* in DD, which was lost after the light pulse, whereas *Cry1* does not correlate with *Tyrosinase* either in DD or after the light pulse (Fig. S3). The fact that the correlation profiles in DD may change after light stimulus favors the hypothesis that Melan-a cells do possess a functional photosensitive system. In fact, the shift in correlation of *Per2* and *Tyrosinase* may represent an important cellular event triggered by white light, which requires further investigation.

The different behaviors of Melan-a and B16–F10 cells in response to WLP could also be due to morpho-physiological differences between the cell lines. It is known that the coupling of SCN neurons is essential for sustained and robust rhythms [11,16,23,49,57]; once dissociated in culture, each SCN neuron oscillates in an independent fashion. The same is true for a population of non-SCN cultured cells: clock gene rhythmic expression of the population damps rapidly [11], and a coupling stimulus, such as glucocorticoid, is required to synchronize the cells, and restore the rhythm. B16–F10 cells exhibit a neuron-like morphology with several cytoplasmic dendrites projecting to neighboring and distant cells, suggesting a putative coupling mechanism; on the contrary, Melan-a cells show short connections only to close cells.

Based on the presence of photopigments in both cell lines and a minor photoresponse by Melan-a cell line as well as the striking dendritic morphology of its malignant counterpart, we hypothesize the following. The poor photoresponse of Melan-a cells may be due to the lack of coupling among the cultured cells; each cell would still possess rhythmic expression of its clock genes, but displaying variable phases, resulting in a null-oscillation of the cell population. Our study, therefore, cannot rule out that white light may still effect individual Melan-a cells, what can only be proven by analyzing single cell rhythm. On the other hand, B16–F10 cells in culture are coupled to each other, due to a more effective physical (dendritic) communication network, thus assuring that all cells oscillate in phase, resulting in a rhythmic clock gene profile displayed by the whole culture. Following this line of reasoning, it has recently been shown that clock gene silencing in human melanocytes increased dendricity what led to increased melanosome transfer to keratinocytes [28]. It is possible that the increased dendricity seen in B16–F10 cells may have resulted from downregulation of the clock exhibited by this cell line as compared to Melan-a cells.

Regardless of which hypothesis will be proven, our data clearly showed that the murine melanoma B16–F10 cells respond differently to WLP when compared to the normal melanocyte cell line Melan-a, suggesting that the carcinogenic process might be responsible for such different physiological responses of B16–F10 cells. It has been recently shown that the light-inducible genes *cry1a* and *per2* oscillate in a circadian manner under LD in health skin tissue of *Danio rerio*, whereas in the fish melanoma the amplitude of the gene oscillation is significantly reduced. In addition to clock genes, the oscillation of key genes related to proper DNA repair was also reduced under LD, and not responsive to WLP in tumoral pigment tissue in comparison to health skin tissue [25]. Interestingly, our data show quite the opposite scenario for mammalian cancer cells; however, in both vertebrate classes, the carcinogenic process affects the clock gene machinery, resulting in a profile not seen in their normal counterparts.

The consequences of clock gene activation in B16–F10 are still unknown but we report here an important finding. Since the clock gene machinery of B16–F10 cells responds to WLP, we speculate that these cells may have acquired this response to external light in order to be free from SCN control. This hypothesis is appreciated since it has been shown that SCN – through a wide and complex network of hormones and neurotransmitters – exerts an important role in controlling key cellular events of peripheral tissues [12,21]. The independence from SCN control over skin cells and the response to external cues would favor cancer growth and progression. In fact, the increased clock gene expression in response to WLP is in line with the fact that B16–F10 cells possess a more sensitive photosensitive system. Therefore, our data opened new perspectives to be further explored in vivo since clock gene machinery activation in cancer cells could favor tumor growth, and if so, could offer interesting pharmacological approaches to treat skin cancer.

As to the light pulse effect on the melanogenesis machinery, the expression of *Tyrosinase* gene was not affected by WLP in Melan-a cells but in B16–F10 cells its expression increased in response to the same stimulus; however, no increase in melanin content was seen in either cell line 24 and 36 h after the WLP.

In the skin, WLP has been shown to elicit immediate pigment darkening (IPD), persistent pigment darkening (PPD), and delayed tanning (DT) [54,73,80]; however, the intensities used in these studies, mostly in human skin, were at least 100-fold higher than the one used in our study. Since melanin quantification was not performed immediately after the WLP we cannot discard that IPD response took place; furthermore, the smaller irradiance we used may have been sufficient to affect clock and *Tyrosinase* genes in B16–F10 cells, but not been enough to activate melanin production downstream.

When the levels of *Tyrosinase* and melanin content are compared between cell lines it becomes clear that melanogenesis is upregulated in B16–F10 cells in comparison to Melan-a cells. It is known that in melanoma melanogenesis is disrupted, what results in increased melanin synthesis [81], due to some direct events like increased *Tyrosinase* expression [39,47,56], disrupted microphthalmia-associated transcription factor (*MITF*) expression [29,86,90] as well as other indirect events that may ultimately deregulate melanin synthesis in melanomas [2,10]. Since WLP increased *Tyrosinase* mRNA levels it would be expected a proportional increase in melanin content but this did not take place in our study. One explanation for this finding may well be that the cascade downstream *Tyrosinase* would be saturated, as the melanogenesis machinery of melanoma cells is upregulated when compared to normal melanocytes, which could prevent further melanin increase despite an increase seen in *Tyrosinase*.

Recently, an elegant study has linked disrupted clock gene machinery expression in human hair follicles and skin with increased melanin content. Knocking down *Bmal1* or *Per1* in melanocytes resulted in upregulation of melanogenesis, and increased melanin content [28]. This was the first study that correlated the local circadian system in melanocytes with the control of melanin synthesis. In fact, our results corroborate the latter findings, as discussed above.

Taken altogether, our data show that both Melan-a and B16–F10 cell lines possess photosensitive system; in the malignant melanocytes this system displays increased sensitivity and enhanced response whereas just a minor effect of white light in Melan-a cells can be seen only when correlation analysis was applied. We also provided evidence of the role of clock genes in regulating melanin synthesis in melanocytes, and that the carcinogenic process affects melanogenesis machinery

probably by decreasing the expression of most clock genes, and increasing *Tyrosinase* expression and melanin content. To the best of our knowledge, this is the first study to show the differential response to WLP regarding *Opn2* and *Opn4* as well as clock gene expression displayed by malignant melanocytes. It is also important to highlight that our findings lead to a better understanding of melanoma carcinogenic process. Our study shows the first evidence linking visible light, opsins, clock genes, and melanoma. This knowledge may be useful for creating new therapy strategies with feasible clinical implications for the treatment of depigmentary disorders as well as be pharmacologically explored in association with traditional therapy in melanoma.

Supplementary data to this article can be found online at http://dx.doi.org/10.1016/j.bbamcr.2016.03.001.

Transparency document

The Transparency document associated with this article can be found in the online version.

Acknowledgments

This work was partially supported by the Sao Paulo Research Foundation (FAPESP, grant 2012/50214-4) and by the National Council of Technological and Scientific Development (CNPq, grant 301293/2011-2). de Assis, L.V.M., Moraes, M.N., and da Silveira Cruz-Machado, S. are fellows of FAPESP (2013/24337-4, 2014/16412-9, 15/04557-5, respectively). We are thankful for the theoretical and methodological insights provided by Prof. Carlos Menck and Mr. Gustavo Satoru as well as for providing the equipment to measure UVA/UVB intensities.

References

[1] A. Balsalobre, F. Damiola, U. Schibler, A serum shock induces circadian gene expression in mammalian tissue culture cells, Cell 93 (6) (1998) 929–937.
[2] B. Bandarchi, C.A. Jabbari, A. Vedadi, R. Navab, Molecular biology of normal melanocytes and melanoma cells, J. Clin. Pathol. 66 (8) (2013) 644–648.
[3] N.W. Bellono, L.G. Kammel, A.L. Zimmerman, E. Oancea, UV light phototransduction activates transient receptor potential A1 ion channels in human melanocytes, Proc. Natl. Acad. Sci. U. S. A. 110 (6) (2013) 2383–2388.
[4] N.W. Bellono, J.A. Najera, E. Oancea, UV light activates a Galphaq/11-coupled phototransduction pathway in human melanocytes, J. Gen. Physiol. 143 (2) (2014) 203–214.
[5] D.C. Bennett, P.J. Cooper, I.R. Hart, A line of non-tumorigenic mouse melanocytes, syngeneic with the B16 melanoma and requiring a tumour promoter for growth, Int. J. Cancer 39 (3) (1987) 414–418.
[6] N.J. Bentley, T. Eisen, C.R. Goding, Melanocyte-specific expression of the human tyrosinase promoter: activation by the microphthalmia gene product and role of the initiator, Mol. Cell. Biol. 14 (12) (1994) 7996–8006.
[7] D.M. Berson, F.A. Dunn, M. Takao, Phototransduction by retinal ganglion cells that set the circadian clock, Science 295 (5557) (2002) 1070–1073.
[8] J.D. Best, E.S. Maywood, K.L. Smith, M.H. Hastings, Rapid resetting of the mammalian circadian clock, J. Neurosci. 19 (2) (1999) 828–835.
[9] G.A. Bjarnason, R.C. Jordan, P.A. Wood, Q. Li, D.W. Lincoln, R.B. Sothern, W.J. Hrushesky, Y. Ben-David, Circadian expression of clock genes in human oral mucosa and skin: association with specific cell-cycle phases, Am. J. Pathol. 158 (5) (2001) 1793–1801.
[10] T. Bogenrieder, M. Herlyn, The molecular pathology of cutaneous melanoma, Cancer Biomark. 9 (1–6) (2010) 267–286.
[11] S.A. Brown, A. Azzi, Peripheral circadian oscillators in mammals, Handb. Exp. Pharmacol. 217 (2013) 45–66.
[12] E.D. Buhr, J.S. Takahashi, Molecular components of the mammalian circadian clock, Handb. Exp. Pharmacol. 217 (2013) 3–27.
[13] L. Calapre, E.S. Gray, M. Ziman, Heat stress: a risk factor for skin carcinogenesis, Cancer Lett. 337 (1) (2013) 35–40.
[14] O. Chiarelli-Neto, A.S. Ferreira, W.K. Martins, C. Pavani, D. Severino, F. Faiao-Flores, S.S. Maria-Engler, E. Aliprandini, G.R. Martinez, P. Di Mascio, M.H. Medeiros, M.S. Baptista, Melanin photosensitization and the effect of visible light on epithelial cells, PLoS One 9 (11) (2014), e113266.
[15] S. Cho, M.H. Shin, Y.K. Kim, J.-E. Seo, Y.M. Lee, C.-H. Park, J.H. Chung, Effects of infrared radiation and heat on human skin aging in vivo, J. Investig. Dermatol. Symp. Proc 14 (1) (2009) 15–19.
[16] J.P. Debruyne, D.R. Weaver, S.M. Reppert, CLOCK and NPAS2 have overlapping roles in the suprachiasmatic circadian clock, Nat. Neurosci. 10 (5) (2007) 543–545.
[17] J.A. Desotelle, M.J. Wilking, N. Ahmad, The circadian control of skin and cutaneous photodamage, Photochem. Photobiol. 88 (5) (2012) 1037–1047.
[18] C. Dibner, U. Schibler, U. Albrecht, The mammalian circadian timing system: organization and coordination of central and peripheral clocks, Annu. Rev. Physiol. 72 (2010) 517–549.
[19] E. Dupont, J. Gomez, D. Bilodeau, Beyond UV radiation: a skin under challenge, Int. J. Cosmet. Sci. 35 (3) (2013) 224–232.
[20] E. Filipski, P. Subramanian, J. Carriere, C. Guettier, H. Barbason, F. Levi, Circadian disruption accelerates liver carcinogenesis in mice, Mutat. Res. 680 (1–2) (2009) 95–105.
[21] L. Fu, C.C. Lee, The circadian clock: pacemaker and tumour suppressor, Nat. Rev. Cancer 3 (5) (2003) 350–361.
[22] S. Gaddameedhi, C.P. Selby, W.K. Kaufmann, R.C. Smart, A. Sancar, Control of skin cancer by the circadian rhythm, Proc. Natl. Acad. Sci. U. S. A. 108 (46) (2011) 18790–18795.
[23] D. Gonze, S. Bernard, C. Waltermann, A. Kramer, H. Herzel, Spontaneous synchronization of coupled circadian oscillators, Biophys. J. 89 (1) (2005) 120–129.
[24] K. Haltaufderhyde, R.N. Ozdeslik, N.L. Wicks, J.A. Najera, E. Oancea, Opsin expression in human epidermal skin, Photochem. Photobiol. 91 (1) (2015) 117–123.
[25] N. Hamilton, N. Diaz-De-Cerio, D. Whitmore, Impaired light detection of the circadian clock in a zebrafish melanoma model, Cell Cycle 14 (8) (2015) 1232–1241.
[26] D. Hanahan, R.A. Weinberg, The hallmarks of cancer, Cell 100 (1) (2000) 57–70 7.
[27] D. Hanahan, R.A. Weinberg, Hallmarks of cancer: the next generation, Cell 144 (5) (2011) 646–674.
[28] J.A. Hardman, D.J. Tobin, I.S. Haslam, N. Farjo, B. Farjo, Y. Al-Nuaimi, B. Grimaldi, R. Paus, The peripheral clock regulates human pigmentation, J. Investig. Dermatol. 135 (4) (2015) 1053–1064.
[29] M. Hartman, M. Czyz, MITF in melanoma: mechanisms behind its expression and activity, Cell. Mol. Life Sci. 72 (7) (2015) 1249–1260.
[30] H. Honigsmann, Erythema and pigmentation, Photodermatol. Photoimmunol. Photomed. 18 (2) (2002) 75–81.
[31] S. Hughes, M.W. Hankins, R.G. Foster, S.N. Peirson, Melanopsin phototransduction: slowly emerging from the dark, Prog. Brain Res. 199 (2012) 19–40.
[32] J. Husse, G. Eichele, H. Oster, Synchronization of the mammalian circadian timing system: light can control peripheral clocks independently of the SCN clock, BioEssays 37 (10) (2015) 1119–1128.
[33] J. Husse, A. Leliavski, A.H. Tsang, H. Oster, G. Eichele, The light–dark cycle controls peripheral rhythmicity in mice with a genetically ablated suprachiasmatic nucleus clock, FASEB J. 28 (11) (2014) 4950–4960.
[34] J. Husse, X. Zhou, A. Shostak, H. Oster, G. Eichele, Synaptotagmin10-Cre, a driver to disrupt clock genes in the SCN, J. Biol. Rhythm. 26 (5) (2011) 379–389.
[35] Y.J. Hwang, H.J. Park, H.J. Hahn, J.Y. Kim, J.H. Ko, Y.W. Lee, Y.B. Choe, K.J. Ahn, Immediate pigment darkening and persistent pigment darkening as means of measuring the ultraviolet A protection factor in vivo: a comparative study, Br. J. Dermatol. 164 (6) (2011) 1356–1361.
[36] M.C. Isoldi, M.D. Rollag, A.M. Castrucci, I. Provencio, Rhabdomeric phototransduction initiated by the vertebrate photopigment melanopsin, Proc. Natl. Acad. Sci. U. S. A. 102 (4) (2005) 1217–1221.
[37] B. Iyengar, The melanocyte photosensory system in the human skin, Springerplus 2 (1) (2013) 158.
[38] M. Izumo, M. Pejchal, A.C. Schook, R.P. Lange, J.A. Walisser, T.R. Sato, X. Wang, C.A. Bradfield, J.S. Takahashi, Differential effects of light and feeding on circadian organization of peripheral clocks in a forebrain Bmal1 mutant, Elife 3 (2014).
[39] K. Jimbow, Y. Miyake, K. Homma, K. Yasuda, Y. Izumi, A. Tsutsumi, S. Ito, Characterization of melanogenesis and morphogenesis of melanosomes by physicochemical properties of melanin and melanosomes in malignant melanoma, Cancer Res. 44 (3) (1984) 1128–1134.
[40] C.H. Jung, E.M. Kim, J.K. Park, S.G. Hwang, S.K. Moon, W.J. Kim, H.D. Um, Bmal1 suppresses cancer cell invasion by blocking the phosphoinositide 3-kinase–Akt–MMP-2 signaling pathway, Oncol. Rep. 29 (6) (2013) 2109–2113.
[41] F.C. Kelleher, A. Rao, A. Maguire, Circadian molecular clocks and cancer, Cancer Lett. 342 (1) (2014) 9–18.
[42] H.-J. Kim, E.D. Son, J.-Y. Jung, H. Choi, T.R. Lee, D.W. Shin, Violet light down-regulates the expression of specific differentiation markers through rhodopsin in normal human epidermal keratinocytes, PLoS One 8 (9) (2013), e73678.
[43] D. Kojima, S. Mori, M. Torii, A. Wada, R. Morishita, Y. Fukada, UV-sensitive photoreceptor protein OPN5 in humans and mice, PLoS One 6 (10) (2011), e26388.
[44] N. Kollias, J.L. Bykowski, Immediate pigment darkening thresholds of human skin to monochromatic (362 nm) ultraviolet A radiation are fluence rate dependent, Photodermatol. Photoimmunol. Photomed. 15 (5) (1999) 175–178.
[45] J.M. Kornhauser, D.E. Nelson, K.E. Mayo, J.S. Takahashi, Photic and circadian regulation of c-fos gene expression in the hamster suprachiasmatic nucleus, Neuron 5 (2) (1990) 127–134.
[46] S.J. Kuhlman, R. Silver, J. Le Sauter, A. Bult-Ito, D.G. Mcmahon, Phase resetting light pulses induce Per1 and persistent spike activity in a subpopulation of biological clock neurons, J. Neurosci. 23 (4) (2003) 1441–1450.
[47] N. Le Fur, W.K. Silvers, S.R. Kelsall, B. Mintz, Up-regulation of specific tyrosinase mRNAs in mouse melanomas with the c2j gene substituted for the wild-type tyrosinase allele: utilization in design of syngeneic immunotherapy models, Proc. Natl. Acad. Sci. U. S. A. 94 (14) (1997) 7561–7565.
[48] Z. Lengyel, C. Lovig, S. Kommedal, R. Keszthelyi, G. Szekeres, Z. Battyani, V. Csernus, A.D. Nagy, Altered expression patterns of clock gene mRNAs and clock proteins in human skin tumors, Tumour Biol. 34 (2) (2013) 811–819.
[49] A.C. Liu, D.K. Welsh, C.H. Ko, H.G. Tran, E.E. Zhang, A.A. Priest, E.D. Buhr, O. Singer, K. Meeker, I.M. Verma, F.J. Doyle III, J.S. Takahashi, S.A. Kay, Intercellular coupling confers robustness against mutations in the SCN circadian clock network, Cell 129 (3) (2007) 605–616.

[50] K.J. Livak, T.D. Schmittgen, Analysis of relative gene expression data using real-time quantitative PCR and the 2(−Delta Delta C(T)) method, Methods 25 (4) (2001) 402–408.
[51] G.J. Lopes, C.C. Gois, L.H. Lima, A.M. Castrucci, Modulation of rhodopsin gene expression and signaling mechanisms evoked by endothelins in goldfish and murine pigment cell lines, Braz. J. Med. Biol. Res. 43 (9) (2010) 828–836.
[52] S. Lopez, S. Alonso, A. Garcia De Galdeano, I. Smith-Zubiaga, Melanocytes from dark and light skin respond differently after ultraviolet B irradiation: effect of keratinocyte-conditioned medium, Photodermatol. Photoimmunol. Photomed. 31 (3) (2015) 149–158.
[54] B.H. Mahmoud, C.L. Hexsel, I.H. Hamzavi, H.W. Lim, Effects of visible light on the skin, Photochem. Photobiol. 84 (2) (2008) 450–462.
[55] N. Matsunaga, K. Itcho, K. Hamamura, E. Ikeda, H. Ikeyama, Y. Furuichi, M. Watanabe, S. Koyanagi, S. Ohdo, 24-hour rhythm of aquaporin-3 function in the epidermis is regulated by molecular clocks, J. Investig. Dermatol. 134 (6) (2014) 1636–1644.
[56] Y. Michaeli, K. Sinik, M. Haus-Cohen, Y. Reiter, Melanoma cells present high levels of HLA-A2-tyrosinase in association with instability and aberrant intracellular processing of tyrosinase, Eur. J. Immunol. 42 (4) (2012) 842–850.
[57] M. Mieda, D. Ono, E. Hasegawa, H. Okamoto, K. Honma, S. Honma, T. Sakurai, Cellular clocks in AVP neurons of the SCN are critical for interneuronal coupling regulating circadian behavior rhythm, Neuron 85 (5) (2015) 1103–1116.
[58] Y. Miyashita, T. Moriya, T. Kubota, K. Yamada, K. Asami, Expression ofmopsin molecule in cultured murine melanocyte, J. Investig. Dermatol. Symp. Proc. 6 (1) (2001) 54–57.
[59] J.A. Mohawk, C.B. Green, J.S. Takahashi, Central and peripheral circadian clocks in mammals, Annu. Rev. Neurosci. 35 (2012) 445–462.
[60] M.N. Moraes, L.H. Lima, B.C. Ramos, M.O. Poletini, A.M. Castrucci, Endothelin modulates the circadian expression of non-visual opsins, Gen. Comp. Endocrinol. 205 (2014) 279–286.
[61] M.N. Moraes, M.O. Poletini, B.C. Ramos, L.H. Lima, A.M.L. Castrucci, Effect of light on expression of clock genes in *Xenopus laevis* melanophores, Photochem. Photobiol. 90 (3) (2014) 696–701.
[62] F. Murisier, S. Guichard, F. Beermann, Distinct distal regulatory elements control tyrosinase expression in melanocytes and the retinal pigment epithelium, Dev. Biol. 303 (2) (2007) 838–847.
[63] S. Panda, I. Provencio, D.C. Tu, S.S. Pires, M.D. Rollag, A.M. Castrucci, M.T. Pletcher, T.K. Sato, T. Wiltshire, M. Andahazy, S.A. Kay, R.N. Van Gelder, J.B. Hogenesch, Melanopsin is required for non-image-forming photic responses in blind mice, Science 301 (5632) (2003) 525–527.
[64] S. Panda, T.K. Sato, A.M. Castrucci, M.D. Rollag, W.J. Degrip, J.B. Hogenesch, I. Provencio, S.A. Kay, Melanopsin (Opn4) requirement for normal light-induced circadian phase shifting, Science 298 (5601) (2002) 2213–2216.
[65] C.L. Partch, C.B. Green, J.S. Takahashi, Molecular architecture of the mammalian circadian clock, Trends Cell Biol. 24 (2) (2014) 90–99.
[66] V.M. Porterfield, H. Piontkivska, E.M. Mintz, Identification of novel light-induced genes in the suprachiasmatic nucleus, BMC Neurosci. 8 (2007) 98.
[67] S. Premi, S. Wallisch, C.M. Mano, A.B. Weiner, A. Bacchiocchi, K. Wakamatsu, E.J. Bechara, R. Halaban, T. Douki, D.E. Brash, Photochemistry. Chemiexcitation of melanin derivatives induces DNA photoproducts long after UV exposure, Science 347 (6224) (2015) 842–847.
[68] I. Provencio, G. Jiang, W.J. De Grip, W.P. Hayes, M.D. Rollag, Melanopsin: an opsin in melanophores, brain, and eye, Proc. Natl. Acad. Sci. U. S. A. 95 (1) (1998) 340–345.
[69] I. Provencio, M.D. Rollag, A.M. Castrucci, Photoreceptive net in the mammalian retina. This mesh of cells may explain how some blind mice can still tell day from night, Nature 415 (6871) (2002) 493.
[70] M. Purschke, H.J. Laubach, R.R. Anderson, D. Manstein, Thermal injury causes DNA damage and lethality in unheated surrounding cells: active thermal bystander effect, J. Investig. Dermatol. 130 (1) (2010) 86–92.
[71] M.R. Ralph, R.G. Foster, F.C. Davis, M. Menaker, Transplanted suprachiasmatic nucleus determines circadian period, Science 247 (4945) (1990) 975–978.
[72] B.C.R. Ramos, M.N.C.M. Moraes, M.O. Poletini, L.H.R.G. Lima, A.M.L. Castrucci, From blue light to clock genes in zebrafish cells, PLoS One 9 (9) (2014), e106252.
[73] M. Randhawa, I. Seo, F. Liebel, M.D. Southall, N. Kollias, E. Ruvolo, Visible light induces melanogenesis in human skin through a photoadaptive response, PLoS One 10 (6) (2015), e0130949.
[74] N.F. Ruby, T.J. Brennan, X. Xie, V. Cao, P. Franken, H.C. Heller, B.F. O'hara, Role of melanopsin in circadian responses to light, Science 298 (5601) (2002) 2211–2213.
[75] C. Sandu, M. Dumas, A. Malan, D. Sambakhe, C. Marteau, C. Nizard, S. Schnebert, E. Perrier, E. Challet, P. Pevet, M.P. Felder-Schmittbuhl, Human skin keratinocytes, melanocytes, and fibroblasts contain distinct circadian clock machineries, Cell. Mol. Life Sci. 69 (19) (2012) 3329–3339.
[76] C. Savvidis, M. Koutsilieris, Circadian rhythm disruption in cancer biology, Mol. Med. 18 (1) (2012) 1249–1260.
[77] Y. Shigeyoshi, K. Taguchi, S. Yamamoto, S. Takekida, L. Yan, H. Tei, T. Moriya, S. Shibata, J.J. Loros, J.C. Dunlap, H. Okamura, Light-induced resetting of a mammalian circadian clock is associated with rapid induction of the mPer1 transcript, Cell 91 (7) (1997) 1043–1053.
[78] H.S. Shim, H. Kim, J. Lee, G.H. Son, S. Cho, T.H. Oh, S.H. Kang, D.S. Seen, K.H. Lee, K. Kim, Rapid activation of CLOCK by Ca^{2+}-dependent protein kinase C mediates resetting of the mammalian circadian clock, EMBO Rep. 8 (4) (2007) 366–371.
[79] G. Sikka, G.P. Hussmann, D. Pandey, S. Cao, D. Hori, J.T. Park, J. Steppan, J.H. Kim, V. Barodka, A.C. Myers, L. Santhanam, D. Nyhan, M.K. Halushka, R.C. Koehler, S.H. Snyder, L.A. Shimoda, D.E. Berkowitz, Melanopsin mediates light-dependent relaxation in blood vessels, Proc. Natl. Acad. Sci. U. S. A. 111 (50) (2014) 17977–17982.
[80] L.R. Sklar, F. Almutawa, H.W. Lim, I. Hamzavi, Effects of ultraviolet radiation, visible light, and infrared radiation on erythema and pigmentation: a review, Photochem. Photobiol. Sci. 12 (1) (2013) 54–64.
[81] A. Slominski, D.J. Tobin, S. Shibahara, J. Wortsman, Melanin pigmentation in mammalian skin and its hormonal regulation, Physiol. Rev. 84 (4) (2004) 1155–1228.
[82] F. Solano, Melanins: skin pigments and much more—types, structural models, biological functions, and formation routes, N. J. Sci. 2014 (2014) 28.
[83] F. Sporl, K. Schellenberg, T. Blatt, H. Wenck, K.P. Wittern, A. Schrader, A. Kramer, A circadian clock in HaCaT keratinocytes, J. Investig. Dermatol. 131 (2) (2011) 338–348.
[84] M. Tanioka, H. Yamada, M. Doi, H. Bando, Y. Yamaguchi, C. Nishigori, H. Okamura, Molecular clocks in mouse skin, J. Investig. Dermatol. 129 (5) (2009) 1225–1231.
[85] M. Tsutsumi, K. Ikeyama, S. Denda, J. Nakanishi, S. Fuziwara, H. Aoki, M. Denda, Expressions of rod and cone photoreceptor-like proteins in human epidermis, Exp. Dermatol. 18 (6) (2009) 567–570.
[86] C. Wellbrock, I. Arozarena, Microphthalmia-associated transcription factor in melanoma development and MAP-kinase pathway targeted therapy, Pigment Cell Melanoma Res. 28 (4) (2015) 390–406.
[87] N.L. Wicks, J.W. Chan, J.A. Najera, J.M. Ciriello, E. Oancea, UVA phototransduction drives early melanin synthesis in human melanocytes, Curr. Biol. 21 (22) (2011) 1906–1911.
[88] S.L. Winter, L. Bosnoyan-Collins, D. Pinnaduwage, I.L. Andrulis, Expression of the circadian clock genes Per1 and Per2 in sporadic and familial breast tumors, Neoplasia 9 (10) (2007) 797–800.
[89] P.A. Wood, X. Yang, W.J. Hrushesky, Clock genes and cancer, Integr. Cancer Ther. 8 (4) (2009) 303–308.
[90] I. Yajima, M.Y. Kumasaka, N.D. Thang, Y. Goto, K. Takeda, M. Iida, N. Ohgami, H. Tamura, O. Yamanoshita, Y. Kawamoto, K. Furukawa, M. Kato, Molecular network associated with MITF in skin melanoma development and progression, J. Skin Cancer 2011 (2011) 730170.
[91] X. Yang, P.A. Wood, C.M. Ansell, D.F. Quiton, E.Y. Oh, J. Du-Quiton, W.J. Hrushesky, The circadian clock gene Per1 suppresses cancer cell proliferation and tumor growth at specific times of day, Chronobiol. Int. 26 (7) (Oct 2009) 1323–1339.
[92] G. Yosipovitch, L. Sackett-Lundeen, A. Goon, C. Yiong Huak, C. Leok Goh, E. Haus, Circadian and ultradian (12 h) variations of skin blood flow and barrier function in non-irritated and irritated skin-effect of topical corticosteroids, J. Investig. Dermatol. 122 (3) (2004) 824–829.
[93] G. Yosipovitch, G.L. Xiong, E. Haus, L. Sackett-Lundeen, I. Ashkenazi, H.I. Maibach, Time-dependent variations of the skin barrier function in humans: transepidermal water loss, stratum corneum hydration, skin surface pH, and skin temperature, J. Investig. Dermatol. 110 (1) (1998) 20–23.
[94] A.R. Young, J.M. Sheehan, UV-induced pigmentation in human skin, in: U.G. Paolo (Ed.) Comprehensive Series in Photosciences, vol. 3, Elsevier 2001, pp. 357–375 (ISBN 1568-461X).
[95] S.B. Zanello, D.M. Jackson, M.F. Holick, Expression of the circadian clock genes clock and period1 in human skin, J. Investig. Dermatol. 115 (4) (2000) 757–760.

Chapter 2: Estradiol differently Affects Melanin Synthesis of Malignant and Normal Melanocytes: A Relationship with Clock and Clock-Controlled genes

The content provided in this chapter has been published in Molecular and Cellular Biochemistry, 2016, 421(1-2):29-39.
DOI: 10.1007/s11010-016-2781-3.

Authors' names: Poletini MO*, de Assis LVM*, Moraes MN, Castrucci AML.
* Joint first authors

Mol Cell Biochem (2016) 421:29–39
DOI 10.1007/s11010-016-2781-3

Estradiol differently affects melanin synthesis of malignant and normal melanocytes: a relationship with clock and clock-controlled genes

Maristela Oliveira Poletini[1] · Leonardo Vinicius Monteiro de Assis[2] · Maria Nathalia Moraes[2] · Ana Maria de Lauro Castrucci[2]

Received: 22 May 2016 / Accepted: 5 August 2016 / Published online: 18 August 2016

Abstract Melanin production within melanocytes is regulated, among others, by estradiol, whose effects on melanogenesis are still not completely elucidated. Here we show that although 10^{-7} M 17β-estradiol (E2) increased tyrosinase mRNA levels in B16-F10 malignant melanocytes, there was a transient decrease and abolishment of the temporal variation of melanin content. Both parameters were much higher in the malignant than in normal Melan-a cells. Considering that silencing clock machinery in human melanocytes increases melanogenesis, we investigated clock gene expression in those cell lines. Except for Melan-a *Bmal1* and B16-F10 *Per2* expression of control cells, *Per1*, *Per2*, and *Bmal1* expression increased independently of cell type or E2 treatment after 24 h. However, melanoma cells showed a marked increase in *Per1* and *Bma11* expression in response to E2 at the same time points, what may rule out E2 as a synchronizer agent since the expression of those genes were not in antiphase. Next, we investigated the expression of *Xpa*, a clock-controlled gene, which in Melan-a cells, peaked at 18 h, and E2 treatment shifted this peak to 24 h, whereas B16-F10 *Xpa* expression peaked at 24 h in both control and E2 group, and it was higher compared to Melan-a cells in both groups. Therefore, malignant and normal melanocytes display profound differences on core elements of the local clock, and how they respond to E2, what is most probably determinant of the differences seen on melanin synthesis and *Tyrosinase* and *Xpa* expression. Understanding these processes at the molecular level could bring new strategies to treat melanoma.

Keywords Murine Melan-a cells · Murine B16-F10 cells · Estradiol · Melanogenesis · Clock genes · *Xpa*

Introduction

The skin is the first line barrier against several potential threatening chemical compounds and biological organisms; in addition, this organ is constantly subject to variation of environmental temperature, humidity and light [1]. Among these factors, visible light and UVA radiation induce melanin production that takes place in lysosome-like structures known as melanosomes [2–4]. Two major pigments are produced in mammalian melanocytes: pheomelanin and eumelanin, both deriving from a common pathway in which tyrosine is the common precursor [5]. Tyrosinase, the key regulatory enzyme of melanogenesis, is responsible for three distinct reactions within melanosomes [6], which may be transferred to neighboring keratinocytes, where they shield the nuclei from the damaging effects of UV radiation [5, 7]. This protective function of melanin is due to its ability to absorb UV photons and buffer UV- and visible light-induced free radicals before they interact with cellular constituents [4, 8, 9]. However, it has been recently shown that UV radiation is able to degrade melanin into smaller fragments, which migrate to the nucleus and, hours after the

Maristela Oliveira Poletini and Leonardo Vinicius Monteiro de Assis contributed equally to this work.

✉ Ana Maria de Lauro Castrucci
amdlcast@ib.usp.br

[1] Department of Physiology and Biophysics, Institute of Biological Sciences, Federal University of Minas Gerais, Belo Horizonte, Minas Gerais, Brazil

[2] Department of Physiology, Institute of Biosciences, University of São Paulo, R. do Matão, Trav. 14, No. 101, São Paulo 05508-900, Brazil

original UV exposure, excited products transfer their energy to DNA, creating mutagenic dimers in the absence of UV radiation [10]. Despite the dual role of melanin, it is well established that DNA damage caused by UV radiation is an important factor that triggers melanin production [4, 9, 11, 12].

Estradiol (E2) affects several aspects of skin function. For example, it stimulates the synthesis, maturation, and turnover of collagen in rats [13] and guinea pigs [14], as well as it increases the synthesis of hyaluronic acid in mice [15]. Estrogens also increase mitotic activity in mouse epidermis [16], and promote enlargement and dendritic formation of human melanocytes in culture [17]. Regarding E2 effect on melanogenesis and pigmentation, the conclusions are controversial since some reports have shown a stimulatory while others an inhibitory hormone action on tyrosinase activity and melanin content [18, 19]. Estrogens seem also to be important factors in epidermal carcinogenesis since they enhance the development of chemical carcinogen-induced squamous cell carcinomas in mice and basal cell carcinomas in rats [20].

It is now well accepted that the molecular basis of the endogenous biological clock is not only expressed in the central clock located in the suprachiasmatic nuclei of the hypothalamus but also widely in the whole body. The core machinery of the biological clock is represented by loops of transcription and translation of clock proteins. In the positive loop CLOCK (Circadian Locomotor Output Cycles Kaput) and BMAL1 (brain and muscle Arnt-like protein 1) heterodimer stimulates the transcription of genes that contain E-box sequence, known as clock-controlled genes (CCGs), and clock genes such as *Pers* (*Period)* and *Crys* (*Cryptochrome*). It is known that *Per* and *Cry* represent the negative loop, which after being translated are targeted to the nucleus where their oligomer inhibits the transcriptional activity of CLOCK/BMAL1 [21–23]. An accessory arm regulates the transcription of *Bmal1*: *Rev-erb-α* inhibits while *Ror* activates *Bmal1* expression. The oscillation of gene and protein levels throughout the day is the molecular basis of the biological clock that allows keeping track of time.

The skin has multi-oscillatory systems that are ultimately responsible for driving its rhythms [1], and the adaptation and fine-tuning of its functions according to the conditions posed by the environment. In fact, it is well established that proliferation rates, transepidermal hydration and water loss (TEWL), temperature, capillary flow, and sebum production [24] oscillate during the day in human and murine skin. Recently aquaporin-3, responsible for regulating water content and TEWL, and *Xeroderma pigmentosum, complementing group A* (*Xpa*), responsible for carrying out DNA repair, have been reported to be clock-controlled genes [25, 26]. Interestingly, melanin synthesis has also been shown to be a clock-regulated event [27].

Circadian clock disruption has been associated with many diseases, including metabolic syndrome, diabetes, and cancer [28–30]. In human melanoma, it has been shown that the clock gene machinery is downregulated in comparison to nontumor skin tissue [31]. Corroborating this finding, our group has recently shown that murine melanoma cells also display a downregulation of clock genes in comparison to normal melanocytes [32]. These data show, therefore, that clock gene downregulation in melanoma may represent an important step in the onset and development of melanoma.

The understanding of skin clock gene modulation by temperature, hormones, UV radiation, and visible light has been deepened by some studies [1, 32–35]. However, as most of the studies have focused on keratinocytes and fibroblasts, most questions concerning melanocytes still remain unanswered, among them: which factors regulate the melanocyte peripheral clock, which processes are clock gene-dependent, how the carcinogenic process affects clock gene expression.

E2 modulates the expression of *Per1* and *Per2* gene in rat [36] and mouse [37] uterus, liver, and kidney [38]. This hormone, therefore, may directly regulate clock gene expression in peripheral tissues. Despite the increasing knowledge of E2 effects on skin, E2 role in the regulation of clock gene machinery in melanocytes has still to be established.

Based on the above, we sought to comparatively evaluate melanin synthesis and the expression of clock genes and DNA repair gene *Xpa* in normal Melan-a and malignant B16-F10 murine melanocytes in response to E2.

Materials and methods

Cell culture

Melan-a or B16-F10 cells were kept in phenol red-free RPMI 1640 (Atena, Campinas, Brazil) supplemented with 14.3 mM $NaHCO_3$, 15 mM HEPES, 10 % fetal bovine serum (FBS, Atena, Campinas, Brazil), and 1 % antibiotic/antimycotic solution (10,000 U/mL penicillin, 10,000 µg/L streptomycin and 25 µg/mL amphotericin B, Life Technologies, Carlsbad, CA, USA), pH 7.2, at 37°C and 5 % CO_2 water-saturated atmosphere. Phorbol 12-myristate 13-acetate (Sigma, St. Louis, MO, USA) at 200 nM was added to Melan-a cell medium, as it is required for proper cell growth [39]. All cell manipulations (medium changes, melanin and RNA extraction) were done under dim red light (7 W Konex bulb and Safe-Light filter GBX-2, Kodak, Rochester, NY, USA).

Experimental design

Melan-a or B16-F10 cells were plated (10^6 and 10^5 cells in 25 cm^2 flask, respectively), kept in constant darkness (DD) at 37 °C for 2 days in a reduced serum concentration (2 %). At the beginning of the 3rd day, the cells were subject to a medium change with 10^{-7} M water-soluble 17β-estradiol (Sigma-Aldrich, St. Louis, MO, USA)-containing medium (E2 group) or only fresh medium (control group). After 2 h, both groups were subject to a second medium change with E2-free medium. Throughout the experiments and in all medium changes phenol red-free RPMI 1640 was supplemented with 2 % FBS. Phorbol 12-myristate 13-acetate at 200 nM was always present in Melan-a cell medium.

For melanin content, cells were harvested immediately, 24, 28, and 32 h after the second medium change. For RNA extraction, cells were harvested immediately after the second medium change, and every 6 h during the next 24 h.

Melanin synthesis

Melan-a or B16-F10 cells were harvested with Tyrode/EDTA solution, and after cell counting, cell suspension was centrifuged at $100\times g$ for 5 min at room temperature, the supernatant was discarded, and 1 M NaOH in 10 % DMSO was added to the cell pellet. The lysate was heated at 80 °C for 2 h and centrifuged at $1050\times g$ for 15 min at room temperature. 200 µL of each sample supernatant was added in duplicates to wells of a flat-bottom plate. Melanin was quantified by absolute absorbance at 475 nm in a plate reader (SpectraMax 250, Molecular Devices, Sunnyvale, CA, USA), and the values interpolated in a standard curve of synthetic melanin (Sigma-Aldrich, St. Louis, MO, USA) ranging from 3.125 to 200 µg/mL. Melanin concentrations were expressed as µg of melanin per 10^6 cells, and compared by Two-way ANOVA, followed by Bonferroni post-test.

Total RNA extraction and reverse transcriptase-polymerase chain reaction (RT-PCR)

Total RNA was extracted with Trizol reagent (Life Technologies, Carlsbad, CA, USA), the RNA pellet was resuspended in DEPC water (Life Technologies, Carlsbad, CA, USA), and treated with DNAse I (turbo-DNA-Free™, Life Technologies, Carlsbad, CA, USA), according to the manufacturer's instructions. RNA concentration (OD260) was determined in a spectrophotometer (Nanodrop, Willmington, DE, USA), and 1–2 µg was reverse transcribed (SuperScript III Reverse Transcriptase, Life Technologies, Carlsbad, CA, USA) with random primers (Life Technologies, Carlsbad, CA, USA), according to the manufacturer's recommended protocol. The reactions were placed in a thermocycler (Ependorff, Hauppauge, NY, USA) set at 65 °C for 5 min, chilling on ice for 1 min, followed by 5 min at 25 °C, 50 min at 50 °C, and 15 min at 70 °C.

Quantitative PCR (qPCR)

qPCR was performed in 96-well plates using a pair of primers spanning introns and a probe specific for the sequences obtained from GenBank (http://www.ncbi.nlm.nih.gov/genbank), designed and synthesized by IDT (Coralville, IA, USA). For simultaneous analysis of *Per1*, *Per2,* and *Bmal1* (*Taqman*®), the solutions contained 300 nM primers, 200 nM probes (Table 1), Supermix 2X (Bio-Rad Laboratories, Hercules, CA, USA, or Life Technologies, Carlsbad, CA, USA), supplemented to final concentrations of 400 µM dNTPs, 6 mM $MgCl_2$, and 0.1 U/µL Platinum Taq DNA polymerase (Life Technologies, São Paulo, SP, Brazil). The solutions already with cDNA were then distributed in triplicate wells for each experimental sample. The reactions were carried out in iCycler or i5 thermal cycler (Bio-Rad Laboratories, Hercules, CA, USA): 1 cycle at 95 °C for 7 min followed by 45 cycles of 30 s at 95 °C and 30 s at 55 °C.

The analysis of *Tyrosinase*, *XPA*, and ribosomal 18S RNA was carried out using SYBR® GreenER 2X mix (KAPA SYBR® FAST, Wilmington, MA, USA), and primers (300 nM for *Tyrosinase* and *XPA,* and 50 nM for 18S RNA, Table 1). The solutions with cDNA were then distributed in duplicate wells for each experimental sample. The reactions were carried out in iCycler (Bio-Rad Laboratories, Hercules, CA, USA): 10 min at 95 °C, followed by 45 cycles of 15 s at 95 °C, 1 min at 60 °C, and 80 cycles of 10 s at 55 °C with gradual increase of 0.5 °C. Ribosomal 18S RNA, which did not vary along time under our experimental conditions (data not shown), was chosen as a reference gene for all gene expression reactions in both TaqMan® and SYBR® GreenER™ methodologies.

Data analysis

qPCR data were analyzed by the $\Delta\Delta c_T$ method [40]. A line, the so-called threshold, was passed through the geometric portions of the amplification curves. The number of cycles where the threshold line crosses the curves is called C_T; the ΔC_T was obtained as the difference between the C_Ts for 18S RNA and the C_T for a gene of interest (corresponding to the average of triplicate or duplicate wells from the same cDNA), at each time studied. The lowest mRNA average obtained from the control cells was set as a calibrator and subtracted from each ΔCT value, thus obtaining the ΔΔCT.

Table 1 Sequences and concentrations of primers and probes, and gene access numbers

Template (access number)	Primers and probes	Final concentration
mPer1	Forward: 5′-AGCAGGTTCAGGCTAACCAGGAAT-3′	300 nM
(NM_0011065.3)	Reverse: 5′-AGGTGTCCTGGTTTCGAAGTGTGT-3′	300 nM
	Probe: 5′-/6FAM/-AGCCTTGTGCCATGGACATGTCTACT/3BHQ_1/-3′	200 nM
mPer2	Forward: 5′-TTCCTACAGCATGGAGCAGGTTGAT-3′	300 nM
(NM_011066)	Reverse: 5′-ATGAGGAGCCAGGAACTCCACAAA-3′	300 nM
	Probe: 5′-/Cy5/-AACGCGGATATGTTTGCTGTGGCTGT/3BHQ_2/-3′	200 nM
mBmal1	Forward: 5′-AGCTTCTGCACAATCCACAGCAC-3′	300 nM
(NM_001243048)	Reverse: 5′-TGTCTGGCTCATTGTCTTCGTCCA-3′	300 nM
	Probe: 5′-/5HEX/-AAAGCTGGCCACCCACGAAGATGGG/3BHQ_1/-3′	200 nM
mXpa	Forward: 5′- GCGATATGAAGCTCTACCTAAA-3′	300 nM
(NM_011728.2)	Reverse: 5′-TTCCTGCCTCACTTCCTTTG-3′	300 nM
mTyrosinase	Forward: 5′-TCCTCCTGGCAGATCATTTGT-3′	300 nM
(NM_011661.4)	Reverse: 5′-TGGTCCCTCAGGTGTTCCA-3′	300 nM
18S RNA	Forward: 5′-CGGCTACCACATCCAAGGAA-3′	50 nM
	Backward: 5′-GCTGGAATTACCGCG GCT-3′	50 nM

This value was used as the negative exponential of base 2 ($2^{-\Delta\Delta CT}$).

To analyze the temporal gene expression of each group, and in each cell line, as well as the comparison between control and E2 groups, the log values of gene expression or the melanin content were averaged ($n = 3$–6 flasks from at least two independent experiments) and plotted as mean ± SEM relative to the lowest value of control group in Melan-a cells. The significance levels of possible differences among time points of the same group or between control and E2-treated cells at the same time point were determined by Two-way ANOVA followed by Bonferroni post-test ($p \leq 0.05$). In cases that the data were very dissimilar but still ANOVA did not indicate a significant difference, Student's *t* test was used as noted in the Figures' legends. Transcript levels or melanin content in Melan-a and B16-F10 cells were also expressed as the temporal mean of all time values along 32 h, and compared by Student's *t* test. All analyses were performed in GraphPad Prism Version 6.0 (La Jolla, CA, USA).

Results

Melanin content did not vary along the time in the control group in Melan-a cells; estradiol had no effect along the time or in comparison with the respective controls (Fig. 1a). On the other hand, in the malignant B16-F10 melanocytes, melanin content temporally varied in the control group with increased levels at 24, 28, and 32 h as compared with 0 h, whereas E2 reduced melanin content 24 and 32 h after the treatment (Fig. 1b), demonstrating a transient inhibitory effect of estradiol on melanogenesis. When melanin content of normal cells was compared to malignant melanocytes, we found that B16-F10 cells possess 25-fold higher level of melanin in comparison to Melan-a cells. This difference is decreased to about 15-fold after E2 treatment (Fig. 1c).

Interestingly, *Tyrosinase* expression was not different between control and E2 groups, along time or at the same time point, in Melan-a cells (Fig. 1d). In B16-F10 cells, E2 induced a temporal variation with a peak of transcription 24 h after the hormone pulse (Fig. 1e). *Tyrosinase* transcripts were higher in the hormone-treated group as compared to the control cells at 12 h. According to what was found for melanin, *Tyrosinase* expression was much higher in both control (40-fold) and E2-treated (55-fold) group of B16-F10 cells in comparison to Melan-a cells (Fig. 1f).

Since we have found temporal changes of melanin levels in malignant melanocytes, we sought to further investigate whether this response had a clock gene-based mechanism. *Per1* (Fig. 2a, b) and *Per2* (Fig. 2c, d) transcripts exhibited a temporal variation in Melan-a and B16-F10 cells in both control and E2-group. E2 had no effect on *Per1* or *Per2* transcripts in both cell types, except of *Per1* mRNA in B16-F10 cells, in which the hormone increased mRNA levels 6, 12, and 18 h after the treatment in comparison to the respective controls (Fig. 2b).

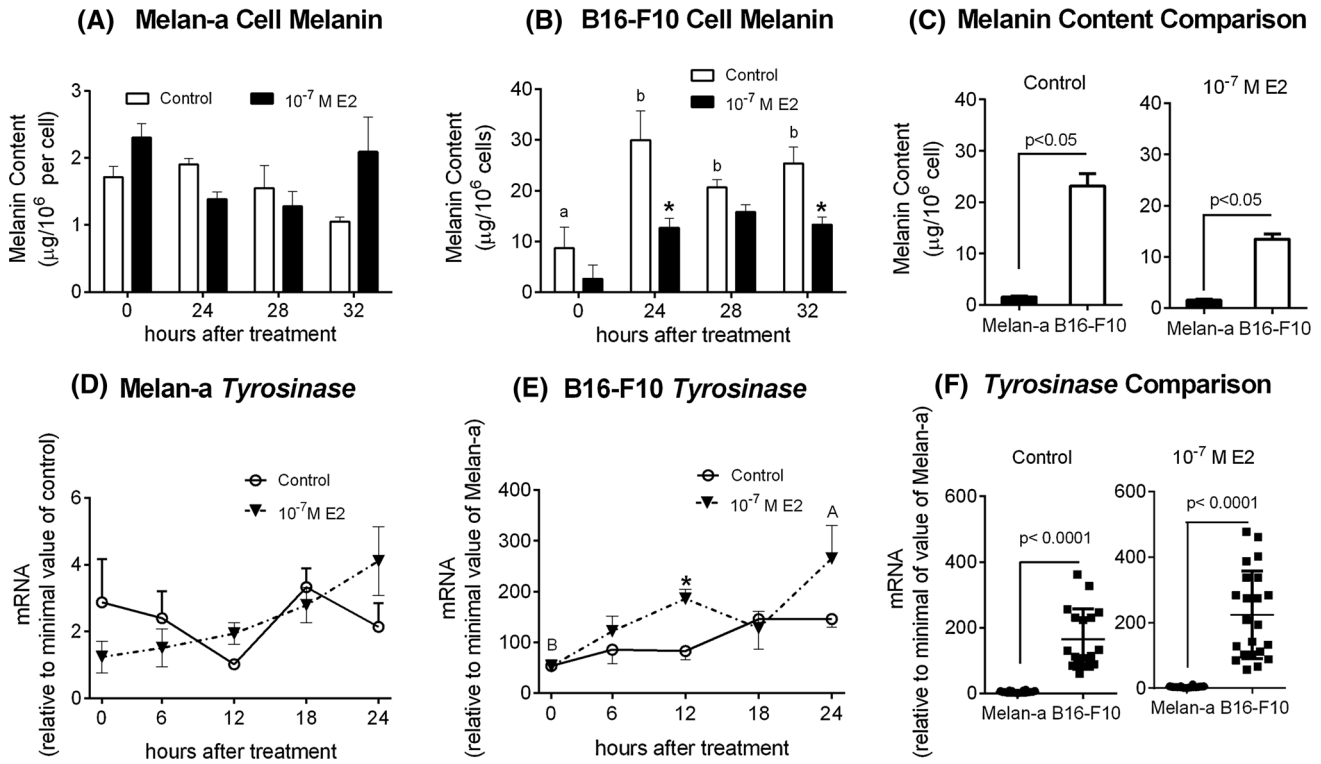

Fig. 1 Melanogenesis in Melan-a and B16-F10 cells. Melanin content in **a** Melan-a (**b**) B16-F10 cells immediately (0 h), 24, 28, and 32 h after estradiol (E2) treatment; **c** Comparison between Melan-a and B16-F10 cells regarding melanin content, presented as the temporal mean ($n = 12$ and 12) of all time values along 32 h in control and E2-treated groups; **d** Tyrosinase mRNA content in Melan-a cells; **e** Tyrosinase mRNA content in B16-F10 cells; **f** Comparison between Melan-a and B16-F10 cells regarding *Tyrosinase* gene expression, presented as the temporal mean ($n = 18$–20) of all time values along 24 h in control and E2-treated groups. In this and in the following Figures, values are expressed as mean ± SEM ($n = 3$–4) except otherwise noted; small letters mean significantly different control values among time points; capital letters mean significantly different E2-group values among time points; asterisk means significantly different values between control and E2-treated cells at the same time point by Student's *t* test (**b**) and (**e**), $p = 0.0078$ and 0.0076, respectively

The oscillatory profile of *Per* genes was not followed by the expected antiphase profile of *Bmal1* expression in Melan-a (Fig. 2e) or B16-F10 (Fig. 2f) cells. E2 did not modify *Bmal1* expression in normal melanocytes (Fig. 2e) but increased *Bmal1* expression 6 and 12 h after treatment in B16-F10 malignant cells (Fig. 2f), what kept *Bmal1* in phase with *Per1* after hormone treatment.

The comparison of clock gene transcripts between malignant and normal cells revealed that *Per1* expression in both control (Fig. 3a) and E2-treated (Fig. 3b) groups, and *Bmal1* in control group (Fig. 3e) did not differ among cell types. However, the expression of *Per2* in control (Fig. 3c) and hormone-treated (Fig. 3d) cells was significantly downregulated whereas *Bmal1* in the hormone-treated group (Fig. 3f) was upregulated in the malignant cell line as compared to Melan-a cells.

Next, we investigated the expression of *Xpa*, a clock-controlled gene, with a prominent role in regulating time-dependent DNA repair [25]. In normal melanocytes, we have found a time-dependent oscillation in the control group with a peak at 18 h in comparison to 12 h (Fig. 4a). After E2 treatment, the expression peak was shifted from 18 to 24 h (Fig. 4a). Differently from normal melanocytes, *Xpa* temporal oscillation in both control and E2 groups of malignant melanocytes peaked at 24 h as compared to 0 h (Fig. 4b). B16-F10 cells showed increased expression of the DNA-repair enzyme in both control and E2-treated groups as compared to Melan-a cells (Fig. 4c).

Discussion

Initially, our group sought to investigate the effect of E2 in melanin synthesis since it was still not fully known how E2 affects melanogenesis in normal and malignant melanocytes, respectively, Melan-a and B16-F10 cells. Our data show that melanin synthesis in normal melanocytes is not affected by E2 treatment; however, in malignant ones melanin synthesis is transiently reduced by E2 treatment. Intriguingly, these results were followed by opposite changes on *Tyrosinase* mRNA levels in malignant melanocytes, in which *Tyrosinase* temporal expression

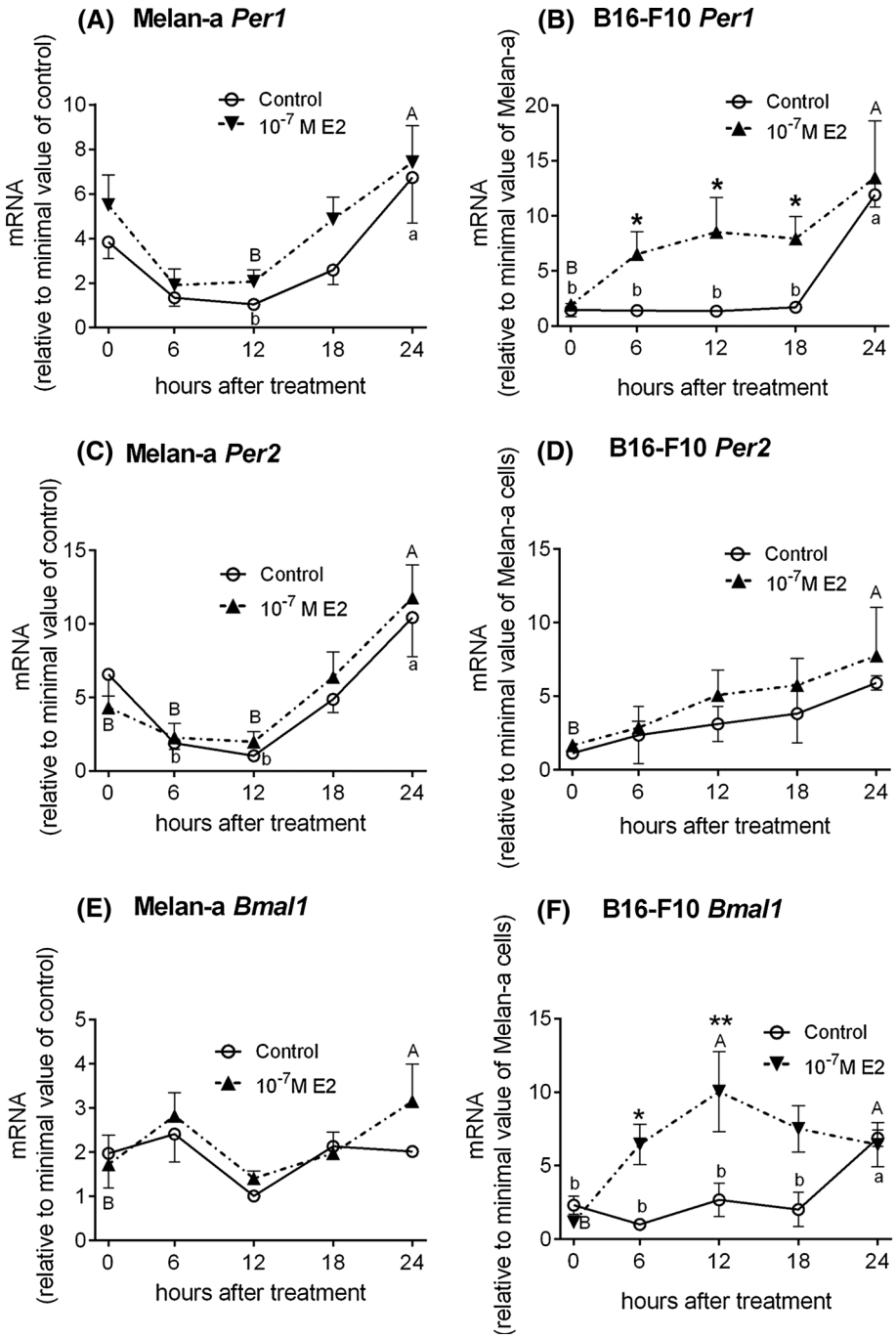

Fig. 2 Temporal expression of clock genes in Melan-a and B16-F10 cells. *Per1* transcripts in **a** Melan-a and **b** B16-F10 cells; *Per2* transcripts in **c** Melan-a and **d** B16-F10 cells; *Bmal1* transcripts in **e** Melan-a and **f** B16-F10 cells. B time point 6 ($p = 0.0107$), 12 ($p = 0.0398$), and 18 ($p = 0.0281$) by Student's t test

increased 24 h after E2 treatment compared to 0 h. One explanation for this may lie on differences shown for the activity and post-translational regulation, and mRNA levels of tyrosinase [7, 41, 42]. Despite similar mRNA expression levels found in melanocytes in dark and light skin [41–43], activity and protein levels of tyrosinase are more pronounced in dark skin melanocytes [41, 44, 45]. It is interesting to mention that the levels of heat shock 70 kDa protein directly correlate with the levels of skin tyrosinase protein [46], what should be further investigated in normal and malignant melanocytes. Following this line, both *Tyrosinase* expression and melanin content were much higher in malignant than in normal melanocytes; moreover, E2 treatment increased *Tyrosinase* gene expression in B16-F10 cells, whereas it had no effect on normal melanocyte. These results highly suggest that the carcinogenic process has impacted signaling pathways within malignant melanocytes leading to different responses to proliferative agents, and gene expression may function very different from normal melanocytes.

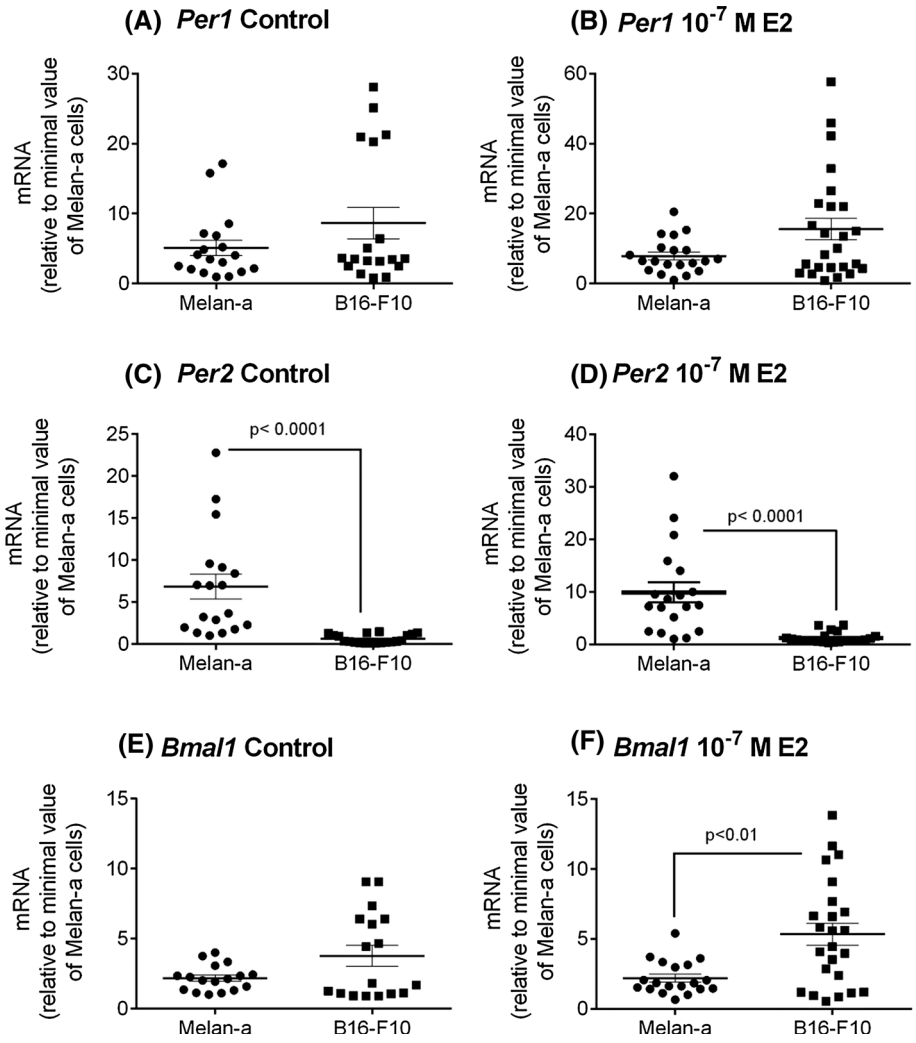

Fig. 3 Comparison between clock gene expression in Melan-a and B16-F10 cells. Data are presented as the temporal mean ($n = 17$–25) of all time values along 24 h in control and E2-treated groups. *Per1* in **a** control group and **b** E2-group; *Per2* in **c** control group and **d** E2-group; *Bmal1* in **e** control group and **f** E2-group

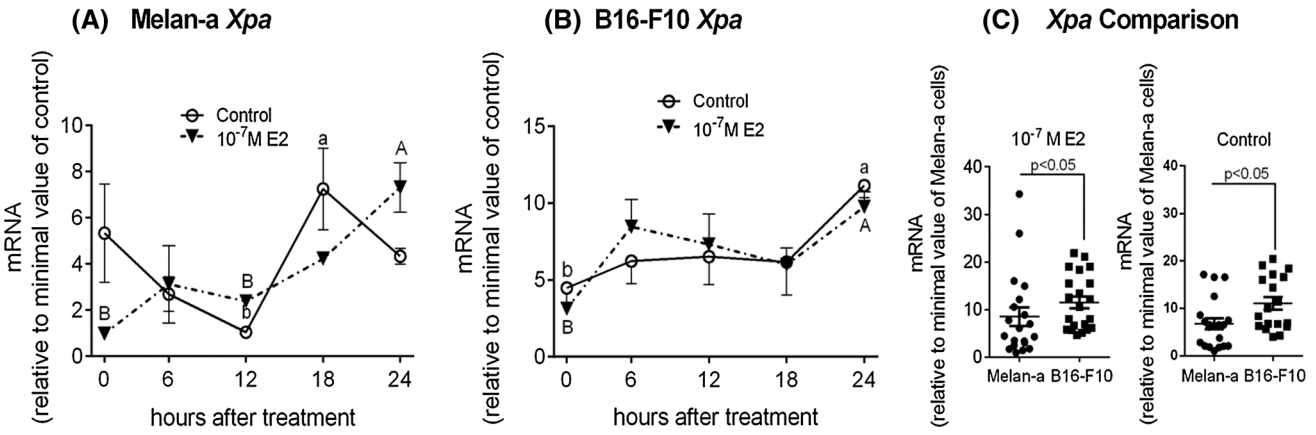

Fig. 4 Temporal expression of *Xpa* gene. **a** Melan-a and **b** B16-F10 cells. **c** Comparison between Melan-a and B16-F10 cells regarding *Xpa* gene expression, presented as the temporal mean ($n = 18$–21) of all time values along 24 h in control and E2-treated groups

It is known that disruption of the clock gene machinery favors tumor growth in many cancers, including melanona [29–31, 47, 48]. Here we observed a time-dependent effect of E2 on melanin synthesis in malignant melanocytes. Based on that, we, therefore, investigated whether this response had a clock component regulation. We analyzed the profile of clock gene expression in response to E2 treatment in both normal and malignant melanocytes.

Except for Melan-a *Bmal1* and B16-F10 *Per2* expression of non-E2 treated cells, *Per1*, *Per2*, and *Bmal1* expression increased independently of cell type or hormone treatment 24 h after handling (medium changes only or E2 treatment). Comparing these data to our previous study in which both Melan-a and B16-F10 cells displayed no temporal variation on clock gene expression in constant conditions and without medium change [32], these results might be attributed to the entrainment induced by medium change—what has been described for other types of cells in culture [49–51].

This effect, however, was still not strong enough to synchronize the clock molecular machinery since, within the frame of analyzed times here, no antiphase relationship between *Pers* and *Bmal1* was seen. This antiphase in clock gene expression profile would be expected in entrained cells in culture since the relationship among *Pers* and *Bmal1* is inhibitory and necessary for the ongoing function of the clock molecular core [52]. Despite of this, melanoma cells showed a marked increase in *Per1* and *Bma1* (but not *Per2*) expression in response to E2, what may be the consequence of an E2 direct effect on *Per1* and *Bmal1* transcript levels without affecting the loop of transcription/translation regulation of clock genes. This hypothesis is reinforced by the fact that the estrogen response element (ERE) has been reported in the *Per* promoter of other cell types [53]; however, it is intriguing that only *Per1* showed a response profile to E2 treatment. Alternatively, this might represent a non-traditional activation of clock genes, shown to be present in malignant melanocytes in response to white light pulse possibly as a consequence of the carcinogenic process [32].

Taken together, our data show that malignant melanocytes are more responsive to E2 treatment when compared to normal ones. The higher E2-sensitivity of malignant cells may be related to E2 proliferative effects on melanoma cells. Interestingly, melanoma has been suggested to be an estrogen-dependent tumor; however, clinical studies have shown no benefits in patients treated with tamoxifen [54–59]. E2 promotes cell proliferation, malignant transformation, and the development of drug resistance. These E2 actions are mediated in a variety of cancer cells by both the classical estradiol receptor alpha (ER-α) via AP1-ligand [60], and consequently activation of transcription of proliferative genes, as well as by MAPK pathway [61–65]. It is known that in mouse melanocytes both pathways interact at the level of CREB phosphorylation which, in turn, promotes melanoma growth and metastasis [66–68]. Together, this may converge with our data on E2-induced *Per1* upregulation, since *Per1* promoter bears responsive elements to CREB, which mediates the induction of *Per1* expression [69].

In 2015, an elegant study showed for the first time that silencing clock molecular core in human melanocytes led to an upregulation of melanogenesis machinery with consequent increase of melanin content [27]. Here we showed no alteration in melanin content in normal melanocytes after E2 treatment or after medium change. We believe that this lack of response is due to no alteration in clock gene expression; on the other hand, in malignant melanocytes, E2 treatment causes an increase in clock gene expression and reduced melanin content. We speculate that the melanin decrease in response to E2 may be due to the upregulation of clock gene transcripts in response to the hormone. It is then interesting to note the inverse relationship between melanin content and clock gene expression levels. It is also important to highlight that this response seems to be hormone specific since an increase in clock gene expression was found in response to white light pulse without any alteration in melanin content [32]. Therefore, our data further support the importance of clock gene expression in regulating melanin synthesis. We provide further evidence that melanocyte pigmentary responses to hormones and light are influenced by clock genes. Based on this, we believe that the modulation of clock genes by hormone and/or light may represent an important advance in our current understanding of the pigmentary process, which may lead to improvements in treatment of depigmentary disorders.

Importantly, we have found profound differences on clock and *Tyrosinase* gene expression between normal and malignant melanocytes not only in terms of responses to E2 treatment but also in terms of magnitude of gene expression. As shown in our previous study [32], *Bmal1* expression was found to be downregulated in B16-F10 cells. Here, however, no difference in this gene expression was found; in addition, in E2-treated group B16-F10 cells showed increased *Bmal1* expression when compared to Melan-a cells. The answer for this apparent contradiction lies on the fact that in the present study medium change was carried out in the control group of the malignant cells, which led to a temporal stimulation of *Bmal1* in this group as well as increased gene expression in the E2-treated group. Thus, the increased sensitivity of B16-F10 cells to E2 is the reason of the increased gene expression in this cell line when compared to normal ones.

These differences might explain the deregulation on melanogenesis in these cells. It is interesting to note that the *Tyrosinase* gene promoter has several regulatory elements, including E-boxes, ultraviolet responsive element (URE), and glucocorticoid responsive element (GRE) sequences [7], which render *Tyrosinase* a clock-controlled gene, CCG. Recently, the pigmentation process in hair follicle has also been shown to be clock-controlled, since silencing *Per1* or *Bmal1* led to increased tyrosinase activity with subsequent increase of melanin content [27]. Therefore, our results are in line with the data from Hardman et al. [27], further supporting the fact that the peripheral

clock is key to the well-organized melanin synthesis in normal melanocytes. Nevertheless, the data shown here associated with our recent study [32] are the first to identify, to the best of our knowledge, the association of disrupted clock gene machinery caused by the carcinogenic process with increased melanin synthesis.

Since B16-F10 is an aggressive melanoma cell line, impairment of the clock machinery may have happened, favoring cancer development. Taking the literature into consideration, this hypothesis is appreciated since it has been shown that disruption of clock machinery favors tumor growth in many cancer types, including melanoma [29–31, 47, 48]. The consequences of these changes on B16-F10 cell metabolism, however, are still largely unknown, but it is plausible to speculate that these alterations in clock gene machinery are associated with the malignant transformation process along with other hallmarks of cancer [70, 71]. Then, interested in evaluating the possible consequences of clock gene disruption in other cellular function, we evaluated the response of *Xpa* expression to E2 treatment.

The excision repair is a multicomponent system that is able to remove nearly all DNA base lesions, being the only system in mice and humans that repair bulky lesions such as cyclobutane pyrimidine dimers, 6–4 photoproducts, and other cisplatin-induced DNA damages [72, 73]. XPA—a member of the xeroderma pigmentosum (XP) family protein—has been shown to oscillate in brain, liver, and skin [25, 74, 75]. XPA expression is in antiphase with CRY1, being higher in the evening than in the morning; its increased expression coincides with the onset of the mouse activity. Remarkably, mice exposed to UV radiation in the morning displayed increased number of skin tumors than those exposed in the afternoon [25]. Therefore, *Xpa* is a CCG that plays an important role in protecting the skin against the detrimental effects of UV. Our data point to the same direction of the latter studies. In Melan-a cells, *Xpa* expression oscillates after medium change with a peak at 18 h, being phase-delayed in the E2-treated group. The role of E2 in influencing *Xpa* expression, or to whether this would interfere in DNA repair in Melan-a cells is still unknown. It is remarkable that E2-elicited response is completely lost in B16-F10 cells, what may be a result of clock machinery disruption. The unresponsive profile of *Xpa* in B16-F10 cells supports our data that the malignant process not only disrupts clock gene machinery, melanin synthesis but also a key gene responsible DNA repair.

Another perspective originated from this study is that B16-F10 cells can be viewed as a model of peripheral oscillator. This statement also arises from our previous study [32], which has shown that these cells express a photosensitive system that perceives white light. In addition to photoreception, B16-F10 cells have the clock core machinery, which is activated by white light or E2. As a consequence of clock gene activation, some outputs are modulated such as *Tyrosinase* and *Xpa* genes, and melanin content. Taken altogether, we suggest that B16-F10 cells can be viewed as a model of disrupted peripheral oscillator, independent of the SCN. We believe that the increased response displayed by B16-F10 cells is due to the fact that these cells are insensitive to SCN-temporal controlling signal, which could ultimately drive cancer development. Based on this, we hypothesize that B16-F10 cells use other cues like white light and hormones to drive its growth. Nevertheless this hypothesis needs in vivo methodological approaches to be proven.

In conclusion, our data show that the carcinogenic process interferes with key regulatory mechanisms present in the melanocyte through clock gene disruption, which could be classified as a new hallmark of cancer [70, 71]. In fact, it has been long known that cancer disrupts several processes within the cell, what favors resistance to apoptosis, angiogenesis, immortality, genome instability and mutation, tumor promoting inflammation, and immune system avoidance [70, 71]. Our study along with many others in the literature [28–32, 76–78] strongly indicates that loss of proper clock machinery functioning with subsequent loss of cellular temporal functions plays an important role in cancer. In fact, we hypothesize that most, if not all, hallmarks of cancer have at their core some component of chronodisruption. Interestingly, in our study, we show that a proliferative agent—E2—has an effect in clock gene expression of malignant melanocytes, which further reinforces the role of estrogens and clock gene in melanoma. Understanding these processes at the molecular level could bring new strategies to treat melanoma.

Acknowledgments This work was partially supported by the Sao Paulo Research Foundation (FAPESP, Grant 2012/50214-4) and by the National Council of Technological and Scientific Development (CNPq, Grant 301293/2011-2 and 303070/2015-3). LVM de Assis and MN Moraes are fellows of FAPESP (2013/24337-4, 2014/16412-9, respectively).

References

1. Sandu C, Dumas M, Malan A, Sambakhe D, Marteau C, Nizard C, Schnebert S, Perrier E, Challet E, Pevet P, Felder-Schmittbuhl MP (2012) Human skin keratinocytes, melanocytes, and fibroblasts contain distinct circadian clock machineries. Cell Mol Life Sci 69:3329–3339. doi:10.1007/s00018-012-1026-1
2. Orlow SJ (1995) Melanosomes are specialized members of the lysosomal lineage of organelles. J Invest Dermatol 105:3–7
3. Marks MS, Seabra MC (2001) The melanosome: membrane dynamics in black and white. Nat Rev Mol Cell Biol 2:738–748. doi:10.1038/35096009
4. Sklar LR, Almutawa F, Lim HW, Hamzavi I (2013) Effects of ultraviolet radiation, visible light, and infrared radiation on erythema and pigmentation: a review. Photochem Photobiol Sci 12:54–64. doi:10.1039/c2pp25152c
5. Lin JY, Fisher DE (2007) Melanocyte biology and skin pigmentation. Nature 445:843–850. doi:10.1038/nature05660

6. Solano F (2014) Melanins: skin pigments and much more—types, structural models, biological functions, and formation routes. N J Sci 2014:28. doi:10.1155/2014/498276
7. Slominski A, Tobin DJ, Shibahara S, Wortsman J (2004) Melanin pigmentation in mammalian skin and its hormonal regulation. Physiol Rev 84:1155–1228. doi:10.1152/physrev.00044.2003
8. McGregor JM, Hawk JLM (1999) Acute effects of ultraviolet radiation on the skin. In: Freedberg IM, Eisen AZ, Wolff K (eds) Fitzpatrick's dermatology in general medicine, 5th edn. McGraw-Hill, New York, pp 1555–1561
9. Dupont E, Gomez J, Bilodeau D (2013) Beyond UV radiation: a skin under challenge. Int J Cosmet Sci 35:224–232. doi:10.1111/ics.12036
10. Premi S, Wallisch S, Mano CM, Weiner AB, Bacchiocchi A, Wakamatsu K, Bechara EJ, Halaban R, Douki T, Brash DE (2015) Photochemistry. Chemiexcitation of melanin derivatives induces DNA photoproducts long after UV exposure. Science 347:842–847. doi:10.1126/science.1256022
11. Eller MS, Ostrom K, Gilchrest BA (1996) DNA damage enhances melanogenesis. Proc Natl Acad Sci USA 93:1087–1092
12. Brenner M, Hearing VJ (2008) The protective role of melanin against UV damage in human skin. Photochem Photobiol 84:539–549. doi:10.1111/j.1751-1097.2007.00226
13. Smith QT, Allison DJ (1966) Changes of collagen content in skin, femur and uterus of 17-beta-estradiol benzoate-treated rats. Endocrinology 79:486–492. doi:10.1210/endo-79-3-486
14. Henneman DH (1968) Effect of estrogen on in vivo and in vitro collagen biosynthesis and maturation in old and young female guinea pigs. Endocrinology 83:678–690. doi:10.1210/endo-83-4-678
15. Sobel H, Lee KD, Hewlett MJ (1965) Effect of estrogen on acid glycosaminoglycans in skin of mice. Biochim Biophys Acta 101:225–229
16. Bullough HF (1947) Epidermal thickness following oestrone injections in the mouse. Nature 159:101–102. doi:10.1038/159101a0
17. Maeda K, Naganuma M, Fukuda M, Matsunaga J, Tomita Y (1996) Effect of pituitary and ovarian hormones on human melanocytes in vitro. Pigment Cell Res 9:204–212
18. Jee SH, Lee SY, Chiu HC, Chang CC, Chen TJ (1994) Effects of estrogen and estrogen receptor in normal human melanocytes. Biochem Biophys Res Commun 199:1407–1412. doi:10.1006/bbrc.1994.1387
19. McLeod SD, Ranson M, Mason RS (1994) Effects of estrogens on human melanocytes in vitro. J Steroid Biochem Mol Biol 49:9–14
20. Lupulescu A (1981) Hormonal regulation of epidermal tumor development. J Invest Dermatol 77:186–195
21. Yamaguchi S, Mitsui S, Yan L, Yagita K, Miyake S, Okamura H (2000) Role of DBP in the circadian oscillatory mechanism. Mol Cell Biol 20:4773–4781
22. Buhr ED, Takahashi JS (2013) Molecular components of the mammalian circadian clock. Handb Exp Pharmacol. doi:10.1007/978-3-642-25950-0_1
23. Partch CL, Green CB, Takahashi JS (2014) Molecular architecture of the mammalian circadian clock. Trends Cell Biol 24:90–99. doi:10.1016/j.tcb.2013.07.002
24. Luber AJ, Ensanyat SH, Zeichner JA (2014) Therapeutic implications of the circadian clock on skin function. J Drugs Dermatol 13:130–144
25. Gaddameedhi S, Selby CP, Kaufmann WK, Smart RC, Sancar A (2011) Control of skin cancer by the circadian rhythm. Proc Natl Acad Sci USA 108:18790–18795. doi:10.1073/pnas.1115249108
26. Matsunaga N, Itcho K, Hamamura K, Ikeda E, Ikeyama H, Furuichi Y, Watanabe M, Koyanagi S, Ohdo S (2014) 24-hour rhythm of aquaporin-3 function in the epidermis is regulated by molecular clocks. J Invest Dermatol 134:1636–1644. doi:10.1038/jid.2014.13
27. Hardman JA, Tobin DJ, Haslam IS, Farjo N, Farjo B, Al-Nuaimi Y, Grimaldi B, Paus R (2015) The peripheral clock regulates human pigmentation. J Invest Dermatol 135:1053–1064. doi:10.1038/jid.2014.442
28. Sukumaran S, Almon RR, DuBois DC, Jusko WJ (2010) Circadian rhythms in gene expression: relationship to physiology, disease, drug disposition and drug action. Adv Drug Deliv Rev 62:904–917. doi:10.1016/j.addr.2010.05.009
29. Savvidis C, Koutsilieris M (2012) Circadian rhythm disruption in cancer biology. Mol Med 18:1249–1260. doi:10.2119/molmed.2012.00077
30. Kelleher FC, Rao Maguire A (2014) Circadian molecular clocks and cancer. Cancer Lett 342:9–18. doi:10.1016/j.canlet.2013.09.040
31. Lengyel Z, Lovig C, Kommedal S, Keszthelyi R, Szekeres G, Battyani Z, Csernus V, Nagy AD (2013) Altered expression patterns of clock gene mRNAs and clock proteins in human skin tumors. Tumour Biol 34:811–819. doi:10.1007/s13277-012-0611-0
32. de Assis LV, Moraes MN, da Silveira Cruz-Machado S, Castrucci AM (2016) The effect of white light on normal and malignant murine melanocytes: a link between opsins, clock genes, and melanogenesis. Biochim Biophys Acta 1863:1119–1133. doi:10.1016/j.bbamcr.2016.03.001
33. Tsuchiya Y, Akashi M, Nishida E (2003) Temperature compensation and temperature resetting of circadian rhythms in mammalian cultured fibroblasts. Genes Cells 8:713–720
34. Sporl F, Schellenberg K, Blatt T, Wenck H, Wittern KP, Schrader A, Kramer A (2011) A circadian clock in HaCaT keratinocytes. J Invest Dermatol 131:338–348. doi:10.1038/jid.2010.315
35. Sandu C, Liu T, Malan A, Challet E, Pevet P, Felder-Schmittbuhl MP (2015) Circadian clocks in rat skin and dermal fibroblasts: differential effects of aging, temperature and melatonin. Cell Mol Life Sci 72:2237–2248. doi:10.1007/s00018-014-1809-7
36. He PJ, Hirata M, Yamauchi N, Hattori MA (2007) Up-regulation of Per1 expression by estradiol and progesterone in the rat uterus. J Endocrinol 194:511–519. doi:10.1677/joe-07-0172
37. Nakamura TJ, Sellix MT, Menaker M, Block GD (2008) Estrogen directly modulates circadian rhythms of PER2 expression in the uterus. Am J Physiol Endocrinol Metab 295:E1025–E1031. doi:10.1152/ajpendo.90392.2008
38. Nakamura TJ, Moriya T, Inoue S, Shimazoe T, Watanabe S, Ebihara S, Shinohara K (2005) Estrogen differentially regulates expression of *Per1* and *Per2* genes between central and peripheral clocks and between reproductive and nonreproductive tissues in female rats. J Neurosci Res 82:622–630. doi:10.1002/jnr.20677
39. Bennett DC, Cooper PJ, Hart IR (1987) A line of non-tumorigenic mouse melanocytes, syngeneic with the B16 melanoma and requiring a tumor promoter for growth. Int J Cancer 39:414–418
40. Livak KJ, Schmittgen TD (2001) Analysis of relative gene expression data using real-time quantitative PCR and the $2^{-\Delta\Delta c_T}$ Method. Methods 25:402-408. doi: 10.1006/meth.2001.1262
41. Naeyaert JM, Eller M, Gordon PR, Park HY, Gilchrest BA (1991) Pigment content of cultured human melanocytes does not correlate with tyrosinase message level. Br J Dermatol 125:297–303
42. Iozumi K, Hoganson GE, Pennella R, Everett MA, Fuller BB (1993) Role of tyrosinase as the determinant of pigmentation in cultured human melanocytes. J Invest Dermatol 100:806–811
43. Haltaufderhyde KD, Oancea E (2014) Genome-wide transcriptome analysis of human epidermal melanocytes. Genomics 104:482–489. doi:10.1016/j.ygeno.2014.09.010
44. Iwata M, Corn T, Iwata S, Everett MA, Fuller BB (1990) The relationship between tyrosinase activity and skin color in human foreskins. J Invest Dermatol 95:9–15
45. Maeda K, Yokokawa Y, Hatao M, Naganuma M, Tomita Y (1997) Comparison of the melanogenesis in human black and light brown melanocytes. J Dermatol Sci 14:199–206

46. Murase D, Hachiya A, Fullenkamp R, Beck A, Moriwaki S, Hase T, Takema Y, Manga P (2016) Variation in Hsp70-1A expression contributes to skin color diversity. J Invest Dermatol. doi:10.1016/j.jid.2016.03.038
47. Filipski E, Subramanian P, Carriere J, Guettier C, Barbason H, Levi F (2009) Circadian disruption accelerates liver carcinogenesis in mice. Mutat Res 680:95–105. doi:10.1016/j.mrgentox.2009.10.002
48. Desotelle JA, Wilking MJ, Ahmad N (2012) The circadian control of skin and cutaneous photodamage. Photochem Photobiol 88:1037–1047. doi:10.1111/j.1751-1097.2012.01099.x
49. Balsalobre A, Damiola F, Schibler U (1998) A serum shock induces circadian gene expression in mammalian tissue culture cells. Cell 93:929–937
50. Yamazaki S, Numano R, Abe M, Hida A, Takahashi R, Ueda M, Block GD, Sakaki Y, Menaker M, Tei H (2000) Resetting central and peripheral circadian oscillators in transgenic rats. Science 288:682–685
51. Hirota T, Okano T, Kokame K, Shirotani-Ikejima H, Miyata T, Fukada Y (2002) Glucose down-regulates Per1 and Per2 mRNA levels and induces circadian gene expression in cultured Rat-1 fibroblasts. J Biol Chem 277:44244–44251. doi:10.1074/jbc.M206233200
52. Albrecht U (2012) Timing to perfection: the biology of central and peripheral circadian clocks. Neuron 74:246–260. doi:10.1016/j.neuron.2012.04.006
53. Gery S, Virk RK, Chumakov K, Yu A, Koeffler HP (2007) The clock gene *Per2* links the circadian system to the estrogen receptor. Oncogene 26:7916–79120. doi:10.1038/sj.onc.1210585
54. Sadoff L, Winkley J, Tyson S (1973) Is malignant melanoma an endocrine-dependent tumor? The possible adverse effect of estrogen. Oncology 27:244–257
55. Buzaid AC, Murren JR, Durivage HJ (1991) High-dose cisplatin with dacarbazine and tamoxifen in the treatment of metastatic melanoma. Cancer 68:1238–1241
56. McClay EF, Mastrangelo MJ, Berd D, Bellet RE (1992) Effective combination chemo/hormonal therapy for malignant melanoma: experience with three consecutive trials. Int J Cancer 50:553–556
57. Bhatia S, Tykodi SS, Thompson JA (2009) Treatment of metastatic melanoma: an overview. Oncology 23:488–496
58. de Giorgi V, Gori A, Alfaioli B, Papi F, Grazzini M, Rossari S, Lotti T, Massi D (2011) Influence of sex hormones on melanoma. J Clin Oncol 29:e94–e95; author reply e96. doi:10.1200/JCO.2010.33.1876
59. Janik ME, Bełkot K, Przybyło M (2014) Is oestrogen an important player in melanoma progression? Contemp Oncol 18:302–306. doi:10.5114/wo.2014.43938
60. Paech K, Webb P, Kuiper GG, Nilsson S, Gustafsson J, Kushner PJ, Scanlan TS (1997) Differential ligand activation of estrogen receptors ERalpha and ERbeta at AP1 sites. Science 277:1508–1510
61. Watters JJ, Campbell JS, Cunningham MJ, Krebs EG, Dorsa DM (1997) Rapid membrane effects of steroids in neuroblastoma cells: effects of estrogen on mitogen activated protein kinase signalling cascade and c-fos immediate early gene transcription. Endocrinology 138:4030–4033. doi:10.1210/endo.138.9.5489
62. Filardo EJ, Quinn JA, Bland KI, Frackelton AR Jr (2000) Estrogen-induced activation of Erk-1 and Erk-2 requires the G protein-coupled receptor homolog, GPR30, and occurs via trans-activation of the epidermal growth factor receptor through release of HB-EGF. Mol Endocrinol 14:1649–1660. doi:10.1210/mend.14.10.0532
63. Davies H, Bignell GR, Cox C, Stephens P, Edkins S, Clegg S, Teague J, Woffendin H, Garnett MJ, Bottomley W, Davis N, Dicks E, Ewing R, Floyd Y, Gray K, Hall S, Hawes R, Hughes J, Kosmidou V, Menzies A, Mould C, Parker A, Stevens C, Watt S, Hooper S, Wilson R, Jayatilake H, Gusterson BA, Cooper C, Shipley J, Hargrave D, Pritchard-Jones K, Maitland N, Chenevix-Trench G, Riggins GJ, Bigner DD, Palmieri G, Cossu A, Flanagan A, Nicholson A, Ho JW, Leung SY, Yuen ST, Weber BL, Seigler HF, Darrow TL, Paterson H, Marais R, Marshall CJ, Wooster R, Stratton MR, Futreal PA (2002) Mutations of the BRAF gene in human cancer. Nature 417:949–954. doi:10.1038/nature00766
64. Kanda N, Watanabe S (2003) 17β-estradiol inhibits oxidative stress-induced apoptosis in keratinocytes by promoting Bcl-2 expression. J Invest Dermatol 121:1500–1509. doi:10.1111/j.1523-1747.2003.12617.x
65. McCubrey JA, Steelman LS, Chappell WH, Abrams SL, Wong EW, Chang F, Lehmann B, Terrian DM, Milella M, Tafuri A, Stivala F, Libra M, Basecke J, Evangelisti C, Martelli AM, Franklin RA (2007) Roles of the Raf/MEK/ERK pathway in cell growth, malignant transformation and drug resistance. Biochim Biophys Acta 1773:1263–1284. doi:10.1016/j.bbamcr.2006.10.001
66. Dobroff AS, Wang H, Melnikova VO, Villares GJ, Zigler M, Huang L, Bar-Eli M (2009) Silencing cAMP-response element-binding protein (CREB) identifies CYR61 as a tumor suppressor gene in melanoma. J Biol Chem 284:26194–26206. doi:10.1074/jbc.M109.019836
67. Hu W, Jin L, Jiang CC, Long GV, Scolyer RA, Wu Q, Zhang XD, Mei Y, Wu M (2013) AEBP1 upregulation confers acquired resistance to BRAF (V600E) inhibition in melanoma. Cell Death Dis 4:e914. doi:10.1038/cddis.2013.441
68. Johannessen CM, Johnson LA, Piccioni F, Townes A, Frederick DT, Donahue MK, Narayan R, Flaherty KT, Wargo JA, Root DE, Garraway LA (2013) A melanocyte lineage program confers resistance to MAP kinase pathway inhibition. Nature 504:138–142. doi:10.1038/nature12688
69. Travnickova-Bendova Z, Cermakian N, Reppert SM, Sassone-Corsi P (2002) Bimodal regulation of mPeriod promoters by CREB-dependent signaling and CLOCK/BMAL1 activity. Proc Natl Acad Sci USA 99:7728–7733. doi:10.1073/pnas.102075599
70. Hanahan D, Weinberg RA (2000) The hallmarks of cancer. Cell 100:57–70
71. Hanahan D, Weinberg RA (2011) Hallmarks of cancer: the next generation. Cell 144:646–674. doi:10.1016/j.cell.2011.02.013
72. Reardon JT, Sancar A (2006) Repair of DNA–polypeptide crosslinks by human excision nuclease. Proc Natl Acad Sci USA 103:4056–4061. doi:10.1073/pnas.0600538103
73. Menck CFM, Munford V (2014) DNA repair diseases: what do they tell us about cancer and aging? Genet Mol Biol 37:220–233
74. Kang TH, Lindsey-Boltz LA, Reardon JT, Sancar A (2010) Circadian control of XPA and excision repair of cisplatin-DNA damage by cryptochrome and HERC2 ubiquitin ligase. Proc Natl Acad Sci USA 107:4890–4895. doi:10.1073/pnas.0915085107
75. Kang TH, Reardon JT, Kemp M, Sancar A (2009) Circadian oscillation of nucleotide excision repair in mammalian brain. Proc Natl Acad Sci USA 106:2864–2867. doi:10.1073/pnas.0812638106
76. Wang Y, Cheng Y, Yu G, Jia B, Hu Z, Zhang L (2016) Expression of PER, CRY, and TIM genes for the pathological features of colorectal cancer patients. Onco Targets Ther 9:1997–2005. doi:10.2147/OTT.S96925
77. Cadenas C, van de Sandt L, Edlund K, Lohr M, Hellwig B, Marchan R, Schmidt M, Rahnenfuhrer J, Oster H, Hengstler JG (2014) Loss of circadian clock gene expression is associated with tumor progression in breast cancer. Cell Cycle 13:3282–3291. doi:10.4161/15384101.2014.954454
78. Fu L, Lee CC (2003) The circadian clock: pacemaker and tumor suppressor. Nat Rev Cancer 3:350–361. doi:10.1038/nrc1072

Chapter 3: Heat Shock Antagonizes UVA-Induced responses in Murine Melanocytes and Melanoma Cells: An Unexpected Interaction

The content provided in this chapter has been published in Photochemical & Photobiological Sciences, 2017, 16(5):633-648. DOI: 10.1039/c6pp00330c.

Authors' names: de Assis LVM, Moraes MN, Castrucci AML.

Photochemical & Photobiological Sciences

PAPER

View Article Online
View Journal | View Issue

Cite this: *Photochem. Photobiol. Sci.*, 2017, **16**, 633

Heat shock antagonizes UVA-induced responses in murine melanocytes and melanoma cells: an unexpected interaction†

Leonardo Vinícius Monteiro de Assis, Maria Nathália Moraes and Ana Maria de Lauro Castrucci*

Received 7th September 2016,
Accepted 21st January 2017

DOI: 10.1039/c6pp00330c

rsc.li/pps

The skin is under the influence of oscillatory factors such as light and temperature. This organ possesses a local system that controls several aspects in a time-dependent manner; moreover, the skin has a well-known set of opsins whose function is still unknown. We demonstrate that heat shock reduces *Opn2* expression in normal Melan-a melanocytes, while the opposite effect is found in malignant B16-F10 cells. In both cell lines, UVA radiation increases the expression of *Opn4* and melanin content. Clock genes and *Xpa*, a DNA repair gene, of malignant melanocytes are more responsive to UVA radiation when compared to normal cells. Most UVA-induced effects are antagonized by heat shock, a phenomenon shown for the first time. Based on our data, the heat produced during UV experiments should be carefully monitored since temperature represents, according to our results, an important confounding factor, and therefore it should, when possible, be dissociated from UV radiation. The responses displayed by murine melanoma cells, if proven to also take place in human melanoma, may represent an important step in cancer development and progression.

1. Introduction

The temporalization and the temporal segregation of physiological processes are crucial for cell and organism homeostasis. Since environmental patterns can be predicted in a 24 h period, the presence of a system capable of keeping track of time, and, based on this information, able to anticipate and regulate the physiology of the organism is key for survival.[1]

The so-called clock genes lie in the core of this system. These genes and their proteins oscillate in a time-dependent fashion, a feature that is responsible for timing through a well-described system of interlaced feedback loops. In short, aryl hydrocarbon receptor nuclear translocator-like protein 1 (BMAL1) forms a heterodimer with CLOCK (Circadian Locomotor Output Cycles Kaput) that binds to E-box sequences in the promoter of *Per* (*Period*) and *Cry* (*Cryptochrome*) genes as well as in other genes known as clock controlled-genes (CGGs), leading to their transcription. After being translated, PER and CRY form a heterodimer, which is phosphorylated by casein kinase δ or ε, an event that targets the PER/CRY heterodimer to the nucleus, where it inhibits the activity of BMAL1/CLOCK; in an additional loop, BMAL1/CLOCK activates the transcription of *nuclear receptor subfamily 1*, *group D*, *member 1/2* (*Rev-Erbα/β*) and *RAR-related orphan receptor alpha/beta* (*RORα/β*) genes. REV-ERBα/β inhibits while RORα/β stimulates *Bmal1* expression. To terminate the repression phase, the degradation of phosphorylated PER and CRY proteins takes place after ubiquitination, and a new cycle begins.[2–4]

The clock gene machinery is the core mechanism in both the central pacemaker, suprachiasmatic nuclei (SCNs), and peripheral pacemakers.[2,5] In the mammalian retina a subset of intrinsically photosensitive retinal ganglion cells perceives the external light through melanopsin (OPN4).[6,7] Once a photon hits OPN4, this information is transformed into electric stimuli which are sent to the SCNs through the retino-hypothalamic tract.[8,9] Based on this information the SCNs are synchronized to the external light/dark cycle, and through stimuli which ultimately reach the entire body, align the whole organism under a single timing.[2] A disruption between the central pacemaker and the peripheral clocks is known to participate in the development of several diseases including cancer.[10–12]

Since the skin is the first barrier between the organism and the environment, the influence of environmental oscillatory factors such as light – in its several wavelengths – and temperature is likely to play an important role in its physiology. The

Laboratory of Comparative Physiology of Pigmentation, Department of Physiology, Institute of Biosciences, University of São Paulo, São Paulo, Brazil.
E-mail: amdlcast@ib.usp.br

†Electronic supplementary information (ESI) available. See DOI: 10.1039/c6pp00330c

light regulation of clock genes in skin cells is still not fully understood. Ultraviolet radiation B (UVB) has been shown to affect clock gene machinery in keratinocytes.[13] We have recently shown that clock genes of malignant melanocytes are more responsive to white light pulse[14] and estradiol[15] as compared to normal ones. The effect of temperature on clock gene expression on SCN and peripheral tissues is better comprehended. Individual SCN neurons are entrained by the temperature cycle but when connected as a single entity no effect of temperature is observed. Thus, the SCN is insensitive to temperature,[16] contrary to peripheral tissues, which were demonstrated to be synchronized by temperature cycles.[16–19] In the skin the temperature cycle plays an important role in the synchronization of human keratinocytes, a feature that is correlated to the temporal regulation of several genes involved in cholesterol homeostasis and differentiation.[20]

The skin has local circadian systems that regulate several processes in a time-dependent fashion,[21–25] for instance, skin barrier protection,[26] transepidermal water loss, pH, and temperature.[27,28] Recently, it has been reported that mice harboring a mutated *Clock* show reduced stratum corneum hydration, which is linked to the reduced expression of *aquaporin 3* levels (*Aqp3*).[29] Another important aspect of the skin that displays a circadian profile is DNA repair: *xeroderma pigmentosum*, *complementation group A* (*XPA*), a DNA repair enzyme, oscillates in murine skin.[30] Another important clock regulated event in the skin is the temporal segregation between the oxidative phosphorylation and the S-phase of the cellular cycle. Interestingly, when *Bmal1* is specifically deleted in keratinocytes, the time-dependent cell division is lost, a fact that, according to the authors, leads to constitutively elevated cell proliferation.[31] Melanogenesis has also been seen to be a time-dependent process, which is upregulated when the clock gene machinery is silenced in normal human melanocytes, ultimately resulting in an increased melanin content.[32] The oscillation of clock gene transcripts has been shown to occur in the skin of mice kept in the light–dark cycle (LD), a profile that is lost when the SCNs are removed.[33] However, there has not been convincing evidence to affirm that these oscillations are solely dependent on the temporal signals arising from the SCNs.[24,33]

Since 2001, it has been known that the skin has a photosensitive system comprised of opsins[14,34–38] whose function was recently started to be elucidated.[39–41] Interestingly, the photopigment system of malignant melanocytes is more sensitive to white light pulse in comparison to normal ones, a feature that is associated with melanopsin (OPN4) migration to the cell membrane and clock gene activation in melanoma cells.[14]

The deleterious effects of UV radiation on the skin are well known;[42,43] interestingly, it has also been shown that heat represents an important – but yet underestimated[44,45] – skin carcinogenic factor.[45–49] Under direct infrared radiation the temperature of human skin increases to more than 40 °C, which is due to the conversion of infrared radiation into heat by the skin.[45] Since the skin is concurrently exposed not only to UV radiation and visible light but also to temperature, it is of great relevance to better understand which effects the two stimuli together would trigger in the skin and in its various cell types. In fact, the hypothetical synergic role of both heat and UV radiation in the development of skin cancer has been set forth;[46] however, to the best of our knowledge, no study in the literature has thus far investigated the synergic effects of UVA radiation and heat shock in the modulation of clock genes and melanin content in skin cells.

Based on the above, we sought to evaluate the gene response profile of opsins, clock genes and *Xpa*, as well as the melanin content, in response to heat shock, UVA radiation or both stimuli in normal (Melan-a) and malignant (B16-F10) murine melanocytes. Our data show for the first time that the clock gene machinery of malignant melanocytes and *Xpa* is more sensitive to UVA radiation when compared to normal melanocytes; in addition, UVA radiation leads to a rapid increase in the melanin content in both normal and malignant melanocytes. Surprisingly, most of the UVA-induced responses are antagonized by heat shock. In this line, we further discuss a putative link between the carcinogenic process and the differential responses in normal melanocytes and melanoma cells to the above-mentioned stimuli, which may advance our knowledge about the development of melanoma as well as serve as a basis for a new pharmacological target.

2. Materials & methods

Cell culture

Melan-a or B16-F10 cells were maintained in RPMI 1640 medium with phenol red (Atená, Campinas, SP, Brazil), supplemented with 14.3 mM $NaHCO_3$, 15 mM HEPES, 10% fetal bovine serum (FBS) (Atená, Campinas, SP, Brazil), and 1% antibiotic/antimycotic solution (10 000 U mL^{-1} penicillin, 10 000 μg mL^{-1} streptomycin, and 25 μg mL^{-1} amphotericin B, Life Technologies, Carlsbad, CA, USA), pH 7.2. The cells were kept at 37 °C and 5% CO_2. During the experiments the cells were maintained in RPMI 1640 without phenol red (Atená, Campinas, SP, Brazil), FBS was reduced to 2%, and 10^{-7} M retinal (*all-trans*, Sigma-Aldrich, St Louis, MO, USA) was added to the media. Phorbol 12-myristate 13-acetate (TPA, Sigma-Aldrich, St Louis, MO, USA) at 200 nM was added to the Melan-a cell medium as it is necessary for appropriate growth and maintenance.[50]

UVA radiation and heat shock

The expression of *Per1* and *Clock*, members of the negative and positive limb of clock machinery, respectively, were analyzed in DD in order to determine the minimal duration necessary to establish free-running conditions, in which despite the fact that each single cell displays its own rhythm, no oscillation is observed in the cell population. Our data showed no oscillation in clock gene expression along a 24 h period after three full days in DD (ESI Fig. 1Sa–d†) demonstrating that three days in DD is enough for both cell lines to free run.

Melan-a or B16-F10 cells were seeded in 25 cm^2 flasks at an initial density of 10^5 and 10^6 cells, respectively, and kept in DD for three days. At the beginning of the 4th day the cells were divided into four groups as follows: (1) constant dark (DD) without handling at 37 °C; (2) increasing temperature from 37 to 40 °C for 40–45 min, in which the cell flasks were wrapped in aluminum foil; (3) increasing temperature from 37 to 40 °C associated with UVA radiation (4.44 kJ m^{-2}, 1.6 W m^{-2} for 40–45 min) and placed together with group (2) in the same incubator; (4) UVA radiation only (4.44 kJ m^{-2}) at 37 ± 0.5 °C. The UVA dose was based on ref. 38, 39 and 41. Cells were collected immediately (ZT 0), 2 (ZT 2), and 6 hours (ZT 6) after the pulse for gene expression and melanin content assays. All cell manipulation during the experiments was carried out under red dim light (7 W Konex bulb and Safe-Light filter GBX-2, Kodak, Rochester, NY, USA).

During all experiments the temperature of the incubator was monitored every 60 s by using a sensor (iLog, Escort Data Loggers, Edison, NJ, USA) placed in a recipient containing MilliQ water. For the groups receiving UVA radiation associated with temperature or only heat shock (flasks wrapped in aluminum foil), the temperature of the incubator was increased as follows: 15 min after UVA lamps were turned on, a 1 °C increase was observed; after a further 15 min the temperature reached 39.5 °C. By the end of the experiment the temperature had been raised further by 0.5 °C (ESI Fig. S3A†). For UVA *per se* experiments, the temperature of the incubator was set to 33 °C, then UVA lamps were turned on and 45 minutes later the temperature had reached 37 °C. The cells were then placed in the incubator and received UVA radiation at 37 °C ± 0.5 °C (ESI Fig. S3B†).

The emission spectrum of the UVA lamps (Model 10077, General Electric, Fairfield, CT, USA) (kindly determined by Dr Elvo Burini Junior, University of São Paulo, using a Spectrometer CAS 140CT and a sensor IOP 120, both from Instrument System, Neumarkter, München, Germany) shows a strong UVA component with a 365 nm emission peak and a minor violet light component (ESI Fig. S2†). The UV radiation was measured in each experiment using a dosimeter (VLX-3W, Vilver Lourmat, Collégien, France) coupled to UVA (355 and 375 nm) and UVB (280 and 320 nm) sensors (kindly provided by Dr Carlos Menck, University of São Paulo). No UVB radiation was detected during irradiation.

Flow cytometry

Propidium iodide (PI) staining is widely used to evaluate apoptosis and the cell cycle profile. This technique is based on the principle that apoptotic cells are characterized by DNA fragmentation with consequent loss of the DNA content. PI is capable of binding and labeling DNA which allows a precise evaluation of the cellular DNA content.[51] Twenty-four and 48 hours after the above-mentioned stimuli, the media were collected, and the cells harvested with a Tyrode/EDTA solution. Both the cell medium and cells were transferred to a tube, and centrifuged at 100*g* for 5 min. The pellet was resuspended in cold ethanol (70%), kept for at least 3 h at −20 °C, washed with PBS (2×), and resuspended in 200 μL of propidium iodide solution (200 μg mL^{-1} of RNase A, 20 μg mL^{-1} of propidium iodide, and 0.1% of Triton X-100 in PBS). The cell suspension in PI solution was kept in the dark for 30 min, washed, and resuspended in PBS. The cell suspension was centrifuged at 100*g* for 5 min between washes. The fluorescence was measured in a flow cytometer (Guava GE Healthcare, Pittsburgh, PA, USA), and a total of 10 000 events were captured per sample.

Total RNA extraction and reverse transcriptase PCR (RT-PCR)

The medium was removed and Tri-Reagent (Ambion, Grand Island, NY, USA) was added directly to the cells. The lysate was subjected to the manufacturer's suggested procedure. The samples were treated with DNAse I (turbo-DNase, Life Technologies, Carlsbad, CA, USA) according to the manufacturer's instructions in order to remove genomic DNA contamination. The RNA concentration and quality (OD_{260}/OD_{280}) were determined in a NanoDrop spectrophotometer (NanoDrop, Wilmington, DE, USA). One to four μg of purified RNA was subjected to reverse transcriptase reaction using random primers (100 ng μL^{-1}) and Superscript III, in addition to the reagents recommended by the enzyme manufacturer (Life Technologies, Carlsbad, CA, USA).

Quantitative PCR (qPCR)

Quantitative PCR was performed with the products of reverse transcription using oligopeptides spanning introns, designed, and synthesized by IDT (Coralville, IA, USA) or Life Technologies (Carlsbad, CA, USA), based on sequences obtained from GenBank (http://www.ncbi.nlm.nih.gov/genbank). All primers exhibited efficiency between 93% and 116%. The access number of each gene, the respective primer sequences, and concentrations are shown in Table 1.

The qPCR reactions were performed through two different protocols: multiplex for simultaneous analysis of multiple genes (*TaqMan*®) and *SYBR*® *GreenER*™. The *TaqMan*® solutions contained *Per1* and *Clock* or *Opn2* and *Bmal1* as the respective primers and fluorescent probes (Table 1), and Supermix 2X (Bio-Rad Laboratories, Hercules, CA, USA). Each experimental cDNA was run in triplicates in 96 well plates. The assays were performed using an i5 thermocycler (Bio-Rad Laboratories, Hercules, CA, USA) under the following conditions: 7 min at 95 °C, followed by 45 cycles of 30 s at 95 °C and 30 s at 55 °C.

The solutions for *Xpa*, *Opn4*, or 18S RNA contained the respective primers (Table 1) and Kapa *SYBR*® Fast qPCR Master Mix 2X (Kapa Biosystems, Wilmington, MA, USA). Each experimental cDNA was run in duplicates in 96 well plates. These assays were performed in an iCycler thermocycler (Bio-Rad Laboratories, Hercules, CA, USA) under the following conditions: 10 min at 95 °C, followed by 45 cycles of 15 s at 95 °C, 1 min at 60 °C, and 80 cycles of 10 s at 55 °C, with a gradual increase of 0.5 °C.

Ribosomal 18S RNA was used as a reference gene in both TaqMan® and *SYBR*® *GreenER*™ methodologies since it did not vary with time under our experimental conditions (data not shown).

Table 1 Sequences and final concentrations of primers and probes. Access numbers are in parentheses

Templates	Primers and probes	Final concentration
Opn2 (NM_145383.1)	Forward: 5′-TGCCACACTTGGAGGTGAAA-3′	300 nM
	Reverse: 5′-ACCACGTAGCGCTCAATGG-3′	300 nM
	Probe: 5′-/6-FAM/-CGCCCTGTGGTCCCTGGTGG/3BHQ_1′	200 nM
Opn4 (NM_001128599.1)	Forward: 5′-ACATCTTCATCTTCAGGGCCA-3′	300 nM
	Reverse: 5′-ACTCACCGCAGCCCTCAC-3′	300 nM
Opn5 (NM_181753.4)	Forward: 5′-TTGAACCACACTGCCCTACC-3′	300 nM
	Reverse: 5′-AACGGCTTGCCTACAACTGAT-3′	300 nM
Per1 (NM_0011065.3)	Forward: 5′-AGCAGGTTCAGGCTAACCAGGAAT-3′	300 nM
	Reverse: 5′-AGGTGTCCTGGTTTCGAAGTGTGT-3′	300 nM
	Probe: 5′-/6FAM/-AGCCTTGTGCCATGGACATGTCTACT/3BHQ_1/-3′	200 nM
Clock (NM_007715.6)	Forward: 5′-CTCTGCTGCCTTTCCACTACAA-3′	300 nM
	Reverse: 5′-TGCTGAGGCTGGTGTTGCT-3′	300 nM
	Probe: 5′-/5HEX/-AGAGCACTTTCCCTCCTTCGCACCA/3BHQ_1/-3′	200 nM
Bmal1 (NM_001243048)	Forward: 5′-AGCTTCTGCACAATCCACAGCAC-3′	300 nM
	Reverse: 5′-TGTCTGGCTCATTGTCTTCGTCCA-3′	300 nM
	Probe: 5′-/5HEX/-AAAGCTGGCCACCCACGAAGATGGG/3BHQ_1-3′	200 nM
Xpa (NM_011728.2)	Forward: 5′-GGCGATATGAAGCTCTACCTAAA-3′	300 nM
	Reverse: 5′-TTCCTGCCTCACTTCCTTTG-3′	300 nM
18S RNA	Forward: 5′-CGGCTACCACATCCAAGGAA-3′	50 nM
	Reverse: 5′-GCTGGAATTACCGCGGCT-3′	50 nM

Melanin quantification

Melan-a and B16-F10 cells were harvested with a Tyrode/EDTA solution, and after cell counting, the cell suspension was centrifuged at 100*g* for 5 min, the supernatant was discarded, and 1 mL of 1 M NaOH (in 10% DMSO) was added to the cell pellet. The lysate was heated at 80 °C for 2 h, centrifuged at 1050*g* for 15 min, and 200 μL of each sample supernatant was added in duplicates to wells of a flat-bottom plate. Melanin was quantified by absolute absorbance at 475 nm in a plate reader (SpectraMax 250, Molecular Devices, Sunnyvale, CA, USA), and the values interpolated in a standard curve of synthetic melanin (Sigma-Aldrich, St Louis, MO, USA) ranging from 3.125 to 200 μg mL^{-1}. The melanin concentration was expressed as μg of melanin per 10^6 cells.

Data and statistical analysis

All data were checked for Gaussian distribution through the D'Agostino–Pearson omnibus and Shapiro–Wilk test. For qPCR analysis, the results in $\log(2^{-\Delta\Delta Ct})$ were used[52] as described previously.[14,15] The log values (from at least two independent experiments) were graphed as mean ± SEM relative to the minimal value expression in the control group (DD condition).

The temporal gene expression and melanin content as well as % of subG1 cells of each group were analyzed by one-way ANOVA followed by Tukey's post-test. The differences in gene expression, % of subG1 cells, and melanin content between the 4 groups (control, exposed to heat shock *per se*, heat shock in association with UVA radiation, and UVA radiation *per se*) were compared by two-way ANOVA followed by the Bonferroni post-test.

Xpa mRNA levels and the melanin content between Melan-a and B16-F10 cells after exposure to the above-mentioned stimuli were compared by unpaired Student's *t* test. Samples that displayed Gaussian distribution were analyzed by the *t* test with Welch correction while those that did not show normal distribution were analyzed by the Mann–Whitney test. Significance was set for $p \leq 0.05$. All analyses were carried out in GraphPad Prism Version 6.0.

3. Results

Effects of heat shock and UVA radiation on cell viability and cycle

We initially evaluated the cytotoxic effects of UVA radiation *per se*, heat shock *per se* and in association with UVA radiation on Melan-a and B16-F10 cells. Using the SubG1 parameter, a commonly used apoptosis marker,[51,53] our data show that the SubG1 cell population was similar in all 4 groups (Fig. 1A and B), 24 and 48 h after the treatments; in addition, no alteration in the cell cycle profile was observed among the groups or time points (Fig. 1C and ESI Tables S1 and S2†). These data, therefore, show that the stimuli did not lead to apoptosis or cell cycle arrest in Melan-a or B16-F10 cells.

Effects of heat shock and UVA radiation on the expression of *Opn2* and *Opn4*

We have recently shown that Melan-a and B16-F10 cells express *Opn2*, *Opn4*, and *S-opsin* but not *M-opsin*.[14] Here we also investigated the presence of *Opn5* – neuropsin – an opsin

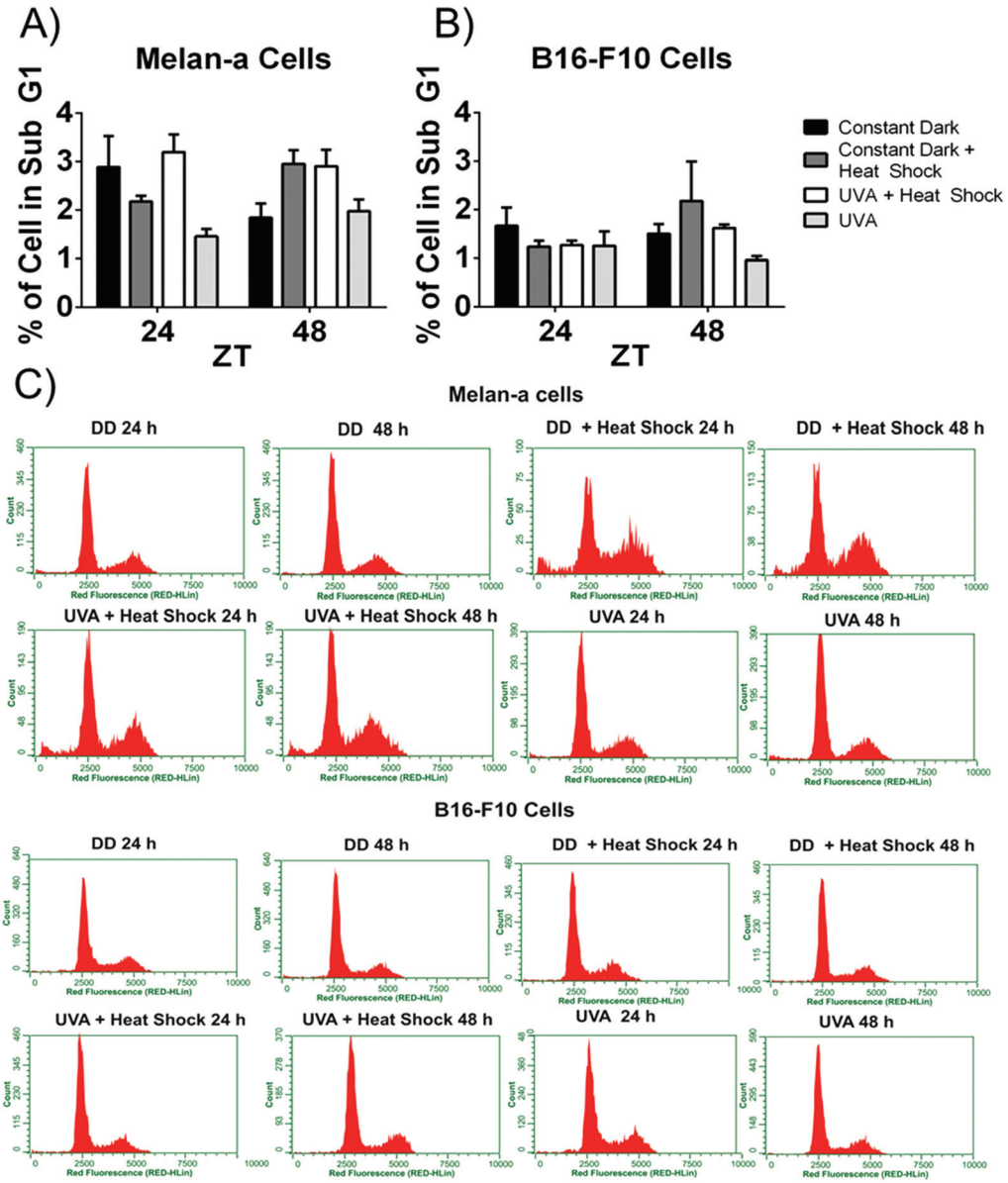

Fig. 1 Effects of heat shock *per se* and UVA radiation in association or not with heat shock in cell cycle and apoptosis, 24 and 48 h after the stimuli. (A) Percentage of Melan-a cells in sub-G1, n = 3–9; (B) percentage of B16-F10 cells in sub-G1, n = 4–10; (C) representative profiles of Melan-a and B16-F10 cell cycles.

known to be activated by UV radiation (absorption maximum at 380 nm), which also participates in the photoentrainment of clock genes in the retina and cornea of mice.[54] Despite the fact that OPN5 has been detected in murine and human skin,[55] neither Melan-a nor B16-F10 cells express *Opn5* (*Ct* value > 36).

Therefore, we evaluated the response profile of the two most expressed opsins in normal and malignant melanocytes – *Opn2* and *Opn4* – to the stimuli described above. In Melan-a cells, no temporal variation of *Opn2* expression was found in the DD group. However, at ZT 2 the heat shock *per se* increased the *Opn2* expression in comparison to ZT 0 and ZT 6 ($p \leq 0.05$), whereas the group exposed to heat shock in association with UVA radiation showed increased *Opn2* expression at ZT 6 in comparison to ZT 0 and ZT 2 ($p \leq 0.05$), and the UVA-exposed group showed increased *Opn2* expression at ZT 6 in comparison to ZT 0 and ZT 2 ($p \leq 0.01$) (Fig. 2A). In B16-F10 cells, *Opn2* showed no temporal variation in any group (Fig. 2B).

A comparison among the stimulated groups demonstrated remarkable results. In Melan-a cells, heat shock *per se* and in association with UVA radiation induced a significant reduction of *Opn2* expression at ZT 6 when compared to control ($p \leq 0.01$) and UVA-exposed ($p \leq 0.001$) groups (Fig. 2A). Interestingly, in malignant melanocytes, the same stimuli, heat shock *per se* and in association with UVA radiation,

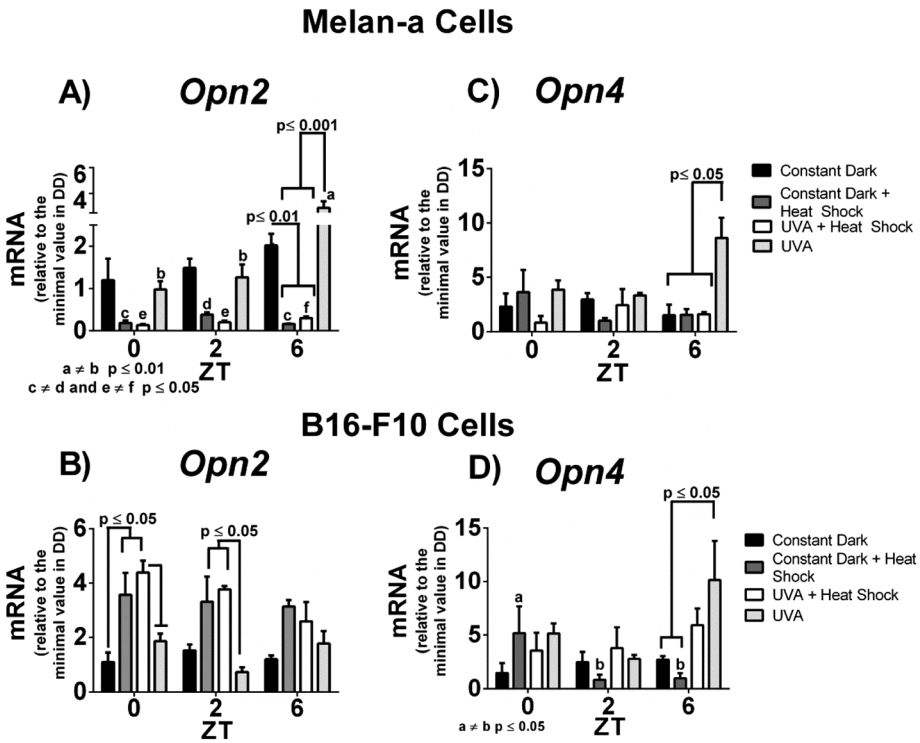

Fig. 2 *Opn2* and *Opn4* mRNA levels in Melan-a and B16-F10 cells immediately (ZT 0), 2 h (ZT 2) and 6 h (ZT 6) after heat shock *per se*, UVA radiation *per se*, and a combination of both stimuli. Gene expression was normalized by 18S RNA transcript and expressed relative to the minimal value of each cell line in the DD control. Gene expression values are shown as mean ± SEM. *p* values are shown in the graphs. (A) Melan-a *Opn2*, *n* = 3–6; (B) B16-F10 *Opn2*, *n* = 3–5; (C) Melan-a *Opn4*, *n* = 3–5; (D) B16-F10 *Opn4*, *n* = 3–5.

increased *Opn2* levels in comparison to the remaining groups ($p \leq 0.05$) at ZT 0 and only to the UVA alone group at ZT 2 (Fig. 2B).

The expression of *Opn4* in normal melanocytes did not oscillate throughout the time in any group (Fig. 2C); on the contrary, in B16-F10 cells, heat shock increased the levels of *Opn4* at ZT 0 when compared to ZT 2 and ZT 6 ($p \leq 0.05$) (Fig. 2D). A feature shared by normal and malignant melanocytes is the fact that UVA pulse leads to increased levels of *Opn4* in comparison to the DD group at ZT 6 ($p \leq 0.05$) (Fig. 2C and D).

This shows that heat shock leads to reduced *Opn2* expression in a UVA radiation independent fashion in Melan-a cells. Interestingly, the antagonistic effect of heat shock over the increasing effect of UVA radiation on *Opn4* expression – as observed in normal melanocytes – was not observed in malignant ones.

Effects of heat shock and UVA radiation on the expression of clock genes

Subsequently, we evaluated the effects of UVA radiation, heat shock *per se* and in association with UVA radiation on normal and malignant melanocytes, assessing clock gene expression. No difference in the temporal expression of *Per1*, *Clock*, or *Bmal1* was observed except for the UVA-exposed group. Cells exposed to UVA radiation showed an increased temporal expression of *Per1* ($p \leq 0.001$), *Clock* ($p \leq 0.001$), and *Bmal1* ($p \leq 0.05$) at ZT 6 in comparison to ZT 0 e ZT 2 (Fig. 3A–C). In addition, in the UVA-exposed group an increase in *Per1* expression in comparison to the group exposed only to heat shock ($p \leq 0.01$), and in *Clock* expression in comparison to the remaining groups was found at ZT 6 ($p \leq 0.001$) (Fig. 3A and B). In the latter, we observed the antagonistic effect of heat shock on the UVA-induced *Clock* expression at ZT 6.

In malignant melanocytes, a temporal oscillation in the expression of *Per1* was only found in the group subjected to heat shock in association with UVA radiation, with an immediate and transitory increase at ZT 0 when compared to ZT 2 and ZT 6 ($p \leq 0.001$) (Fig. 4A). No temporal difference in the expression of *Clock* or *Bmal1* was observed in any group except for the UVA-exposed cells: the expression of *Clock* was higher at ZT 6 in comparison to the same group at ZT 0 and ZT 2 ($p \leq 0.05$), whereas the *Bmal1* expression was higher at ZT 0 and ZT 6 in comparison to ZT 2 ($p \leq 0.05$) (Fig. 4B and C). Concerning B16-F10 cell responses to the various stimuli, heat shock in association with UVA radiation elicited a remarkable increase in *Per1* expression as compared to the other groups at ZT 0 ($p \leq 0.01$) (Fig. 4A). As for the *Clock* expression, it was significantly higher in cells exposed to UVA radiation in all time points in comparison to the remaining groups (Fig. 4B), whereas *Bmal1* transcripts showed increased levels in response to the same stimulus at ZT 0 and ZT 6 when compared to the remaining groups (Fig. 4C). Interestingly, we observed that both *Clock* and *Bmal1* were subjected to the antagonistic action of heat shock on the UVA-induced gene expression.

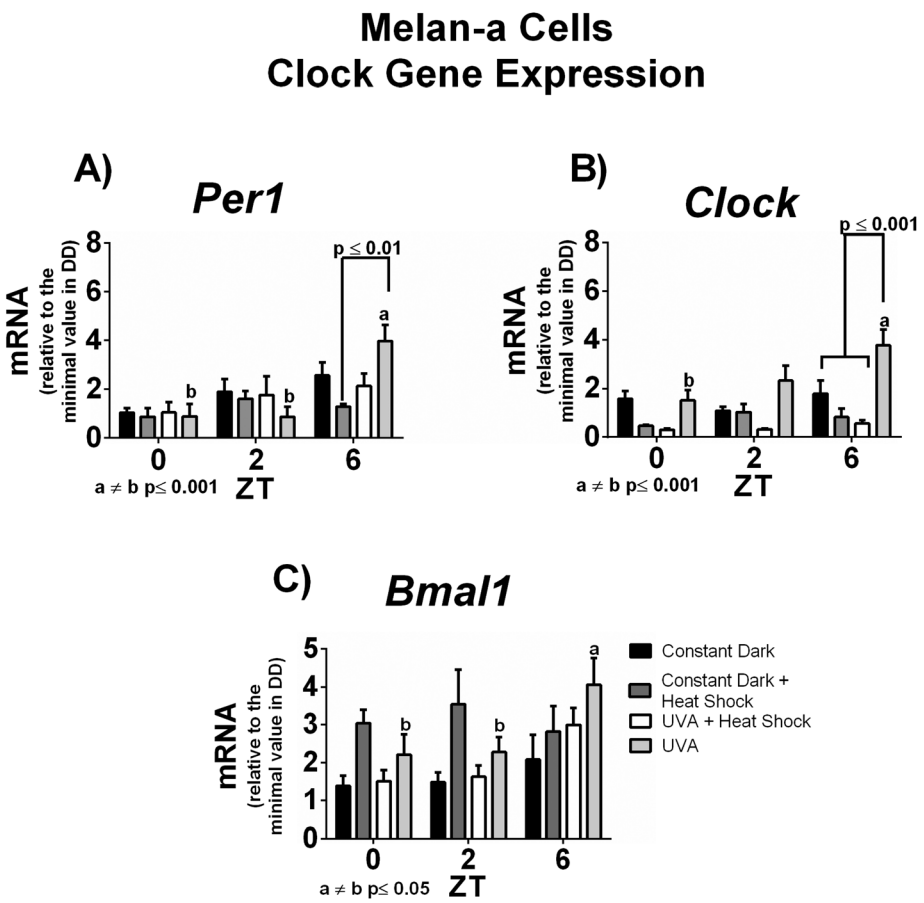

Fig. 3 Clock gene mRNA levels in Melan-a cells immediately (ZT 0), 2 h (ZT 2) and 6 h (ZT 6) after heat shock *per se*, UVA radiation *per se*, and a combination of both stimuli. Gene expression was normalized by 18S RNA transcript and expressed relative to the minimal value in the DD control. Gene expression values are shown as mean ± SEM. *p* values are shown in the graphs. (A) Melan-a *Per1*, $n = 3–7$; (B) Melan-a *Clock*, $n = 4–7$; (C) Melan-a *Bmal1*, $n = 3–6$.

Effects of heat shock and UVA radiation on *Xpa* expression

After evaluating opsin and clock gene expression, we analyzed *Xpa* expression. The protein XPA, encoded by *Xpa*, acts as a DNA repair enzyme known to oscillate in murine skin in the anti-phase with CRY1.[30] Our data show that *Xpa* expression is very stable in Melan-a cells, only oscillating in the UVA-exposed group, exhibiting a slight temporal increase at ZT 6 in comparison to ZT 0 ($p \leq 0.05$) (Fig. 5A).

In B16-F10 cells the expression of *Xpa* did not display any temporal oscillation in either group. In cells exposed to UVA radiation *per se*, *Xpa* expression increased at ZT 0 and ZT 6 in comparison to the other groups at the same time points ($p \leq 0.05$ and $p \leq 0.01$ respectively). These findings show that UVA radiation rapidly increases *Xpa* expression; however, when associated with heat shock the stimulatory effect of UVA radiation on this gene is lost, which again shows the inhibitory effect of heat shock on UVA-induced responses (Fig. 5B).

It is worth emphasizing the different response profiles between normal and malignant melanocytes: in Melan-a cells UVA radiation did not affect *Xpa* expression while in B16-F10 cells the same stimulus increased the *Xpa* transcript levels when compared to the other groups. A comparison of *Xpa* in Melan-a and B16-F10 cells further shows that *Xpa* mRNA is downregulated in malignant melanocytes (Fig. 5C).

Effect of heat shock and UVA radiation on the melanin content

In Melan-a cells an oscillatory profile in the melanin content was observed in all groups except the DD control: the melanin increase was higher at ZT 0, decreasing at ZT 2 and ZT 6 for all experimental groups; the most significant increase was seen in UVA-stimulated cells at ZT 0 ($p \leq 0.0001$) (Fig. 6A). These findings, therefore, show that UVA radiation leads to a rapid, expressive, and transitory increase in melanin content, which is characteristic of the immediate pigment darkening (IPD).[56] Remarkably, if UVA radiation was associated with heat shock, IPD was drastically reduced, once again showing the antagonistic effect of heat shock over UVA radiation (Fig. 6A).

Unlike normal melanocytes, in B16-F10 cells no oscillation in the melanin content was observed except in the UVA-treated cells: a rapid, expressive, and transitory increase in the melanin content was found at ZT 0 ($p \leq 0.0001$), which decreased at ZT 2 and ZT 6 (Fig. 6B). Similar to Melan-a cells, the same antagonistic profile of heat shock over UVA radiation

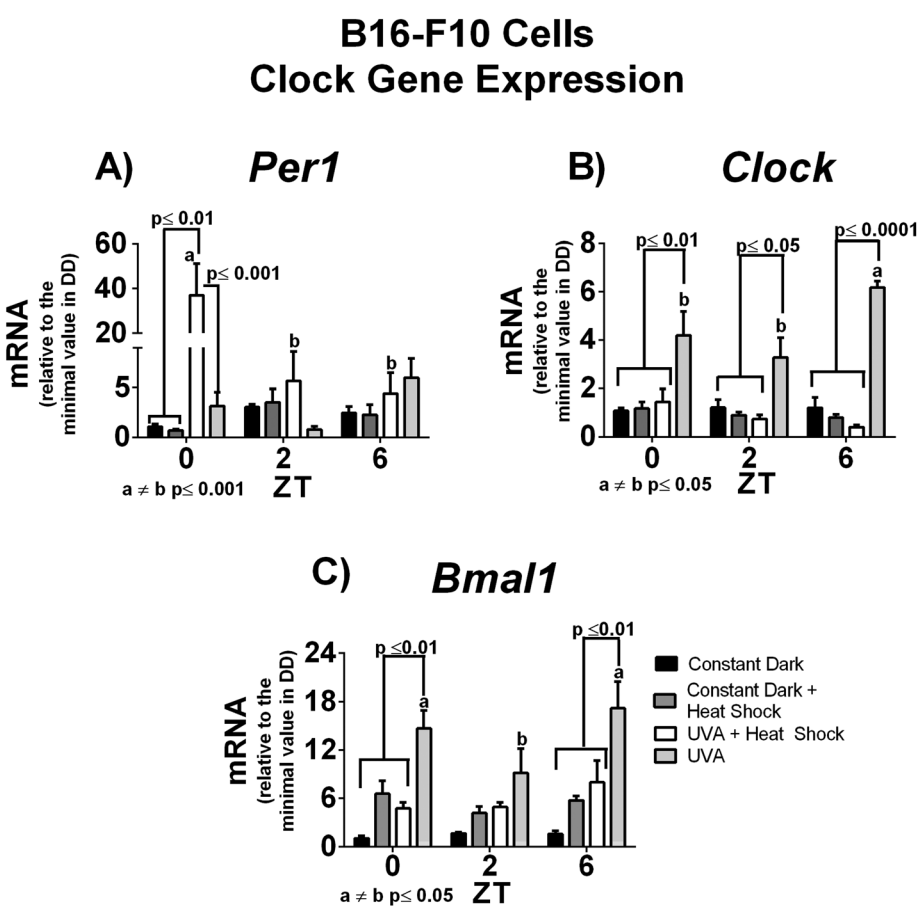

Fig. 4 Clock gene mRNA levels in B16-F10 cells immediately (ZT 0), 2 h (ZT 2) and 6 h (ZT 6) after heat shock *per se*, UVA radiation *per se*, and a combination of both stimuli. Gene expression was normalized by 18S RNA transcript and expressed relative to the minimal value in the DD control. Gene expression values are shown as mean ± SEM. *p* values are shown in the graphs. (A) B16-F10 *Per1*, *n* = 3–5; (B) B16-F10 *Clock*, *n* = 3–4; (C) B16-F10 *Bmal1*, *n* = 3–5.

in the melanin content was seen in malignant melanocytes (Fig. 6B).

We have previously shown that the melanin content is upregulated in malignant melanocytes in comparison to normal cells;[14,15] here we additionally show that the melanin content is higher not only in the B16-F10 DD control group (Fig. 7A), but also in all three experimental groups (Fig. 7B–D) in comparison to the respective groups of Melan-a cells. These findings further reinforce the fact that melanogenesis machinery is upregulated and likely to be disrupted in malignant melanocytes in comparison to normal cells.

4. Discussion

It is interesting to highlight that in nature the skin is exposed to UV radiation and heat in a concurrent fashion; nevertheless, most studies have focused on understanding the effects of UV radiation *per se* on the skin better. Nowadays, the beneficial and deleterious effects of UV radiation on the skin have been well established; however, few studies have analyzed in depth the effect of heat shock on this organ, and thus far, it is poorly understood how UV radiation and heat shock interact in the regulation of several skin features.

Effects of UVA radiation and heat shock on the expression of *Opn2* and *Opn4*

Rhodopsin or OPN2 is a visual pigment essential for image formation, expressed in retinal rods. The importance of OPN2 in the visual process is clearly shown in patients harboring *Opn2* mutation, a condition that leads to autosomal dominant retinitis pigmentosa or congenital stationary night blindness.[57]

Melanopsin or OPN4 is a non-visual opsin[58–60] shown to be expressed in a subset of intrinsically photosensitive retinal ganglion cells,[7] which participates in the photo-entrainment of SCN.[6] Recently, it was shown that OPN4 is expressed in blood vessels where it mediates a blue light-dependent relaxation.[61] Our previous study has also shown that both normal and malignant melanocytes express *Opn4* and OPN4, which is a putative candidate to mediate white light effects on these cells.[14]

Few studies have evaluated the functionality of the photosensitive system within the skin and its cells. UVA radiation

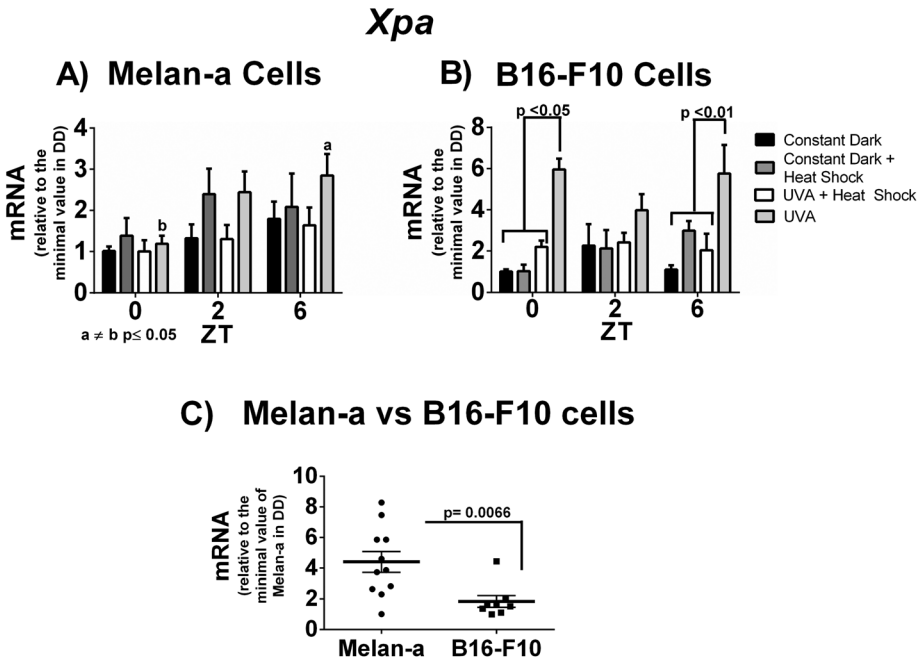

Fig. 5 *Xpa* mRNA levels in Melan-a and B16-F10 cells immediately (ZT 0), 2 h (ZT 2) and 6 h (ZT 6) after heat shock *per se*, UVA radiation *per se*, and a combination of both stimuli. Gene expression was normalized by 18S RNA transcript and expressed relative to the minimal value of each cell line in the DD control in (A) and (B) and to the minimal value of Melan-a cells in DD in (C). Gene expression values are shown as mean ± SEM. *p* values are shown in the graphs. (A) Melan-a *Xpa*, *n* = 3–7; (B) B16-F10 *Xpa*, *n* = 3–4; (C) comparison of *Xpa* levels in Melan-a and B16-F10 cells.

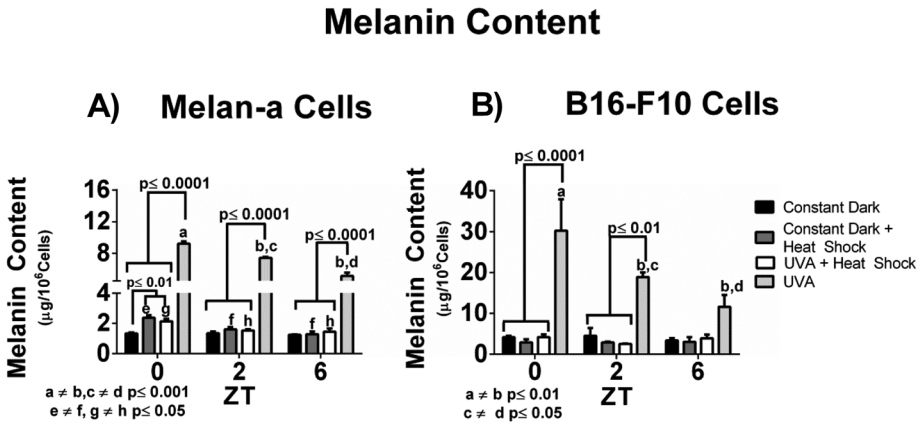

Fig. 6 Melanin content in Melan-a and B16-F10 cells immediately (ZT 0), 2 h (ZT 2) and 6 h (ZT 6) after heat shock *per se*, UVA radiation *per se*, and a combination of both stimuli. Melanin concentration is expressed in µg per 10^6 cells. *p* values are shown in the graphs. (A) Melan-a, *n* = 3–10; (B) B16-F10, *n* = 3–6.

and violet light have been shown to increase the expression of *Opn2* as well as negatively regulate the expression of differentiation markers, a process dependent on OPN2.[40] In human melanocytes, UVA radiation leads to a fast melanin synthesis, which is dependent on OPN2 signaling.[41] An intriguing fact is that the maximal peak of absorption of this opsin is approximately 500 nm,[62] and in order to respond to UVA, it should also be stimulated by a much shorter wavelength.

In normal melanocytes our data show that heat shock associated or not to UVA radiation led to a significant reduction of *Opn2* when compared to the control group or UVA alone. This finding is different from the one proposed by Kim and coworkers[40] who showed that UVA radiation increases the expression of *Opn2* in keratinocytes, but agrees with Haltaufderhyde and coworkers[38] who also found no effect of UVA radiation on human melanocytes and keratinocytes. It should be stressed that Kim and colleagues[40] used a 2 to 20-fold higher UV dose whereas Haltaufderhyde and colleagues[38] applied a similar UV dose as compared to our study (4.4 kJ m^{-2}).

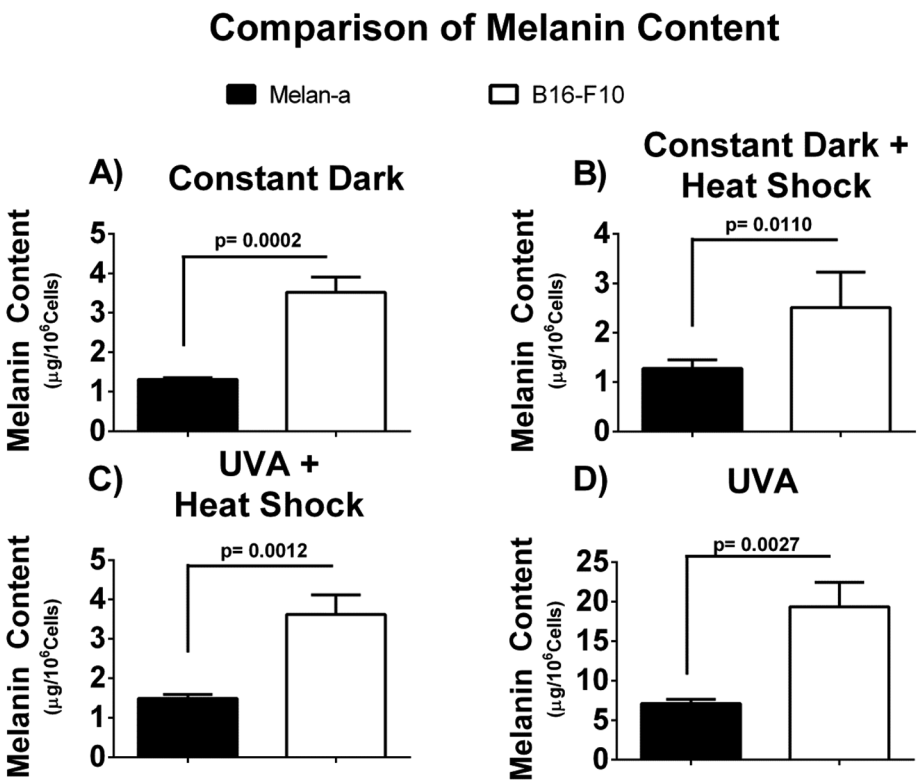

Fig. 7 Comparison of the melanin content in Melan-a and B16-F10 cells. The histogram is the average of melanin concentrations at ZT 0, ZT 2 and ZT 6. *p* values are shown in the graphs. (A) DD control, *n* = 15 and 12 for Melan-a and B16-F10 cells respectively; (B) heat shock, *n* = 16 and 12 for Melan-a and B16-F10 cells respectively; (C) UVA associated with heat shock, *n* = 16 and 12 for Melan-a and B16-F10 cells respectively; (D) UVA, *n* = 12 for both Melan-a and B16-F10 cells.

While heat shock reduced the expression of *Opn2* in Melan-a cells, the same stimulus increased the expression of this opsin in B16-F10 cells. The physiological relevance of these findings has yet to be established. In contrast to *Opn2*, *Opn4* transcript levels in normal melanocytes were not affected by any stimuli except UVA radiation. At ZT 6 we have found an increase of *Opn4* levels when compared to the remaining groups. When heat shock was applied in association with UVA radiation no increase is found, which shows a heat inhibitory effect. In malignant melanocytes we have found a temporal increase of *Opn4* transcripts only in the heat-exposed group. As for the UVA group, although no temporal variation was seen, a remarkable increase of *Opn4* expression took place as compared to DD and heat-exposed cells; however, the antagonistic effect of heat was not found. It should be stressed that the modification in the transcription levels of *Opn4* and *Opn2* in both cell types may not result in a proportional increase or decrease in the protein levels.

We have previously shown that *Opn4* was irresponsive to white light pulse in normal melanocytes, but exhibited an increase in response to this stimulus in malignant cells.[14] It is difficult to discuss our data on *Opn4* in light of the literature, since we are the first to report the expression of OPN4 in murine normal and malignant melanocytes,[14] and its response to white light,[14] heat and UVA (this work). Taken together, the data indicate that the malignant melanocytes show an increased response to heat shock and UVA radiation, despite the fact that *Opn2* and *Opn4* were severely downregulated as compared to normal melanocytes.[14]

Effects of UVA radiation and heat shock on the expression of clock genes

The effect of UV radiation is widely known in several skin traits such as pigmentation, DNA damage, reactive oxygen species generation, and cancer development.[42,43,63,64] Besides UV radiation – a classic factor associated with skin cancer – heat has been investigated over the past few years as a possible skin cancer risk factor.[46,65] It has been reported that heat shock itself leads to morphological changes in melanocytes such as an increased number of dendrites.[66] In the skin UVB-induced apoptosis and cell cycle arrest have been shown to be antagonized by heat stress applied after UVB radiation.[67] The survival of damaged cells could represent an important factor for skin carcinogenesis.[67] Within this line of thought, non-melanoma skin cancer in ten surveyed regions of USA not only correlated with the ambient UV dose but also with the average daily maximal temperature in the summer.[68] In our study UVA radiation was applied concomitantly with heat while in the study by Calapre and coworkers[67] heat stress was given after UVB exposure. Corroborating evidence by a study from our

laboratory has shown that the effects driven by light were different when heat was also applied.[69] In this study[69] it was demonstrated that the expression of *hsp90 aa1*, a gene that encodes a heat shock protein, was 2-fold lower when embryonic cells of *Danio rerio* were kept in the light–dark cycle and subjected to a 33 °C heat shock for one hour in comparison to heat shock alone. Therefore, it is of great interest to better understand the concurrent effects of heat shock with UV radiation and visible light.

The clock gene machinery of Melan-a cells was responsive to UVA radiation since a temporal increase was found in *Per1*, *Clock* and *Bmal1* transcripts. *Clock* showed increased expression in the UVA-stimulated cells when compared to all other groups. Interestingly, this increase is inhibited if UVA radiation is associated with heat shock, a phenomenon shown here for the first time. On the other hand, the clock gene machinery of B16-F10 cells was seen to be more sensitive than their normal counterparts, and responsive to heat shock and UVA radiation, as it has been previously shown for white light pulse[14] and estradiol.[15] Based on these data, one may say that the negative arm of the clock gene machinery is activated by heat shock and UVA radiation, a feature shown for the first time. *Bmal1* and *Clock* – members of the positive limb of the clock molecular core – are only responsive to UVA radiation *per se*. The increased clock gene levels shown here may not necessarily result in increased protein levels but the fact that the clock gene machinery of malignant melanocytes is more responsive than the one from normal melanocytes is of great relevance.

Our data further reinforce that the clock gene machinery of B16-F10 cells is downregulated in comparison to normal melanocytes as previously shown.[14,15] This downregulation might lead to the loss of temporal control of several physiologically relevant processes along evolution (teleost fish melanophores;[70] human melanocytes).[32] In fact, the downregulation of clock genes is a common feature in several cancers including skin cancer.[10,12,71] Recently, the impairment of clock genes in melanocytes has been suggested as a new therapy for skin depigmentation disorders.[32]

The consequences of the increased response of B16-F10 cells with subsequent clock gene activation require further studies; however, the fact that malignant melanocytes are more sensitive and responsive to white light pulse[14] and estradiol[15] as well as to UVA radiation and heat shock may represent an important step in the tumorigenic process, which can be classified as a new hallmark of cancer.[15,72,73]

Effect of UVA radiation and heat shock on the expression of *Xpa*

The excision repair process has several components and is able to remove almost all damaged DNA; this system is the only responsible for removing bulky DNA lesions such as cyclobutane pyrimidine dimers (CPD), 6,4 photoproducts (6-4 PP), and damage induced by cisplatin.[64] XPA, a member of this system, has been shown to oscillate in a circadian fashion in the mouse brain, liver, and skin.[30,74,75] In the latter, XPA protein levels were shown to be in the antiphase with CRY1. The peak of XPA occurs at night, coinciding with the onset of the locomotor activity of mice. The importance of XPA in the skin was shown when mice exposed to UVB radiation in the morning – when the levels of XPA were low – exhibited an increased number of skin tumors in comparison to those exposed at night,[30] which strongly suggests that *Xpa* and XPA are controlled by the skin clock.

Since DNA repair is less efficient in the morning, the UVB-induced damage is associated with DNA polymerase stalling in regions harboring unrepaired DNA damage, which leads to increased p53 activity with subsequent apoptosis and erythema.[76] Recently, we have demonstrated that *Xpa* expression is phase-delayed in response to estradiol in normal melanocytes; however, this response is lost in melanoma cells.[15] In this same study[15] we have found that *Xpa* levels are upregulated in melanoma cells when compared to melanocytes, which is different from what is shown here; however, in the latter study medium change was performed, a fact that led to a temporal increase in *Xpa* levels. Therefore under basal conditions *Xpa* expression is smaller in melanoma cells in comparison to normal melanocytes.

In normal cells, *Xpa* mRNA levels only oscillate in the UVA exposed group whereas malignant melanocytes exposed to UVA radiation displayed increased levels of *Xpa* when compared to all other groups. When UVA radiation was associated with heat shock the antagonistic effect was observed, which prevented the UVA-induced increase in *Xpa* levels. It should be highlighted that the reduced gene expression in malignant cells, which may not be translated into reduced protein levels, may not impair DNA repair, as it has been previously shown that 20% of XPA is enough to carry out genomic repair.[77]

Our data show that – despite being less expressed in malignant melanocytes than in normal cells – *Xpa* was responsive to UVA radiation only in B16-F10 cells. Following this line, the genomic instability results in gene mutation, which is associated with resistance to apoptosis in cancer. The combination of these two factors – increased gene mutation and apoptosis resistance – is known as one of the hallmarks of cancer.[72,73] Therefore, the response of *Xpa* towards UVA radiation might be involved in a putative DNA repair process which may contribute to apoptosis resistance – a widely known feature of melanoma.[78,79]

Effect of UVA radiation and heat shock on the melanin content

Melanogenesis, a characteristic process of pigment cells, is widely known to be deregulated in melanoma.[80,81] In both normal and malignant cell lines, no oscillation in the melanin content was found in the DD control group, whereas a remarkable increase in the melanin content was seen immediately after UVA radiation, which slightly decreased at ZT 2 and ZT 6. In normal melanocytes a slight, acute, and transient increase was found in response to heat shock *per se*, a profile very similar to the immediate pigment darkening (IPD).[56]

The melanin content increase in response to heat was originally shown more than a century ago by Meirowsky

(Meirowsky, 1909 in ref. 82); such an oxygen-dependent phenomenon was neglected for several decades[82–84] which resulted in a lack of studies correlating the effect of high temperature with the melanin content. It has been described that human melanocytes exposed to 42 °C for one hour exhibited increased dendricity when compared to the control. The prolonged exposure during three days resulted in increased levels of p53 and p21 as well as tyrosinase activity in the same fashion as did UVB radiation.[84] Thus, it would be expected that the temperature increase caused by UV radiation would accelerate and/or act synergistically in melanin synthesis;[85] however, a limitation of these studies is that the effects of UV radiation and heat on the skin were analyzed in an isolated fashion and never in a concurrent way.

In 1981 it was shown that the maximal tyrosinase activity of Himalayan mice take places at lower temperatures in comparison to the normal body temperature.[86] Since the skin is constantly exposed to fluctuation of temperatures, its temperature is usually lower than the core temperature.[87] Based on that, an interesting study[88] showed that at 31 °C a reduction of the melanin content and tyrosinase activity is found when compared to melanocytes kept at 37 °C.

The lack of similar studies in the literature does not allow an in depth discussion of our results; however, normal melanocytes showed an immediate melanin increase in response to heat shock, a fact that did not take place in malignant melanocytes. Thus, we speculate that the melanogenesis machinery of malignant melanocytes is maximally activated as a result of the carcinogenic process, since the average of melanin content under all experimental conditions is 3 to 4-fold higher than in normal cells. A second phenomenon shown here is the response profile of both cell lines to UVA radiation. Due to the short time interval and fast decay of the melanin content, the melanin increase seen here is IPD, which according to the literature is a result of the oxidation of pre-existing melanin.[56] Accordingly, the immediate increase in response to all stimuli in Melan-a cells, and to UVA in both normal and malignant melanocytes showed a time-dependent decrease, which is characteristic of oxidation, not a synthesis process. Interestingly, in human melanocytes it has been suggested that the IPD process is a result of a fast melanin synthesis.[41]

Our data corroborate the study by Hardman and colleagues[32] who found that the disruption of clock genes increases the melanin content in normal human melanocytes. In fact, the melanin content of malignant melanocytes is significantly higher in comparison to the normal ones, a fact that is likely linked to the downregulation of clock genes. Within this line of thought we have recently shown that estradiol does not affect the melanin content in normal melanocytes; however, in malignant cells estradiol reduces melanin levels. It is worth to highlight an inverse relationship between clock genes activation and melanin content in response to estradiol in malignant melanocytes.[15] In the latter estradiol was shown to increase clock gene expression as well as to reduce the melanin content, a fact that seems to be hormone-specific[15] since white light pulse[14] and UVA radiation (these data) increase the clock gene expression in malignant melanocytes with an increased melanin content only in cells exposed to UVA radiation.

It is known that murine and human pigmentary systems display some differences particularly due to the fact that furry animals lack active melanogenesis in their adult epidermis, except in non-hair-bearing sites such as the ear, nose and paws, and it is more pronounced in the hair follicle bulb.[80,81] Human skin, on the other hand, has an active melanogenesis process in both the epidermis and hair follicles. Moreover, most of the protection from UV radiation in mice is carried out by the fur and not by melanin itself; in humans melanin is the main source of protection from UV radiation.[80,81] Due to these differences as well as others,[80] our findings should be further evaluated in human skin.

5. Perspectives

Most events shown here in response to UVA were antagonized by heat shock. Since in nature both factors are present in a concurrent way, it is interesting to speculate their relevance for the cell and organism physiology. Thus, should we expect that the effects of these concurrent stimuli reflect the summation or the synergistic addition? Or would it be more plausible to speculate that both stimuli act in an antagonistic fashion, and the net result would be a mitigation of their individual effects? Following this reasoning, the physiological response evoked by these stimuli together would depend on the intensity of each one.

Based on this, our data warn us about the effect of heat in experiments using UV radiation since it is a common feature of the UV apparatus to generate heat. Thus, the heat produced during UV experiments should be carefully monitored since the temperature represents, according to our results, an important confounding factor, and therefore it should be dissociated from UV in experiments using UV radiation.

Finally, we acknowledge that although we are the first to show the inhibitory profile of heat when associated with UVA radiation, we describe here a biological principle occurring under specific experimental conditions in murine melanocyte and melanoma lines without evidence of reproducibility in any other mammalian experimental system or organ and as yet of unclear biological relevance.

Competing interests

None to declare.

Author contributions

All authors designed the study. L. V. M. de Assis acquired the data. L. V. M. de Assis and M. N. Moraes analyzed the data. L. V. M. de Assis drafted the manuscript, and M. N. Moraes and A. M. L. Castrucci critically revised the draft. All authors have approved the final version of the manuscript

and agreed to be accountable for all aspects of the study in ensuring that questions related to the accuracy or integrity of any part of the study are appropriately investigated and resolved. All persons designated as authors qualify for authorship, and all those who qualify for authorship are listed.

Abbreviations

6-4 PP	6,4 Photoproducts
Aqp3	Aquaporin 3 gene
BMAL1	Aryl hydrocarbon receptor nuclear translocator-like protein 1
Bmal1	Aryl hydrocarbon receptor nuclear translocator-like protein 1 gene
CLOCK	Circadian locomotor output cycles kaput protein
Clock	Circadian locomotor output cycles kaput gene
CPD	Cyclobutane pyrimidine dimers
CRY	Cryptochrome protein
Cry	Cryptochrome gene
DD	Constant dark
FBS	Fetal bovine serum
IPD	Immediate pigment darkening
LD	Light–dark cycle
PER	Period protein
Per	Period gene
PI	Propidium iodide
Rev-Erbα/β	RAR-related orphan receptor alpha/beta gene
RORα/β	Nuclear receptor subfamily 1, group D, member 1/2 gene
SCNs	Suprachiasmatic nuclei
TPA	Phorbol 12-myristate 13-acetate
UVB	Ultraviolet B radiation
XPA	Xeroderma pigmentosum, complementation group A protein
Xpa	Xeroderma pigmentosum, complementation group A gene
ZT	Zeitgeber time

Acknowledgements

This work was partially supported by the Sao Paulo Research Foundation (FAPESP, grant 2012/50214-4) and by the National Council of Technological and Scientific Development (CNPq, grants 301293/2011-2 and 303070/2015-3). L. V. M. de Assis and M. N. Moraes are fellows of FAPESP (2013/24337-4 and 2014/16412-9, respectively). We are thankful to Prof. Carlos Frederico Martins Menck and Mr Gustavo Satoru Kajitani (both from the Institute of Biomedical Science, University of São Paulo) for providing theoretical and methodological insights and advices as well as for providing equipment to measure UVA/UVB irradiance. We also thank Dr Elvo Burini Junior (the Institute of Environment and Energy, University of São Paulo) for carrying out the spectrum analysis of the UVA lamps used in this study.

References

1 J. B. Hogenesch and H. R. Ueda, Understanding systems-level properties: timely stories from the study of clocks, *Nat. Rev. Genet.*, 2011, **12**, 407–416.
2 S. A. Brown and A. Azzi, Peripheral circadian oscillators in mammals, *Handb. Exp. Pharmacol.*, 2013, **217**, 45–66.
3 E. D. Buhr and J. S. Takahashi, Molecular components of the Mammalian circadian clock, *Handb. Exp. Pharmacol.*, 2013, **217**, 3–27.
4 J. A. Mohawk, C. B. Green and J. S. Takahashi, Central and peripheral circadian clocks in mammals, *Annu. Rev. Neurosci.*, 2012, **35**, 445–462.
5 M. R. Ralph, R. G. Foster, F. C. Davis and M. Menaker, Transplanted suprachiasmatic nucleus determines circadian period, *Science*, 1990, **247**, 975–978.
6 S. Panda, I. Provencio, D. C. Tu, S. S. Pires, M. D. Rollag, A. M. Castrucci, M. T. Pletcher, T. K. Sato, T. Wiltshire, M. Andahazy, S. A. Kay, R. N. Van Gelder and J. B. Hogenesch, Melanopsin is required for non-image-forming photic responses in blind mice, *Science*, 2003, **301**, 525–527.
7 I. Provencio, M. D. Rollag and A. M. Castrucci, Photoreceptive net in the mammalian retina. This mesh of cells may explain how some blind mice can still tell day from night, *Nature*, 2002, **415**, 493.
8 D. M. Berson, F. A. Dunn and M. Takao, Phototransduction by retinal ganglion cells that set the circadian clock, *Science*, 2002, **295**, 1070–1073.
9 S. Hughes, M. W. Hankins, R. G. Foster and S. N. Peirson, Melanopsin phototransduction: slowly emerging from the dark, *Prog. Brain Res.*, 2012, **199**, 19–40.
10 K. G. Baron and K. J. Reid, Circadian misalignment and health, *Int. Rev. Psychiatry*, 2014, **26**, 139–154.
11 F. C. Kelleher, A. Rao and A. Maguire, Circadian molecular clocks and cancer, *Cancer Lett.*, 2014, **342**, 9–18.
12 C. Savvidis and M. Koutsilieris, Circadian rhythm disruption in cancer biology, *Mol. Med.*, 2012, **18**, 1249–1260.
13 S. Kawara, R. Mydlarski, A. J. Mamelak, I. Freed, B. Wang, H. Watanabe, G. Shivji, S. K. Tavadia, H. Suzuki, G. A. Bjarnason, R. C. Jordan and D. N. Sauder, Low-dose ultraviolet B rays alter the mRNA expression of the circadian clock genes in cultured human keratinocytes, *J. Invest. Dermatol.*, 2002, **119**, 1220–1223.
14 L. V. de Assis, M. N. Moraes, S. da Silveira Cruz-Machado and A. M. Castrucci, The effect of white light on normal and malignant murine melanocytes: A link between opsins, clock genes, and melanogenesis, *Biochim. Biophys. Acta*, 2016, **1863**, 1119–1133.
15 M. O. Poletini, L. V. M. de Assis, M. N. Moraes and A. M. L. Castrucci, Estradiol Differently Affects Melanin Synthesis of Malignant and Normal Melanocytes - a Relationship With Clock and Clock Controlled Genes, *Mol. Cell. Biochem.*, 2016, **421**, 29–39.
16 E. D. Buhr, S. H. Yoo and J. S. Takahashi, Temperature as a universal resetting cue for mammalian circadian oscillators, *Science*, 2010, **330**, 379–385.

17 U. Abraham, A. E. Granada, P. O. Westermark, M. Heine, A. Kramer and H. Herzel, Coupling governs entrainment range of circadian clocks, *Mol. Syst. Biol.*, 2010, **6**, 438.
18 S. A. Brown, G. Zumbrunn, F. Fleury-Olela, N. Preitner and U. Schibler, Rhythms of mammalian body temperature can sustain peripheral circadian clocks, *Curr. Biol.*, 2002, **12**, 1574–1583.
19 C. Saini, J. Morf, M. Stratmann, P. Gos and U. Schibler, Simulated body temperature rhythms reveal the phase-shifting behavior and plasticity of mammalian circadian oscillators, *Genes Dev.*, 2012, **26**, 567–580.
20 F. Sporl, K. Schellenberg, T. Blatt, H. Wenck, K. P. Wittern, A. Schrader and A. Kramer, A circadian clock in HaCaT keratinocytes, *J. Invest. Dermatol.*, 2011, **131**, 338–348.
21 D. Gutierrez and J. Arbesman, Circadian Dysrhythmias, Physiological Aberrations, and the Link to Skin Cancer, *Int. J. Mol. Sci.*, 2016, **17**, 621.
22 A. J. Luber, S. H. Ensanyat and J. A. Zeichner, Therapeutic implications of the circadian clock on skin function, *J. Drugs Dermatol.*, 2014, **13**, 130–134.
23 M. S. Matsui, E. Pelle, K. Dong and N. Pernodet, Biological Rhythms in the Skin, *Int. J. Mol. Sci.*, 2016, **17**, 801.
24 M. V. Plikus, E. N. Van Spyk, K. Pham, M. Geyfman, V. Kumar, J. S. Takahashi and B. Andersen, The circadian clock in skin: implications for adult stem cells, tissue regeneration, cancer, aging, and immunity, *J. Biol. Rhythms*, 2015, **30**, 163–182.
25 C. Sandu, M. Dumas, A. Malan, D. Sambakhe, C. Marteau, C. Nizard, S. Schnebert, E. Perrier, E. Challet, P. Pevet and M. P. Felder-Schmittbuhl, Human skin keratinocytes, melanocytes, and fibroblasts contain distinct circadian clock machineries, *Cell. Mol. Life Sci.*, 2012, **69**, 3329–3339.
26 G. Yosipovitch, L. Sackett-Lundeen, A. Goon, C. Yiong Huak, C. Leok Goh and E. Haus, Circadian and ultradian (12 h) variations of skin blood flow and barrier function in non-irritated and irritated skin-effect of topical corticosteroids, *J. Invest. Dermatol.*, 2004, **122**, 824–829.
27 I. Le Fur, A. Reinberg, S. Lopez, F. Morizot, M. Mechkouri and E. Tschachler, Analysis of circadian and ultradian rhythms of skin surface properties of face and forearm of healthy women, *J. Invest. Dermatol.*, 2001, **117**, 718–724.
28 G. Yosipovitch, G. L. Xiong, E. Haus, L. Sackett-Lundeen, I. Ashkenazi and H. I. Maibach, Time-dependent variations of the skin barrier function in humans: transepidermal water loss, stratum corneum hydration, skin surface pH, and skin temperature, *J. Invest. Dermatol.*, 1998, **110**, 20–23.
29 N. Matsunaga, K. Itcho, K. Hamamura, E. Ikeda, H. Ikeyama, Y. Furuichi, M. Watanabe, S. Koyanagi and S. Ohdo, 24-hour rhythm of aquaporin-3 function in the epidermis is regulated by molecular clocks, *J. Invest. Dermatol.*, 2014, **134**, 1636–1644.
30 S. Gaddameedhi, C. P. Selby, W. K. Kaufmann, R. C. Smart and A. Sancar, Control of skin cancer by the circadian rhythm, *Proc. Natl. Acad. Sci. U. S. A.*, 2011, **108**, 18790–18795.
31 M. Geyfman, V. Kumar, Q. Liu, R. Ruiz, W. Gordon, F. Espitia, E. Cam, S. E. Millar, P. Smyth, A. Ihler, J. S. Takahashi and B. Andersen, Brain and muscle Arnt-like protein-1 (BMAL1) controls circadian cell proliferation and susceptibility to UVB-induced DNA damage in the epidermis, *Proc. Natl. Acad. Sci. U. S. A.*, 2012, **109**, 11758–11763.
32 J. A. Hardman, D. J. Tobin, I. S. Haslam, N. Farjo, B. Farjo, Y. Al-Nuaimi, B. Grimaldi and R. Paus, The peripheral clock regulates human pigmentation, *J. Invest. Dermatol.*, 2015, **135**, 1053–1064.
33 M. Tanioka, H. Yamada, M. Doi, H. Bando, Y. Yamaguchi, C. Nishigori and H. Okamura, Molecular clocks in mouse skin, *J. Invest. Dermatol.*, 2009, **129**, 1225–1231.
34 B. Iyengar, The melanocyte photosensory system in the human skin, *SpringerPlus*, 2013, **2**, 158.
35 G. J. Lopes, C. C. Gois, L. H. Lima and A. M. Castrucci, Modulation of rhodopsin gene expression and signaling mechanisms evoked by endothelins in goldfish and murine pigment cell lines, *Braz. J. Med. Biol. Res.*, 2010, **43**, 828–836.
36 Y. Miyashita, T. Moriya, T. Kubota, K. Yamada and K. Asami, Expression of opsin molecule in cultured murine melanocyte, *J. Invest. Dermatol. Symp. Proc.*, 2001, **6**, 54–57.
37 M. Tsutsumi, K. Ikeyama, S. Denda, J. Nakanishi, S. Fuziwara, H. Aoki and M. Denda, Expressions of rod and cone photoreceptor-like proteins in human epidermis, *Exp. Dermatol.*, 2009, **18**, 567–570.
38 K. Haltaufderhyde, R. N. Ozdeslik, N. L. Wicks, J. A. Najera and E. Oancea, Opsin expression in human epidermal skin, *Photochem. Photobiol.*, 2015, **91**, 117–123.
39 N. W. Bellono, L. G. Kammel, A. L. Zimmerman and E. Oancea, UV light phototransduction activates transient receptor potential A1 ion channels in human melanocytes, *Proc. Natl. Acad. Sci. U. S. A.*, 2013, **110**, 2383–2388.
40 H. J. Kim, E. D. Son, J. Y. Jung, H. Choi, T. R. Lee and D. W. Shin, Violet light down-regulates the expression of specific differentiation markers through Rhodopsin in normal human epidermal keratinocytes, *PLoS One*, 2013, **8**, e73678.
41 N. L. Wicks, J. W. Chan, J. A. Najera, J. M. Ciriello and E. Oancea, UVA phototransduction drives early melanin synthesis in human melanocytes, *Curr. Biol.*, 2011, **21**, 1906–1911.
42 E. Dupont, J. Gomez and D. Bilodeau, Beyond UV radiation: a skin under challenge, *Int. J. Cosmet. Sci.*, 2013, **35**, 224–232.
43 L. R. Sklar, F. Almutawa, H. W. Lim and I. Hamzavi, Effects of ultraviolet radiation, visible light, and infrared radiation on erythema and pigmentation: a review, *Photochem. Photobiol. Sci.*, 2013, **12**, 54–64.
44 C. Fortes and E. de Vries, Nonsolar occupational risk factors for cutaneous melanoma, *Int. J. Dermatol.*, 2008, **47**, 319–328.
45 H. S. Lee, D. H. Lee, S. Cho and J. H. Chung, Minimal heating dose: a novel biological unit to measure infrared irradiation, *Photodermatol., Photoimmunol. Photomed.*, 2006, **22**, 148–152.

46 L. Calapre, E. S. Gray and M. Ziman, Heat stress: a risk factor for skin carcinogenesis, *Cancer Lett.*, 2013, **337**, 35–40.
47 J. S. Dover, T. J. Phillips and K. A. Arndt, Cutaneous effects and therapeutic uses of heat with emphasis on infrared radiation, *J. Am. Acad. Dermatol.*, 1989, **20**, 278–286.
48 L. H. Kligman, Intensification of ultraviolet-induced dermal damage by infrared radiation, *Arch. Dermatol. Res.*, 1982, **272**, 229–238.
49 L. H. Kligman and A. M. Kligman, Reflections on heat, *Br. J. Dermatol.*, 1984, **110**, 369–375.
50 D. C. Bennett, P. J. Cooper and I. R. Hart, A line of non-tumorigenic mouse melanocytes, syngeneic with the B16 melanoma and requiring a tumour promoter for growth, *Int. J. Cancer*, 1987, **39**, 414–418.
51 C. Riccardi and I. Nicoletti, Analysis of apoptosis by propidium iodide staining and flow cytometry, *Nat. Protoc.*, 2006, **1**, 1458–1461.
52 K. J. Livak and T. D. Schmittgen, Analysis of relative gene expression data using real-time quantitative PCR and the 2(-Delta Delta C(T)) Method, *Methods*, 2001, **25**, 402–408.
53 M. Kajstura, H. D. Halicka, J. Pryjma and Z. Darzynkiewicz, Discontinuous fragmentation of nuclear DNA during apoptosis revealed by discrete "sub-G1" peaks on DNA content histograms, *Cytometry, Part A*, 2007, **71**, 125–131.
54 E. D. Buhr, W. W. Yue, X. Ren, Z. Jiang, H. W. Liao, X. Mei, S. Vemaraju, M. T. Nguyen, R. R. Reed, R. A. Lang, K. W. Yau and R. N. Van Gelder, Neuropsin (OPN5)-mediated photoentrainment of local circadian oscillators in mammalian retina and cornea, *Proc. Natl. Acad. Sci. U. S. A.*, 2015, **112**, 13093–13098.
55 D. Kojima, S. Mori, M. Torii, A. Wada, R. Morishita and Y. Fukada, UV-sensitive photoreceptor protein OPN5 in humans and mice, *PLoS One*, 2011, **6**, e26388.
56 Y. J. Hwang, H. J. Park, H. J. Hahn, J. Y. Kim, J. H. Ko, Y. W. Lee, Y. B. Choe and K. J. Ahn, Immediate pigment darkening and persistent pigment darkening as means of measuring the ultraviolet A protection factor in vivo: a comparative study, *Br. J. Dermatol.*, 2011, **164**, 1356–1361.
57 S. D. McAlear, T. W. Kraft and A. K. Gross, 1 rhodopsin mutations in congenital night blindness, *Adv. Exp. Med. Biol.*, 2010, **664**, 263–272.
58 M. C. Isoldi, M. D. Rollag, A. M. Castrucci and I. Provencio, Rhabdomeric phototransduction initiated by the vertebrate photopigment melanopsin, *Proc. Natl. Acad. Sci. U. S. A.*, 2005, **102**, 1217–1221.
59 M. N. Moraes, L. H. Lima, B. C. Ramos, M. O. Poletini and A. M. Castrucci, Endothelin modulates the circadian expression of non-visual opsins, *Gen. Comp. Endocrinol.*, 2014, **205**, 279–286.
60 I. Provencio, G. Jiang, W. J. De Grip, W. P. Hayes and M. D. Rollag, Melanopsin: An opsin in melanophores, brain, and eye, *Proc. Natl. Acad. Sci. U. S. A.*, 1998, **95**, 340–345.
61 G. Sikka, G. P. Hussmann, D. Pandey, S. Cao, D. Hori, J. T. Park, J. Steppan, J. H. Kim, V. Barodka, A. C. Myers, L. Santhanam, D. Nyhan, M. K. Halushka, R. C. Koehler, S. H. Snyder, L. A. Shimoda and D. E. Berkowitz, Melanopsin mediates light-dependent relaxation in blood vessels, *Proc. Natl. Acad. Sci. U. S. A.*, 2014, **111**, 17977–17982.
62 H. Imai, V. Kefalov, K. Sakurai, O. Chisaka, Y. Ueda, A. Onishi, T. Morizumi, Y. Fu, K. Ichikawa, K. Nakatani, Y. Honda, J. Chen, K. W. Yau and Y. Shichida, Molecular properties of rhodopsin and rod function, *J. Biol. Chem.*, 2007, **282**, 6677–6684.
63 M. Brenner and V. J. Hearing, The protective role of melanin against UV damage in human skin, *Photochem. Photobiol.*, 2008, **84**, 539–549.
64 C. F. M. Menck and V. Munford, DNA repair diseases: What do they tell us about cancer and aging?, *Genet. Mol. Biol.*, 2014, **37**, 220–233.
65 S. Cho, M. H. Shin, Y. K. Kim, J. E. Seo, Y. M. Lee, C. H. Park and J. H. Chung, Effects of infrared radiation and heat on human skin aging in vivo, *J. Invest. Dermatol. Symp. Proc.*, 2009, **14**, 15–19.
66 V. Cavallari, R. Cicciarello, V. Torre, M. E. Gagliardi, F. Albiero, R. Palazzo, M. Siragusa and C. Schipis, Chronic heat-induced skin lesions (erythema ab Igne): ultrastructural studies, *Ultrastruct. Pathol.*, 2001, **25**, 93–97.
67 L. Calapre, E. S. Gray, S. Kurdykowski, A. David, P. Hart, P. Descargues and M. Ziman, Heat-mediated reduction of apoptosis in UVB-damaged keratinocytes in vitro and in human skin ex vivo, *BMC Dermatol.*, 2016, **16**, 6.
68 J. C. van der Leun, R. D. Piacentini and F. R. de Gruijl, Climate change and human skin cancer, *Photochem. Photobiol. Sci.*, 2008, **7**, 730–733.
69 R. Jerônimo, M. N. Moraes, L. V. M. de Assis, B. C. Ramos, T. C. Rocha and A. M. L. Castrucci, Thermal Stress in Danio rerio: a Link between Temperature, Light, Thermo-TRP Channels, and Clock Genes, *J. Therm. Biol.*, 2016, Accepted manuscript.
70 N. Hamilton, N. Diaz-de-Cerio and D. Whitmore, Impaired light detection of the circadian clock in a zebrafish melanoma model, *Cell Cycle*, 2015, **14**, 1232–1241.
71 Z. Lengyel, C. Lovig, S. Kommedal, R. Keszthelyi, G. Szekeres, Z. Battyani, V. Csernus and A. D. Nagy, Altered expression patterns of clock gene mRNAs and clock proteins in human skin tumors, *Tumour Biol.*, 2013, **34**, 811–819.
72 D. Hanahan and R. A. Weinberg, The hallmarks of cancer, *Cell*, 2000, **100**, 57–70.
73 D. Hanahan and R. A. Weinberg, Hallmarks of cancer: the next generation, *Cell*, 2011, **144**, 646–674.
74 T. H. Kang, L. A. Lindsey-Boltz, J. T. Reardon and A. Sancar, Circadian control of XPA and excision repair of cisplatin-DNA damage by cryptochrome and HERC2 ubiquitin ligase, *Proc. Natl. Acad. Sci. U. S. A.*, 2010, **107**, 4890–4895.
75 T. H. Kang, J. T. Reardon, M. Kemp and A. Sancar, Circadian oscillation of nucleotide excision repair in mammalian brain, *Proc. Natl. Acad. Sci. U. S. A.*, 2009, **106**, 2864–2870.

76 S. Gaddameedhi, C. P. Selby, M. G. Kemp, R. Ye and A. Sancar, The circadian clock controls sunburn apoptosis and erythema in mouse skin, *J. Invest. Dermatol.*, 2015, **135**, 1119–1127.
77 A. R. Muotri, M. C. N. Marchetto, M. F. Suzuki, K. Okazaki, C. F. P. Lotfi, G. Brumatti, G. P. Amarante-Mendes and C. F. M. Menck, Low amounts of the DNA repair XPA protein are sufficient to recover UV-resistance, *Carcinogenesis*, 2002, **23**, 1039–1046.
78 A. Daponte, P. A. Ascierto, A. Gravina, M. Melucci, S. Scala, A. Ottaiano, E. Simeone, G. Palmieris and G. Comella, Temozolomide and cisplatin in avdanced malignant melanoma, *Anticancer Res.*, 2005, **25**, 1441–1447.
79 H. Helmbach, E. Rossmann, M. A. Kern and D. Schadendorf, Drug-resistance in human melanoma, *Int. J. Cancer*, 2001, **93**, 617–622.
80 A. Slominski, D. J. Tobin, S. Shibahara and J. Wortsman, Melanin pigmentation in mammalian skin and its hormonal regulation, *Physiol. Rev.*, 2004, **84**, 1155–1228.
81 J. Y. Lin and D. E. Fisher, Melanocyte biology and skin pigmentation, *Nature*, 2007, **445**, 843–850.
82 G. H. Findlay and L. W. Van der Merwe, The Meirowsky phenomenon. Colour changes in melanin according to temperature and redox potential, *Br. J. Dermatol.*, 1966, **78**, 572–576.
83 K. Maeda and M. Hatao, Involvement of photooxidation of melanogenic precursors in prolonged pigmentation induced by ultraviolet A, *J. Invest. Dermatol.*, 2004, **122**, 503–509.
84 K. Nakazawa, F. Sahuc, O. Damour, C. Collombel and H. Nakazawa, Regulatory effects of heat on normal human melanocyte growth and melanogenesis: comparative study with UVB, *J. Invest. Dermatol.*, 1998, **110**, 972–977.
85 T. B. Fitzpatrick and G. Szabo, Part III: General Considerations of Skin Pigmentation: The Melanocyte: Cytology and Cytochemistry1, *J. Invest. Dermatol.*, 1959, **32**, 197–206.
86 S. H. Kidson and B. C. Fabian, The effect of temperature on tyrosinase activity in Himalayan mouse skin, *J. Exp. Zool.*, 1981, **215**, 91–97.
87 F. G. Benedict, W. R. Miles and A. Johnson, The Temperature of the Human Skin, *Proc. Natl. Acad. Sci. U. S. A.*, 1919, **5**, 218–222.
88 D. S. Kim, S. H. Park, S. B. Kwon, Y. H. Joo, S. W. Youn, U. D. Sohn and K. C. Park, Temperature regulates melanin synthesis in melanocytes, *Arch. Pharmacal Res.*, 2003, **26**, 840–845.

Chapter 4: Melanopsin, a Canonical Light Receptor, Mediates Thermal Activation of Clock Genes

The content provided in this chapter has been published in Scientific Reports, 2017, 7 13977. DOI: 10.1038/s41598-017-13939-3.

Authors' names: Moraes MN*, de Assis LVM*, Magalhães-Marques KK, Poletini MO, Lima LHRG, Castrucci AML.

* Joint first authors

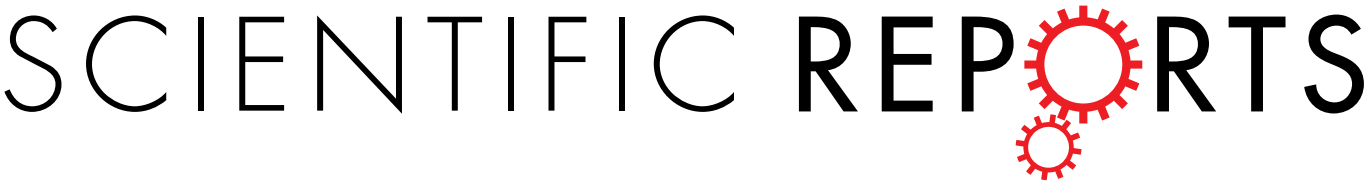

OPEN

Melanopsin, a Canonical Light Receptor, Mediates Thermal Activation of Clock Genes

Received: 9 June 2017
Accepted: 3 October 2017
Published online: 25 October 2017

Maria Nathália Moraes[1], Leonardo Vinícius Monteiro de Assis[1], Keila Karoline Magalhães-Marques[1], Maristela Oliveira Poletini[2], Leonardo Henrique Ribeiro Graciani de Lima[1] & Ana Maria de Lauro Castrucci[1,3]

Melanopsin (OPN4) is a photo-pigment found in a small subset of intrinsically photosensitive ganglion cells (ipRGCs) of the mammalian retina. These cells play a role in synchronizing the central circadian pacemaker to the astronomical day by conveying information about ambient light to the hypothalamic suprachiasmatic nucleus, the site of the master clock. We evaluated the effect of a heat stimulus (39.5 °C) on clock gene (*Per1 and Bmal1*) expression in cultured murine Melan-a melanocytes synchronized by medium changes, and in B16-F10 melanoma cells, in the presence of the selective OPN4 antagonist AA92593, or after OPN4 knockdown by small interfering RNA (siRNA). In addition, we evaluated the effects of heat shock on the localization of melanopsin by immunocytochemistry. In both cell lines melanopsin was found in a region capping the nucleus and heat shock did not affect its location. The heat-induced increase of *Per1* expression was inhibited when melanopsin was pharmacologically blocked by AA92593 as well as when its protein expression was suppressed by siRNA in both Melan-a and B16-F10 cells. These data strongly suggest that melanopsin is required for thermo-reception, acting as a thermo-opsin that ultimately feeds the local circadian clock in mouse melanocytes and melanoma cells.

The canonical role of melanopsin (OPN4) is to act as a photo-pigment in the mammalian intrinsically photosensitive retinal ganglion cells (ipRGCs)[1]. These cells play a role in synchronizing the central circadian pacemaker[2] to the astronomical day by conveying information about ambient light to the hypothalamic suprachiasmatic nucleus (SCN), the site of the master clock[3]. Another function of melanopsin that was recently described is its participation in early visual system formation[4]. Upon photo-activation of mammalian ipRGCs, OPN4 triggers a signaling cascade leading to phospholipase C activation and subsequent opening of transient potential receptor channels, TRPC6/7, which ultimately leads to membrane depolarization[5].

ipRGC axons release glutamate at the SCN neurons, increasing *Per* transcripts which reset the clock gene machinery. The biological mechanism of keeping track of time takes place through positive and negative interlaced feedback loops (reviewed in[6]). In summary, CLOCK and BMAL1 form a heterodimer that activates *Per* and *Cry* genes. PER and CRY proteins dimerize and after phosphorylation by casein kinases, are targeted to the nucleus, inhibiting the action of CLOCK/BMAL1. Once PER/CRY heterodimers are degraded, their inhibitory effect is reduced, and then CLOCK/BMAL1 is freed to start a new cycle of transcription. The core of clock gene machinery, described above, is stabilized by Rev-Erbα/β and RORα/β, whose transcripts are induced by CLOCK/BMAL1; Rev-Erbα/β inhibits while RORα/β activates *Bmal1*[6].

A local temporal controlling machinery has been found in almost every organ tested, comprising a multi-oscillatory system. These peripheral clocks are under the SCN control, which ensures that the whole organism is orchestrated in a single timing zone, allowing a harmonic working relationship among organs and systems[6–8].

Interestingly, rhodopsin (OPN2), classically associated with image formation in arthropods and vertebrates[9], has been demonstrated to participate in *Drosophila* temperature sensing. *Drosophila* larvae lacking rhodopsin lose

[1]Department of Physiology, Institute of Biosciences, University of São Paulo, São Paulo, Brazil. [2]Department of Physiology and Biophysics, Institute of Biological Sciences, Federal University of Minas Gerais, Minas Gerais, Brazil. [3]Department of Biology, University of Virginia, Charlottesville, VA, USA. Maria Nathália Moraes and Leonardo Vinícius Monteiro de Assis contributed equally to this work. Correspondence and requests for materials should be addressed to A.M.d.L.C. (email: amdlcast@ib.usp.br)

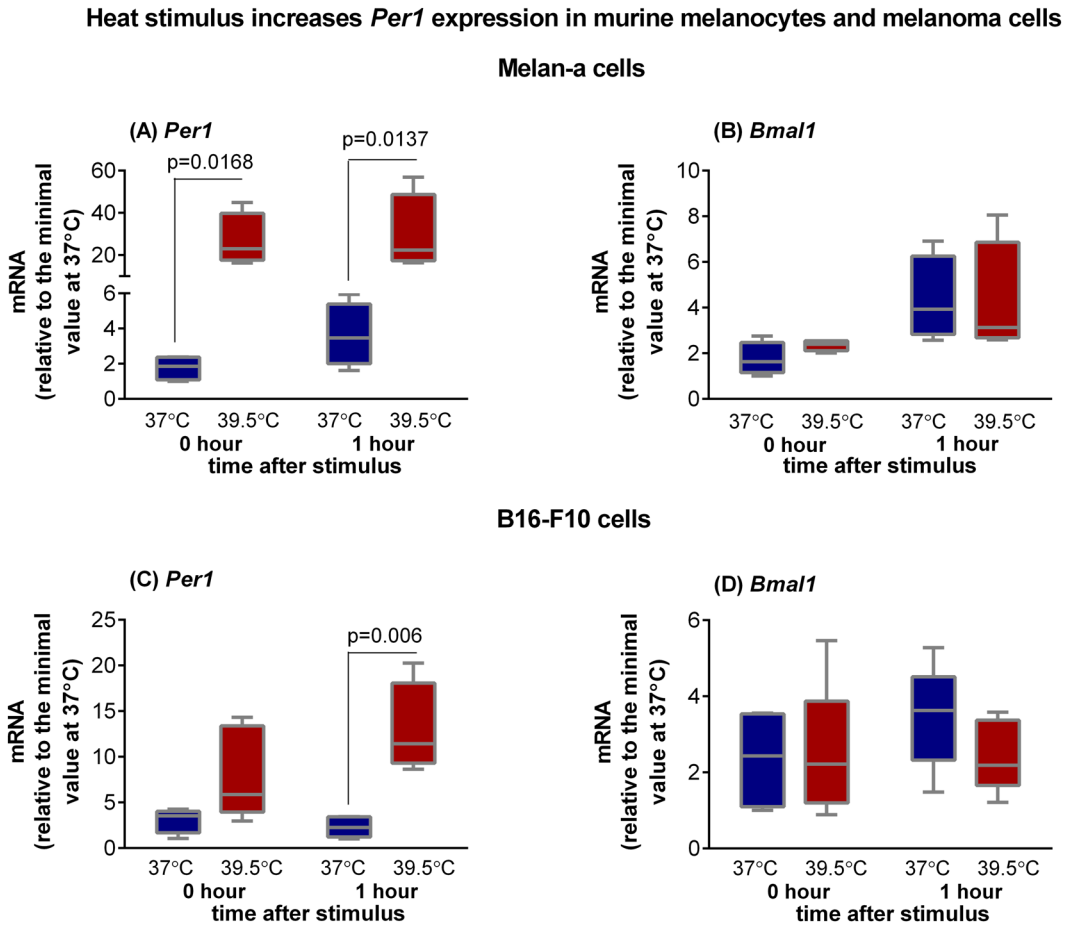

Figure 1. Expression of *Per1* (**A** and **C**) and *Bmal1* (**B** and **D**) in murine Melan-a melanocytes and B16-F10 melanoma cells after heat stimulus (39.5 °C). Melan-a or B16-F10 cells were kept for 3 days in constant dark and temperature (37 °C). In the beginning of the 4th day, Melan-a cells were synchronized by two medium changes and after further 24 hours they were heat-stimulated (39.5 °C) during 1 h. B16-F10 cells were heat stimulated in the beginning of the 4th day. Total RNA was extracted immediately and 1 h after the end of the stimulus for Melan-a and B16-F10 cells. Boxplots show the median, quartiles, maximum, and minimum expression values of each gene transcript normalized by 18S ribosomal RNA (for Melan-a cells) and *Rpl37a* (for B16-F10 cells), and expressed relative to the minimal value at 37 °C (N = 4–6). Statistical analysis was performed by Two-way ANOVA followed by Bonferroni post-test.

the ability of thermo-discrimination[10–12], which can be rescued by the targeted expression of mouse melanopsin[10]. In addition, melanopsin has been recently reported in murine blood vessels[13], in which it mediates blue-light dependent photo-relaxation. Since the vascular physiology is under circadian control[14], one may suggest that melanopsin could act as sensor that ultimately feeds the local temporal controlling system. Following this line, our group has shown that melanopsin and rhodopsin are expressed in murine melanocytes and melanoma cells where they may participate in a photo-sensitive system[15]. Based on these findings, we questioned whether an opsin could also function as a thermo-sensor in mammalian cells, conveying temperature information to the clock gene machinery of cutaneous melanocytes, cells known to be exposed to cycles of environmental light and temperature[16].

Results and Discussion

We evaluated the effect of a heat stimulus (39.5 °C) on clock gene expression in cultured Melan-a melanocytes and B16-F10 melanoma cells. Cells were maintained for three days under constant darkness and temperature (37 °C), a situation in which each cell displays its own rhythm of clock gene expression, usually leading to undetectable rhythm of the cell culture[17]. Melan-a cells exposed to 1 h heat pulse (39.5 °C) showed no difference from control cells in *Per1*, and *Bmal1* expression 0, 1 and 2 h after the stimulus (Supplemental Fig. 1). Because no effect was found in non-synchronized melanocytes, our next step was to repeat the same assay in cells synchronized by two medium changes[18,19]. In fact, 24 h after cell synchronization, heat shock led to increased *Per1* (0 and 1 h after the stimulus, Fig. 1A) but not *Bmal1* (Fig. 1B) expression. On the other hand, heat shock induced *Per1* increase in B16-F10 cells in constant dark condition 1 h after the end of the stimulus (Fig. 1C). Again, *Bmal1* was irresponsive to heat shock (Fig. 1D).

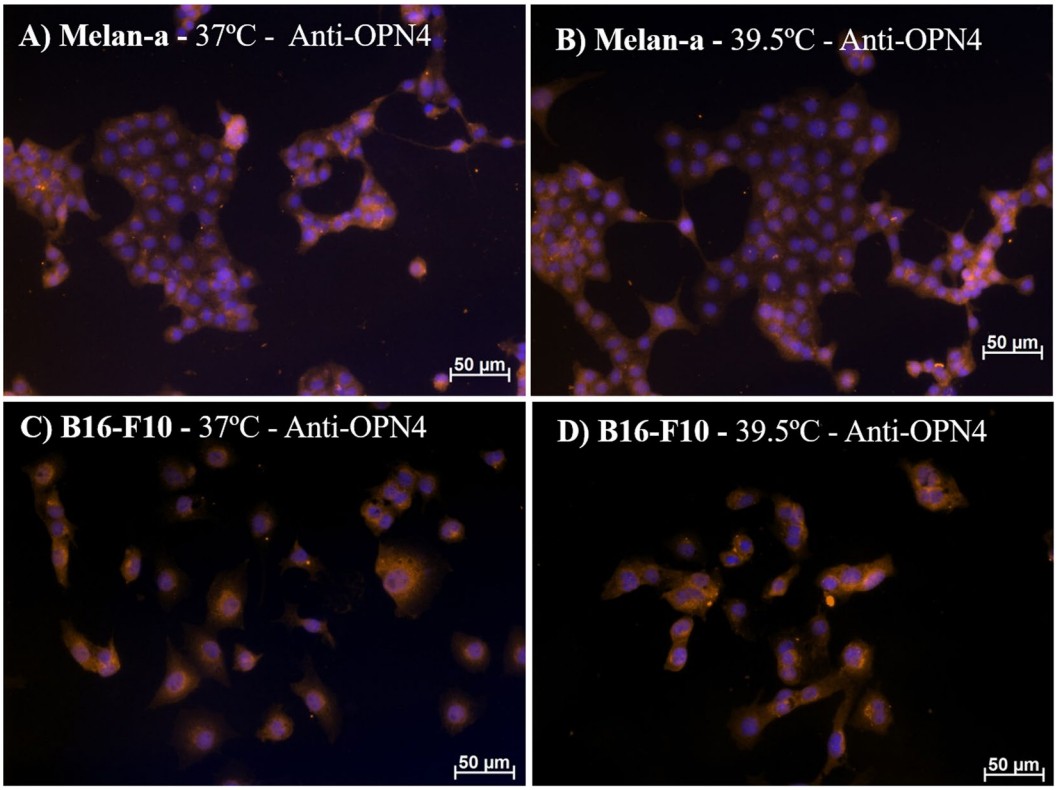

Figure 2. Representative fields of melanopsin (OPN4) immunostaining in Melan-a (**A**,**B**) and B16-F10 (**C**,**D**) cells. Cells were kept in DD for 3 days and at the beginning of the 4th day, cells were divided into 2 groups: (1) Control group kept in constant dark and temperature (37 °C); (2) group in constant dark and exposed to 1 h heat stimulus (39.5 °C). Twenty-four hours later the medium was removed and the cells were fixed with 4% paraformaldehyde. DAPI stained nuclei in blue and OPN4 immunopositivity (1:500 antiserum), revealed with a Cy3-labeled secondary antibody, in orange. Photomicrographies were taken with Axiocam MRm camera (Zeiss) and pseudocolored with Axiovision software (Zeiss). Scale bar 50 µm (200x magnification).

In agreement with these findings a 15-min white light pulse (WLP) applied to desynchronized Melan-a cells did not alter clock gene expression in comparison to cells kept in constant dark (DD) condition. Interestingly, in B16-F10 cells the expression of *Per1*, *Per2*, and *Bmal1* was upregulated in response to WLP[15]. Although the effects of heat shock or light pulse were not observed in desynchronized Melan-a cells, we cannot rule out that this stimulus may have affected the clock machinery of single cells, which would remain uncoupled to each other, and therefore, the overall oscillation would be unnoticed in the cell population. Another point of view is related to morpho-physiological differences between normal and malignant melanocytes, the latter showing denser dendritic projections among cells, a feature that probably allows more efficient cellular coupling[15].

Temperature cycles have been shown to alter rhythmic parameters of clock genes in peripheral tissues[20], and are a strong *zeitgeber* in normal murine keratinocytes[21] and fibroblasts[22]. To our knowledge, this is the first report that a short heat pulse affects clock gene machinery in murine melanocytes and melanoma cells. In fact, in non-mammalian vertebrates, we have already shown that heat shock increases the expression of clock genes in the photosensitive teleost ZEM-2S cell line, but only when cells were synchronized by light/dark (LD) cycles[23].

Previous studies using Melan-a and B16-F10 cells[15] and human and mouse spermatozoa[24] showed immunolabeling of melanopsin in regions capping the nucleus. We have shown that a 15-min WLP promoted OPN4 translocation from nucleus region to the cytoplasm and cell membrane in B16-F10 cells 24 h after the stimulus[15]. Based on these findings, we investigated whether heat shock was also capable of inducing melanopsin translocation in Melan-a and B16-F10 cells. Our results demonstrate that the cytoplasm and the nucleus capping location of OPN4 in both cell lines was not altered 24 h after the heat shock of 39.5 °C (Fig. 2A–D), suggesting that OPN4 is not required to be inserted into the membrane to detect heat stimulus. In another line of thought, one may consider that the basal level of membrane-bound OPN4 may be enough to detect heat and trigger heat-induced responses in murine melanocytes and melanoma cells.

We then pharmacologically inhibited melanopsin with the antagonist AA92593, shown to be specific because it competes with retinaldehyde for the melanopsin retinal binding site which is very distinct from other opsins. Its administration to mice *in vivo* specifically and reversibly modified melanopsin-dependent light responses including the pupillary light reflex and light aversion[25]. Our data show that the increase of *Per1* level induced by heat in Melan-a and B16-F10 cells was significantly reduced in the presence of the melanopsin antagonist (Fig. 3A,C) whereas *Bmal1* expression was not affected (Fig. 3B,D). Surprisingly, in Melan-a cells the group incubated with the antagonist and kept at 37 °C showed a statistically significant increase of *Per1* transcript when compared

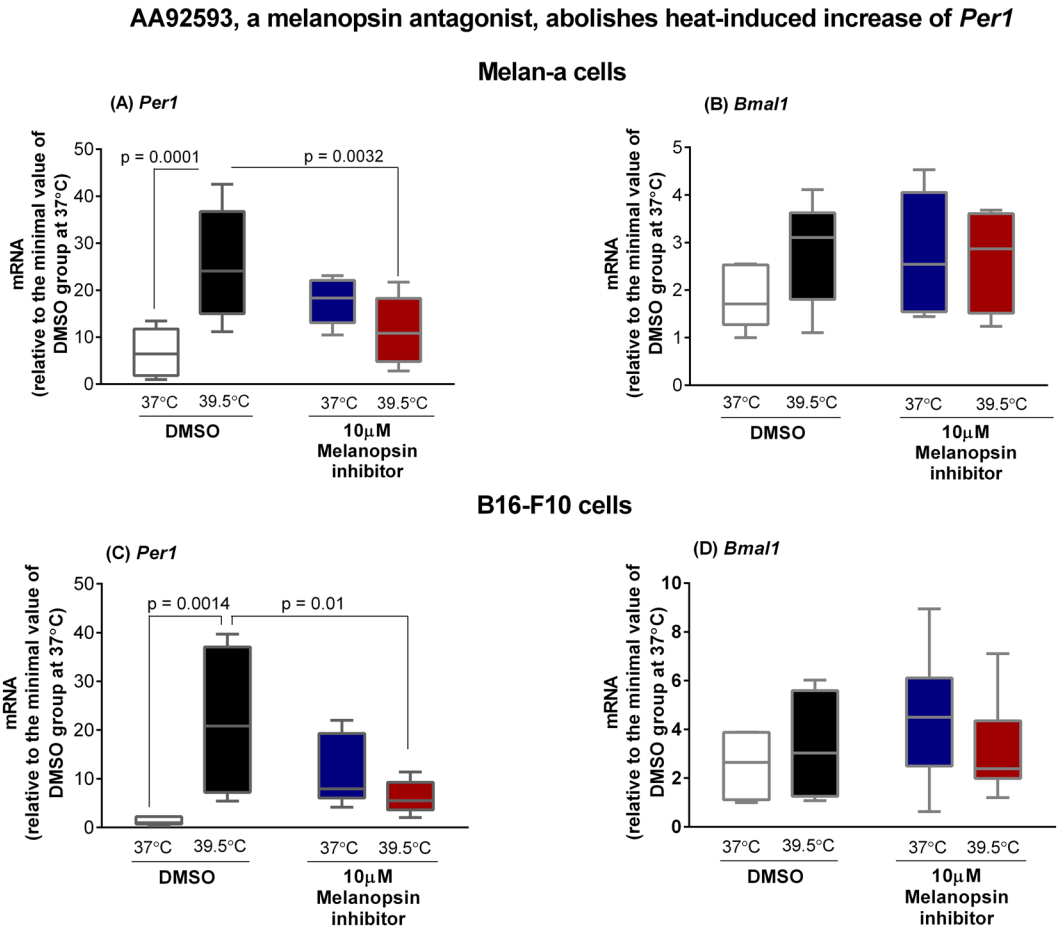

Figure 3. Expression of *Per1* (**A** and **C**) and *Bmal1* (**B** and **D**) in murine Melan-a melanocytes and B16-F10 melanoma cells after heat stimulus (39.5 °C) in the presence of AA92593. Melan-a or B16-F10 cells were kept for 3 days in constant dark and temperature (37 °C). In the beginning of the 4th day, Melan-a cells were synchronized by two medium changes, and after further 24 hours cells were heat-stimulated. For B16-F10 cells, the heat shock (39.5 °C) was applied at the beginning of the 4th day. In both scenarios, cells were divided into four groups: (1) control group at 37 °C in the presence of DMSO (0.1%); (2) heat-stimulated (39.5 °C) group in the presence of DMSO (0.1%); (3) group kept at 37 °C in the presence of AA92593 (10 μM), a selective OPN4 antagonist; (4) heat-stimulated (39.5 °C) group in the presence of AA92593 (10 μM). Total RNA was extracted immediately and 1 h after the end of the stimulus for Melan-a and B16-F10 cells, respectively. Boxplots show the median, quartiles, maximum, and minimum expression values of each gene transcript normalized by *Rpl 37a* and expressed relative to the minimal value of DMSO group at 37 °C (N = 5–9). Statistical analysis was performed by One-way ANOVA followed by Tukey's test.

to DMSO-treated control group ($p = 0.0478$, Fig. 3A); a phenomenon that showed no statistical significance ($p = 0.08$) in B16-F10 cells. The apparent intrinsic effect of AA92593 on control cells kept at 37 °C could be due to the following reasons: I) melanopsin acts as a thermosensor, and when inhibited, the cell would lose its ability to sense temperature, and the response would resemble the heat-evoked behavior; II) another possibility lies on a partial agonistic activity of AA92593 which, although not reported by Jones and co-workers[25], could explain the response found in the control group treated with AA92593; III) since AA92593 is a competitive melanopsin antagonist, its presence in the retinal-binding pocket of melanopsin leads to the displacement of retinal, which could trigger a downstream signaling that would ultimately result in *Per1* increased expression.

Next, we performed gene knockdown assays using the endoribonuclease-prepared siRNAs (esiRNA), which consist of a heterogeneous mixture of siRNAs against murine melanopsin mRNA. These siRNAs selectively suppress gene expression with low off-target effects[26]. In fact, we show a significant reduction of *Opn4* transcription as well as melanopsin protein level 48 h after transfection in Melan-a cells (Fig. 4A,B,E). In B16-F10 cells, although the mRNA levels of melanopsin did not decrease 48 h after transfection (Fig. 4F), a fact that could be due to a faster mRNA turnover, OPN4 protein level was drastically reduced (Fig. 4C,D). Then, our next step was to heat shock Melan-a and B16-F10 cells with reduced melanopsin expression, and the results demonstrated that the heat-induced increase of *Per1* was significantly reduced in both cell lines (Fig. 5A,C) while no effect on *Bmal1* expression was found (Fig. 5B,D). We have demonstrated that an opsin in a skin cell type can be activated not only by photons[15] but also by thermal energy. In fact, thermo-isomerization of rhodopsin and cone opsins

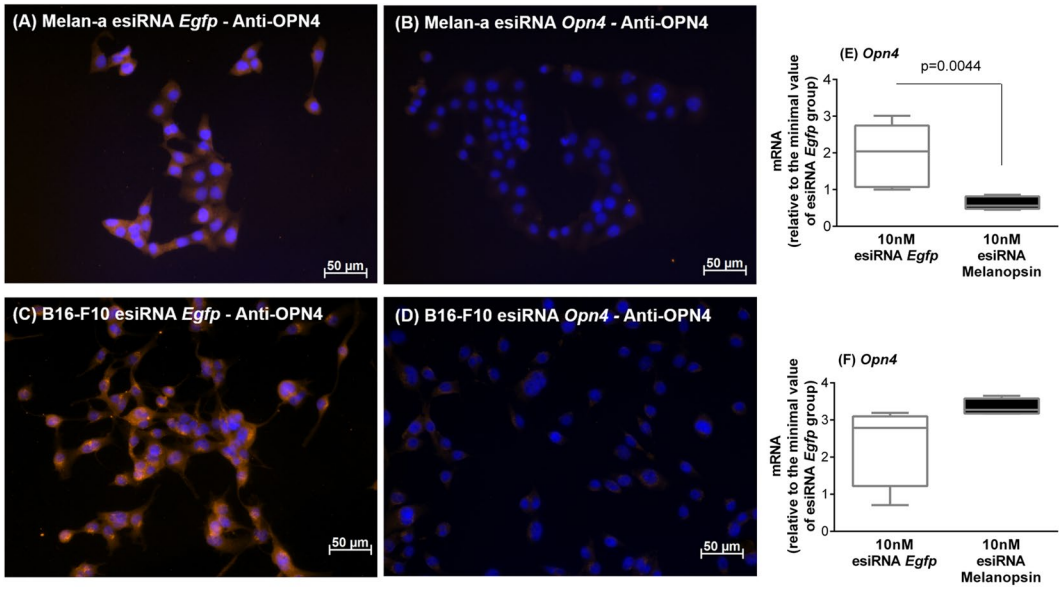

Figure 4. Representative fields of melanopsin (OPN4) immunostaining in Melan-a (**A**,**B**) and B16-F10 (**C**,**D**) cells. Cells were kept in DD for 24 hours, on the 2nd day, were transfected with esiRNA against melanopsin or EGFP (both at 10 nM), and 48 h after transfection the cells were immunostained for melanopsin (OPN4). (**A** and **C**) esiRNA against mRNA of EGFP transfected cells (control group) and (**B** and **D**) esiRNA against mRNA of OPN4 transfected cells. Photo-micrographies were obtained with 200 x magnification in an inverted fluorescence microscope Axiovert 40CFL (Zeiss, Oberkochen, Germany) with a mercury lamp of 50 W, and DAPI (excitation 358 and emission 463 nm) and Cy3 (excitation 549 and emission 562 nm) filters. **Melanopsin gene and protein knockdown by endoribonuclease-prepared siRNAs (esiRNA).** Gene expression of *Opn4* (melanopsin encoding gene) in esiRNA against mRNA of EGFP (control group) or of melanopsin transfected cells. Melan-a (**E**) or B16-F10 (**F**) cells were kept during three days in constant dark and temperature (37 °C). At the beginning of the 4th day, Melan-a cells were synchronized by two medium changes, and after further 24 hours they were transfected with esiRNA. B16-F10 cells were transfected at the beginning of the 4th day. In both cases, gene expression was evaluated 48 h after transfection with esiRNA. Boxplots show the median, quartiles, maximum, and minimum expression values of each gene transcript normalized by *Rpl 37a* and expressed relative to the minimal value of the esiRNA EGFP group kept at 37 °C (N = 5–6). Statistical analysis was performed by Student's t test.

has been shown to occur and it requires about half the energy necessary to photo-activate the photo-pigment[27]. Therefore, taken together our results clearly demonstrate– for the first time – the involvement of melanopsin in thermo-responses of mammalian cells.

According to Colin Pittendrigh *Escape from Light* theory[28], higher temperatures are found during the photo-phase of the day and, therefore, temperature and light are environmental entities exerting simultaneous selective pressures on the organisms. It is not surprising, therefore, that light and temperature may be perceived by the same conserved proteins, having in mind that photo- and thermo-sensitive systems probably co-evolved during evolution. Considering that the skin is constantly exposed to both physical stimuli[16], it is relevant to better understand how the skin perceives heat and light. In fact, our data add another layer of complexity for this system: an opsin, which is classically a light sensor, also acts as a thermo-sensor that ultimately feeds the local circadian clock. Interestingly, the opsin-mediated clock gene activation is conserved in malignant melanocytes, which warrants further investigation whether this event was pro- or anti-tumorigenic. Within this line, it has been recently shown that clock gene machinery of melanoma cells is suppressed[15,29], but clock gene activation by dexamethasone, forskolin, or heat shock results in reduced melanoma proliferation *in vitro* and *in vivo* without leading to cell death[29]. Taken altogether, our data bring convincing evidence of a new role for a canonical mammalian light sensor, which challenges the current paradigm that mammalian opsins exclusively function as photo-pigments.

Material and Methods

Cell Culture. Immortalized murine Melan-a melanocytes and B16-F10 malignant melanocytes were cultured in RPMI 1640 medium without phenol red (Atená, Campinas, SP, Brazil), supplemented with 14.3 mM $NaHCO_3$, 15 mM HEPES, 10% fetal bovine serum (FBS) (Atená, Campinas, SP, Brazil), 1% antibiotic/antimycotic solution (10,000 U/mL penicillin, 10,000 µg/mL streptomycin, and 25 µg/mL amphotericin B, ThermoFisher, Waltham, MA, USA), and 100 nM of *all-trans* retinal (Sigma-Aldrich, St. Louis, MO, USA). Phorbol 12-myristate 13-acetate (TPA, Sigma-Aldrich, St. Louis, MO, USA) at 200 nM was added to Melan-a medium, since it is required to maintain cell viability in culture[30]. The pH was adjusted to 7.2, and the cells were kept at constant temperature (37 °C) with 5% CO_2. Previous cell maintenance and experiment set up were carried out under ambient lighting.

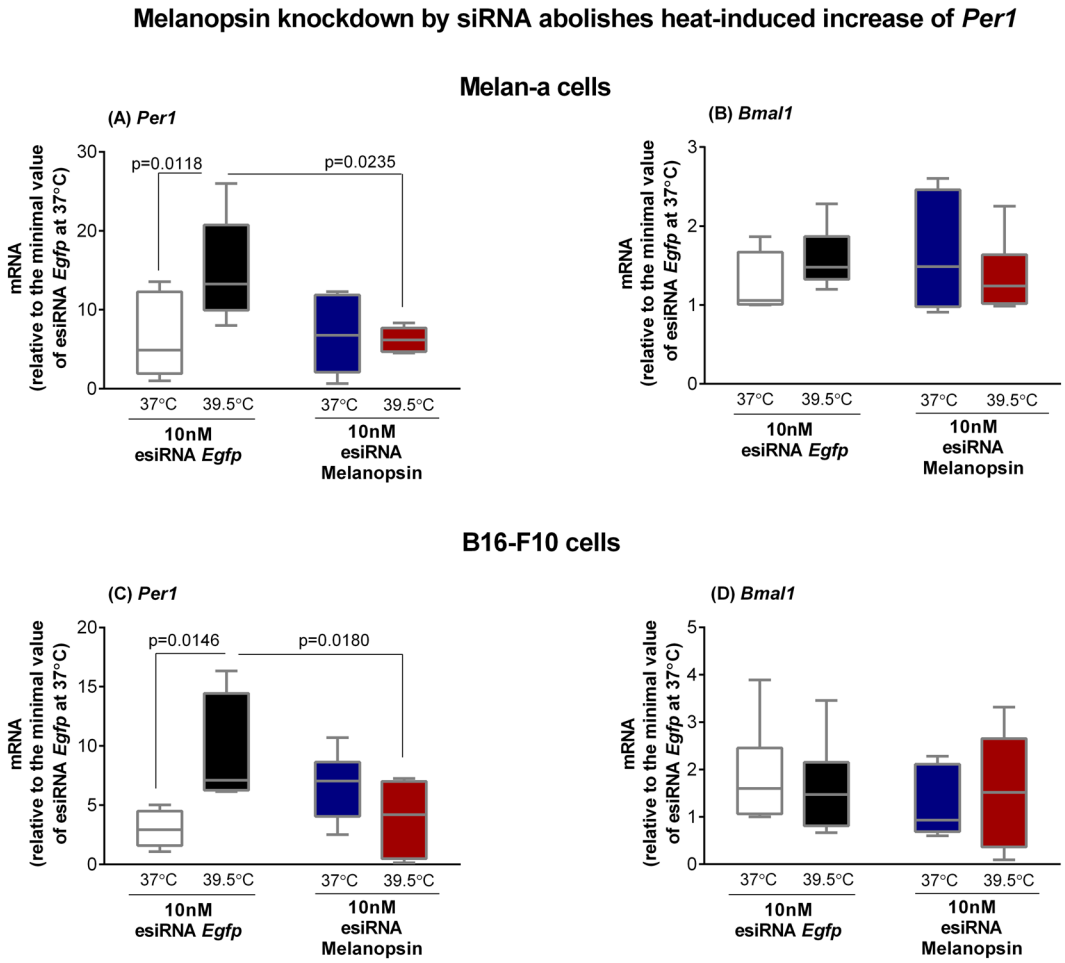

Figure 5. Expression of *Per1* (**A** and **C**) and *Bmal1* (**B** and **D**) in esiRNA transfected murine Melan-a melanocytes and B16-F10 melanoma cells after heat stimulus (39.5 °C). Melan-a or B16-F10 cells were kept during three days in constant dark and temperature (37 °C). At the beginning of the 4th day, Melan-a cells were synchronized by two medium changes, and after further 24 h cells were transfected with esiRNA against melanopsin or EGFP (both at 10 nM) using Lipofectamine 3000 transfection kit. B16-F10 cells were transfected with esiRNA, as described above, at the beginning of the 4th day. In both experimental scenarios, 48 hours after transfection, cells were divided into four groups: (1) control group at 37 °C in the presence of esiRNA EGFP (10 nM); (2) heat-stimulated (39.5 °C) group in the presence of esiRNA EGFP (10 nM); (3) group at 37 °C in the presence of esiRNA melanopsin (10 nM); (4) heat-stimulated (39.5 °C) group in the presence of esiRNA melanopsin (10 nM). Boxplots show the median, quartiles, maximum, and minimum expression values of each gene transcript normalized by *Rpl 37a* and expressed relative to the minimal value of the esiRNA EGFP group at 37 °C (N = 5–11). Total RNA was extracted immediately and 1 h after the end of the stimulus for Melan-a and B16-F10 cells, respectively. Statistical analysis was performed by One-way ANOVA followed by Tukey's test.

Experimental Design. In all experiments, Melan-a and B16-F10 cells were maintained in the medium described above but FBS was reduced to 2% (experimental medium). Cell manipulation during the experiments was carried out under red dim light (7 W Konex bulb and Safe-Light filter GBX-2, Kodak, Rochester, NY, USA). For all protocols described below, Melan-a and B16-F10 cells were kept in constant dark and temperature (37 °C) during 3 days. At the beginning of the 4th day the medium of Melan-a cells was changed twice with a 2-hour interval, after which the cells were kept in DD during further 24 h. This procedure has been shown to synchronize clock genes in this cell line[31].

Effect of Heat Stimulus on Clock Gene Machinery of Melan-a and B16-F10 Cells. Melan-a or B16-F10 cells were seeded at the density of 10^6 and 10^5 cells respectively in 25 cm^2 flasks. In the beginning of the 4th or 5th day (24 h after medium changes), B16-F10 and Melan-a cells were, respectively, heat-stimulated (39.5 °C) during 1 h while the control group remained at 37 °C. Total RNA was initially extracted immediately, 1 and 2 h after the end of the heat stimulus, and the time points showing maximal response of clock gene expression were adopted for subsequent assays.

Effect of Heat Stimulus on OPN4 Localization in Melan-a and B16-F10 Cells. Immunocytochemistry assays were performed as previously described[15]. A peptide comprised by the 15 N-terminal amino acid sequence of mouse melanopsin (Genbank accession NP_038915) with an appended C-terminal cysteine (MDSPSGPRVLSSLTQC) (Uniformed Services University of the Health Biomedical Instrumentation Center, Bethesda, MD, USA) was conjugated to keyhole limpet hemocyanin and used to immunize rabbits (Covance Labs, Denver, PA, USA). The antisera were used with no further purification[1]. Previous studies showed that increasing the concentration of the antigenic peptide led to the loss of immunoreactivity by pre-absorption in a dose-dependent manner, and that retinas of OPN4 knockout mice showed lack of immunoreactivity[32].

Melan-a or B16-F10 cells were seeded (10^4/well) into 8-chamber slides in the experimental medium as described above. The cells were kept in DD at 37 °C for 3 days and at the beginning of the 4th day they were divided into 2 groups: the control remained in DD at 37 °C while the experimental group was exposed to 1 h of heat stimulus (39.5 °C). Twenty-four hours later the medium was removed and the cells were fixed in 4% paraformaldehyde as described below.

To verify the effectiveness of the *Opn4* silencing Melan-a or B16-F10 cells were seeded (10^4/well) into 8-chamber slides and kept in DD for 24 hours. On the 2nd day, the cells were transfected with esiRNA, and immunostaining of OPN4 was performed 48 h after transfection. The cells were incubated in the primary antibody anti-melanopsin (1:500, Covance Laboratories, Denver, PA, USA) overnight at 4 °C. A Cy3-labeled anti-rabbit secondary antibody (1:500, Jackson Immunolab, West Grove, PA, USA) was applied for 1 h at room temperature. Photo-micrographies were obtained with 200 x magnification in an inverted fluorescence microscope Axiovert 40CFL (Zeiss, Oberkochen, Germany) with a mercury lamp of 50 W, and DAPI (excitation 358 and emission 463 nm) and Cy3 (excitation 549 and emission 562 nm) filters.

Pharmacological Inhibition of Melanopsin. We used the selective competitive antagonist of melanopsin, AA92593 (Sigma-Aldrich, St. Louis, MO, USA), at 10 µM, based on a previous study[25]. Melan-a and B16-F10 cells were seeded at the density of 10^6 and 10^5 cells respectively in 25 cm^2 flasks, and after the procedure described in the Experimental Design section, they were divided into four groups: (1) control group at 37 °C in the presence of DMSO (0.1%); (2) heat-stimulated group (39.5 °C) in the presence of DMSO (0.1%); (3) group kept at 37 °C in the presence of the OPN4 antagonist AA92593 (10 µM); (4) heat-stimulated group (39.5 °C) in the presence of AA92593 (10 µM). Total RNA of Melan-a cells was extracted immediately and of B16-F10 cells 1 h after the end of the heat stimulus.

Melanopsin Knockdown by Endoribonuclease Small Interfering RNA (esiRNA). We used esiRNA as gene silencing tool (Sigma-Aldrich, St. Louis, MO, USA) that targets mouse *Opn4* variants 1 and 2 (access numbers NM_001128599.1 and NM_013887.2). The esiRNA results from the cleavage of long double-stranded RNA (dsRNA). This process generates a heterogeneous mixture of siRNAs, all of which target the same mRNA of interest. This methodology provides highly selective gene suppression with lower off-target effects than single or pooled siRNAs[26]. As a control for our experiments, we used an esiRNA that targets the mRNA of Enhanced Green Fluorescent Protein (EGFP), which can be used as a negative control in systems that lack this protein.

Melan-a or B16-F10 cells were seeded (10^5 and 5×10^4/well respectively) in a 12-well plate, and after the procedure described in the Experimental Design section they were transfected with esiRNA against melanopsin or EGFP (both at 10 nM) using Lipofectamine 3000 transfection kit (ThermoFisher, Waltham, MA, USA) according to the manufacturer's instructions.

To verify the functional role of melanopsin in perceiving heat, Melan-a or B16-F10 cells were divided into four groups 48 hours after transfection: (1) control group transfected with esiRNA EGFP (10 nM) at 37 °C; (2) heat-stimulated (39.5 °C) group transfected with esiRNA EGFP (10 nM); (3) group transfected with esiRNA melanopsin (10 nM) at 37 °C; (4) heat-stimulated (39.5 °C) group transfected with esiRNA melanopsin (10 nM). Total RNA was extracted immediately after the end of heat stimulus and gene expression of *Opn4* (melanopsin encoding gene) was assessed by qPCR as previously described[15] in Melan-a and B16-F10 cells transfected with esiRNA against EGFP (control group) or against melanopsin mRNA. Lipofectamine 3000 displayed no effect *per se* on clock gene expression (data not shown).

RNA Extraction, Purification, and cDNA Synthesis. RNA was extracted with trizol (Ambion, Carlsbad, CA, USA), and purified (Direct-zol™ Zymo Research, Irvine, CA, USA) according to the manufacturers' instructions. RNA concentration and quality (OD260/OD280) were determined in a NanoDrop spectrophotometer (NanoDrop, Wilmington, DE, USA), and 1 µg of total RNA was reverse transcribed to cDNA using random hexamer primers and *Superscript III*, following the manufacturer's instruction (ThermoFisher, Waltham, MA, USA).

Quantitative PCR. Quantitative PCR reactions were performed in an iQ5 thermocycler (Bio-Rad Laboratories, Hercules, CA, USA) with the products of reverse transcription using primers spanning introns, designed, and synthesized by IDT (Coralville, IA, USA), and based on sequences obtained from GenBank (http://www.ncbi.nlm.nih.gov/genbank). The access number of each gene, the respective primer sequences, and concentrations are shown in Table 1. The qPCR reactions were performed using two different protocols: multiplex for simultaneous analysis of multiple genes (TaqMan®) and SYBR® GreenER™. The TaqMan® solutions contained *Per1* and *Bmal1* respective primers and fluorescent probes (Table 1), and iQ Multiplex Powermix (Bio-Rad Laboratories, Hercules, CA, USA) or Kapa Probe Fast qPCR Mix 2X (Kapa Biosystems, Wilmington, MA, USA). Each experimental cDNA was run in triplicates (1 µl of cDNA per reaction) in 96 well plates. The assays were performed under the following conditions: 7 min at 95 °C, followed by 45 cycles of 30 s at 95 °C and 30 s at 55 °C.

Templates	Primers and probes	Final Concentration
Per1 (NM_0011065.3)	Forward: 5′-AGCAGGTTCAGGCTAACCAGGAAT-3′	300 nM
	Reverse: 5′-AGGTGTCCTGGTTTCGAAGTGTGT-3′	300 nM
	Probe:5′-/6FAM/AGCCTTGTGCCATGGACATGTCTACT/BHQ_1/-3′	200 nM
Bmal1 (NM_001243048)	Forward: 5′-AGCTTCTGCACAATCCACAGCAC-3′	300 nM
	Reverse: 5′-TGTCTGGCTCATTGTCTTCGTCCA-3′	300 nM
	Probe:5′-/5HEX/-AAAGCTGGCCACCCACGAAGATGGG/BHQ_1–3′	200 nM
Opn4 (NM_001128599.1)	Forward: 5′-ACATCTTCATCTTCAGGGCCA-3′	300 nM
	Reverse: 5′-ACTCACCGCAGCCCTCAC-3′	300 nM
Rpl37a (NM_009084.4)	Forward: GCATGAAAACAGTGGCCGGT	300 nM
	Reverse: CAGGGTCACACAGTATGTCTCAAAA	300 nM
18S RNA	Forward: 5′-CGGCTACCACATCCAAGGAA-3′	50 nM
	Reverse: 5′-GCTGGAATTACCGCGGCT-3′	50 nM

Table 1. Sequences and Final Concentrations of Primers and Probes. Access Numbers in Between Parentheses.

The solutions for *Opn4*, *Rpl 37a* or 18S RNA contained the respective primers (Table 1) and Kapa SYBR® Fast qPCR Master Mix 2X (Kapa Biosystems, Wilmington, MA, USA). Each experimental cDNA was run in duplicates (1 µl of cDNA per well) in 96 well plates. These assays were performed under the following conditions: 10 min at 95 °C, followed by 45 cycles of 15 s at 95 °C, 1 min at 60 °C, and 80 cycles of 10s at 55 °C, with a gradual increase of 0.5 °C. Ribosomal 18S RNA and *Rpl 37a* were used as reference genes in both TaqMan® and SYBR® GreenER™ methodologies since they did not vary with time under our experimental conditions.

Statistical Analyses. To analyze qPCR data, we used the $2^{-\Delta\Delta CT}$ method as previously described[33]. The temporal effect of heat stimulus on clock gene expression of Melan-a and B16-F10 cells was analyzed by Two-way ANOVA followed by Bonferroni post-test. For the pharmacological and gene knockdown assays, Student's *t* test or One-way ANOVA followed by Tukey post-test were used according to the number of groups. Significance was set for $p < 0.05$. All analyses were carried out in GraphPad Prism Version 6.0 (La Jolla, CA, USA).

References

1. Provencio, I., Rollag, M. D. & Castrucci, A. M. L. Photoreceptive net in the mammalian retina. This mesh of cells may explain how some blind mice can still tell day from night. *Nature* **415**(6871), 493 (2002).
2. Panda, S. *et al*. Melanopsin is required for non-image-forming photic responses in blind mice. *Science* **301**(5632), 525–527 (2003).
3. Ralph, M. R., Foster, R. G., Davis, F. C. & Menaker, M. Transplanted suprachiasmatic nucleus determines circadian period. *Science* **247**(4945), 975–978 (1990).
4. Allen, A. E., Storchi, R., Martial, F. P., Bedford, R. A. & Lucas, R. J. Melanopsin contributions to the representation of images in the early visual system. *Curr. Biol.* **27**(11), 1623–1632 (2017).
5. Hughes, S. *et al*. Signalling by melanopsin (OPN4) expressing photosensitive retinal ganglion cells. *Eye (Lond)* **30**(2), 247–254 (2016).
6. Takahashi, J. S. Transcriptional architecture of the mammalian circadian clock. *Nat. Rev. Genet.* **18**(3), 164–179 (2017).
7. Husse, J., Eichele, G. & Oster, H. Synchronization of the mammalian circadian timing system: Light can control peripheral clocks independently of the SCN clock: alternate routes of entrainment optimize the alignment of the body's circadian clock network with external time. *Bioessays* **37**(10), 1119–1128 (2015).
8. Bass, J. & Lazar, M. A. Circadian time signatures of fitness and disease. *Science* **354**(6315), 994–999 (2016).
9. Terakita, A. & Nagata, T. Functional properties of opsins and their contribution to light-sensing physiology. *Zoolog. Sci.* **31**(10), 653–659 (2014).
10. Shen, W. L. *et al*. Function of rhodopsin in temperature discrimination in *Drosophila*. *Science* **331**, 1333–1336 (2011).
11. Sokabe, T., Chen, H. C., Luo, J. & Montell, C. A. A switch in thermal preference in Drosophila larvae depends on multiple rhodopsins. *Cell Rep.* **17**, 336–344 (2016).
12. Leung, N. Y. & Montell, C. Unconventional roles of opsins. *Annu. Rev. Cell Dev. Biol.* https://doi.org/10.1146/annurev-cellbio-100616-060432 (2017).
13. Sikka, G. *et al*. Melanopsin mediates light-dependent relaxation in blood vessels. *Proc. Natl. Acad. Sci. USA* **111**(50), 17977–17982 (2014).
14. Richards, J., Diaz, A. N. & Gumz, M. L. Clock genes in hypertension: novel insights from rodent models. *Blood Press. Monit.* **19**(5), 249–254 (2014).
15. de Assis, L. V., Moraes, M. N., da Silveira Cruz-Machado, S. & Castrucci, A. M. L. The effect of white light on normal and malignant murine melanocytes: A link between opsins, clock genes, and melanogenesis. *Biochim. Biophys. Acta* **1863**, 1119–1133 (2016).
16. Slominski, A. T. *et al*. Sensing the environment: Regulation of local and global homeostasis by the skin neuroendocrine system. *Adv. Anat. Embryol. Cell Biol.* **212**, v–115 (2012).
17. de Assis, L. V., Moraes, M. N. & Castrucci, A. M. L. Heat shock antagonizes UVA-induced responses in murine melanocytes and melanoma cells: an unexpected interaction. *Photochem. Photobiol. Sci.* **16**, 633–648 (2017).
18. Liu, A. C. *et al*. Intercellular coupling confers robustness against mutations in the SCN circadian clock network. *Cell* **129**(3), 605–616 (2007).
19. Brown, S. A. & Azzi, A. Peripheral circadian oscillators in mammals. *Handb. Exp. Pharmacol.* (**217**), 45–66 (2013).
20. Buhr, E. D., Yoo, S. H. & Takahashi, J. S. Temperature as a universal resetting cue for mammalian circadian oscillators. *Science* **330**, 379–385 (2010).
21. Sporl, F. *et al*. A circadian clock in HaCaT keratinocytes. *J. Invest. Dermatol.* **131**(2), 338–348 (2011).
22. Saini, C., Morf, J., Stratmann, M., Gos, P. & Schibler, U. Simulated body temperature rhythms reveal the phase-shifting behavior and plasticity of mammalian circadian oscillators. *Genes Dev.* **26**(6), 567–580 (2012).
23. Jeronimo, R. *et al*. Thermal stress in *Danio rerio*: A link between temperature, light, thermo-TRP channels, and clock genes. *J. Thermal Biol.* **68**(A), 128–138 (2017).

24. Pérez-Cerezales, S. *et al.* Involvement of opsins in mammalian sperm thermotaxis. *Sci. Rep.* **5**, 16146 (2015).
25. Jones, K. A. *et al.* Small-molecule antagonists of melanopsin-mediated phototransduction. *Nature Chem. Biol.* **9**(10), 630–635 (2013).
26. Theis, M. & Buchholz, F. MISSION esiRNA for RNAi screening in mammalian cells. *J. Visual Exp*. **39**, pii 2008. Advance online publication. https://doi.org/10.3791/2008 (2010).
27. Wang, T., Facciotti, M. T. & Duan, Y. Schiff base switch II precedes the retinal thermal isomerization in the photocycle of bacteriorhodopsin. *PLoS* **8**(7), e69882 (2013).
28. Pittendrigh, C. S. Temporal organization: reflections of a Darwinian clock-watcher. *Annu. Rev. Physiol.* **55**, 17–54 (1993).
29. Kiessling, S. *et al.* Enhancing circadian clock function in cancer cells inhibits tumor growth. *BMC Biol.* **15**(1), 13 (2017).
30. Bennett, D. C., Cooper, D. C. & Hart, I. R. A line of non-tumorigenic mouse melanocytes, syngeneic with the B16 melanoma and requiring a tumour promoter for growth. *Int. J. Cancer* **39**(3), 414–418 (1987).
31. Poletini, M. O., de Assis, L. V., Moraes, M. N. & Castrucci, A. M. L. Estradiol differently affects melanin synthesis of malignant and normal melanocytes: a relationship with clock and clock-controlled genes. *Mol. Cell Biochem.* **421**(1–2), 29–39 (2016).
32. Panda, S. *et al.* Melanopsin (Opn4) requirement for normal light-induced circadian phase shifting. *Science* **298**(5601), 2213–2216 (2002).
33. Livak, K. J. & Schmittgen, T. D. Analysis of relative gene expression data using real-time quantitative PCR and the 2(-Delta Delta C(T)) Method. *Methods* **25**(4), 402–428 (2001).

Acknowledgements

This work was partially supported by the Sao Paulo Research Foundation (FAPESP, grant 2012/50214-4) and by the National Council of Technological and Scientific Development (CNPq, grants 301293/2011-2 and 303070/2015-3). MN Moraes, LVM de Assis, and LHRG Lima are fellows of FAPESP (2014/16412-9, 2013/24337-4 and 2009/53533-0 respectively). We are thankful to Prof. Ignacio Provencio from the University of Virginia for providing theoretical and methodological insights and thoughtful discussions.

Author Contributions

All authors designed the study. M.N.M., L.V.M.D.A. and K.K.M.M. acquired and analyzed the data. M.N.M. and L.V.M.D.A. drafted the manuscript. A.M.L.C. discussed the data and critically revised the draft. All authors have approved the final version of the manuscript and agreed to be accountable for all aspects of the study in ensuring that questions related to the accuracy or integrity of any part of the study are appropriately investigated and resolved. All persons designated as authors qualify for authorship, and all those who qualify for authorship are listed.

Additional Information

Supplementary information accompanies this paper at https://doi.org/10.1038/s41598-017-13939-3.

Competing Interests: The authors declare that they have no competing interests.

Publisher's note: Springer Nature remains neutral with regard to jurisdictional claims in published maps and institutional affiliations.

Chapter 5: Melanopsin and Rhodopsin Mediate UVA-Induced Immediate Pigment Darkening: Unravelling the Photosensitive System of the Skin

The content provided in this chapter has been published in European Journal of Cell Biology, 2018, 97(3):150-162. DOI: 10.1016/j.ejcb.2018.01.004.

Authors' names: de Assis LVM, Moraes MN, Magalhães-Marques KK, Castrucci AML.

European Journal of Cell Biology 97 (2018) 150–162

Contents lists available at ScienceDirect

European Journal of Cell Biology

journal homepage: www.elsevier.com/locate/ejcb

Research paper

Melanopsin and rhodopsin mediate UVA-induced immediate pigment darkening: Unravelling the photosensitive system of the skin

Leonardo Vinícius Monteiro de Assis[a], Maria Nathalia Moraes[a], Keila Karoline Magalhães-Marques[a], Ana Maria de Lauro Castrucci[a,b,*]

[a] Laboratory of Comparative Physiology of Pigmentation, Department of Physiology, Institute of Biosciences, University of São Paulo, São Paulo, Brazil
[b] Department of Biology, University of Virginia, Charlottesville, VA, USA

ARTICLE INFO

Keywords:
Immediate pigment darkening (IPD)
Ultraviolet A radiation (UVA)
Melanocytes and melanoma
Opsins and light sensors

ABSTRACT

The mammalian skin has a photosensitive system comprised by several opsins, including rhodopsin (OPN2) and melanopsin (OPN4). Recently, our group showed that UVA (4.4 kJ/m^2) leads to immediate pigment darkening (IPD) in murine normal and malignant melanocytes. We show the role of OPN2 and OPN4 as UVA sensors: UVA-induced IPD was fully abolished when OPN4 was pharmacologically inhibited by AA9253 or when OPN2 and OPN4 were knocked down by siRNA in both cell lines. Our data, however, demonstrate that phospholipase C/protein kinase C pathway, a classical OPN4 pathway, is not involved in UVA-induced IPD in either cell line. Nonetheless, in both cell types we have shown that: a) intracellular calcium signal is necessary for UVA-induced IPD; b) the involvement of CaMK II, whose inhibition, abolished the UVA-induced IPD; c) the role of CAMK II/NOS/sGC/cGMP pathway in the process since inhibition of either NOS or sGC abolished the UVA-induced IPD. Taken altogether, we show that OPN2 and OPN4 participate in IPD induced by UVA in murine normal and malignant melanocytes through a conserved common pathway. Interestingly, upon knockdown of OPN2 or OPN4, the UVA-driven IPD is completely lost, which suggests that both opsins are required and cooperatively signal in murine both cell lines. The participation of OPN2 and OPN4 system in UVA radiation-induced response, if proven to take place in human skin, may represent an interesting pharmacological target for the treatment of depigmentary disorders and skin-related cancer.

Significance statement

Opsins are light sensors present in the eye and skin; however, the role and functionality of the cutaneous photosensitive system remain poorly understood. Some evidence, on the other hand, has demonstrated that opsins mediate melanin synthesis and differentiation processes in melanocytes and keratinocytes, respectively. In this study, our group provides further insights into the opsin-based system of the skin. We demonstrate that two opsins, melanopsin and rhodopsin, act cooperatively as UVA radiation sensors in murine melanocytes and melanoma cells, participating in immediate pigment darkening through a shared pathway that involves calcium and cGMP. Thus, we suggest that this system can be pharmacologically targeted to improve the treatment of depigmentary diseases.

1. Introduction

The skin is the first barrier between the external environment and the organism, being constantly exposed to several threatening chemicals, temperature, ultraviolet radiation (UVR) and visible light, and pathogens (Calapre et al., 2013; Cho et al., 2009; Desotelle et al., 2012; Dupont et al., 2013; Luber et al., 2014; Mohania et al., 2017; Purschke et al., 2010). Since the skin is continuously challenged by the environment, it is not surprising that it has complex mechanisms of defense such as – but not limited to – immune (Bangert et al., 2011) and neuroendocrine responses (Slominski et al., 2012b), increasing epidermal thickness and cytokeratin, normal shedding of epidermal squamous layers and apoptosis of damaged cells (Brenner and Hearing, 2008), DNA repair system (Brenner and Hearing, 2008; Dakup and Gaddameedhi, 2016; Gaddameedhi et al., 2011; Gaddameedhi et al., 2015; Nasti and Timares, 2015), and skin pigmentary system that acts as a natural sunscreen (Brenner and Hearing, 2008; Lin and Fisher, 2007; Nasti and Timares, 2015; Solano, 2014).

The cutaneous pigmentary system synthesizes melanin (Slominski et al., 2012a), which exerts a complex photo-protective role that mainly consists in photo-absorption and free radical scavenger properties

* Corresponding author at: Departamento de Fisiologia, Instituto de Biociências, Universidade de São Paulo, R. do Matão, trav. 14, no. 101, São Paulo, 05508-900, Brazil.
E-mail address: amdlcast@ib.usp.br (A.M.d.L. Castrucci).

https://doi.org/10.1016/j.ejcb.2018.01.004
Received 6 October 2017; Received in revised form 12 January 2018; Accepted 19 January 2018

(Brenner and Hearing, 2008; Nasti and Timares, 2015). The melanogenic process takes place within melanosomes in which tyrosine is hydroxylated into L-dihydroxyphenylalanine (L-DOPA) followed by its oxidation to dopaquinone, steps known to be catalyzed by tyrosinase. The melanogenesis is then divided into two pathways ultimately resulting in eumelanin or pheomelanin production. In the latter process dopaquinone synthesis is dependent on cysteine, which reacts with dopaquinone forming cysteinyl-dopa that is later converted into quinoleimine, alanine-hydroxyl dihydrobenzothazine, and then polymerizes into pheomelanin. Interestingly, pheomelanin has been associated with a poor protective effect as it is photo-unstable and may be linked to increased risk of skin cancer (Brenner and Hearing, 2008; Nasti and Timares, 2015; Williams et al., 2011). For eumelanin formation, dopachrome is spontaneously converted into 5,6-dihydroxyindole (DHI) or, through dopachrome tautomerase activity (tyrosinase-related protein-2 (TRP-2 or DCT)), into 5,6-dihydroxyindole-2-carboxylic acid (DHICA). Finally, polymerization of indoles and quinones originates eumelanin that is transferred to adjacent keratinocytes where it shields the nuclei, providing a protection against the deleterious effect of UVR and visible light on DNA (Gillbro and Olsson, 2011; Nasti and Timares, 2015; Slominski et al., 2004; Solano, 2014). It should be mentioned that in murine skin, melanogenesis predominantly occurs in hair follicles, whereas in human skin melanin is synthesized in both epidermis and hair follicle (Lin and Fisher, 2007; Slominski and Paus, 1993; Slominski et al., 2005; Lin and Fisher, 2007).

It has long been accepted that light skin people are significantly more prone to develop skin cancer when compared to dark skin ones – a fact that demonstrates the protective effect of melanin (Bradford, 2009; Gloster and Neal, 2006; Halder and Bang, 1988; Yamaguchi et al., 2007). Nevertheless, melanin and active melanogenesis can negatively affect the outcome of patients with advanced melanomas (Slominski et al., 1998; Slominski et al., 2014; Slominski et al., 2015). In fact, higher melanin content may favor a poor prognosis since it has been demonstrated *in vitro* that inhibition of melanogenesis enhances the antitumoral efficiency of radiotherapy (Brozyna et al., 2008), chemotherapy, or immune cells (Slominski et al., 2009). Corroborating reports have also shown that patients with melanotic melanoma exhibited significantly shorter survival than those with amelanotic lesions (Brozyna et al., 2013; Brozyna et al., 2016). In addition, evidences have pointed that chemiexcitation of melanin derivatives hours after UVR leads to DNA photoproducts, which indicates that melanin may also have carcinogenic properties (Premi et al., 2015). Therefore, melanin can play a dual role in melanoma development and progression (Slominski et al., 2015).

Melanogenesis is a tightly regulated process known to be influenced by a wide variety of hormones (Allil et al., 2008; Kadekaro et al., 2004; Lopes et al., 2010; Luchs et al., 2008; Marwan et al., 1985; Poletini et al., 2016; Sarti et al., 2004; Scarparo et al., 2007; Scarparo et al., 2004; Scarparo et al., 2000; Slominski et al., 2004; Slominski et al., 2000; Slominski et al., 2013; Souza et al., 2003; Videira et al., 2013) and UVR and visible light (Brenner and Hearing, 2008; Chakraborty et al., 1999; de Assis et al., 2017; de Assis et al., 2016; Gillbro and Olsson, 2011; Lin and Fisher, 2007; Yamaguchi et al., 2007). In response to UVR, skin pigmentation proceeds in several distinct steps. Initially, a transient pigmentation, known as immediate pigment darkening (IPD), takes places within minutes, and fades away in minutes to hours. Classically, UVA radiation – but not UVB – (Black et al., 1985; Honigsmann et al., 1986; Jimbow et al., 1973; Pathak et al., 1962) as well as visible light (Jimbow et al., 1973; Mahmoud et al., 2008; Mahmoud et al., 2010; Pathak et al., 1962; Randhawa et al., 2015; Rosen et al., 1990; Sklar et al., 2013; Williams et al., 2011) have been associated with IPD. The wavelength that promotes the strongest IPD response is 340 nm, with doses ranging from 10 to 20 kJ/m^2. When skin is exposed to doses higher than 100 kJ/m^2, the IPD is more intense and the persistent pigment darkening (PPD) happens. Both IPD and PPD are believed to result from oxidation and redistribution of pre-existing melanin that can last up to 24 h and blend with another pigmentary process: the delayed tanning (DT), known to be dependent on *de novo* synthesis of tyrosinase and melanin (Mahmoud et al., 2008; Sklar et al., 2013). Both UVA and UVB can lead to DT, but UVA-induced DT is preceded by IPD and/or PPD without erythema while the UVB-induced DT is preceded by erythema (Mahmoud et al., 2008; Sklar et al., 2013).

The genesis of IPD is a poorly comprehended process as compared to the other pigmentary responses such as DT (Mahmoud et al., 2008; Sklar et al., 2013). IPD was first observed in skin of corpses exposed to irradiation from a lamp with a quartz filter. This evidence is suggestive that IPD takes place independently of skin cell viability as a result of an acellular photochemical reaction (Hausser, 1938 and Miescher and Minder, 1939 apud Honigsmann et al., 1986). It has been previously shown that IPD may take place in response to UVA radiation at temperatures as different as 0 °C and 37 °C (Honigsmann et al., 1986). Contrary to this report, recent data from our lab have shown that IPD triggered by UVA radiation is antagonized by heat shock when both stimuli are applied together (de Assis et al., 2017), thus indicating that IPD may be temperature-dependent.

The functional relevance of IPD is still unclear. It has been speculated that the pigment generated during IPD would protect the skin against the deleterious effect of UV radiation; however, even though this hypothesis is the most intuitive, studies have shown that the pigment generated in IPD does not absorb in the UVR spectrum. Therefore, it is accepted that IPD does not protect against UVR deleterious effects (Black et al., 1985; Honigsmann, 2002; Honigsmann et al., 1986; Willis et al., 1972). And, corroborating this hypothesis, an elegant study has demonstrated that IPD-induced pigment mainly absorbs in the white light spectrum, and weakly in the UV wavelengths (Moan et al., 2012). Nevertheless, it protects against photo-degradation of folate and other chromophores present in the skin (Moan et al., 2012). In agreement with these findings, it has been set forth that folate protection in addition to DNA protection would be the key role of skin pigmentary response (Branda and Eaton, 1978; Jablonski and Chaplin, 2010).

The skin has long been known to possess light sensors (Bellono et al., 2013; Bellono et al., 2014; de Assis et al., 2017; de Assis et al., 2016; Haltaufderhyde et al., 2015; Kim et al., 2013; Miyashita et al., 2001; Regazzetti et al., 2017; Toh et al., 2016; Tsutsumi et al., 2009; Wicks et al., 2011), *i.e.*, a system of opsins that is virtually the same present in the retina (Buhr et al., 2015; Lamb, 2013; Solomon and Lennie, 2007); however, the role and functionality of this light sensitive system in the skin has only recently started to be unraveled (Bellono et al., 2013; Bellono et al., 2014; de Assis et al., 2017; de Assis et al., 2016; Kim et al., 2013; Wicks et al., 2011). It is worth to emphasize that the majority of studies in the literature reporting the effects elicited by UVR and visible light has not taken into consideration the photosensitive system of the skin. Thus, could the well-known described cutaneous effects exerted by visible light and UV radiation be mediated by photopigments known to be present in the skin? To start addressing this gap in our knowledge, we evaluated which signaling pathways participate in the IPD response of the photosensitive murine melanocytes and melanoma cells to UVA radiation.

2. Material and methods

2.1. Cell culture

Melan-a melanocytes or B16-F10 melanoma cells were maintained in RPMI 1640 medium without phenol red (Atená, Campinas, SP, Brazil), supplemented with 14.3 mM $NaHCO_3$, 15 mM HEPES, 10% fetal bovine serum (FBS) (Atená, Campinas, SP, Brazil), 1% antibiotic/antimycotic solution (10,000 U/mL penicillin, 10,000 μg/mL streptomycin, and 25 μg/mL amphotericin B, Thermo Fisher, Waltham, MA, USA), and 10^{-7} M retinal (*all-trans* Sigma-Aldrich, St. Louis, MO, USA) at pH 7.2, 37 °C and 5% CO_2. During the experiments, the cells were maintained in the same medium, and FBS was reduced to 2%. Phorbol 12-

myristate 13-acetate (TPA, Sigma-Aldrich, St. Louis, MO, USA) at 200 nM was added to Melan-a cell medium as it is necessary for proper growth and maintenance (Bennett et al., 1987). Cell manipulation during the experiments was carried out under red dim light (7 W Konex bulb and Safe-Light filter GBX-2, Kodak, Rochester, NY, USA).

2.2. Evaluation of signaling pathways evoked by UVA radiation

The cells were seeded in 6-well plates at the initial density of 10^6 and 10^5cells for Melan-a and B16-F10 cells, respectively, and were kept at 37 °C during three days in constant dark (DD). In the beginning of the 4th day, the experimental groups were stimulated with UVA radiation (4.44 kJ/m^2, 1.6 W/m^2 during 45–55 min) at 37 °C (de Assis et al., 2017), and the control group remained at 37 °C in DD. This UVA dose was previously shown to promote neither cell death nor cell cycle arrest 24 or 48 h after the stimulus (de Assis et al., 2017). The temperature of the incubator was carefully monitored every 60 s (iLog, Escort Data Loggers, USA), and the dose of UVA radiation was measured with a UV dosimeter (VLX-3W, Vilver Lourmat, France) coupled to UVA (355 a 375 nm) and UVB (280 a 320 nm) sensors. We have not detected any UVB radiation during the experiments. In this and in the next experimental designs, the cells were harvested immediately after the ending of the stimulus for melanin staining and quantification, and tyrosinase assay.

2.2.1. Pharmacological strategies

To investigate the intracellular components involved in the UVA-induced melanin increase, Melan-a or B16-F10 cells were divided into four groups: (1) cells kept in DD; (2) cells kept in DD in the presence of each specific pharmacological blocker; (3) cells stimulated with UVA radiation; (4) cells stimulated with UVA radiation in the presence of each specific pharmacological blocker. Thirty minutes before UVA stimulus, the inhibitor was added to the medium and remained in contact with the cells throughout the experiments. All inhibitors (Table 1 lists the inhibitors and the respective concentrations) were purchased from Enzo Life Sciences (Plymouth Meeting, PA, USA), except for the guanylyl cyclase inhibitor (Merck, Kenilworth, NJ, USA). Stock solutions were prepared in dimethylsulfoxide (DMSO, Merck, Kenilworth, NJ, USA) with maximal concentration of 1% in the culture medium, except for L-NAME and SQ-22536 which were dissolved in sterile water. The effects of DMSO *per se* were previously analyzed, and no effect on melanin content was seen (Supplementary Fig. 1). Forskolin, an adenylyl cyclase stimulator (Enzo Life Sciences, Plymouth Meeting, PA, USA, dissolved in sterile water) was added to the cells at the beginning of 4th day, and remained in the medium during all experiment.

2.2.2. Gene silencing by endoribonuclease-prepared siRNAs – esiRNA

To specifically target *Opn2* and *Opn4* mRNAs, we used esiRNAs (Merck, Kenilworth, NJ, USA) which silence mouse *Opn2* (Access Number NM_145383) and mouse *Opn4* variants 1 and 2 (Access Number NM_001128599.1 and NM_013887.2, respectively). EsiRNAs result from the cleavage of long double-stranded RNAs (dsRNAs) that generates a heterogeneous mixture of siRNAs, which targets the same mRNA. This methodology provides a more effective and selective gene knockdown with reduced off-target effects than single or pooled siRNAs (Theis and Buchholz, 2011). We used an esiRNA that targets enhanced Green Fluorescent Protein (*Egfp*), as a negative control, since our cell lines do not express this protein.

Melan-a or B16-F10 cells were seeded into 12-well plates at the density of 10^5 and 2×10^4 cells, respectively. After three days in DD, the cells were transfected with 10 nM esiRNA against *Opn2*, *Opn4*, or *Egfp* using Lipofectamine 3000 transfection kit (ThermoFisher, Waltham, MA, USA) according to the manufacturer's instructions. Forty-eight hours after transfection, protein knockdown was confirmed by immunocytochemistry (Supplementary Fig. 2).

Our next step was to challenge Melan-a or B16-F10 cells in which OPN2 and OPN4 protein levels were reduced with UVA radiation. After transfection, the cells were divided into the following groups: (1) cells kept in DD; (2) cells kept in DD in the presence of each esiRNA; (3) cells stimulated with UVA radiation as described above; (4) cells stimulated with UVA radiation in the presence of each esiRNA. Melanin content was evaluated immediately after the ending of UVA stimulus.

Table 1
List of pharmacological reagents.

Inhibitor	Concentration
AA92593, melanopsin antagonist	100 µM
U-73122, phospholipase C, PLC, inhibitor	1, 3 or 9 µM
1-[6-[[(17b)-3-methoxyestra-1,3,5(10)-trien-17-yl]amino] hexyl]-1H-pyrrole-2,5-dione	
BAPTA-AM, calcium chelator.	10 or 50 µM
1,2-bis(o-aminophenoxy)ethane-N,N,N9,N9-tetraacetic acid	
RO 31-8220, protein kinase C, PKC, inhibitor	2.5 µM
2-{1-[3-(amidinothio)propyl]-1H-indol-3-yl}-3-(1-methylindol-3-yl)maleimide methanesulfonate	
Salt	
KN-93, calcium/calmodulin kinase II, CAMK II, inhibitor	3 or 9 µM
N-[2-[[[3-(4-chlorophenyl)-2-propenyl]methylamino]methyl] phenyl]-	
N-(2-hydroxyethyl)-4-methoxybenzenesulphonamide	
SQ-22536, adenylyl cyclase inhibitor	20 µM
9-(tetrahydro-2-furanyl)-9Hpurin-	
6-amine	
L-NAME, NO synthase, NOS, inhibitor	10 mM
L-NG-nitroargininemethyl ester	
2 ODQ, guanylyl cyclase inhibitor	50 µM
3 1H-[1,2,4]Oxadiazolo[4,3-a]quinoxalin-1-one	

All the above-mentioned drugs, except for L-NAME and SQ-22536, were dissolved in DMSO. *Per* se effect of DMSO at the maximal concentration used (1%) was ruled out in melanocytes and melanoma cells.

2.3. Melanin staining – Fontana Masson

Melan-a or B16-F10 cells were seeded into 12-well plates at the density of 10^5 and 5×10^4 cells, respectively. After three days in DD, cells were exposed to UVA radiation (4.44 kJ/m^2, 1.6 W/m^2 during 45–55 min). Immediately after the end of stimulus, the medium was removed, and cells were fixed in 4% paraformaldehyde (Electron Microscopy Sciences, Hatfield, PA, USA) in phosphate-buffered saline (PBS) at 4 °C for 30 min. Then, Fontana-Masson staining was performed accordingly to the manufacturer's instructions (Easy Path, São Paulo, Brazil, Cat. N. EP-11-20024). After the end of the procedure, the cells were immediately analyzed in an inverted microscopy, Axiovert 40CFL (Zeiss, Oberkochen, Germany) with a mercury lamp of 50 W. Bright field photo-micrographics were taken and for a better visualization of the cells, cell autoflorescence was acquired using a Cy3 filter (excitation 549 and emission 562 nm) filter. All images were processed in ZEN Lite software for Windows

2.4. Melanin quantification

After UVA stimulation, a 500 µL aliquot of the medium was collected and transferred to a 1.5 mL tube, and 500 µL of 1 M NaOH (10% DMSO) was added. Next, the remaining medium was removed, and the cells were harvested using Tyrode/EDTA solution. For each cell containing well, an aliquot (200 µL) of the cell suspension was collected and used for cell count in a Neubauer chamber. The residual volume of

the cell suspension (800 µL) was centrifuged at 100 x g during 5 min. The supernatant was discarded and 1 mL of 1 M NaOH (10% DMSO) was added. The melanin containing tubes were heated at 80 °C during 2 h, after which the samples were centrifuged at 1050 × *g* during 15 min, and the supernatant was collected.

Each sample was added in duplicate (200 µL) to wells of a 96-well flat-bottom plate, and total absorbance was measured at 475 nm. The values were interpolated in a standard curve of synthetic melanin (Sigma-Aldrich, St. Louis, MO, USA), ranging from 1.5625 µg/mL to 20 µg/mL. Total melanin content is shown as the total of intra- and extracellular melanin content normalized by the cell number in each well. The statistical analyses were performed with the raw data, which are graphed as the percentage relative to the mean of each cell line group that received the inhibitor, in each condition.

2.5. Immunocytochemistry

Immunocytochemistry assay was performed as previously described (de Assis et al., 2016). Briefly, Melan-a or B16-F10 cells were seeded at the density of 10^4 cells per well into 8-chamber slides and kept in DD for 24 h. On the 2nd day, cells were transfected with esiRNA, and immunostaining of melanopsin (OPN4) and rhodopsin (OPN2) was performed 48 h after transfection. The cells were incubated in primary antibodies anti-melanopsin (1:500, Covance Laboratories, Denver, PA, USA) or anti-rhodopsin (1:25, sc-15382, Santa Cruz Biotechnology, Dallas, TX, USA) overnight at 4 °C. A Cy3-labeled anti-rabbit secondary antibody (1:500, Jackson Immunolab, West Grove, PA, USA) was applied for 1 h at room temperature. Photo-micrographies were obtained with 200× magnification in an inverted fluorescence microscope Axiovert 40CFL (Zeiss, Oberkochen, Germany) with a mercury lamp of 50 W, and DAPI (excitation 358 and emission 463 nm) and Cy3 (excitation 549 and emission 562 nm) filters. All images were processed in ZEN Lite software for Windows.

2.6. Tyrosinase activity

Tyrosinase activity was measured based on previous studies (Kim et al., 2016; Tomita et al., 1992; Tuerxuntayi et al., 2014) with slight modifications. After UVA radiation stimulation, the medium was discarded, and the cells were harvested with Tyrode/EDTA solution and centrifuged at 100 × *g* during 5 min. The pellet was rinsed with PBS followed by a centrifugation at 1050 × *g* during 5 min. The pellet was incubated with Tris-HCL (0.1 M, 1% Triton X-100, pH 6.8) during 1 h at −20 °C. After this period, the samples were thawed at room temperature and centrifuged at 14,000 × *g* during 10 min.

The supernatant was transferred to a 1.5 mL tube, and protein concentration was determined by the BCA method according to the manufacturer's instructions (Thermo Fisher, Waltham, MA, USA). A volume containing 60 µg of protein and 20 µL of 10 mM L-DOPA (pH 6.8) was added to a 96-well flat bottom plate, completing with Tris-HCL solution up to 200 µL. After incubation at 37 °C during 1 h, total absorbance of each sample in duplicate was measured at 475 nm. The statistical analyses were performed with the raw data and the results are shown as percentage relative to the mean of the control group of each cell line. Comparison of tyrosinase activity between Melan-a and B16-F10 cells was also performed using raw data, and the results are expressed as percentage relative to the mean in Melan-a cells in DD.

2.7. Data and statistical analyses of in vitro data

The values (from at least two independent experiments) were graphed as mean ± SEM. Melanin content of each group was analyzed by One-way ANOVA followed by Tukey post-test. Tyrosinase activity in control and UVA-exposed group from the same cell line was analyzed by Student's *t*-test. The comparison of tyrosinase activity between cell lines in the same experimental condition (DD or UVA-exposed group) was also analyzed by Student's *t*-test. Samples that showed Gaussian distribution were analyzed by *t*-test with Welch correction while those that did not show normal distribution were analyzed by Mann-Whitney test. Significance was set for $p < 0.05$. All analyses were carried out in GraphPad Prism Version 7.0.

2.8. Bioinformatics analyses of GTEX database

We evaluated the expression of opsin-encoding genes in human skin samples from The Genotype-Tissue Expression (GTEx) (Consortium, 2015). RNASeq data (TcgaTargetGtex_RSEM_Hugo_norm_count) from unexposed and sun-exposed (n = 233 and 324, respectively) skins were downloaded from UCSC Xena browser (http://xena.ucsc.edu) in December 2017. Gene expression values were calculated using RSEM and log2(x + 1) transformed. All samples were checked for normality by D'Agostino & Pearson test. Mann-Whitney test was performed between unexposed and sun-exposed skin for each gene.

3. Results

The putative candidates that could ultimately perceive UVA radiation would be OPN1SW (maximal absorption peak of 430 nm) and/or OPN4 (maximal absorption peak of 480 nm) (Hughes et al., 2012; Solomon and Lennie, 2007). Retinal OPN2 has been previously shown to absorb approximately in 550 nm (Lucas et al., 2014); intriguingly, in human melanocytes and keratinocytes OPN2 was reported to absorb in the violet (380–420 nm) and UVA wavelengths (Kim et al., 2013; Wicks et al., 2011). Another strong candidate could be neuropsin, OPN5, that also absorbs in the UVA wavelength range (Buhr et al., 2015; Kojima et al., 2011); however, OPN5 is not expressed in our cell lines (de Assis et al., 2017). Recently, another opsin, peropsin, has been demonstrated to be expressed in human skin and keratinocytes as it contributes to UVA-driven calcium influx in keratinocytes (Toh et al., 2016); however, peropsin expression was not investigated in this study. Thus, there remain three opsin candidates, OPN1SW, OPN2, and OPN4, as the putative UVA sensors in Melan-a and B16-F10 cells.

Initially, we used Fontana-Masson staining to provide a better visualization of the UVA-driven IPD in normal and malignant melanocytes, which was previously demonstrated by our group (de Assis et al., 2017). Immediately after UVA exposure, melanin content was increased in both cell types compared to control group (Fig. 1), a fact that corroborates our melanin measurements carried out in this study. Then, we investigated the role of OPN4 in the UVA-driven melanin content increase that takes place in normal and malignant melanocytes using a specific OPN4 antagonist, AA92593 (Jones et al., 2013). Since DMSO was used at the maximal concentration of 1%, we first analyzed the effects of DMSO *per se*, which were ruled out in both DD and UVA-exposed melanocytes and melanoma cells (Supplementary Fig. 1). Our data show that UVA radiation led to 50–85% increase of melanin content in both normal and malignant melanocytes (Fig. 2A–B). It is interesting to note that 100 µM AA92593 partially blocked the UVA-induced melanin increase in Melan-a cells, but not in B16-F10 cells; however, when given in a reduced concentration (10 µM) the antagonist blocked the increase of melanin content in both cell lines (Fig. 2A–B).

Next, we confirmed the pharmacological data using gene knockdown strategies. Protein levels of OPN2 and OPN4 were significantly reduced in Melan-a and B16-F10 cells transfected with the respective esiRNAs (Figs. 3A–D; 4A–D , and Supplementary Fig. 2). Interestingly, in normal and malignant melanocytes when OPN4 protein levels were diminished, a profound reduction of the UVA-induced melanin increase was observed (Figs. 3E and 4E), which corroborated the results with the melanopsin antagonist. The presence of OPN4 in human skin was not detected in two studies (Haltaufderhyde et al., 2015; Regazzetti et al., 2017); however, we evaluated the presence of *OPN4* as well as other opsins in human skin transcriptome data. In fact, human skin expresses

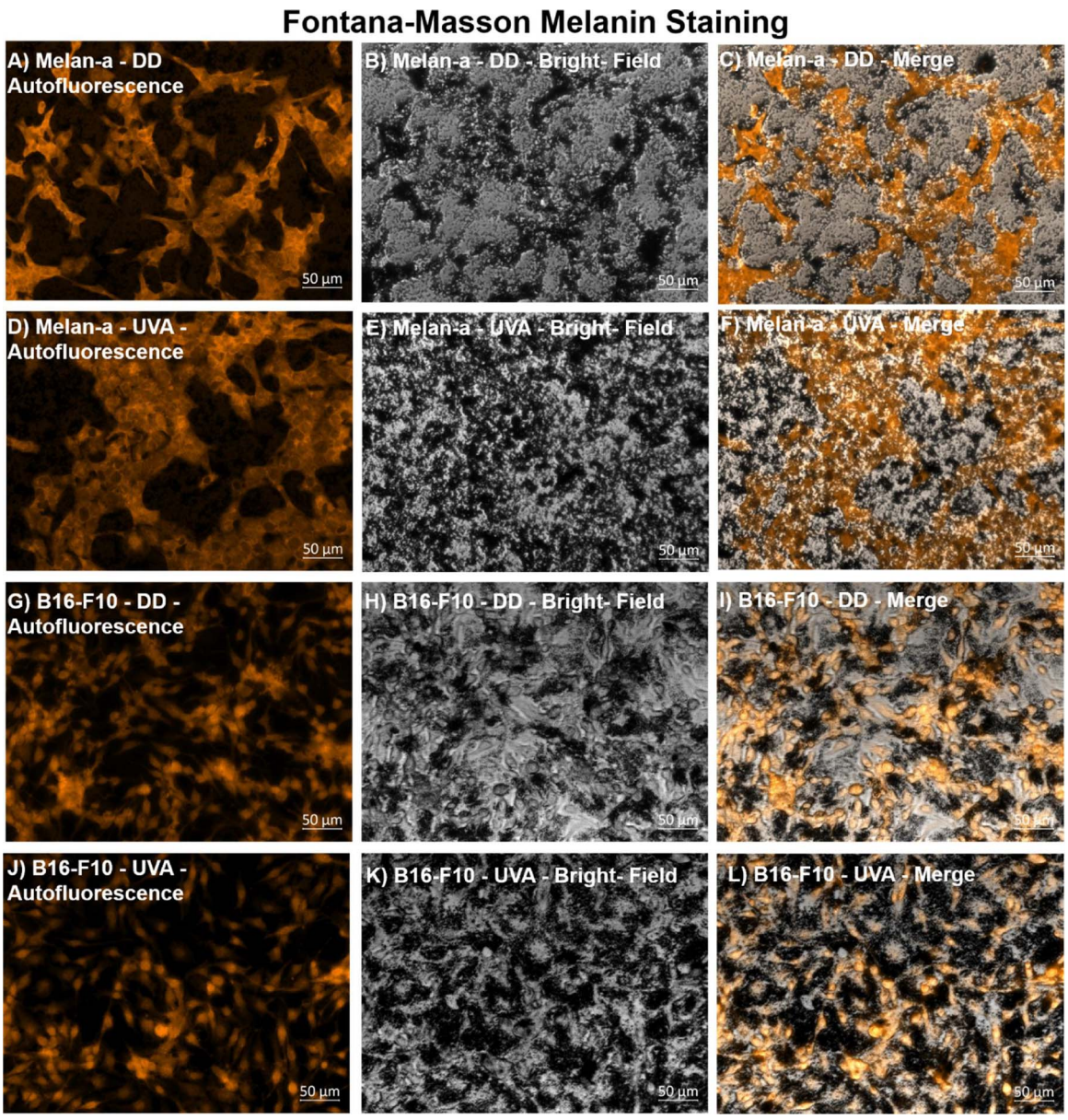

Fig. 1. Representative images of Fontana-Masson stained murine Melan-a melanocytes and B16-F10 melanoma cells exposed to UVA radiation in comparison to non-UVA exposed groups. The staining procedure was performed immediately after the end of UVA stimulus. Autofluorescence (A, D, G, and J) was captured using inverted microscopy, Axiovert 40CFL (Zeiss, Oberkochen, Germany) with a mercury lamp of 50 W and a filter with excitation 549 and emission 562 nm. Bright field photo-micrographies (B, E, H, and K) were also taken with the same equipment. Bright field- and autofluorescence photo-micrographies were processed in ZEN Lite software for Windows, adjusted to min/max function, and are shown as merge of the previous images (C, F, I, and L).

OPN1SW, *OPN1MW*, *OPN2*, *OPN3*, *OPN4*, and *OPN5*. Interestingly, the expression of *OPN1LW* and *OPN4* is higher in sun-exposed skin as compared to unexposed skin, whereas *OPN5* expression is higher in unexposed skin (Fig. 5). Surprisingly, in both Melan-a and B16-F10 cells OPN2 also seems to participate in the UVA-driven melanin content increase since knockdown of OPN2 led to a reduction of UVA-induced increase of melanin content (Figs. 3E and 4E). These evidences agree with previous studies (Kim et al., 2013; Wicks et al., 2011), which have reported the non-canonical role of OPN2 as a UVA sensor.

Since we have shown that both OPN2 and OPN4 participate in the UVA-induced increase of melanin content in melanocytes and melanoma cells, our next step was to investigate the evoked signaling pathways. In the retinal ganglion cells, the photo-isomerization of *cis*-retinal – which is bound to OPN4 – into *all-trans* retinal activates a signaling pathway dependent on $G_{\alpha q}$ protein and phospholipase C (PLC), ultimately leading to the opening of the transient receptor potential (TRP) C6/7 channel and increase of cytosolic calcium level (Hughes et al., 2012). Based on this knowledge, we first analyzed the canonical OPN4 signaling pathway which takes place in the retina (Hughes et al., 2012).

Initially, we blocked PLC with 9 µM U73122 (Wicks et al., 2011), which was cytotoxic to both normal and malignant melanocytes (data not shown). We then reduced the concentration to 1 µM (Lopes et al., 2010; Moraes et al., 2015; Ramos et al., 2014), which induced the loss of UVA-triggered increase in melanin content in normal melanocytes (Fig. 6A); however, the blockade of PLC had no effect on UVA-evoked response of malignant melanocytes (Fig. 6B) even at higher concentration (3 µM, data not shown). These data suggest that in normal melanocytes UVA recruits PLC (Fig. 6A) while in malignant melanocytes this pathway does not participate in the UVA-driven increase of melanin content (Fig. 6B).

Next, we investigated the role of calcium in the UVA-dependent

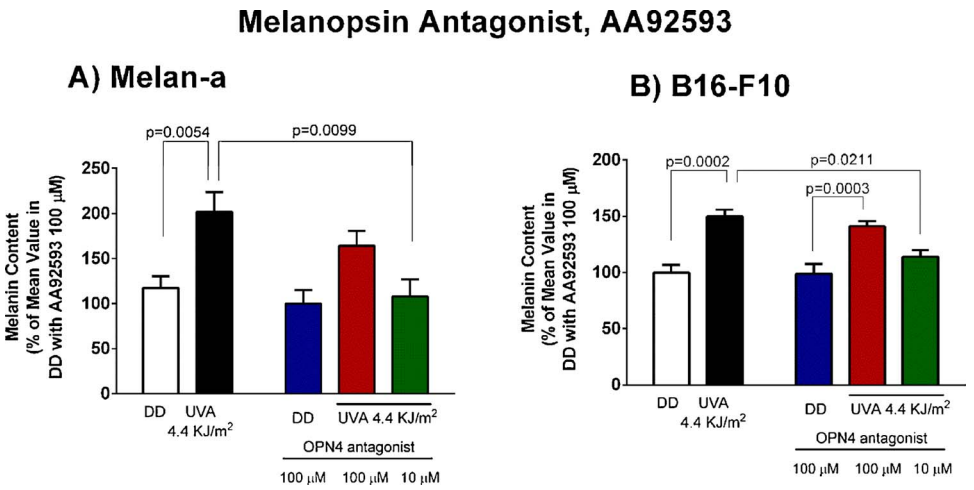

Fig. 2. Melanin content increase induced by UVA radiation in murine Melan-a melanocytes (A) and B16-F10 melanoma cells (B) in the presence of the melanopsin antagonist, AA92593. Melanin in both cell lines was immediately extracted after UVA radiation. Melanin levels are expressed as the mean percentage (n = 4-10), ± SEM, of the values in 100 μM AA92593-treated cells in DD; p values are shown in the graphs.

process by chelating the cation with BAPTA-AM at 10 μM based on previous studies (Lopes et al., 2010; Wicks et al., 2011). BAPTA-AM at 10 μM did not abolish the UVA-induced increase of melanin content in Melan-a cells (data not shown), but significantly reduced melanin content in the malignant cell line (Fig. 6D). We then increased BAPTA-AM concentration to 50 μM which was able to inhibit the UVA-induced response in normal melanocytes (Fig. 6C). Therefore, our results indicate that calcium was signaling the UVA-induced melanin increase in both normal and malignant melanocytes. It should be mentioned, however, that in Melan-a cells, since PLC was activated, calcium probably came from internal stores as well as through cell membrane channels. On the other hand, PLC was not activated in B16-F10 cells, thus calcium most probably came from the extracellular compartment. This hypothesis is strengthened by the loss of UVA-driven IPD in both melanocytes and melanoma cell lines in the presence of 100 μM ruthenium red (data not shown), a broad inhibitor of TRP and other calcium permeable channels (Bellono et al., 2013; Clapham et al., 2005).

Since calcium was an important player in the melanin content increase in response to UVA radiation, we investigated whether protein kinase C (PKC) or CAM kinase II (calcium-dependent protein kinase/calmodulin II) participated in this response. As we had shown evidence that PLC participated in the UVA-induced response in Melan-a cells, it would be expected diacylglycerol (DAG) and inositol trisphosphate (IP_3) production: DAG could modulate TRP channels (Bellono et al., 2014) as well as lead to PKC activation, while IP_3 would mobilize calcium from intracellular storages (Kadamur and Ross, 2013).

We then inhibited PKC with 2.5 μM RO 31-8220 (Lopes et al., 2010), which was ineffective on normal melanocytes (Fig. 7A). Although PLC seemed not to be mobilized in the response of malignant melanocytes to UVA radiation, atypical PKC could still be a player in a DAG/Ca^{2+}-independent manner, since this type of PKC is frequently activated in cancer cells (Parker et al., 2014). Based on this, we also used RO 31-8220 in malignant melanocytes, but the response to UVA was unaffected (Fig. 7B) similarly to normal cells (Fig. 7A). Since PKC involvement in this UVA-driven process was ruled out, our next step was to investigate whether CaMK II participated in this response. To do so, we specifically inhibited CaMK II with 3 μM KN-93 (Lopes et al., 2010; Ramos et al., 2014), which did not prevent the melanin increase induced by UVA radiation in normal melanocytes (data not shown), but blocked UVA-elicited response in B16-F10 melanoma cells (Fig. 7D). When KN-93 concentration was increased to 9 uM, an inhibition was

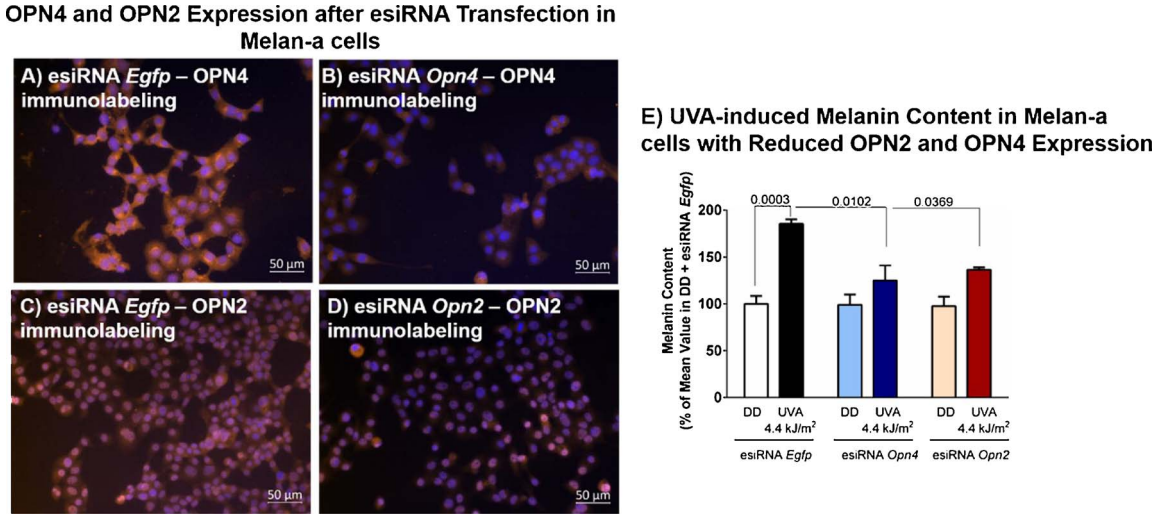

Fig. 3. Representative fields of OPN2 and OPN4 immunostained Melan-a cells. (A) OPN4 staining in cells kept in DD and transfected with esiRNA against *Egfp*; (B) OPN4 staining in cells kept in DD and transfected with esiRNA against *Opn4*; (C) OPN2 in Melan-a cells kept in DD and transfected with esiRNA against *Egfp*; (D) OPN2 in cells kept in DD and transfected with esiRNA against *Opn2*. DAPI stained nuclei in blue and immunopositivity in orange for OPN4 or OPN2 with 1:500 or 1:25 antiserum, respectively, revealed with a Cy3-labeled secondary antibody in orange. Photomicrographies were taken with Axiocam MRm camera (Zeiss) and pseudocolored with Axiovision software (Zeiss). Scale bar 50 μm (200 × magnification). (E) UVA-induced melanin content in Melan-a cells transfected with esiRNA against *Egfp*, *Opn2*, and *Opn4*. Melanin was immediately extracted after UVA radiation. Melanin levels are expressed as the mean percentage (n = 4-5), ± SEM, of the values in cells transfected with esiRNA against *Egfp* in DD; p values are shown in the graphs. (For interpretation of the references to colour in this figure legend, the reader is referred to the web version of this article.)

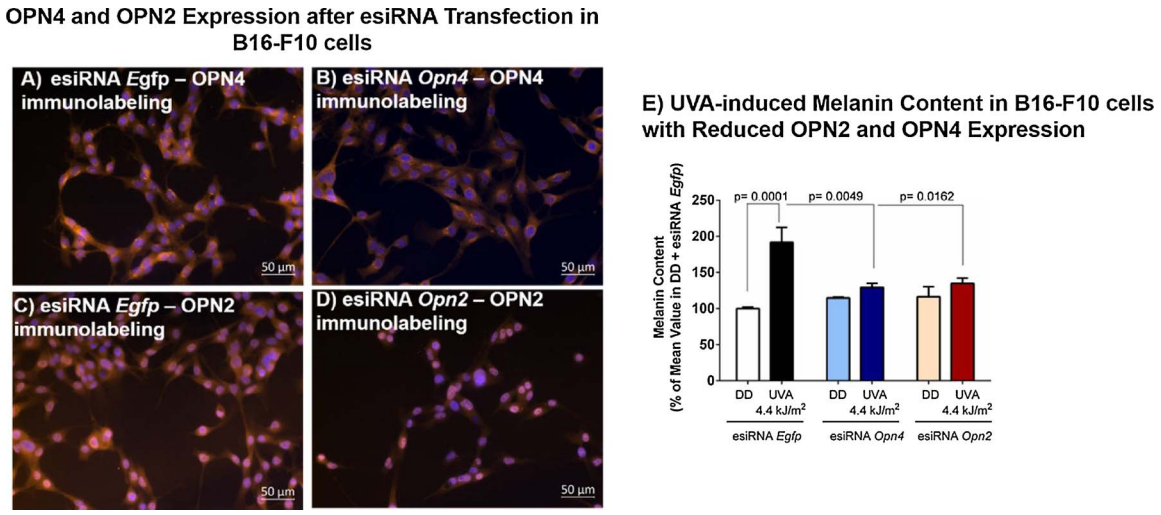

Fig. 4. Representative fields of OPN2 and OPN4 immunostained B16-F10 cells. (A) OPN4 staining in cells kept in DD and transfected with esiRNA against *Egfp*; (B) OPN4 staining in cells kept in DD and transfected with esiRNA against *Opn4*; (C) OPN2 in B16-F10 cells kept in DD and transfected with esiRNA against *Egfp*; (D) OPN2 in cells kept in DD and transfected with esiRNA against *Opn2*. DAPI stained nuclei in blue and immunopositivity in orange for OPN4 or OPN2 with 1:500 or 1:25 antiserum, respectively, revealed with a Cy3-labeled secondary antibody in orange. Photomicrographies were taken with Axiocam MRm camera (Zeiss) and pseudocolored with Axiovision software (Zeiss). Scale bar 50 µm (200× magnification). (E) UVA-induced melanin content in B16-F10 cells transfected with esiRNA against *Egfp*, *Opn2*, and *Opn4*. Melanin was immediately extracted after UVA radiation. Melanin levels are expressed as the mean percentage (n = 4-5), ± SEM, of the values in cells transfected with esiRNA against *Egfp* in DD; p values are shown in the graphs. (For interpretation of the references to colour in this figure legend, the reader is referred to the web version of this article.)

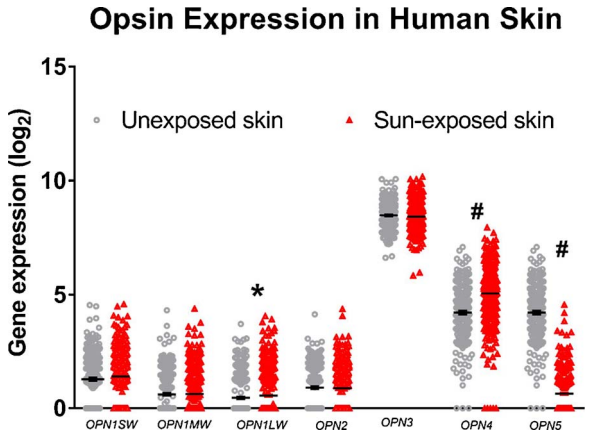

Fig. 5. Evaluation of opsin-encoding genes in unexposed and sun-exposed human skin (n = 233 and 324, respectively). Human skin shows detectable levels of *OPN1SW*, *OPN1MW*, *OPN1LW*, *OPN2*, *OPN3*, *OPN4*, and *OPN5*. Comparison of opsin-encoding genes in unexposed and sun- exposed skin was performed by Mann-Whitney test. Data are shown as scatter plot ± SEM. * p = 0.0040 and # p = < 0.0001.

now seen in the response of normal melanocytes (Fig. 7C).

It is well known that CaMK II phosphorylates nitric oxide synthase (NOS), which catalyzes the nitric oxide (NO) synthesis. NO is an easily permeable gas which activates soluble guanylyl cyclases (sGC), an event that ultimately results in cyclic GMP (cGMP) formation (Francis et al., 2010). In order to further investigate whether CaMK II/NO/sGC/cGMP pathway was responsible for the UVA-induced increase of melanin content in both normal and malignant melanocytes, we used the NOS inhibitor, L-NAME, at 10 mM (Campos et al., 2007; Ramos et al., 2014). In fact, when NOS was inhibited the increase of melanin content induced by UVA radiation was prevented, demonstrating the involvement of this pathway in both cell lines (Fig. 8A and B). When we specifically inhibit the sGC with 50 µM ODQ (Chan and Fiscus, 2003; Matsunaga et al., 2014), the UVA-induced increase of melanin content was also lost in both normal and malignant melanocytes (Fig. 8C and D).

Since the cAMP/PKA pathway is known to be important in triggering the *de novo* synthesis of melanin (Nery and Castrucci, 1997; Slominski et al., 2004), our next step was to evaluate its participation in the IPD induced by UVA. In the presence of 10 µM forskolin, an adenylyl cyclase activator (Fimia and Sassone-Corsi, 2001; Seino and Shibasaki, 2005), both normal and malignant melanocytes kept in DD showed an increase of melanin content similar to cells exposed to UVA radiation (Fig. 9A and B). However, the participation of cAMP/PKA pathway was ruled out when adenylyl cyclase was inhibited with 20 µM SQ-22536 (Fimia and Sassone-Corsi, 2001; Seino and Shibasaki, 2005) and no reduction of the UVA-induced response was found in Melan-a and B16-F10 cells (Fig. 9C and D).

The genesis of IPD process is still controversial and the literature is scarce. *De novo* synthesis of melanin is not accepted to occur in IPD, being an event known to take place only in delayed tanning (Mahmoud et al., 2008; Rosen et al., 1990; Sklar et al., 2013). In our model, the UVA-driven IPD process is likely due to photo-oxidation of melanin precursors, and not to *de novo* melanin synthesis, as we have previously demonstrated the acute and transient increase in melanin content, which returned to basal level 6 h after the UVA stimulus (de Assis et al., 2017). Corroborating this classical view of IPD, we have shown that tyrosinase activity was not increased in normal and malignant melanocytes after UVA radiation (Fig. 10A–C). In melanoma cells tyrosinase activity was 30% higher than in the normal melanocytes (Fig. 10C), which has been demonstrated before (Fuller, 1987; Jimenez et al., 1988; Slominski et al., 1983).

4. Discussion

We have provided evidence that OPN2 of murine melanocytes and melanoma cells participates in the IPD process, corroborating previous studies (Bellono et al., 2013; Wicks et al., 2011), further supporting the notion that OPN2 in the skin is in fact a UVA sensor as previously appreciated (Kim et al., 2013; Wicks et al., 2011). But we are the first to show that OPN4 is also a UVA sensor in normal and malignant murine melanocytes. In the pharmacological assays using the specific inhibitor, AA92593, there was not a dose-response relationship, what is intriguing and not yet fully understood, and should be subject of future investigation. Nevertheless, the implication of OPN4 in UV-induced responses suggested by the pharmacological assays was confirmed by knockdown strategies, thus further demonstrating the role of OPN4 as UVA sensor.

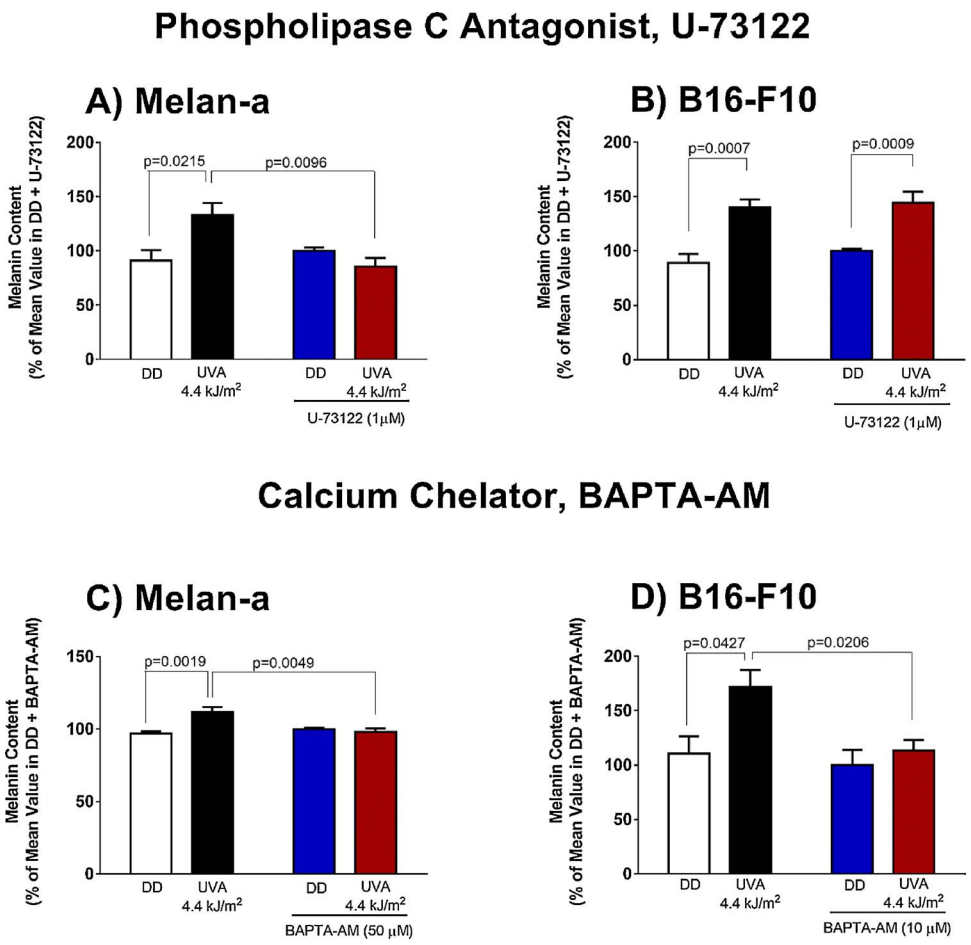

Fig. 6. Melanin content increase induced by UVA radiation in murine Melan-a melanocytes (A, C) and B16-F10 melanoma cells (B, D) in the presence of the phospholipase inhibitor, U-73122 (A, B), or the calcium chelator, BAPTA-AM (C, D). Melanin in both cell lines was immediately extracted after UVA radiation. Melanin levels are expressed as the mean percentage (n = 4–7), ± SEM, of the values in cells treated with each inhibitor in DD; p values are shown in the graphs.

OPN4 has been shown to be expressed in murine blood vessels and to participate in blue-light dependent relaxation through a cGMP-dependent pathway (Sikka et al., 2014). OPN4 is traditionally found in the mammalian retina and participates in the synchronization of the central oscillator (Hughes et al., 2012; Panda et al., 2003; Panda et al., 2002); our data in cutaneous cells further reinforce the intriguing role of opsins outside the eye as recently reviewed (Leung and Montell, 2017). In fact, our group has demonstrated – for the first time – that OPN4 detects thermal energy and feeds the local molecular clock of murine melanocytes and melanoma cells (Moraes et al., 2017). However, in human melanocytes and skin *OPN4* was not detected through qPCR (Haltaufderhyde et al., 2015; Regazzetti et al., 2017) but recent RNASeq analysis from The Genotype-Tissue Expression (GTEx) (Consortium, 2015) shows detectable levels of *OPN4* as well as *OPN1SW*, *OPN1MW*, *OPN1LW, OPN2*, *OPN3*, and *OPN5*. Nevertheless, the role of OPN4 in human models is still unknown and requires further evaluation.

It is worth to highlight that despite the fact that OPN2 and OPN4 act as UVA sensors in murine Melan-a and B16-F10 cells, upon knockdown of either opsin, the UVA-induced increase of melanin content was totally lost. Therefore, these data suggest an unexpected level of interaction between OPN2 and OPN4, for the first time shown here, in which the removal of a single opsin completely abolishes UVA-driven IPD in both cell lines. Thus, the IPD process induced by UVA seems to be dependent on a cooperative action between OPN2 and OPN4. It is interesting to mention that OPN2 was shown to be organized as dimers in rod photoreceptors (Gunkel et al., 2015), thus, strengthening the possibility of cooperativity between OPN2 and OPN4.

Some studies have also suggested that IPD is independent of structural integrity (Honigsmann, 2002), thus, it could be considered an acellular process; however, its reversion requires intracellular mechanisms (Honigsmann et al., 1986). An elegant study has shown migration and dispersion of melanosomes in keratinocytes 18 h after UVA radiation: in basal conditions the melanin granules cap the nucleus, but after UVA exposure they migrate to the cell periphery (Lavker and Kaidbey, 1982). In fact, this pattern of translocation has been suggested as an explanation of the skin darkening shown to occur in keratinocytes (Lavker and Kaidbey, 1982) and melanocytes (Jimbow et al., 1973); however, this melanosome migration does not take place in IPD (Beitner and Wennersten, 1985; Honigsmann et al., 1986), and thus the migration of melanosomes is still an open question (Mahmoud et al., 2008; Sklar et al., 2013). A second mechanism that could explain IPD is the melanosome transfer from melanocytes to keratinocytes (Beitner and Wennersten, 1985; Jimbow et al., 1973); but no evidence was found during IPD (Honigsmann et al., 1986). Within this line, a recent *in vitro* study using co-culture of melanocytes and keratinocytes demonstrated that UVA or UVB leads to calcium influx and contributes to melanosome transfer through a signaling pathway dependent on retinal, calcium, PLC, and TRPM1 (Hu et al., 2017). The third, and most accepted, mechanism proposed for IPD is the photo-oxidation of melanin precursors in response to UVA radiation and visible light (Honigsmann et al., 1986; Pathak et al., 1962; Pathak and Stratton, 1968; Sklar et al., 2013).

In the opposite direction of this traditional view, recent studies have provided evidence that human melanocytes exposed to UVA radiation show an IPD process that is dependent on OPN2, retinal, PLC, IP_3, DAG, intra- and extracellular calcium, which ultimately lead to a fast melanin synthesis (Bellono et al., 2013; Bellono et al., 2014; Wicks et al., 2011). Our data, nevertheless, showed that new melanin synthesis did not account for the IPD process in murine Melan-a melanocytes and B16-

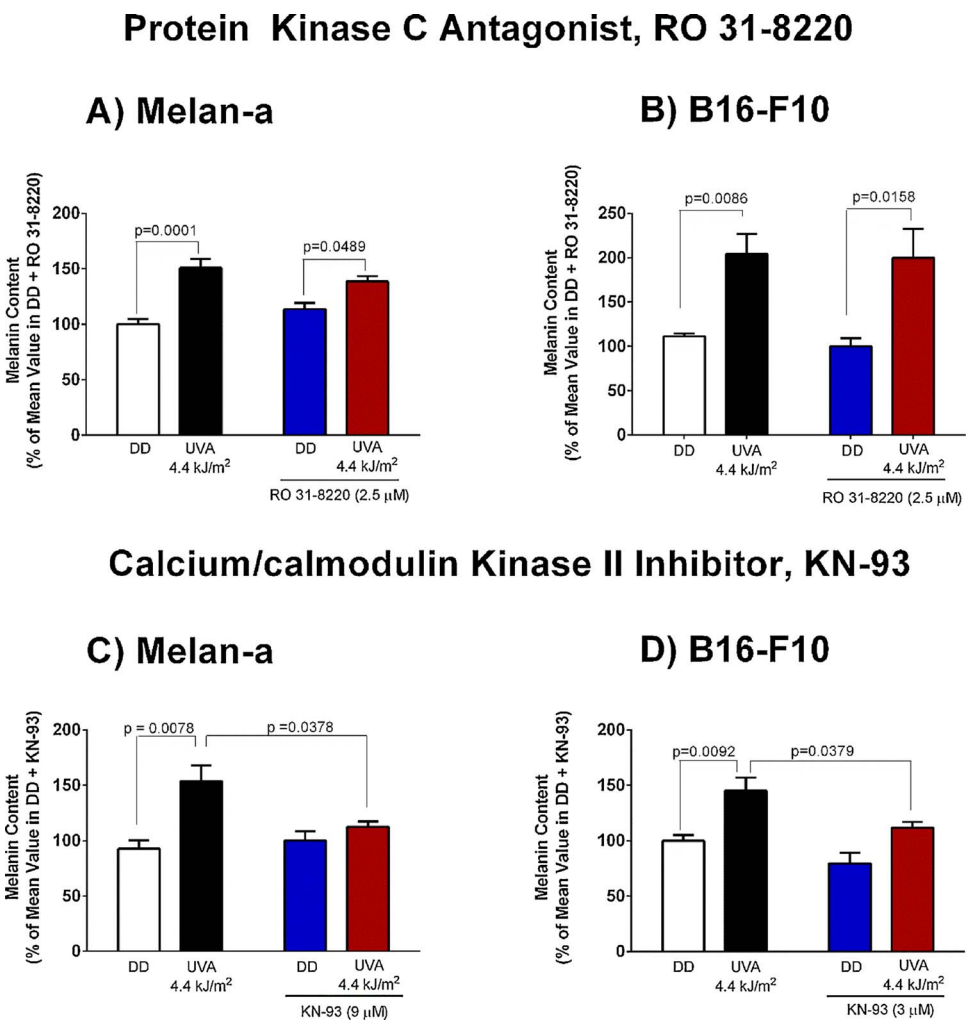

Fig. 7. Melanin content increase induced by UVA radiation in murine Melan-a melanocytes (A, C) and B16-F10 melanoma cells (B, D) in the presence of the protein kinase C inhibitor, RO 31-8220 (A, B), or the calcium/calmodulin kinase II inhibitor, KN-93 (C, D). Melanin in both cell lines was immediately extracted after UVA radiation. Melanin levels are expressed as the mean percentage (n = 4–6), ± SEM, of the values in cells treated with each inhibitor in DD; p values are shown in the graphs.

F10 melanoma cells. In fact, in a previous study we described that the UVA-driven IPD is reversible (de Assis et al., 2017), and probably a result of fast oxidation of pre-melanin precursors into melanin. The signaling pathways for IPD in murine and human melanocytes share some common steps such as the participation of opsins and calcium; however, the studies performed in human melanocytes, as shown above, brought compelling evidence that melanin synthesis – but not melanin oxidation – takes place.

The two protocols were very different, but we believe that the major difference lies in the fact that the UV apparatus used in the human studies (Bellono et al., 2013; Bellono et al., 2014; Wicks et al., 2011) showed a minor UVB wavelength, whereas in our study no UVB wavelength was detected (de Assis et al., 2017). Even though UVB does not lead to a fast melanin synthesis (Wicks et al., 2011), a putative synergism between UVA and UVB may have occurred. Corroborating this hypothesis, UVB is known to activate corticotropin-releasing factor (CRF) and proopiomelanocortin (POMC) peptides (namely alpha-melanocyte stimulating hormone, beta-endorphin, and adrenocorticotropin) (Skobowiat et al., 2011), an event that could have contributed for the melanin synthesis profile found by Wicks and colleagues (Wicks et al., 2011). Another striking difference is that the irradiance used in human melanocytes was approximately 60-fold higher (100 W/m^2) (Bellono et al., 2013; Wicks et al., 2011) than the irradiance used by our group (1.6 W/m^2) (de Assis et al., 2017). The final dosages were also different since human melanocytes were exposed to 10–50 kJ/m^2 (Bellono et al., 2013; Wicks et al., 2011) while in our study the cells were exposed to 4.4 kJ/m^2. The length of exposure to UV radiation lasted from seconds to minutes in human cells, because of the high irradiance, while in our study the cells were exposed during 45–55 min to obtain a much lower dosage. Wicks and colleagues (Wicks et al., 2011) found that the melanin synthesis is UVR-dose dependent (10–50 kJ/m^2) 8 h after the stimulus whereas our findings showed an immediate melanin increase after UVA exposure with decreased levels 6 h later (de Assis et al., 2017).

Since the pigments generated during IPD do not absorb in the UV wavelength, *i.e.*, do not protect DNA against the radiation deleterious effects, the relevance and importance of this process has been long questioned (Black et al., 1985; Honigsmann, 2002; Honigsmann et al., 1986; Miyamura et al., 2011; Moan et al., 2012; Willis et al., 1972). Contrary to this view, a recent and interesting study demonstrated that IPD protects the skin and the subcutaneous tissues against the deleterious effects of visible light, which is known to penetrate deeply, and reach the dermal capillaries (Mahmoud et al., 2010; Moan et al., 2012; Sikka et al., 2014; Sklar et al., 2013). Based on this evidence it has been proposed that IPD provides an excellent protection against photosensitization and degradation of folate derivatives and other chromophores present in the skin such as porphirins, flavins, pterins, which are known to absorb in the visible light spectrum (Moan et al., 2012).

Photo-degradation of folate and its metabolite, methyltetrahydrofolate 5MTHF, in response to UVA radiation and visible light reduces folate levels, which significantly impairs cellular division. Therefore, protection of folate and other chromophores against UV and light is in fact a strong adaptive selective event (Jablonski and Chaplin, 2010). Corroborating these findings, it has been set forth that folate protection in addition to DNA protection – a classic known process – would be the key role of pigmentary response in the skin (Branda and

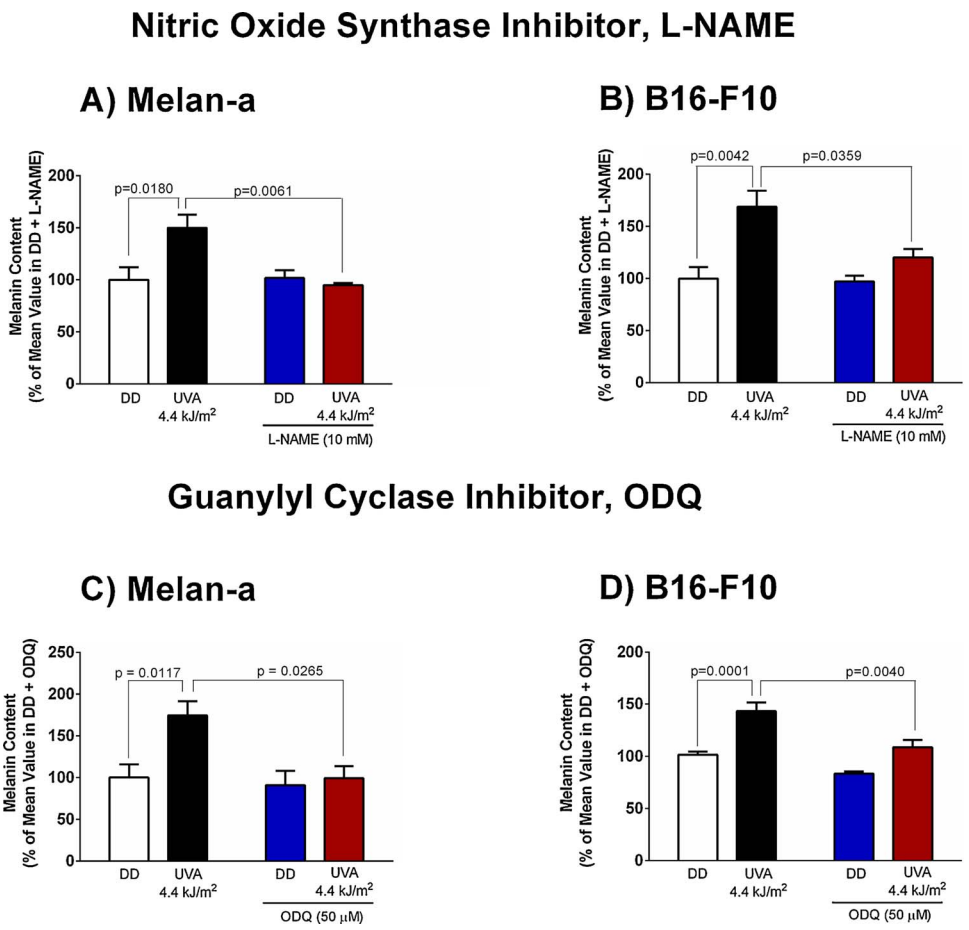

Fig. 8. Melanin content increase induced by UVA radiation in murine Melan-a melanocytes (A, C) and B16-F10 melanoma cells (B, D) in the presence of the nitric oxide synthase inhibitor, L-NAME (A, B), or the guanylyl cyclase inhibitor, ODQ (C, D). Melanin in both cell lines was immediately extracted after UVA radiation. Melanin levels are expressed as the mean percentage (n = 3-11), ± SEM, of the values in cells treated with each inhibitor in DD; p values are shown in the graphs.

Eaton, 1978; Jablonski and Chaplin, 2010).

The role of opsins mediating the pigmentary process has been shown in delayed tanning (DT): blue light leads to DT *via* OPN3-dependent signaling, calcium, CAMK II, CREB, ERK, p38, culminating in MITF phosphorylation (Regazzetti et al., 2017). Blue light has also been shown to stimulate hair follicle growth *via* OPN3 (Buscone et al., 2017). Therefore, both IPD and DT, hallmarks of the pigmentary process, have been demonstrated to depend on opsins, which may be of great clinical interest.

Taken altogether, we have shown that both normal and malignant melanocytes have a functional photosensitive system in which OPN2 and OPN4 act as UVA sensors. Both normal and malignant melanocytes share some signaling components, CAMK II/NOS/cGMP, which lead to immediate increase of melanin content in response to UVA. Accordingly, it has been previously shown that UVA radiation increases cGMP levels in mice skin (Allanson et al., 2006) and NO in human skin from several donors (Holliman et al., 2017). Our findings, therefore, demonstrate that the IPD process is not an abiotic process, caused by fast and reversible chemical reactions, but it involves a membrane-bound light sensor with complex intracellular signaling pathways.

These data in murine models contribute to the better understanding of the photosensitive system within the skin, which is still poorly comprehended. OPN2 has been shown to act as a UVA sensor in human melanocytes and keratinocytes (Wicks et al., 2011; Kim et al., 2013), which is in line with our findings. Therefore, the photosensitive system in murine and human skin exhibits a significant degree of conservation. Even though our data show an interesting role of OPN4 in murine cells, its role in human model is still unknown; however, we speculate – based on the conserved characteristics in both systems – that OPN4 in human skin could display a potential role in mediating light-based events. Therefore, if our findings were validated in humans, we suggest that the photosensitive system could become an interesting pharmacological target for the treatment of depigmentary disorders as well as skin-related cancer. As the functionality of this system starts to be understood new perspectives for therapies and pharmacological intervention become closer to reality.

Author contributions

de Assis, L.V.M., Moraes, M.N., and Castrucci, A.M.L. designed the study. de Assis, L.V.M. and Magalhães-Marques, K. acquired the data. de Assis, L.V.M. and Moraes, M.N. analyzed the data. de Assis, L.V.M drafted the manuscript. de Assis, L.V.M., Moraes, M.N., and Castrucci, A.M.L. critically revised the draft. All authors have approved the final version of the manuscript and agreed to be accountable for all aspects of the study in ensuring that questions related to the accuracy or integrity of any part of the study are appropriately investigated and resolved. All persons designated as authors qualify for authorship, and all those who qualify for authorship are listed.

Competing interests

None to declare.

Acknowledgements

This work was partially supported by the Sao Paulo Research Foundation (FAPESP, grant 2012/50214-4) and by the National Council of Technological and Scientific Development (CNPq, grants 301293/2011-2 and 303070/2015-3). L.V.M. de Assis and M.N. Moraes are fellows of FAPESP (2013/24337-4 and 2014/16412-9, respectively). We are thankful to Prof. Carlos Frederico Martins Menck for providing

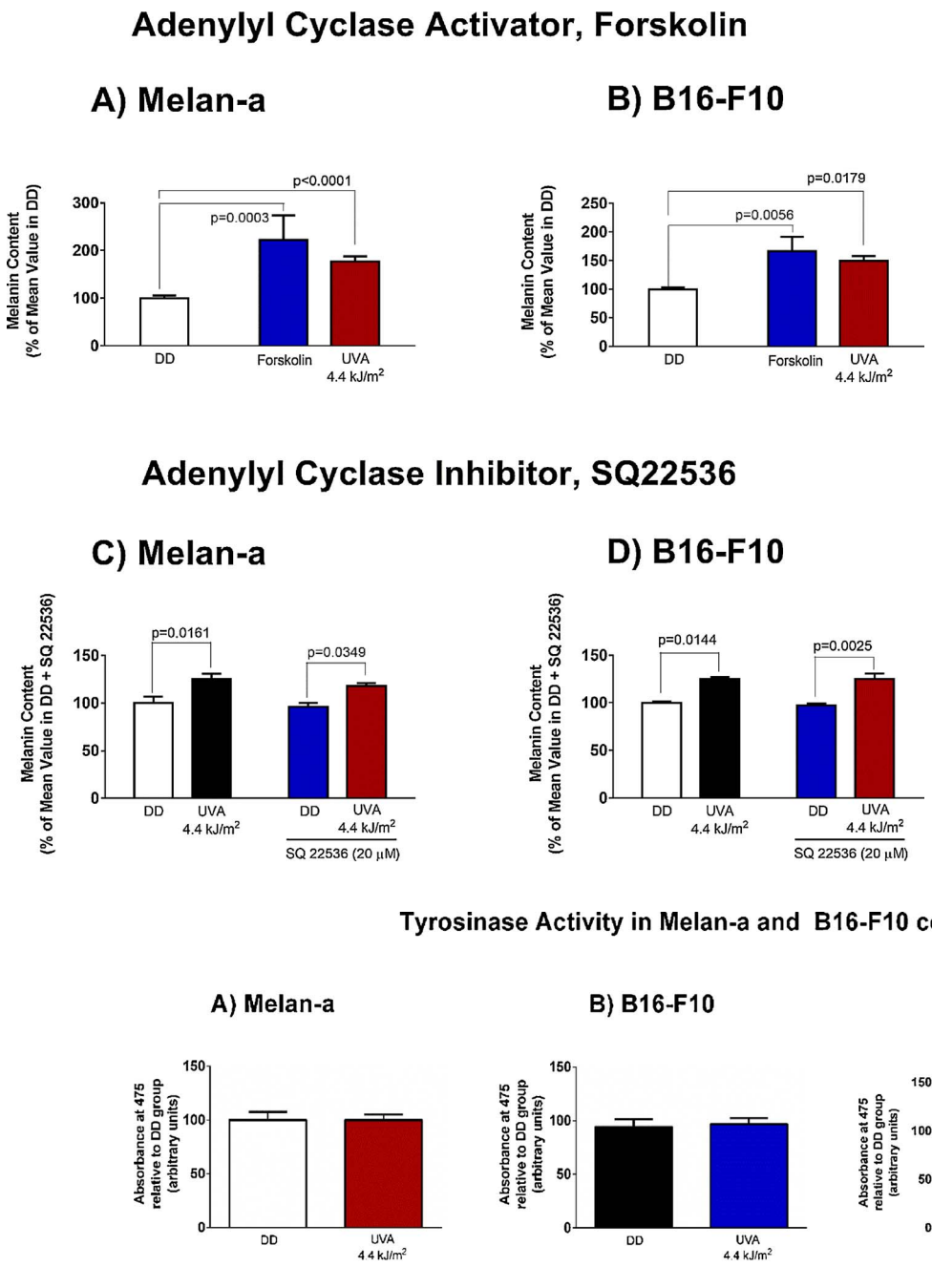

Fig. 9. Melanin content increase induced by UVA radiation or forskolin in murine Melan-a melanocytes (A) and B16-F10 melanoma cells (B). (C) and (D) show melanin content in Melan-a and B16-F10 cells, respectively, after UVA radiation in the absence or presence of the adenylyl cyclase inhibitor, SQ22536. Melanin in both cell lines was immediately extracted after UVA radiation. Melanin levels are expressed as the mean percentage (n = 3–11), ± SEM, of the values in DD control cells (A and B) or in SQ22536-treated cells in DD (C and D); p values are shown in the graphs.

Fig. 10. Tyrosinase activity in murine Melan-a melanocytes (A) and B16-F10 melanoma cells (B) exposed to UVA radiation. Cells were harvested immediately after UVA radiation. In (C) comparison of tyrosinase activity between Melan-a and B16-F10 cells in DD or exposed to UVA radiation. Tyrosinase levels are expressed as the mean percentage (n = 5–9), ± SEM, of the values in DD control cells; p values are shown in the graphs.

the equipment to measure UVA/UVB irradiance. We thank Gabriela Sarti Kinker for assisting in the analysis of GTEX data.

Appendix A. Supplementary data

Supplementary data associated with this article can be found, in the online version, at https://doi.org/10.1016/j.ejcb.2018.01.004.

References

Allanson, M., Domanski, D., Reeve, V.E., 2006. Photoimmunoprotection by UVA (320–400 nm) radiation is determined by UVA dose and is associated with cutaneous cyclic guanosine monophosphate. J. Invest. Dermatol. 126, 191–197.

Allil, P.A., Visconti, M.A., Castrucci, A.M., Isoldi, M.C., 2008. Photoperiod and testosterone modulate growth and melanogenesis of s91 murine melanoma. Med. Chem. 4, 100–105.

Bangert, C., Brunner, P.M., Stingl, G., 2011. Immune functions of the skin. Clin. Dermatol. 29, 360–376.

Beitner, H., Wennersten, G., 1985. A qualitative and quantitative transmission electronmicroscopic study of the immediate pigment darkening reaction. Photodermatol 2, 273–278.

Bellono, N.W., Kammel, L.G., Zimmerman, A.L., Oancea, E., 2013. UV light phototransduction activates transient receptor potential A1 ion channels in human melanocytes. Proc. Natl. Acad. Sci. U. S. A. 110, 2383–2388.

Bellono, N.W., Najera, J.A., Oancea, E., 2014. UV light activates a Galphaq/11-coupled phototransduction pathway in human melanocytes. J. Gen. Physiol. 143, 203–214.

Bennett, D.C., Cooper, P.J., Hart, I.R., 1987. A line of non-tumorigenic mouse melanocytes, syngeneic with the B16 melanoma and requiring a tumour promoter for growth. Int. J. Cancer 39, 414–418.

Black, G., Matzinger, E., Gange, R.W., 1985. Lack of photoprotection against UVB-induced erythema by immediate pigmentation induced by 382 nm radiation. J. Invest. Dermatol. 85, 448–449.

Bradford, P.T., 2009. Skin cancer in skin of color. Dermatol. Nurs. 21, 170–177 206; quiz 178.
Branda, R.F., Eaton, J.W., 1978. Skin color and nutrient photolysis: an evolutionary hypothesis. Science 201, 625–626.
Brenner, M., Hearing, V.J., 2008. The protective role of melanin against UV damage in human skin. Photochem. Photobiol. 84, 539–549.
Brozyna, A.A., VanMiddlesworth, L., Slominski, A.T., 2008. Inhibition of melanogenesis as a radiation sensitizer for melanoma therapy. Int. J. Cancer 123, 1448–1456.
Brozyna, A.A., Jozwicki, W., Carlson, J.A., Slominski, A.T., 2013. Melanogenesis affects overall and disease-free survival in patients with stage III and IV melanoma. Hum. Pathol. 44, 2071–2074.
Brozyna, A.A., Jozwicki, W., Roszkowski, K., Filipiak, J., Slominski, A.T., 2016. Melanin content in melanoma metastases affects the outcome of radiotherapy. Oncotarget 7, 17844–17853.
Buhr, E.D., Yue, W.W., Ren, X., Jiang, Z., Liao, H.W., Mei, X., Vemaraju, S., Nguyen, M.T., Reed, R.R., Lang, R.A., Yau, K.W., Van Gelder, R.N., 2015. Neuropsin (OPN5)-mediated photoentrainment of local circadian oscillators in mammalian retina and cornea. Proc. Natl. Acad. Sci. U. S. A. 112, 13093–13098.
Buscone, S., Mardaryev, A.N., Raafs, B., Bikker, J.W., Sticht, C., Gretz, N., Farjo, N., Uzunbajakava, N.E., Botchkareva, N.V., 2017. A new path in defining light parameters for hair growth: discovery and modulation of photoreceptors in human hair follicle. Lasers Surg. Med. 49, 705–718.
Calapre, L., Gray, E.S., Ziman, M., 2013. Heat stress: a risk factor for skin carcinogenesis. Cancer Lett. 337, 35–40.
Campos, A.C., Molognoni, F., Melo, F.H., Galdieri, L.C., Carneiro, C.R., D'Almeida, V., Correa, M., Jasiulionis, M.G., 2007. Oxidative stress modulates DNA methylation during melanocyte anchorage blockade associated with malignant transformation. Neoplasia 9, 1111–1121.
Chakraborty, A.K., Funasaka, Y., Slominski, A., Bolognia, J., Sodi, S., Ichihashi, M., Pawelek, J.M., 1999. UV light and MSH receptors. Ann. N. Y. Acad. Sci. 885, 100–116.
Chan, S.L., Fiscus, R.R., 2003. Guanylyl cyclase inhibitors NS2028 and ODQ and protein kinase G (PKG) inhibitor KT5823 trigger apoptotic DNA fragmentation in immortalized uterine epithelial cells: anti-apoptotic effects of basal cGMP/PKG. Mol. Hum. Reprod. 9, 775–783.
Cho, S., Shin, M.H., Kim, Y.K., Seo, J.E., Lee, Y.M., Park, C.H., Chung, J.H., 2009. Effects of infrared radiation and heat on human skin aging in vivo. J. Invest. Dermatol. Symp. Proc. 14, 15–19.
Clapham, D.E., Julius, D., Montell, C., Schultz, G., 2005. International Union of Pharmacology: XLIX. Nomenclature and structure-function relationships of transient receptor potential channels. Pharmacol. Rev. 57, 427–450.
Consortium, G.T., 2015. Human genomics. the genotype-tissue expression (GTEx) pilot analysis: multitissue gene regulation in humans. Science (N. Y.) 348, 648–660.
Dakup, P., Gaddameedhi, S., 2016. Impact of the circadian clock on UV-induced DNA damage response and photocarcinogenesis. Photochem. Photobiol. 93, 293–303.
Desotelle, J.A., Wilking, M.J., Ahmad, N., 2012. The circadian control of skin and cutaneous photodamage. Photochem. Photobiol. 88, 1037–1047.
de Assis, S., Moraes, A.M., da Silveira Cruz-Machado, A.M., 2016. The effect of white light on normal and malignant murine melanocytes: a link between opsins, clock genes, and melanogenesis. Biochim. Biophys. Acta. 1863, 1119–1133.
de Assis, M.N., Moraes, A.M., Castrucci, A.M., 2017. Heat shock antagonizes UVA-induced responses in murine melanocytes and melanoma cells: an unexpected interaction. Photochem. Photobiol. Sci. 16, 633–648.
Dupont, E., Gomez, J., Bilodeau, D., 2013. Beyond UV radiation: a skin under challenge. Int. J. Cosmet. Sci. 35, 224–232.
Fimia, G.M., Sassone-Corsi, P., 2001. Cyclic AMP signalling. J. Cell Sci. 114, 1971–1972.
Francis, S.H., Busch, J.L., Corbin, J.D., Sibley, D., 2010. cGMP-dependent protein kinases and cGMP phosphodiesterases in nitric oxide and cGMP action. Pharmacol. Rev. 62, 525–563.
Fuller, B.B., 1987. Activation of tyrosinase in mouse melanoma cell cultures. In Vitro Cell. Dev. Biol. 23, 633–640.
Gaddameedhi, S., Selby, C.P., Kaufmann, W.K., Smart, R.C., Sancar, A., 2011. Control of skin cancer by the circadian rhythm. Proc. Natl. Acad. Sci. U. S. A. 108, 18790–18795.
Gaddameedhi, S., Selby, C.P., Kemp, M.G., Ye, R., Sancar, A., 2015. The circadian clock controls sunburn apoptosis and erythema in mouse skin. J. Invest. Dermatol. 135, 1119–1127.
Gillbro, J.M., Olsson, M.J., 2011. The melanogenesis and mechanisms of skin-lightening agents–existing and new approaches. Int. J. Cosmet. Sci. 33, 210–221.
Gloster Jr., H.M., Neal, K., 2006. Skin cancer in skin of color. J. Am. Acad. Dermatol. 55, 741–760 quiz 761–744.
Gunkel, M., Schoneberg, J., Alkhaldi, W., Irsen, S., Noe, F., Kaupp, U.B., Al-Amoudi, A., 2015. Higher-order architecture of rhodopsin in intact photoreceptors and its implication for phototransduction kinetics. Structure 23, 628–638.
Halder, R.M., Bang, K.M., 1988. Skin cancer in blacks in the United States. Dermatol. Clin. 6, 397–405.
Haltaufderhyde, K., Ozdeslik, R.N., Wicks, N.L., Najera, J.A., Oancea, E., 2015. Opsin expression in human epidermal skin. Photochem. Photobiol. 91, 117–123.
Holliman, G., Lowe, D., Cohen, H., Felton, S., Raj, K., 2017. Ultraviolet radiation-induced production of nitric oxide: a multi-cell and multi-donor analysis. Sci. Rep. 7, 11105.
Honigsmann, H., Schuler, G., Aberer, W., Romani, N., Wolff, K., 1986. Immediate pigment darkening phenomenon: a reevaluation of its mechanisms. J. Invest. Dermatol. 87, 648–652.
Honigsmann, H., 2002. Erythema and pigmentation. Photodermatol. Photoimmunol. Photomed. 18, 75–81.
Hu, Q.M., Yi, W.J., Su, M.Y., Jiang, S., Xu, S.Z., Lei, T.C., 2017. Induction of retinal-dependent calcium influx in human melanocytes by UVA or UVB radiation contributes to the stimulation of melanosome transfer. Cell Prolif. 50, e12372.
Hughes, S., Hankins, M.W., Foster, R.G., Peirson, S.N., 2012. Melanopsin phototransduction: slowly emerging from the dark. Prog. Brain Res. 199, 19–40.
Jablonski, N.G., Chaplin, G., 2010. Human skin pigmentation as an adaptation to UV radiation. Proc. Natl. Acad. Sci. U. S. A. 107, 8962–8968.
Jimbow, K., Pathak, M.A., Fitzpatrick, T.B., 1973. Effect of ultraviolet on the distribution pattern of microfilaments and microtubules and on the nucleus in human melanocytes. Yale J. Biol. Med. 46, 411–426.
Jimenez, M., Kameyama, K., Maloy, W.L., Tomita, Y., Hearing, V.J., 1988. Mammalian tyrosinase: biosynthesis, processing, and modulation by melanocyte-stimulating hormone. Proc. Natl. Acad. Sci. U. S. A. 85, 3830–3834.
Jones, K.A., Hatori, M., Mure, L.S., Bramley, J.R., Artymyshyn, R., Hong, S.P., Marzabadi, M., Zhong, H., Sprouse, J., Zhu, Q., Hartwick, A.T., Sollars, P.J., Pickard, G.E., Panda, S., 2013. Small-molecule antagonists of melanopsin-mediated phototransduction. Nat. Chem. Biol. 9, 630–635.
Kadamur, G., Ross, E.M., 2013. Mammalian phospholipase C. Annu. Rev. Physiol. 75, 127–154.
Kadekaro, A.L., Andrade, L.N., Floeter-Winter, L.M., Rollag, M.D., Virador, V., Vieira, W., Castrucci, A.M., 2004. MT-1 melatonin receptor expression increases the antiproliferative effect of melatonin on S-91 murine melanoma cells. J. Pineal Res. 36, 204–211.
Kim, H.J., Son, E.D., Jung, J.Y., Choi, H., Lee, T.R., Shin, D.W., 2013. Violet light downregulates the expression of specific differentiation markers through Rhodopsin in normal human epidermal keratinocytes. PLoS One 8, e73678.
Kim, Y.M., Cho, S.E., Seo, Y.K., 2016. The activation of melanogenesis by p-CREB and MITF signaling with extremely low-frequency electromagnetic fields on B16F10 melanoma. Life Sci. 162, 25–32.
Kojima, D., Mori, S., Torii, M., Wada, A., Morishita, R., Fukada, Y., 2011. UV-sensitive photoreceptor protein OPN5 in humans and mice. PLoS One 6, e26388.
Lamb, T.D., 2013. Evolution of phototransduction, vertebrate photoreceptors and retina. Prog. Retin. Eye Res. 36, 52–119.
Lavker, R.M., Kaidbey, K.H., 1982. Redistribution of melanosomal complexes within keratinocytes following UV-A irradiation: a possible mechanism for cutaneous darkening in man. Arch. Dermatol. Res. 272, 215–228.
Leung, N.Y., Montell, C., 2017. Unconventional roles of opsins. Annu. Rev. Cell Dev. Biol. 33, 241–264.
Lin, J.Y., Fisher, D.E., 2007. Melanocyte biology and skin pigmentation. Nature 445, 843–850.
Lopes, G.J., Gois, C.C., Lima, L.H., Castrucci, A.M., 2010. Modulation of rhodopsin gene expression and signaling mechanisms evoked by endothelins in goldfish and murine pigment cell lines. Braz. J. Med. Biol. Res. 43, 828–836.
Luber, A.J., Ensanyat, S.H., Zeichner, J.A., 2014. Therapeutic implications of the circadian clock on skin function. J. Drugs Dermatol. 13, 130–134.
Lucas, R.J., Peirson, S., Berson, D.M., Brown, T.M., Cooper, H.M., Czeisler, C.A., Figueiro, M.G., Gamlin, P.D., Lockley, S.W., O'Hagan, J.B., Price, L.L.A., Provencio, I., Skene, D.J., Brainard, G.C., 2014. Measuring and using light in the melanopsin age. Trends Neurosci. 37, 1–9.
Luchs, A., Sumida, D.H., Visconti, M.A., Castrucci, A.M., 2008. Biological effects of insulin on murine melanoma cells and fish erythrophoroma cells: a comparative study. Gen. Comp. Endocrinol. 156, 218–223.
Mahmoud, B.H., Hexsel, C.L., Hamzavi, I.H., Lim, H.W., 2008. Effects of visible light on the skin. Photochem. Photobiol. 84, 450–462.
Mahmoud, B.H., Ruvolo, E., Hexsel, C.L., Liu, Y., Owen, M.R., Kollias, N., Lim, H.W., Hamzavi, I.H., 2010. Impact of long-wavelength UVA and visible light on melanocompetent skin. J. Invest. Dermatol. 130, 2092–2097.
Marwan, M.M., Abdel Malek, Z.A., Kreutzfeld, K.L., Hadley, M.E., Wilkes, B.C., Hruby, V.J., Castrucci, A.M., 1985. Stimulation of S91 melanoma tyrosinase activity by superpotent alpha-melanotropins. Mol. Cell. Endocrinol. 41, 171–177.
Matsunaga, T., Yamaji, Y., Tomokuni, T., Morita, H., Morikawa, Y., Suzuki, A., Yonezawa, A., Endo, S., Ikari, A., Iguchi, K., El-Kabbani, O., Tajima, K., Hara, A., 2014. Nitric oxide confers cisplatin resistance in human lung cancer cells through upregulation of aldo-keto reductase 1B10 and proteasome. Free Radic. Res. 48, 1371–1385.
Miyamura, Y., Coelho, S.G., Schlenz, K., Batzer, J., Smuda, C., Choi, W., Brenner, M., Passeron, T., Zhang, G., Kolbe, L., Wolber, R., Hearing, V.J., 2011. The deceptive nature of UVA tanning versus the modest protective effects of UVB tanning on human skin. Pigm. Cell Melanoma Res. 24, 136–147.
Miyashita, Y., Moriya, T., Kubota, T., Yamada, K., Asami, K., 2001. Expression of opsin molecule in cultured murine melanocyte. J. Invest. Dermatol. Symp. Proc. 6, 54–57.
Moan, J., Nielsen, K.P., Juzeniene, A., 2012. Immediate pigment darkening: its evolutionary roles may include protection against folate photosensitization. FASEB J. 26, 971–975.
Mohania, D., Chandel, S., Kumar, P., Verma, V., Digvijay, K., Tripathi, D., Choudhury, K., Mitten, S.K., Shah, D., 2017. Ultraviolet radiations: skin defense-damage mechanism. Adv. Exp. Med. Biol. 996, 71–87.
Moraes, M.N., Ramos, B.C., Poletini, M.O., Castrucci, A.M., 2015. Melanopsins: localization and phototransduction in Xenopus laevis melanophores. Photochem. Photobiol. 91, 1133–1141.
Moraes, M.N., de Assis, L.V.M., Magalhães-Marques, K.K., Poletini, M.O., Lima, L.H.R.G., Castrucci, A.M.L., 2017. Melanopsin, a canonical light receptor, mediates thermal activation of clock genes. Sci. Rep. 7, 13977.
Nasti, T.H., Timares, L., 2015. MC1R, eumelanin and pheomelanin: their role in determining the susceptibility to skin cancer. Photochem. Photobiol. 91, 188–200.
Nery, L.E., Castrucci, A.M., 1997. Pigment cell signalling for physiological color change. Comp. Biochem. Physiol. A Physiol. 118, 1135–1144.
Panda, S., Sato, T.K., Castrucci, A.M., Rollag, M.D., DeGrip, W.J., Hogenesch, J.B.,

Provencio, I., Kay, S.A., 2002. Melanopsin (Opn4) requirement for normal light-induced circadian phase shifting. Science 298, 2213–2216.
Panda, S., Provencio, I., Tu, D.C., Pires, S.S., Rollag, M.D., Castrucci, A.M., Pletcher, M.T., Sato, T.K., Wiltshire, T., Andahazy, M., Kay, S.A., Van Gelder, R.N., Hogenesch, J.B., 2003. Melanopsin is required for non-image-forming photic responses in blind mice. Science 301, 525–527.
Parker, P.J., Justilien, V., Riou, P., Linch, M., Fields, A.P., 2014. Atypical Protein Kinase Cι as a human oncogene and therapeutic target. Biochem. Pharmacol. 88, 1–11.
Pathak, M.A., Stratton, K., 1968. Free radicals in human skin before and after exposure to light. Arch. Biochem. Biophys. 123, 468–476.
Pathak, M.A., Riley, F.J., Fitzpatrick, T.B., Curwen, W.L., 1962. Melanin formation in human skin induced by long-wave ultra-violet and visible light. Nature 193, 148–150.
Poletini, M.O., de Assis, L.V., Moraes, M.N., Castrucci, A.M., 2016. Estradiol differently affects melanin synthesis of malignant and normal melanocytes: a relationship with clock and clock-controlled genes. Mol. Cell. Biochem. 421, 29–39.
Premi, S., Wallisch, S., Mano, C.M., Weiner, A.B., Bacchiocchi, A., Wakamatsu, K., Bechara, E.J., Halaban, R., Douki, T., Brash, D.E., 2015. Photochemistry: chemiexcitation of melanin derivatives induces DNA photoproducts long after UV exposure. Science 347, 842–847.
Purschke, M., Laubach, H.J., Anderson, R.R., Manstein, D., 2010. Thermal injury causes DNA damage and lethality in unheated surrounding cells: active thermal bystander effect. J. Invest. Dermatol. 130, 86–92.
Ramos, B.C., Moraes, M.N., Poletini, M.O., Lima, L.H., Castrucci, A.M., 2014. From blue light to clock genes in zebrafish ZEM-2S cells. PLoS One 9, e106252.
Randhawa, M., Seo, I., Liebel, F., Southall, M.D., Kollias, N., Ruvolo, E., 2015. Visible light induces melanogenesis in human skin through a photoadaptive response. PLoS One 10, e0130949.
Regazzetti, C., Sormani, L., Debayle, D., Bernerd, F., Tulic, M.K., De Donatis, G.M., Chignon-Sicard, B., Rocchi, S., Passeron, T., 2017. Melanocytes sense blue light and regulate pigmentation through the Opsin3. J. Invest. Dermatol. 138, 171–178.
Rosen, C.F., Jacques, S.L., Stuart, M.E., Gange, R.W., 1990. Immediate pigment darkening: visual and reflectance spectrophotometric analysis of action spectrum. Photochem. Photobiol. 51, 583–588.
Sarti, M.S., Visconti, M.A., Castrucci, A.M., 2004. Biological activity and binding of estradiol to SK-Mel 23 human melanoma cells. Braz. J. Med. Biol. Res. 37, 901–905.
Scarparo, A.C., Visconti, M.A., de Oliveira, A.R., Castrucci, A.M., 2000. Adrenoceptors in normal and malignant human melanocytes. Arch. Dermatol. Res. 292, 265–267.
Scarparo, A.C., Sumida, D.H., Patrao, M.T., Avellar, M.C., Visconti, M.A., Castrucci, A.M.L., 2004. Catecholamine effects on human melanoma cells evoked by alpha1-adrenoceptors. Arch. Dermatol. Res. 296, 112–119.
Scarparo, A.C., Isoldi, M.C., de Lima, L.H.R.G., Visconti, M.A., Castrucci, A.M.L., 2007. Expression of endothelin receptors in frog, chicken, mouse and human pigment cells. Comp. Biochem. Physiol. A Mol. Integr. Physiol. 147, 640–646.
Seino, S., Shibasaki, T., 2005. PKA-dependent and PKA-independent pathways for cAMP-regulated exocytosis. Physiol. Rev. 85, 1303–1342.
Sikka, G., Hussmann, G.P., Pandey, D., Cao, S., Hori, D., Park, J.T., Steppan, J., Kim, J.H., Barodka, V., Myers, A.C., Santhanam, L., Nyhan, D., Halushka, M.K., Koehler, R.C., Snyder, S.H., Shimoda, L.A., Berkowitz, D.E., 2014. Melanopsin mediates light-dependent relaxation in blood vessels. Proc. Natl. Acad. Sci. U. S. A. 111, 17977–17982.
Sklar, L.R., Almutawa, F., Lim, H.W., Hamzavi, I., 2013. Effects of ultraviolet radiation, visible light, and infrared radiation on erythema and pigmentation: a review. Photochem. Photobiol. Sci. 12, 54–64.
Skobowiat, C., Dowdy, J.C., Sayre, R.M., Tuckey, R.C., Slominski, A., 2011. Cutaneous hypothalamic-pituitary-adrenal axis homolog: regulation by ultraviolet radiation. Am. J. Physiol. Endocrinol. Metab. 301, E484–493.
Slominski, A., Paus, R., 1993. Melanogenesis is coupled to murine anagen: toward new concepts for the role of melanocytes and the regulation of melanogenesis in hair growth. J. Clin. Invest. Dermatol. 101, 90s–97s.
Slominski, A., Scislowski, P.W., Bomirski, A., 1983. Tyrosinase activity in primary cell culture of amelanotic melanoma cells. Biosci. Rep. 3, 1027–1034.
Slominski, A., Paus, R., Mihm, M.C., 1998. Inhibition of melanogenesis as an adjuvant strategy in the treatment of melanotic melanomas: selective review and hypothesis. Anticancer Res. 18, 3709–3715.
Slominski, A., Wortsman, J., Luger, T., Paus, R., Solomon, S., 2000. Corticotropin releasing hormone and proopiomelanocortin involvement in the cutaneous response to stress. Physiol. Rev. 80, 979–1020.
Slominski, A., Tobin, D.J., Shibahara, S., Wortsman, J., 2004. Melanin pigmentation in mammalian skin and its hormonal regulation. Physiol. Rev. 84, 1155–1228.
Slominski, A., Wortsman, J., Plonka, P.M., Schallreuter, K.U., Paus, R., Tobin, D.J., 2005. Hair follicle pigmentation. J. Clin. Invest. Dermatol. 124, 13–21.
Slominski, A., Zbytek, B., Slominski, R., 2009. Inhibitors of melanogenesis increase toxicity of cyclophosphamide and lymphocytes against melanoma cells. Int. J. Cancer 124, 1470–1477.
Slominski, A., Zmijewski, M.A., Pawelek, J., 2012a. L-tyrosine and L-dihydroxyphenylalanine as hormone-like regulators of melanocyte functions. Pigm. Cell Melanoma Res. 25, 14–27.
Slominski, A.T., Zmijewski, M.A., Skobowiat, C., Zbytek, B., Slominski, R.M., Steketee, J.D., 2012b. Sensing the environment: regulation of local and global homeostasis by the skin's neuroendocrine system. Adv. Anat. Embryol. Cell Biol. 212, 1–115 v, vii.
Slominski, A.T., Zmijewski, M.A., Zbytek, B., Tobin, D.J., Theoharides, T.C., Rivier, J., 2013. Key role of CRF in the skin stress response system. Endocr. Rev. 34, 827–884.
Slominski, A., Kim, T.K., Brozyna, A.A., Janjetovic, Z., Brooks, D.L., Schwab, L.P., Skobowiat, C., Jozwicki, W., Seagroves, T.N., 2014. The role of melanogenesis in regulation of melanoma behavior: melanogenesis leads to stimulation of HIF-1alpha expression and HIF-dependent attendant pathways. Arch. Biochem. Biophys. 563, 79–93.
Slominski, R.M., Zmijewski, M.A., Slominski, A.T., 2015. The role of melanin pigment in melanoma. Exp. Dermatol. 24, 258–259.
Solano, F., 2014. Melanins: skin pigments and much more—types, structural models, biological functions, and formation routes. New J. Sci. 2014, 28.
Solomon, S.G., Lennie, P., 2007. The machinery of colour vision. Nat. Rev. Neurosci. 8, 276–286.
Souza, A.V., Visconti, M.A., Castrucci, A.M., 2003. Melatonin biological activity and binding sites in human melanoma cells. J. Pineal Res. 34, 242–248.
Theis, M., Buchholz, F., 2011. High-throughput RNAi screening in mammalian cells with esiRNAs. Methods 53, 424–429.
Toh, P.P., Bigliardi-Qi, M., Yap, A.M., Sriram, G., Bigliardi, P., 2016. Expression of peropsin in human skin is related to phototransduction of violet light in keratinocytes. Exp. Dermatol. 25, 1002–1005.
Tomita, Y., Maeda, K., Tagami, H., 1992. Melanocyte-stimulating properties of arachidonic acid metabolites: possible role in postinflammatory pigmentation. Pigment Cell Res. 5, 357–361.
Tsutsumi, M., Ikeyama, K., Denda, S., Nakanishi, J., Fuziwara, S., Aoki, H., Denda, M., 2009. Expressions of rod and cone photoreceptor-like proteins in human epidermis. Exp. Dermatol. 18, 567–570.
Tuerxuntayi, A., Liu, Y.Q., Tulake, A., Kabas, M., Eblimit, A., Aisa, H.A., 2014. Kaliziri extract upregulates tyrosinase, TRP-1, TRP-2 and MITF expression in murine B16 melanoma cells. BMC Complement. Altern. Med. 14, 166.
Videira, I.F.d.S., Moura, D.F.L., Magina, S., 2013. Mechanisms regulating melanogenesis. An. Bras. Dermatol. 88, 76–83.
Wicks, N.L., Chan, J.W., Najera, J.A., Ciriello, J.M., Oancea, E., 2011. UVA phototransduction drives early melanin synthesis in human melanocytes. Curr. Biol. CB 21, 1906–1911.
Williams, P.F., Olsen, C.M., Hayward, N.K., Whiteman, D.C., 2011. Melanocortin 1 receptor and risk of cutaneous melanoma: a meta-analysis and estimates of population burden. Int. J. Cancer 129, 1730–1740.
Willis, I., Kligman, A., Epstein, J., 1972. Effects of long ultraviolet rays on human skin: photoprotective or photoaugmentative. J. Invest. Dermatol. 59, 416–420.
Yamaguchi, Y., Brenner, M., Hearing, V.J., 2007. The regulation of skin pigmentation. J. Biol. Chem. 282, 27557–27561.

Chapter 6: Non-Metastatic Cutaneous Melanoma Induces Chronodisruption in Central and Peripheral Circadian Clocks

The content provided in this chapter has been published in International Journal of Molecular Sciences, 2018, 3;19(4). E1065. DOI: 10.3390/ijms19041065.

Authors' names: de Assis LVM[*], Moraes MN[*], Magalhães-Marques KK, Kinker GS, da Silveira Cruz-Machado S, Castrucci AML.

[*] Joint first authors

International Journal of
Molecular Sciences

MDPI

Article

Non-Metastatic Cutaneous Melanoma Induces Chronodisruption in Central and Peripheral Circadian Clocks

Leonardo Vinícius Monteiro de Assis [1,†], Maria Nathália Moraes [1,†], Keila Karoline Magalhães-Marques [1], Gabriela Sarti Kinker [2], Sanseray da Silveira Cruz-Machado [2] and Ana Maria de Lauro Castrucci [1,3,*]

1 Laboratory of Comparative Physiology of Pigmentation, Department of Physiology, Institute of Biosciences, University of São Paulo, São Paulo 05508-900, Brazil; deassis.leonardo@usp.br (L.V.M.d.A.); nathalia.moraes@usp.br (M.N.M.); keilamagalhaesmarques@gmail.com (K.K.M.-M.)
2 Laboratory of Chronopharmacology, Department of Physiology, Institute of Biosciences, University of São Paulo, São Paulo 05508-900, Brazil; gabriela.kinker@hotmail.com (G.S.K.); sanseray@hotmail.com (S.d.S.C.-M.)
3 Department of Biology, University of Virginia, Charlottesville, VA 22904, USA
* Correspondence: amdlcast@ib.usp.br; Tel.: +55-11-3091-7523
† These authors contributed equally to this work.

Received: 30 January 2018; Accepted: 29 March 2018; Published: 3 April 2018

Abstract: The biological clock has received increasing interest due to its key role in regulating body homeostasis in a time-dependent manner. Cancer development and progression has been linked to a disrupted molecular clock; however, in melanoma, the role of the biological clock is largely unknown. We investigated the effects of the tumor on its micro- (TME) and macro-environments (TMaE) in a non-metastatic melanoma model. C57BL/6J mice were inoculated with murine B16-F10 melanoma cells and 2 weeks later the animals were euthanized every 6 h during 24 h. The presence of a localized tumor significantly impaired the biological clock of tumor-adjacent skin and affected the oscillatory expression of genes involved in light- and thermo-reception, proliferation, melanogenesis, and DNA repair. The expression of tumor molecular clock was significantly reduced compared to healthy skin but still displayed an oscillatory profile. We were able to cluster the affected genes using a human database and distinguish between primary melanoma and healthy skin. The molecular clocks of lungs and liver (common sites of metastasis), and the suprachiasmatic nucleus (SCN) were significantly affected by tumor presence, leading to chronodisruption in each organ. Taken altogether, the presence of non-metastatic melanoma significantly impairs the organism's biological clocks. We suggest that the clock alterations found in TME and TMaE could impact development, progression, and metastasis of melanoma; thus, making the molecular clock an interesting pharmacological target.

Keywords: cancer; melanoma; tumor microenvironment; tumor macroenvironment; central and peripheral clocks; chronodisruption

1. Introduction

Over the past decades, an overwhelming number of studies clearly established the importance of time in physiology and homeostasis of the organism. The daily pattern of light and temperature over 24 h is detected by a complex and elegant biological clock machinery. Endogenous rhythms are found from bacteria to humans, relying on similar time keeping systems. In mammals, the hypothalamic suprachiasmatic nucleus (SCN) is the central neural oscillator able to respond to cyclic environmental changes of lighting through a retinal melanopsin-dependent process. This photo-pigment, expressed

in a subpopulation of retinal ganglion cells [1,2], translates light information into electrical signals, through the isomerization of *cis*- into all-*trans* retinal, with subsequent activation of downstream signaling and release of glutamate and pituitary adenylyl cyclase activating peptide (PACAP) by the retinal hypothalamic tract at the SCN neurons [3]. The SCN then shares this temporal information with several areas of the brain that ultimately control most biological processes. In fact, in a harmonic condition there is only a single time zone within the organism [4–7].

The molecular basis of the temporal control is an intertwined and complex regulatory system of transcriptional feedback loops involving several genes in the core of the clock molecular machinery [4,6,8,9]. The proteins coded by *Clock* (Circadian Locomotor Output Cycles Kaput) and *Bmal1* (also known as ARNTL, Aryl hydrocarbon receptor nuclear translocator-like protein 1) form heterodimers CLOCK/BMAL1 which migrate to the nucleus and stimulate the transcription of *Per* (Period) and *Cry* (Cryptochrome). After translation, PER/CRY heterodimers are formed and, through phosphorylation by casein kinases, are targeted to the nucleus where they inhibit BMAL1/CLOCK action. This central loop of regulation is fine-tuned by another loop in which BMAL1/CLOCK activates the nuclear receptor subfamily 1, group D, member 1/2 (*Nr1d1*/2 also known as *Rev-Erbα*/*β*) and RAR-related orphan receptor alpha/beta (*Nr1f1*/*2* also known as *RORα*/*β*). REV-ERBα/β and ROR*α*/*β* compete for the orphan receptor response element (RORE) sequence present in *Bmal1* promoter: REV-ERB*α*/*β* stimulates while ROR*α*/*β* inhibits *Bmal1* expression. A new cycle of transcription restarts when the inhibitory effect of PER/CRY decreases, mainly due to the degradation of both proteins [8–11]. The above-mentioned process takes about 24 h to complete and the components of this system have been detected in almost every murine and human cell [8]. In fact, each organ has its own molecular clock, i.e., peripheral clocks, which are influenced by the SCN [9,12]. It is of importance to highlight that CLOCK/BMAL1 also activates the transcription of several clock-controlled genes (CCGs) in a tissue-specific manner, which ultimately contributes to the temporal control of biological processes in the organism. Based on these, clock genes have received increasing interest due to their key role in regulating the body homeostasis [4,6,8,9]. Interestingly, chronodisruption, i.e., loss of internal coherence among the biological clocks, has been linked to the development of cancer [13–19], metabolic dysfunctions, and psychiatric disorders [4,5,20–22].

Melanoma is an aggressive cancer whose incidence has significantly increased over the past decades [23,24]. Melanoma represents 4% of all skin-related cancers but accounts for approximately 80% of all deaths [25]. Although most patients present a localized disease with subsequent surgical excision of the primary tumor, a significant portion of patients develops metastases [26]. In fact, metastatic melanoma is a fatal disease with patients displaying an overall survival of approximately 5 months [27]. Etiologically, melanoma is a multifactorial disease and is associated with chronic environmental and artificial UV exposure, sunburn history in early childhood, reduced skin pigmentation, melanocytic nevi, family history, and genetic susceptibility [23,24]. Interestingly, melatonin, a classic regulator of circadian rhythms [28], is synthesized locally by the skin—a remarkable neuroendocrine system [29]; in this tissue melatonin acts as a protective agent against UV-induced damage [30], but it role as a regulator of the skin molecular clocks is still unclear.

Several genes play a significant role in the development of melanoma. In initial stages, mutation on *BRAF*, *NRAS*, and *NF1* are frequently found while during progression mutations on *TERT*, *CDKN2A*, *ARID1A*, *PTEN*, and *TP53* are observed [31]. In recent years, the landscape of melanoma treatment has significantly changed with the introduction of newer drugs that target BRAF, and its downstream molecule MEK, as well as antibodies that block immune checkpoints such as CTLA-4, PD-1 and its ligand (PD-L1) [32–35]. In addition to the classic genes related to development and progression of melanoma, as mentioned above clock genes are known to be frequently altered in several types of cancer [14,15,17,18]. Understanding how clock genes are altered in melanoma has become an attractive field of study.

Within this line, our group has shown that the molecular clock of cultured malignant melanocytes is significantly downregulated in comparison to its normal counterpart [16,36,37]. Clinical data

show that clock proteins are significantly less expressed in melanoma and in nonmalignant nevus compared to adjacent skin of human samples; in addition, clock genes and proteins correlate with clinicopathological characteristics such as Breslow thickness [38]. An interesting study showed that intra-melanoma tumor dexamethasone injections led to cell cycle arrest with consequent reduction of tumor growth in vivo. This antitumor action is due to dexamethasone-induced activation of the melanoma molecular clock, as the ablation of *Bmal1* resulted in inhibition of the observed glucocorticoid effect [39].

Increasing evidence has implicated the tumor microenvironment (TME) as an important player in tumor development and progression [40,41]. TME contains several cell types such as: immune cells, tumor-associated macrophages and neutrophils, myeloid-derived suppressor cells, fibroblasts, adipocytes, vascular endothelial cells, and lymphatic endothelial cells [41]. This environment not only provides a physical location for all these cells but plays a significant role in development, metastasis, and treatment-related resistance of cancer [40–44].

On the other hand, the crosstalk between the tumor and its macroenvironment (TMaE), i.e., distant organs and tissues, has been less investigated. The best-known example is the cancer-induced cachexia, characterized by progressive loss of muscle mass that cannot be reversed by nutritional support [45–47]. This syndrome is mainly due to increased levels of serum cytokines, tumor-derived inflammatory factors, and others secreted by the host in response to the tumor presence [45–47]. Other characteristics of TMaE are generalized immune system suppression and altered coagulation capacity [48]. In fact, such alterations in the TMaE are the main source of cancer-related death rather than the effects of tumor growth and metastases themselves [48]. Recently, tumors have also been shown to impact the TMaE through the modulation of molecular clocks. An elegant study demonstrated that a non-metastatic lung adenocarcinoma rewires the time-dependent hepatic metabolism via a pro-inflammatory pathway, with no change in the clock core machinery [49]. In another model, a non-metastatic breast cancer, an altered pattern of clock gene expression was found in liver of the tumor-bearing mice [50].

Our goal in this study was to evaluate whether a non-metastatic melanoma, achieved by subcutaneous inoculation of B16-F10 murine melanoma cells in C57BL/6J mice, affected the machinery of peripheral clocks present in tumor-adjacent skin, lung, and liver (common sites of metastasis), as well as the central SCN oscillator. In addition, we also evaluated the behavior of tissue-specific genes facing the challenge imposed by the tumor.

2. Results and Discussion

2.1. Effects of Tumor Microenvironment (TME) on Clock and Clock-Controlled Genes of Tumor-Adjacent Skin and Melanoma

Chronodisruption in cancer is often analyzed by comparing the levels of clock genes and/or proteins in single time points between tumor samples, tumor-adjacent and/or healthy tissues; however, to the best of our knowledge, there has not been a study that evaluated the oscillatory process along 24 h of the molecular clock in tumor and tumor-adjacent tissue.

Our in vivo analysis of 24 h gene expression showed an oscillatory profile of *Per1* and *Bmal1*, which were in antiphase (Figure 1), a well-established feature of a functional clock [8]. *Per1* levels were decreased at ZT14 (Figure 1A) and *Bmal1* levels at ZT2 and ZT14 (Figure 1B) in tumor-adjacent skin and tumor as compared to control skin. The oscillatory profile of *Per1* was absent in tumor-adjacent skin and very attenuated in tumor samples (Figure 1A), whereas the temporal oscillation of *Bmal1* was sustained, but severely reduced in amplitude, in both tumor-adjacent skin and tumor itself (Figure 1B).

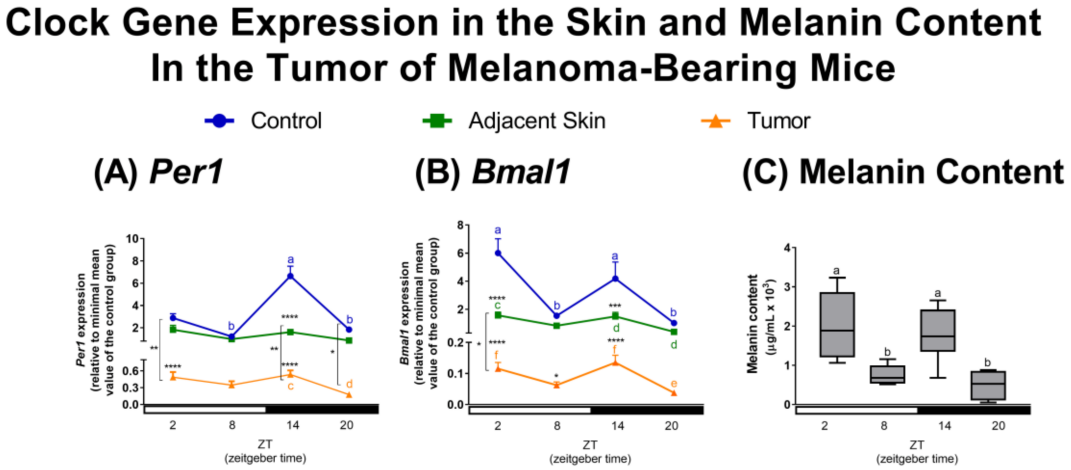

Figure 1. (**A**,**B**) Non-metastatic skin melanoma affects clock gene expression in skin. Expression of (**A**) *Per1*, (**B**) *Bmal1* in control skin, tumor-adjacent skin, and tumor samples. Letters represent significant differences in gene expression within the same group, Two-Way ANOVA followed by Tukey post-test. In (**A**) $a \neq b$, $p < 0.01$, and $c \neq d$, $p < 0.05$. In (**B**) $a \neq b$, $p < 0.01$, $c \neq d$, $p < 0.01$, and $e \neq f$, $p < 0.05$. Significant differences among groups were demonstrated by Two-Way ANOVA followed by Bonferroni post-test, and are represented by asterisks having the control skin as reference. Differences between tumor-adjacent skin and tumor samples are indicated by brackets. * $p < 0.05$, ** $p < 0.01$, *** $p < 0.001$, **** $p < 0.0001$. Values are presented as the mean expression (n = 3–7) ± SEM of the gene of interest normalized by Rpl37a RNA, relative to the minimal value of skin control group. (**C**) Temporal tumor melanin content. Boxplots show the median, quartiles, maximum, and minimum melanin contents. Melanin content was normalized by total protein. Letters represent statistical temporal differences in melanin content as revealed by One-Way ANOVA followed by Tukey post-test. $a \neq b$, $p < 0.05$.

These results indicate that *Per1* and *Bmal1* expression levels are significantly impaired in both tumor-adjacent skin and tumor samples when compared to skin of control, non-inoculated, animals resulting in loss of oscillatory profile of *Per1*. The assumption of "healthiness" of tumor-adjacent skin has resulted in its use as control in skin-related studies [38,51]. In fact, a compelling argument for the use of tumor-adjacent skin is that its morphology is preserved and no sign of malignization is found [51]; however, this traditional view has been recently challenged. Transcriptome analysis comparing heathy, tumor-adjacent tissue, and tumor samples from eight types of tumors, revealed that the tumor-adjacent tissue represents an intermediate state between heathy and tumor tissue [51]. Interestingly, tumor-adjacent is influenced by the pro-inflammatory signals originating from the tumor itself [51]. In fact, our data clearly corroborate this intermediate state of the tumor-adjacent skin. Thus, in addition to the findings reported by Aran and colleagues [51], our findings add another layer of complexity: The disruption of the molecular clock. Therefore, these results warn for further caution in using tumor-adjacent tissue as control.

Since melanogenesis is a clock-controlled process [16,36,52,53], we evaluated the melanin content in tumor samples along 24 h. To the best of our knowledge, we are the first to show a circadian profile of tumor melanin content. Interestingly, the oscillation of melanin content (Figure 1C) showed a similar profile to the one found for *Bmal1* gene (Figure 1B) in the tumor samples: It peaked at ZT2 and ZT14 and had its lowest values at ZT8 and ZT20 (Figure 1C).

We found a positive correlation between *Per1* or *Bmal1* expression with melanin content of tumor samples (Table 1). Previous studies have demonstrated a negative relationship between clock gene expression and melanin content [16,36,53]; however, these studies have used homogeneous melanocyte cell culture while in our study we used the whole skin and tumor samples. In the skin, melanocytes represent only 8% of the epidermal cell population [54] while in the tumor there are several cell types

that make up the TME [41]. Therefore, the difference in gene correlation could be explained by the presence of skin or tumor cell types other than pigment cells.

Table 1. Genes whose expression values correlate with melanin content of matched tumor-bearing mice.

Tissue	Gene Expression vs. Melanin Content	*r* Value	R^2	*p* Value
Tumor-Adjacent Skin	*Per1*	0.4761	0.2266	0.0394
	Bmal1	0.6469	0.285	0.0021
	Opn2	0.7513	0.5644	0.0003
	Opn4	−0.7837	0.09481	0.0001
	Xpa	0.5037	0.1475	0.0199
	Pparγ	−0.5956	0.3751	0.0133
Tumor	*Per1*	0.5805	0.337	0.0073
	Bmal1	0.5651	0.3194	0.0076
	Opn2	0.5368	0.2159	0.0147
	Opn4	−0.6067	0.368	0.0098
	Xpa	−0.5817	0.3383	0.0071
Lungs	*Bmal1*	−0.5015	0.2515	0.0403
Liver	*Per1*	−0.5327	0.1618	0.0356
SCN	*Per1*	0.5543	0.3072	0.0112
	Bmal1	−0.5933	0.352	0.0046
	cFos	0.6481	0.42	0.002

Positive or negative *r* values indicate positive or negative correlation, respectively, between gene expression in a given tissue and melanin content from tumor samples. Only the genes with significant *p* values are shown. *Mus musculus* gene nomenclature according http://www.informatics.jax.org/mgihome/nomen/gene.shtml.

Although the tumor molecular clock was severely downregulated, the oscillatory profile found for melanin content favors the hypothesis that the disrupted tumor clock may still evoke time-dependent local responses. Alternatively, but not exclusively, another hypothesis would be that SCN timing signals or environmental cues feed the tumor clock. Our data could lead to an interesting outcome if proven in patients. It is known that melanin content in melanoma tumors is a prognostic factor since patients harboring tumors with increased melanin content display reduced survival compared to amelanotic melanomas [55]. The presence of melanin in metastatic melanoma is a key factor that contributes to the reduced success of radiotherapy [55]. Accordingly, in vitro studies have provided evidence that inhibiting melanin synthesis improves radiotherapy success in melanoma cell lines [56]. Based on these findings, one could speculate a better outcome of a time-modulated radiotherapy or chemotherapy regimens at the time points where tumors show reduced melanin content; however, this hypothesis needs to be validated in clinical trials.

In addition to clock genes, we also evaluated some tissue-specific genes that are involved in proliferation [57,58], detection of light and/or heat [16,59], and DNA repair in tumor-adjacent skin and the tumor itself [60]. Members of the *Ppar* family have been described as direct targets of the CLOCK/BMAL1 dimer through its binding to E-box element present in *Ppar* promoter [61]. *Pparγ* participates in pigmentation and antiproliferative processes in melanocytes and melanoma cells, respectively [57,58]. In our model, *Pparγ* expression was higher at ZT20 in comparison to the remaining ZTs in control skin. No oscillatory profile was found in tumor-adjacent skin or in tumor samples. In the former, due to the overall increase of expression in ZTs 2, 8 and 14 (although not statistically significant), and in the latter due to the dramatic reduction of *Pparγ* transcripts at ZT20 as compared to control skin (Figure 2A). The loss of oscillatory profile of *Pparγ* expression in the skin

of tumor-bearing mice may represent important tumorigenic process that contributes to the loss of temporalization of the proliferative process, a common event in cancer [62]. In fact, *Pparγ* expression in tumor-adjacent skin showed a negative correlation with tumor melanin which was lost in tumor samples (Table 1).

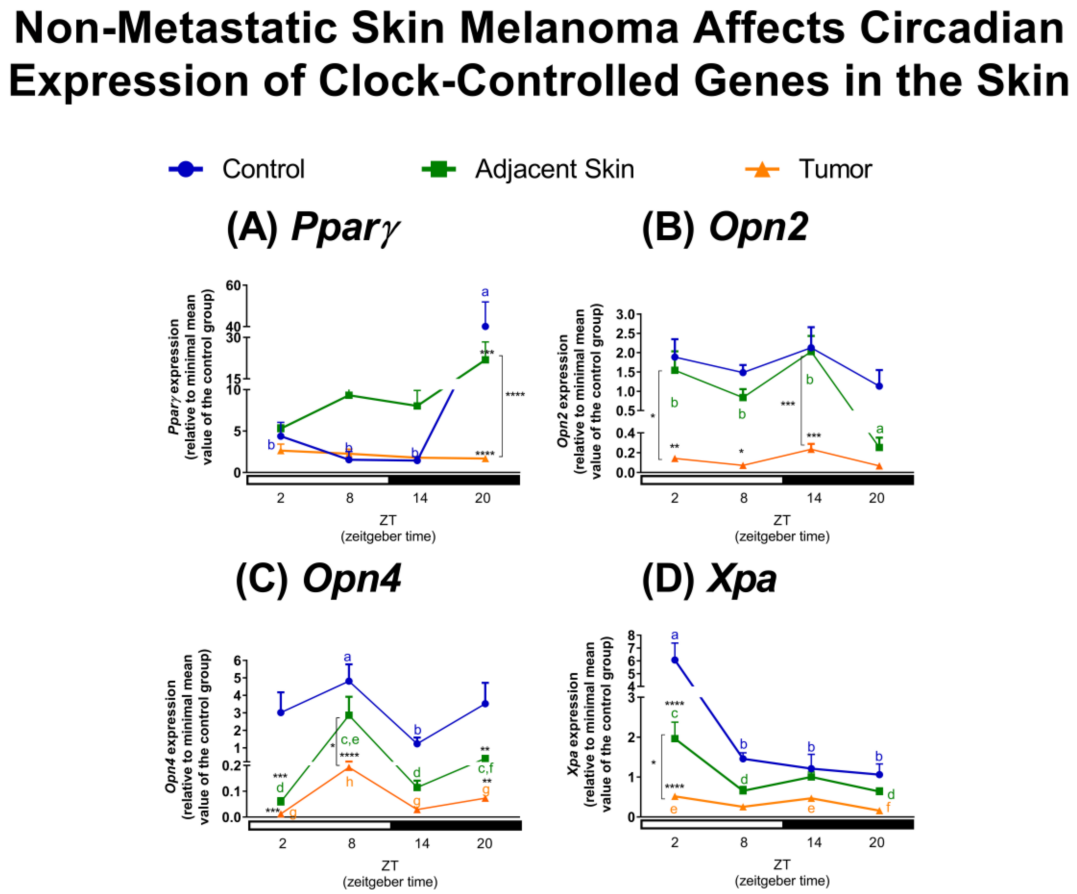

Figure 2. Non-metastatic skin melanoma affects clock-controlled gene expression in skin. Expression of (**A**) *Pparγ*, (**B**) *Opn2*, (**C**) *Opn4* and (**D**) *Xpa* in control skin, tumor-adjacent skin, and tumor samples. Letters represent significant differences in gene expression within the same group, Two-Way ANOVA followed by Tukey post-test. In (**A**) $a \neq b$, $p < 0.01$. In (**B**) $a \neq b$, $p < 0.01$. In (**C**) a ≠ b, $p < 0.05$, c ≠ d, $p < 0.0001$, e ≠ f, $p < 0.05$ and g ≠ h, $p < 0.01$. In (**D**) a ≠ b, $p < 0.001$, c ≠ d, $p < 0.01$ and e ≠ f, $p < 0.05$. Significant differences among groups were demonstrated by Two-Way ANOVA followed by Bonferroni post-test, and are represented by asterisks having the control skin as reference. Differences between tumor-adjacent skin and tumor samples are indicated by brackets. * $p < 0.05$, ** $p < 0.01$, *** $p < 0.001$, **** $p < 0.0001$. Values are presented as the mean expression (n = 3–7) ± SEM of the gene of interest normalized by Rpl37a RNA, relative to the minimal value of skin control group.

The functionality of the photo- and thermo-sensitive systems of the skin is still an ongoing field of studies and their role in pigmentary response and hair follicle growth has been demonstrated [63–66]. In the skin, OPN2 has been implicated as a sensor of UVA radiation and violet light, participating in pigmentation and differentiation of skin cells [66,67]. In normal and malignant murine melanocytes, we have also demonstrated that OPN2 acts as a UVA radiation sensor [63]. In the present study, *Opn2* did not show a circadian oscillatory profile in control skin or tumor samples; however, in tumor-adjacent skin *Opn2* level was dramatically reduced at night (ZT20) in comparison to the remaining ZTs. In tumor samples *Opn2* expression was significantly reduced in most time points when compared to control

and tumor-adjacent skin (Figure 2B). The reduction of *Opn2* transcripts in melanoma tumor in vivo corroborates previous similar findings in cultured melanoma cells [16].

Interestingly, our group detected OPN4, classically found in the retina [1,68], in murine normal and malignant melanocytes [16]. We showed that OPN4 is a UVA radiation sensor [63], and acts in conjunction with OPN2 to mediate the immediate pigmentary process (IPD) [63]. In healthy skin, as well as in tumor-adjacent skin and tumor, *Opn4* expression peaked during the light phase, showing an oscillatory profile which was reduced in amplitude in the tumor (Figure 2C). Since the knowledge of the biological processes regulated by this system in cancer is still scarce, it is hard to grasp the consequences of such reduced gene expression. Nevertheless, higher levels of OPN3 were demonstrated to sensitize hepatocellular carcinoma to 5-fluorouracil. The reduction of OPN3 activates an anti-apoptotic pathway while overexpression of OPN3 inactivates this pathway, thus, favoring chemical-induced cell death [69]. Still in this line, a recent study demonstrated that upon stimulation with blue light, human colon cancer cell lines display decreased viability with increased autophagy, but not apoptosis, compared to non-irradiated cells. Remarkably, all these effects were lost upon knockdown of *OPN3* [70].

Regarding the correlation of opsins and tumor melanin content, we have found that in tumor-adjacent skin and tumor, *Opn2* and *Opn4* correlate positively and negatively, respectively, with melanin content of tumor (Table 1). It is of interest to further investigate the role of opsins and melanin content since OPN2 and OPN4 are UVA sensors and participate in IPD process in melanocytes [63].

Xeroderma Pigmentosum, Complementation Group A (XPA) protein is a DNA repair enzyme, reported to oscillate along 24 h in murine skin [60]. Here, we found that *Xpa* transcripts peaked at ZT2 in control skin, an event that was conserved in tumor-adjacent skin and tumor samples, although with reduced amplitude similarly to other genes analyzed in the skin (Figure 2D). Interestingly, mice exposed to UVB radiation in the morning, when XPA protein levels were low, demonstrated increased skin cancer incidence as compared to mice exposed to the same radiation at night [60]. In our study, *Xpa* transcripts showed higher levels in the light phase and reduced expression in the other ZTs, which is in agreement with previous report of XPA protein peak at ZT10 [60]. Within this line, a recent report demonstrated that an evening cisplatin-based regimen is less toxic than morning treatment in wild type mice, since XPA in the kidney oscillates in a time-dependent manner, leading to more efficient DNA damage removal in the evening compared to the morning. This time-dependent event was lost in *Per1/2* KO animals; however, *Per1/2* KO mice displayed increased immune system activation which led to increased tumor shrinkage in response to cisplatin in comparison to wild type mice [71]. In our study, *Xpa* in tumor-adjacent skin positively correlates with melanin content while in tumor the correlation was negative (Table 1). This difference could be related to different DNA repair capabilities between both tissues; furthermore, melanoma tumors with increased melanin content are more aggressive and resistant to cancer treatment [55,56,72]. We thus suggest that the increased aggressiveness may be associated with reduced DNA repair with consequent increase in gene mutation. Therefore, *Xpa* was significantly affected by the tumor process, which could ultimately favor the malignization of adjacent tissue due to impaired DNA repair process. Further experiments need to be done to validate this hypothesis.

Based on the previous in vivo molecular data, we decided to evaluate the expression of the above-mentioned genes in human samples of healthy skins [73] and primary melanomas [74]. Clinical data analyses show that most of all clock genes, clock-controlled genes, and opsins were less expressed in primary melanoma samples compared to healthy skin. A table containing clinicopathological data from patients with primary melanoma and healthy skin is provided (Supplementary Table S1). In fact, based on the expression levels of these genes, we were able to cluster them in a pattern that clearly distinguishes primary melanoma from healthy skin (Figure 3). Interestingly, primary melanomas show increased *OPN1SW* and *OPN3* expression in comparison to healthy skin, in opposition to all remaining opsins, which are less expressed (Table 2). Therefore, the role of opsins in cancer is an intriguing field that requires further evaluation.

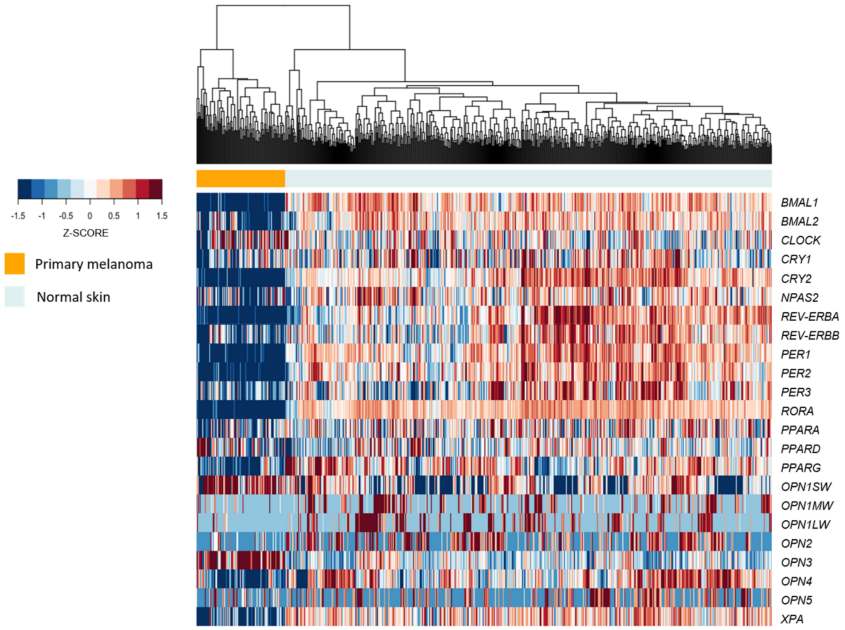

Figure 3. The molecular clock machinery is repressed in human primary melanomas compared to normal skin. Unsupervised hierarchical clustering of 557 GTEx normal (sun and non-sun exposed) skin samples and 104 TCGA primary melanomas according to the expression of clock and clock-controlled genes. Clusters were defined based on the Euclidean distance using complete linkage.

Table 2. Comparison of gene expression between human healthy skins and primary melanomas.

Genes	Expression Mean ± (SEM)		Mann—Whitney Test
	GTEx Normal Skin (n = 557)	TCGA Primary Melanoma (n = 104)	p Value
BMAL1	10.525 (0.023)	7.553 (0.08)	**<0.0001**
BMAL2	9.45 (0.024)	7.19 (0.183)	**<0.0001**
CLOCK	9.975 (0.015)	10.028 (0.079)	**0.019**
CRY1	9.623 (0.024)	9.073 (0.089)	**<0.0001**
CRY2	12.301 (0.023)	9.737 (0.062)	**<0.0001**
NPAS2	11.251 (0.022)	10.346 (0.125)	**<0.0001**
REV-ERBA	13.968 (0.051)	10.057 (0.08)	**<0.0001**
REV-ERBB	10.826 (0.025)	9.625 (0.111)	**<0.0001**
PER1	14.388 (0.033)	10.801 (0.087)	**<0.0001**
PER2	11.217 (0.03)	8.404 (0.073)	**<0.0001**
PER3	10.842 (0.036)	9.816 (0.089)	**<0.0001**
RORA	13.75 (0.031)	7.351 (0.141)	**<0.0001**
PPARA	10.24 (0.022)	9.696 (0.079)	**<0.0001**
PPARD	11.419 (0.014)	11.525 (0.077)	0.921
PPARG	8.08 (0.047)	6.029 (0.135)	**<0.0001**
OPN1SW	1.358 (0.047)	2.873 (0.135)	**<0.0001**
OPN1MW	0.624 (0.039)	0.219 (0.058)	**<0.0001**
OPN1LW	0.628 (0.04)	0.113 (0.039)	**<0.0001**
OPN2	0.898 (0.04)	0.29 (0.056)	**<0.0001**
OPN3	8.452 (0.027)	10.357 (0.129)	**<0.0001**
OPN4	4.709 (0.056)	2.503 (0.149)	**<0.0001**
OPN5	0.706 (0.039)	0.554 (0.09)	0.093
XPA	8.898 (0.012)	8.002 (0.065)	**<0.0001**

Expression levels were estimated using upper-quartile normalized RSEM. Mean expression is shown as transformed log2(x + 1), where x = RSEM. p values in bold indicate significant differences between healthy skin and primary melanoma tumor. *Homo sapiens* gene nomenclature according to https://www.genenames.org/about/guidelines.

In summary, the presence of tumor and TME has been previously shown to lead to a pro-inflammatory process in adjacent tissue [51], and according to our data, also promotes a chronodisruption in adjacent skin. In addition to the molecular clock, we observed that the expression and/or oscillatory profile of key genes involved in skin proliferation, pigmentation, photo- and thermo-sensitive systems, and DNA repair processes was significantly affected by TME in vivo. The data by Aran and colleagues [51] in association with ours caution against the use of adjacent skin as a "healthy" tissue, since it displays an intermediate phenotype between healthy skin and tumor samples. All these molecular changes clearly demonstrated that tumor-adjacent skin is significantly affected by TME, and that these alterations—especially in the molecular clock—could be linked to the progression of skin cancer.

2.2. Effects of Tumor Macroenvironment (TMaE) on Clock and Clock-Controlled Genes of Lung, Liver and SCN

The investigation of the influence of a circumscribed tumor over distant organs is an attractive approach. Although tumors can be confined to a restricted place, even encapsulated, some tumor-derived molecules may be released into the bloodstream. For instance, tumors secrete growth factor-, mRNA- and miRNA-containing micro-vesicles, which can be found in the blood of cancer patients and are important players in the metastatic process (reviewed in [47]). Along this line, a recent study reported that exosomes derived from B16-F10 cells are positive for mRNA and miRNA molecules, which affect the epigenetic landscape and mitochondrial respiration in cytotoxic T cells [75]. Classical effects of TMaE are related to cancer-associated cachexia, systemic inflammation, immune system suppression, and altered coagulation [47,48]. All the previous effects clearly demonstrate the ability of tumors to communicate with the whole organism.

In this study we evaluated two organs commonly affected by melanoma metastasis—lung and liver [76]. In agreement with previous reports of oscillatory profile of clock genes in the lung [77–80], we showed that lungs of control mice display an oscillatory profile of *Per1* with increased expression at ZTs 8, 14, and 20 in comparison to ZT2. In tumor-bearing mice, lung *Per1* transcripts also exhibited an oscillatory profile, however, with lower amplitude of expression at ZT14 as compared to control mice (Figure 4A). *Bmal1* expression was detected in anti-phase with *Per1* in control animals, with higher level of transcripts at ZT2 in comparison to ZTs 8 and 14 (Figure 4B). In tumor-bearing animals, the circadian oscillation of *Bmal1* was abolished due to a remarkable reduction on transcripts at ZT2 in comparison to control lungs (Figure 4B), and in this case the anti-phase relationship between *Per1* and *Bmal1* was lost. In lungs of control and tumor-bearing mice, *Reverb-α* expression peaked at ZT8, but with a remarkable reduction in amplitude in the tumor-bearing animals (Figure 4C).

It is known that several respiratory parameters such as expiratory flow and lung volume exhibit a circadian pattern [81,82]. Interestingly, this temporal pattern may be altered by oxidative stress evoked by environmental smoke and pollution, jet lag, or pro-inflammatory mediators among others [81]. For instance, nuclear factor (erythroid-derived 2)-like 2 (NRF2), a major antioxidant player, was demonstrated to be a lung CCG and to participate in a time-dependent oxidative/fibrotic lung damage [83]. An elegant study using lung adenocarcinoma demonstrated that jet lag and genetic mutation of *Per2* or *Bmal1* accelerates carcinogenesis with consequent reduction on survival. The lack of clock genes in the lungs resulted in increased c-Myc expression, proliferation, and metabolic dysregulation [84]. Here we demonstrated that the presence of non-metastatic tumor significantly affected the molecular clock of lungs, leading to reduction of *Per1* and *Reverb-α* transcripts and complete loss of *Bmal1* oscillatory pattern, likely resulting in a chronodisruption scenario. Our data suggest that chronodisruption induced by the primary tumor might favor the success of melanoma cells migration and establishment of tumoral environment in the lungs, what still needs to be validated.

In addition to clock genes, we also evaluated *Xpa* expression in lungs of control and tumor-bearing mice. No oscillatory profile was found in lungs of control mice while an oscillatory pattern was found in lungs of tumor-bearing mice: *Xpa* expression was higher at ZTs 8 and 14 than at ZTs 2 and 20,

and significantly higher than in control mice (Figure 4D), which could be related to increased DNA damage in this tissue.

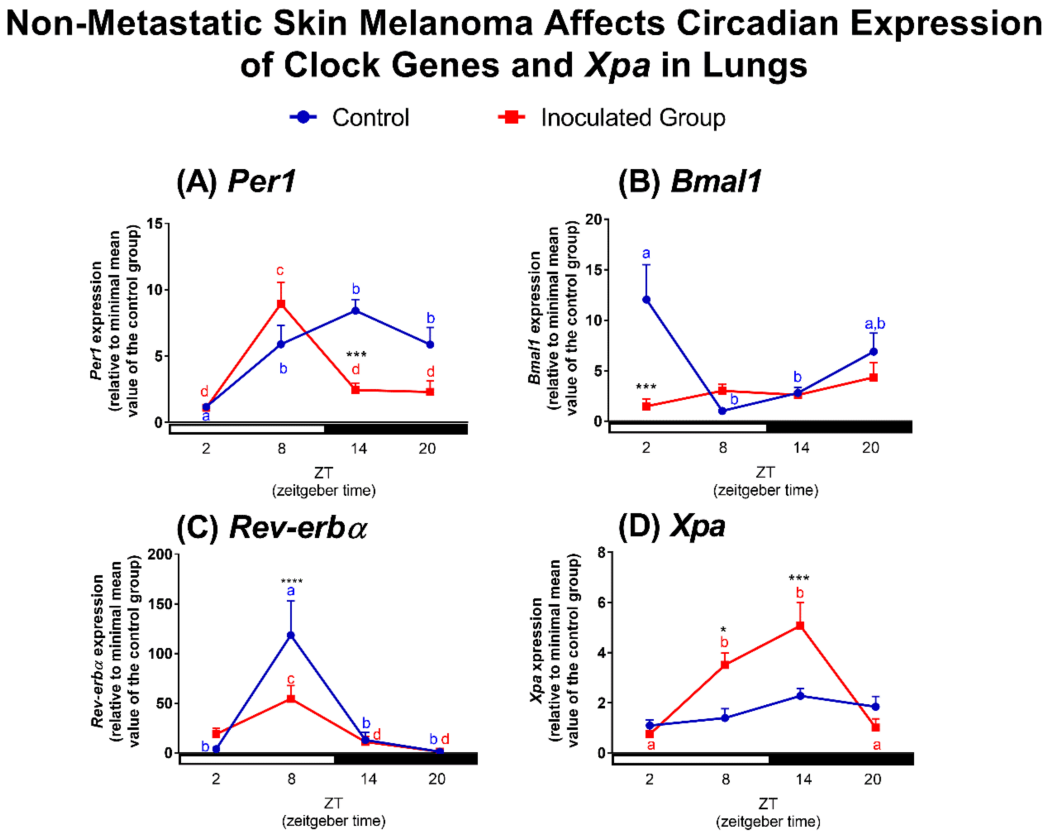

Figure 4. Non-metastatic skin melanoma affects circadian expression of clock genes and *Xpa* in lungs. Expression of (**A**) *Per1*, (**B**) *Bmal1*, (**C**) *Reverb-α* and (**D**) *Xpa* in lungs of control and tumor-bearing mice. Letters represent significant differences in gene expression within the same group, Two-Way ANOVA followed by Bonferroni post-test. In (**A**) $a \neq b$, $p < 0.05$ and $c \neq d$, $p < 0.001$. In (**B**) $a \neq b$, $p < 0.01$. In (**C**) $a \neq b$, $p < 0.0001$ and $c \neq d$, $p < 0.05$. In (**D**) $a \neq b$, $p < 0.01$. Significant differences between control and tumor-bearing mice were demonstrated by Two-Way ANOVA followed by Bonferroni post-test, and are represented by asterisks having the control lung as reference. * p <0.05, *** p <0.001, **** p <0.0001. Values are presented as the mean expression (n = 4–6) ± SEM of the gene of interest normalized by 18S RNA, relative to the minimal value found in the control group.

Approximately 10% of all liver transcripts are known to display temporal variation. Among them, several enzymes that participate in cholesterol and lipid metabolism are expressed in a 24-h daily rhythm [85]. Accordingly, it has been shown that plasma triglyceride and cholesterol levels also oscillate along 24 h [86]. In this way, knockout animals of clock components exhibit impairment of lipid metabolism [87–90] which is related with development of several diseases [4,5,20–22], including cancer [13–15,17–19]. Here we demonstrated, in agreement with the literature reports [78,91,92], that *Per1*, *Bmal1*, and *Reverb-α* display a temporal oscillation in the liver of control mice. *Per1* expression was higher at ZT8 in comparison to the other ZTs; this pattern was conserved in tumor-bearing mice but in these animals *Per1* transcripts remained higher for an additional 6 h (up to ZT14) in comparison to control mice (Figure 5A). We also found an antiphase relationship between liver *Per1* and *Bmal1*. The expression of the latter gene was found to oscillate along 24 h, peaking at ZT2. The oscillatory profile of *Bmal1* was lost in tumor-bearing mice since at ZT2 *Bmal1* expression was significantly reduced when compared to control mice (Figure 5B). The classic antiphase relationship between *Per1* and *Bmal1* observed in the control mice was completely lost in tumor-bearing mice, as a consequence of the

shift of *Per1* expression peak and the reduction of *Bmal1* expression and loss of its circadian rhythm. Since *Reverb-α* shows a prominent role in circadian metabolism [93,94], we evaluated its expression in our model. *Reverb-α* exhibited identical oscillatory profile to *Bmal1* gene, with attenuated amplitude at ZT2 in liver of tumor-bearing mice (Figure 5C).

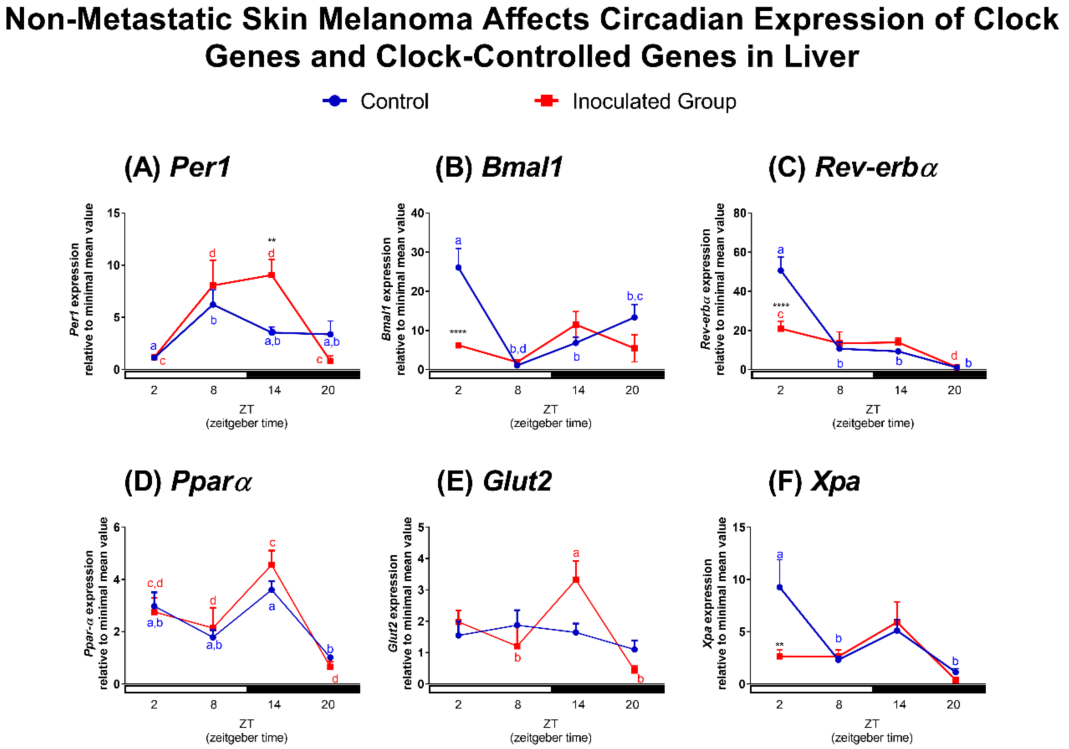

Figure 5. Non-metastatic skin melanoma affects circadian expression of clock genes and clock-controlled genes in liver. Expression of (**A**) *Per1*, (**B**) *Bmal1*, (**C**) *Reverb-α*, (**D**) *Pparα*, (**E**) *Glut2* and (**F**) *Xpa* in liver of control and tumor-bearing mice. Letters represent significant differences in gene expression within the same group, Two-Way ANOVA followed by Bonferroni post-test. In (**A**) $a \neq b$, $p < 0.05$ and $c \neq d$, $p < 0.01$. In (**B**) $a \neq b$, $p < 0.001$, $c \neq d$, $p < 0.05$. In (**C**) $a \neq b$, $p < 0.0001$, $c \neq d$, $p < 0.05$. In (**D**) $a \neq b$ and $c \neq d$, $p < 0.05$. In (**E**) $a \neq b$, $p < 0.05$. In (**F**) $a \neq b$, $p < 0.05$. Significant differences between control and tumor-bearing mice were demonstrated by Two-Way ANOVA followed by Bonferroni post-test, and are represented by asterisks having the control liver as reference ** $p < 0.01$, **** $p < 0.0001$. Values are presented as the mean expression (n = 4–6) ± SEM of the gene of interest normalized by 18S RNA, relative to the minimal value found in the control group.

Pparα, a CCG, is an important regulator of liver lipid homeostasis since PPARα participates in fatty acid metabolism and ketogenesis [95]. In livers of control animals, *Pparα* expression was higher at ZT14 in comparison to ZT20, a pattern that was still evident in tumor-bearing mice (Figure 5D). We also evaluated the expression of *Glut2*, a gene that encodes a glucose transporter [96,97]. *Glut2* transcripts did not show an oscillatory pattern in control mice; however, in tumor-bearing mice, *Glut2* expression was higher at ZT14 in comparison to ZTs 8 and 20 (Figure 5E). Liver *Xpa* transcripts were higher at ZT2 in comparison to ZTs 8 and 20 in control animals while this oscillatory profile was absent in tumor-bearing mice, as at ZT2, its expression was significantly reduced (Figure 5F). Within this line, Hojo and colleagues [50] found that a non-metastatic breast cancer results in increased oxidative stress in the liver. Due to the similarities in both experimental protocols ([50] and ours), we suggest that liver of tumor-bearing mice may show increased oxidative stress and damage, which could be associated with altered glucose metabolism and DNA repair.

Interestingly, C57BL/6J wild type mice subject to chronic jet lag showed significantly reduced lifespan, spontaneous hepatocellular carcinoma, which is preceded by non-alcoholic fatty liver disease that progress to hepatic steatosis and fibrosis. In addition, these jet-lagged mice had increased hepatic triglycerides and free fatty acids, which was related with insulin resistance [17]. Based on a largescale circadian metabolomics, it was found that most of the analyzed metabolites displayed robust circadian rhythms in control mice; however, jet-lagged mice exhibited a genome-wide gene deregulation and liver metabolic dysfunction with nuclear receptor-controlled cholesterol/bile acids among the top deregulated pathways [17]. In fact, bile acids, besides being a physiological detergent that facilitates intestinal absorption, are also an inflammatory agent that rapidly activates nuclear receptors and cell signaling pathways, which ultimately regulate lipid, glucose, and energy metabolism. The transcriptional regulation of CYP7A1 (cholesterol 7α-hydroxylase), which is the rate limiting enzyme in bile acid biosynthesis, occurs at several levels, mainly related to the levels of plasma cholesterol [98]. In addition to its canonical role, bile acids also stimulate the secretion of pro-inflammatory cytokines from Kupffer cells (liver resident macrophages). This leads to the activation of tumor necrosis factor (TNFα) receptor signaling and mitogen-activated protein kinase (MAPK)/JNK pathway, which results in the repression of *Cyp7a1* [99]. Interestingly, *Reverb-α* negatively regulates *Cyp7a1* by the repression of liver receptor homologue-1 (LRH-1), a known hepatic activator of *Cyp7a1* [100]. In line with the previous data, global or tissue-specific double knockout mice *Rev-erbα*$^{-/-}$/*Rev-erbβ*$^{-/-}$ show elevated plasma triglyceride levels and hepatic steatosis [87,94].

We clearly demonstrated that a non-metastatic melanoma tumor can significantly impair the molecular clock of lungs and liver, indicating a chronodisruption scenario. Taken together the literature and our results, we can hypothesize that TMaE effects on liver and lungs may be due to at least two different mechanisms: (1) change of the temporal profile of clock genes what leads to deregulation of tissue-specific CCGs; (2) activation of immune system that ultimately affects the organ physiology. Within this line, our results open a question whether the altered clock components of distant organs may be a direct or indirect consequence of tumor. In fact, a pioneering study by Masri and colleagues [49] showed that a non-metastatic lung adenocarcinoma rewires, through an inflammatory pathway, several liver clock-controlled metabolic processes, which ultimately impairs insulin, glucose, and lipid metabolism. In similar fashion inoculation of breast cancer cells, in a non-metastatic cancer model, evokes an altered pattern of clock gene expression and increased oxidative stress in liver (not kidney) [50].

Although the results are comparable, important experimental differences should be pointed. Masri and colleagues used a Cre-lox genetic model that leads to activation of the oncogene *Kras* and deletion of *Tp53* (p53-coding gene), and the animals were euthanized 4 months later [49]. Hojo and colleagues [50] used 4T-1 breast cancer cell line subcutaneously injected into mammary gland, and the mice were euthanized 7 days after inoculation. Therefore, comparisons between both studies should be made with caution. The experimental protocol used by Marsi and colleagues [49] mimics a more physiological situation since tumor developed over the course of 4 months. Due to the long experimental setup, the cancer-induced perturbation of the molecular clock may have been compensated, which could explain the lack of alteration of the core clock. On the other hand, Hojo and coworkers [50] used an acute model of tumorigenesis which may have induced an inflammatory process and immune system activation, events that could contribute to the altered profile of the molecular clock profile. Our protocol is similar to the one used by the latter authors, what suggests that the circadian alteration of the clock may be due to the activation of immune system.

Based on the fact that lung and liver peripheral clocks were disrupted in tumor-bearing animals, we questioned whether the SCN would still be fully functional in tumor-bearing mice. In SCN of control mice, *Per1* transcripts showed an oscillatory profile with higher levels in the scotophase (ZT14) in comparison to the light phase (ZT2 and ZT8) as well as at ZT20, a pattern that was maintained in tumor-bearing mice (Figure 6A). *Bmal1* transcripts also showed an oscillatory profile in SCN of control mice peaking at ZT2 in antiphase with *Per1*. Surprisingly, in SCN of tumor-bearing mice, the oscillatory

profile of *Bmal1* expression, was lost due to a significant transcript reduction at ZT2 in comparison to SCN of control mice (Figure 6B).

We then analyzed *cFos* expression, a gene known to be acutely induced by light, as a marker of neuronal activity [101]. In SCN of control mice, *cFos* expression showed a temporal variation with higher expression at ZT14. In tumor bearing-mice an increased expression of *cFos* was found at ZT2 in comparison to control mice (Figure 6C), which resulted in a phase shift of gene expression phase from ZT14 to ZT2. *cFos* expression was upregulated in tumor-bearing mice compared to control, a fact that could indicate that SCN neuronal activity was increased in response to TMaE, the understanding of which requires additional studies. Therefore, our data clearly show for the first time, that a non-metastatic melanoma impairs the molecular clock function of the central oscillator, mainly due to the reduction of *Bmal1* expression and consequent loss of oscillatory profile and of the antiphase relationship between *Per1* and *Bmal1*.

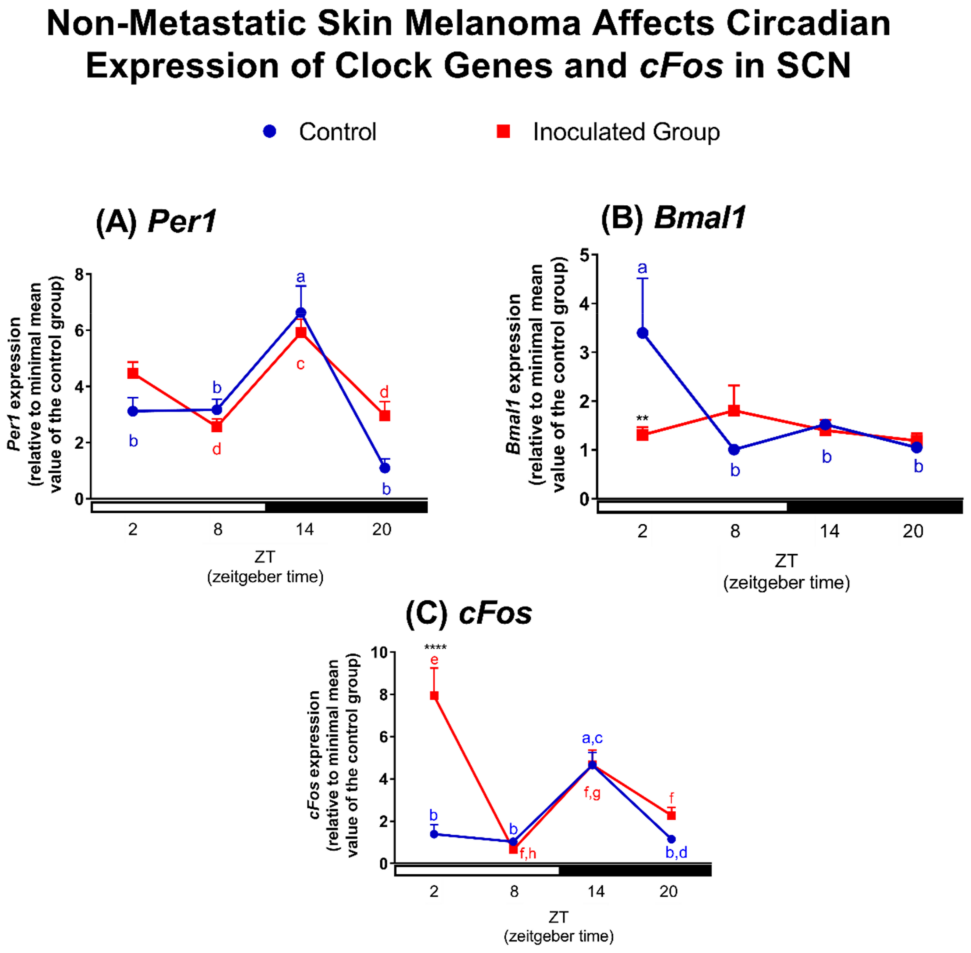

Figure 6. Non-metastatic skin melanoma affects circadian expression of clock genes and *cFos* in SCN. Expression of (**A**) *Per1*, (**B**) *Bmal1* and (**C**) *cFos* in SCN of control and tumor-bearing mice. Letters represent significant differences in gene expression within the same group, Two-Way ANOVA followed by Bonferroni post-test. In (**A**) $a \neq b$, $p < 0.01$ and $c \neq d$, $p < 0.05$. In (**B**) $a \neq b$, $p < 0.05$. In (**C**) $a \neq b$ and $c \neq d$, $p < 0.05$, $e \neq f$, $p < 0.01$ and $g \neq h$, $p < 0.001$. Significant differences between control and tumor-bearing mice were demonstrated by Two-Way ANOVA followed by Bonferroni post-test, and are represented by asterisks having the control SCN as reference. ** $p < 0.01$, **** $p < 0.0001$. Values are presented as the mean expression (n = 3–7) ± SEM of the gene of interest normalized by Rpl37a RNA, relative to the minimal value found in the control group.

To the best of our knowledge, no study has evaluated the effect of tumor presence on the molecular clock of the central oscillator. In fact, these are intriguing results since the SCN is known to be resistant to genetic perturbation due to its strong coupling [9,102]. The disruption of the central oscillator is disastrous to the entire organism due to its crucial control of temporal organization [8,12], since important biological processes such as immune system activation [103,104], metabolism [105–107], endocrine system physiology [108,109], DNA repair [110] are controlled by the central oscillator in a time-dependent fashion.

It is interesting to highlight that in all analyzed tissues, *Bmal1* disruption paralleled the carcinogenic process. It is known that *Bmal1* is the only clock gene whose removal leads to arrhythmia as no redundant compensatory mechanism exists [12,111,112]. However, BMAL1 protein is regulated by a variety of circadian mechanisms such as phosphorylation, SUMOylation, ubiquitination, acetylation, *O*-GlcNAcylation and *S*-nitrosylation [113]. Additionally, several factors like oxidative stress, nutritional and inflammatory signals significantly affect BMAL1 protein stability and function, thus modifying the organ physiology [113]. Taken altogether, *Bmal1* is an interesting candidate marker for chronodisruption and melanoma development.

Our results bring compelling evidence that a non-metastatic melanoma significantly affects the molecular machinery of both central and peripheral clocks. These data are strengthened by the correlation between tumor melanin content and clock genes. For instance, tumor melanin content negatively correlated with the expression of *Bmal1* and *Per1* in lungs and liver, respectively. Intriguingly, the expression of both genes in SCN samples also negatively correlated with the tumor melanin content. Therefore, as melanin content increases, the expression of clock gene decreases in central and peripheral clocks. Based on these data, we suggest that these clock-related modifications could partially explain the clinical results showing that highly pigmented melanomas are more aggressive than amelanotic ones [55].

We hypothesize that alterations in the clock machinery may be an important step during the onset and progression of the metastatic process as well as could be involved in the development of the classical TMaE alterations such as cachexia, immune system suppression, and altered coagulation. Neither previous reports [49,50] nor the present study evaluated whether the tumor-induced genetic alterations favor tumor metastasis. Further studies are required to establish the consequences of TMaE-induced changes of the molecular clock in cancer development and metastasis. If validated, clock gene and CCG machinery may become an interesting pharmacological target.

The data presented in this manuscript have established important findings regarding the effects of a non-metastatic melanoma on the functioning of central and peripheral clocks. We showed that melanoma tumor exhibits a profound reduction in the expression of clock genes. Of note, melanoma tumors showed an oscillatory profile in melanin content, an event that if proven clinically true, could represent an important treatment strategy since an elevated tumor melanin content has been associated with poor prognosis and limited response to radiotherapy [55]. The presence of tumor is also deleterious to the adjacent tissue, which presented an intermediate phenotype between control skin and tumor, warning against the use of tumor-adjacent tissue as control samples. The TME likely presented alterations in some important skin physiological processes, such as light and temperature detection, proliferation, and DNA repair; however, further functional-based studies are required.

Regarding TMaE, our data and the cited literature suggest that some tumor-originated molecules may be released into the bloodstream and exert distant effects. In fact, classic alterations of TMaE such as cachexia, systemic inflammation, immune system suppression, and altered coagulation, are well known [47,48]; however, chronodisruption has been recently added to the myriad of TMaE features [49,50]. Within this line, our data provide compelling evidence that chronodisruption, in a non-metastatic model of melanoma, takes place in organs other than the tumor-adjacent skin (Figure 7). These findings, therefore, suggest that chronodisruption could impact melanoma development and progression. The pharmacological targeting of clock components of peripheral tissues might represent an important improvement in oncological treatment [39,114].

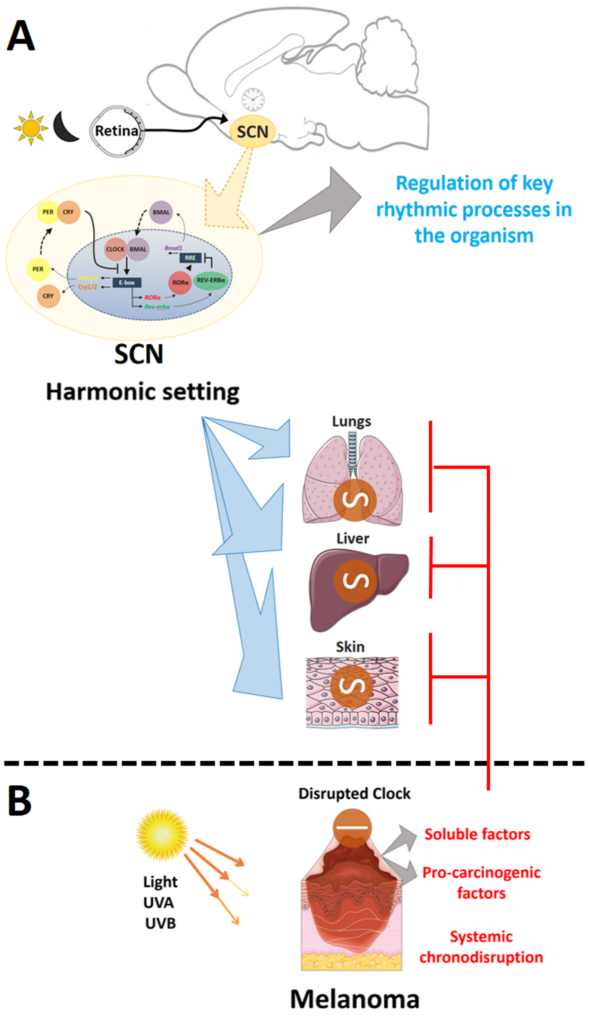

Figure 7. Non-metastatic melanoma leads to systemic chronodisruption in peripheral and central clocks in mice. (**A**) In a physiological situation melanopsin-expressing retinal cells translate the photic information into glutamate release at the suprachiasmatic nucleus (SCN)—the central clock. The SCN then adjusts its molecular clock, comprised by several circadian oscillatory genes, to the environmental light-dark information (24 h duration). The SCN feeds the external time information to several regulatory regions of the brain, which control many biological processes. In fact, in a harmonic setting all biological processes within the organism are in phase and aligned to the external time, thus ensuring a homeostatic condition among all organs and systems; (**B**) However, this systemic harmonic condition is lost when a localized and non-metastatic melanoma is present. Our data show that the effects TME and TMaE lead, respectively, to a chronodisruption scenario in adjacent skin and in distant organs (lungs, liver, and SCN). In addition, TME and TMaE not only disrupt the molecular clock but also affect key tissue-specific regulatory genes. Based on the literature, we suggest that these tumor-induced effects are due to the presence of soluble factors which leak from the encapsulated tumor into the bloodstream, thus triggering systemic chronodisruption.

3. Material and Methods

3.1. In Vivo Procedures

Experimental procedures were performed according the protocol approved by the Ethics Committee for Animal Use (CEUA IB/USP, number 255/16, approved on 14 June 2016). The experiments were conducted on 45 C57BL/6J mice (provided by the Institute of Biomedical Sciences vivarium, University of São Paulo, originally acquired from Jackson Laboratories), ranging

from eight to sixteen-week old. Animals were subcutaneously inoculated in the right flank with 2×10^6 B16-F10 cells (kindly donated by Prof. Roger Chammas, Faculty of Medicine, University of São Paulo), resuspended in sterile phosphate buffered saline (PBS). Control mice received the same volume of sterile PBS. B16-F10 cells are a metastatic melanoma line capable of forming distant metastasis [115] and the development of metastasis depends on several factors including injection site, number of inoculated cells, and others [115]. In our experimental model no metastasis was observed, and every animal was inspected for the presence of metastasis points in all organs after the euthanasia. Mice were individually placed in standard propylene cages with access to food and water *ad libitum*, kept at 22 °C ± 2 under a 12:12 light/dark cycle (1000–1200 lux white LED light, ranging from 420 to 750 nm). Lights were on at 7 a.m. (ZT0) and off at 7 p.m. The experiments lasted 14 days, and on the 15th day the mice were euthanized with CO_2 at ZTs 2 (9 a.m.), 8 (3 p.m.), 14 (9 p.m.), and 20 (3 a.m.), and the death was assured by cervical dislocation. At ZTs 14 and 20 all experimental procedures were carried with assistance of night goggles in complete darkness.

The animals were decapitated, the heads wrapped in aluminum foil in the absence of light and placed in dry ice. Then, the ambient light was turned on, and samples of skin (2 cm^2), liver and lungs from control animals, and of tumor-adjacent skin, tumor, liver, and lungs from melanoma-bearing mice were excised, placed in dry ice, and stored at −80 °C until processing. For SCN isolation, brains were dissected at 4 °C after removal of excess of cranial meninge. Coronal sections were performed using the optic nerves and the base of the posterior hypothalamus as reference. Anterior hypothalamic area was dissected and the SCN was identified by the location of the optic chiasm and third ventricle, and approximately 3 mm thick portion was removed and processed for RNA extraction (Supplementary Figure S1). Because mouse SCN expresses vasoactive intestinal peptide [116], confirmation of *Vip* expression was performed by quantitative PCR.

3.2. TME and TMaE Effects in the Organism

To evaluate the effects of TME, we determined gene expression in skin of control mice and tumor-adjacent skin of tumor-bearing mice. The effects of TMaE were assessed by determining the expression of clock genes, clock-controlled genes, and tissue-specific genes in lung, liver, and SCN of control and tumor-inoculated animals.

3.3. Total RNA Extraction and Reverse Transcriptase-Polymerase Chain Reaction (RT-PCR)

Small fragments of tissue were homogenized in TRIzol (Thermo Fisher Scientific, Waltham, MA, USA), and total RNA was extracted and purified according to the kit manufacturer's instructions (Direct-zol™ RNA MiniPrep, Zymo Research, Irvine, CA, USA). RNA concentration (OD_{260}) was determined in a spectrophotometer (Nanodrop, Willmington, DE, USA), and 1 µg was subject to reverse transcription with SuperScript III Reverse Transcriptase, random hexamer primers, and other reagents according to the manufacturer's instructions (Thermo Fisher Scientific, Waltham, MA, USA).

3.4. Quantitative PCR (qPCR)

The products of 1 µL of RT-PCR were subject to quantitative PCR reactions using species-specific primers (Table 3) spanning introns, based on sequences obtained from GenBank (http://www.ncbi.nlm.nih.gov/genbank), designed by Primer Blast (http://www.ncbi.nlm.nih.gov/genbank) or Primer Quest (IDT, Coralville, IA, USA), and synthesized by IDT. Rpl37a RNA or ribosomal 18S RNA was used to normalize the expression values of the genes of interest. Prior to this selection, we ascertained that both normalizers did not vary among time points under the various experimental conditions.

Table 3. Sequences and concentrations of primers and probes, and gene access numbers.

Templates (Access Number)	Primers and Probes	Final Concentration
Per1 (NM_0011065.3)	Forward: 5′-AGCAGGTTCAGGCTAACCAGGAAT-3′ Reverse: 5′-AGGTGTCCTGGTTTCGAAGTGTGT-3′ Probe: 5′-/6FAM/-AGCTTGTGCCATGGACATGTCTACT/BHQ_1/-3′	300 nM 300 nM 200 nM
Bmal1 (NM_001243048)	Forward: 5′-AGCTTCTGCACAATCCACAGCAC-3′ Reverse: 5′-TGTCTGGCTCATTGTCTTCGTCCA-3′ Probe: 5′-/5HEX/-AAAGCTGGCCACCCACGAAGATGGG/BHQ_1/-3′	300 nM 300 nM 200 nM
Pparγ (NM_001127330.2)	Forward: 5′-TGTGGGGATAAAGCATCAGGC-3′ Reverse: 5′-CCGGCAGTTAAGATCACACCTAT-3′	300 nM 300 nM
Pparα (NM_011144.6)	Forward: 5′-ACGTTTGTGGCTGGTCAAGT-3′ Reverse: 5′-TGGAGAGAGGGTGTCTGTGAT-3′	300 nM 300 nM
Reverb-α (NM_145434.4)	Forward: 5′-AAGACATGACGACCCTGGAC-3′ Reverse: 5′-CCATGCCATTCAGCTTGGTAAT-3′	300 nM 300 nM
Glut2 (NM_031197.2)	Forward: 5′-TGTTGGGGCCATCAACATGA-3′ Reverse: 5′-GGCGAATTTATCCAGCAGCAC-3′	300 nM 300 nM
Xpa (NM_011728.2)	Forward: 5′-GGCGATATGAAGCTCTACCTAAA-3′ Reverse: 5′-TTCCTGCCTCACTTCCTTTG-3′	300 nM 300 nM
cFos (NM_010234.2)	Forward: 5′-TACTACCATTCCCCAGCCGA-3′ Reverse: 5′-GCTGTCACCGTGGGGATAAA-3′	300 nM 300 nM
Opn2 (NM_145383.1)	Forward: 5′-TGCCACACTTGGAGGTGAAA-3′ Reverse: 5′-ACCACGTAGCGCTCAATGG-3′	300 nM 300 nM
Opn4 (NM_001128599.1)	Forward: 5′-ACATCTTCATCTTCAGGGCCA-3′ Reverse: 5′-ACTCACCGCAGCCCTCAC-3′	300 nM 300 nM
Rpl37a RNA (NM_009084.4)	Forward: 5′-GCATGAAAACAGTGGCCGGT-3′ Reverse: 5′-AGGGTCACACAGTATGTCTCAAAA-3′	300 nM 300 nM
18S RNA	Forward: 5′-CGGCTACCACATCCAAGGAA-3′ Reverse: 5′-GCTGGAATTACCGCGGCT-3′	50 nM 50 nM

For simultaneous analysis of *Per1* and *Bmal1*, multiplex reactions containing cDNA, 300 nM primers, 200 nM fluorescent probes and KAPA PROBE FAST 2× (Kapa Biosystems, Wilmington, MA, USA) were run in triplicates for each experimental cDNA sample. Independent solutions for the remaining genes were prepared with cDNA, specific primers (300 nM) and KAPA SYBR FAST 2× (Kapa Biosystems, Wilmington, MA, USA), and run in duplicates. Reactions were carried out in the following conditions: for multiplex assays, in iQ5 thermocycler (Bio-Rad Laboratories, Hercules, CA, USA), 3 min at 95 °C followed by 45 cycles of 15 s at 95 °C and 60 s at 60 °C; for SYBR Green assays in iQ5 or iCycler thermocycler (Bio-Rad Laboratories, Hercules, CA, USA), 10 min at 95 °C, followed by 45 cycles of 15 s at 95 °C, 1 min at 60 °C, and 80 cycles of 10 s at 55 °C with a gradual rise of 0.5 °C. Negative controls without templates were routinely included.

3.5. Melanin Quantification

Melanin content was determined from tumor samples based on a previous study [117]. Briefly, a portion of the tumor was collected, lysed in 1% Triton X-100 in PBS, and kept at 4 °C to allow complete lysis. After vigorous agitation, the samples were centrifuged during 30 min at 14,000× *g* (4 °C) to separate soluble and insoluble fractions. The supernatant was used to quantify total protein by BCA according to the manufacturer's instruction (Thermo Fisher Scientific, Waltham, MA, USA). The insoluble fraction containing the melanin pellet was resuspended in 1 mL of 1 M NaOH in 10% DMSO and heated at 80 °C during 2 h. Samples were then centrifuged at 1050× *g* for 15 min, the supernatant was transferred to new tubes, and 200 µL of each sample were added in duplicate to wells of a flat-bottom plate. Melanin was quantified by absolute absorbance at 475 nm in a plate reader (SpectraMax 250, Molecular Devices, Sunnyvale, CA, USA), and the values interpolated in a standard curve of synthetic melanin (Sigma-Aldrich, St. Louis, MO, USA) ranging from 3.125 to 200 µg/mL [16,36,37,63]. Values were plotted as µg/mL × 10^3 previously normalized by protein concentration.

3.6. RNAseq Datasets

Gene expression and clinical data of 104 primary melanomas from The Cancer Genoma Atlas (TCGA) and 557 normal skins (sun and non-sun exposed) from Genotype-Tissue Expression (GTEx) were downloaded from the UCSC XENA Browser (http://xena.ucsc.edu) TCGA and GTEx gene expression data were generated using the Illumina HiSeq 2000 RNA sequencing platform, quantified using RSEM, upper quartile normalized and log2(x + 1) transformed. Unsupervised hierarchical clustering was performed using the Euclidean distance and complete linkage. Gene expression data were checked for normality using the D'Agostino & Pearson test. Comparisons between normal skin samples and primary melanomas were performed using the Mann-Whitney test. Analyses were conducted in the R statistical environment (https://www.r-project.org).

3.7. Experimental Data Analyses

Gene expression was quantified according the $2^{-\Delta\Delta Ct}$ method [118], as previously described [119]. ΔC_t was determined by subtracting the normalizer C_t from the C_t of the gene of interest at the same time point, both corresponding to the average of duplicate (SybrGreen assays) or triplicate (multiplex assays) wells of the same cDNA. The smaller mean value obtained from control mice was subtracted from all other values, for each tissue for both control and tumor-bearing mice, obtaining the $\Delta\Delta C_t$, which was used as a negative exponential of base 2 ($2^{-\Delta\Delta Ct}$).

The log values were obtained from at least three animals from two independent experiments. Data are shown as the mean ± SEM. To determine the significance of differences between time points within the same group or the temporal differences between control and tumor-bearing mice, logarithmic data were compared by Two-Way ANOVA followed by Bonferroni or Tukey post-test.

Melanin content of tumor samples was analyzed by One-Way ANOVA followed by Tukey post-test. The analysis of gene correlation with melanin content of matched tumor-bearing mice were carried out using the logarithmic gene expression values for each tissue. Data were checked for normality using the D'Agostino & Pearson test; samples that display a Gaussian distribution were analyzed according to Pearson correlation while non-parametric data were analyzed by Spearman correlation.

In all scenarios, $p < 0.05$ was established to reject the null hypothesis.

Supplementary Materials: The following are available online at http://www.mdpi.com/1422-0067/19/4/1065/s1.

Acknowledgments: This work was partially supported by the Sao Paulo Research Foundation (FAPESP, grant 2012/50214-4) and by the National Council of Technological and Scientific Development (CNPq, grants 301293/2011-2 and 303070/2015-3). Leonardo Vinícius Monteiro de Assis, Maria Nathália Moraes, Sanseray da Silveira Cruz-Machado, Gabriela Sarti Kinker are fellows of FAPESP (2013/24337-4, 2014/16412-9, 2015/04557-5, and 2014/16412-9 respectively). We thank Renata Alves dos Santos for providing an excellent care for our mice.

Author Contributions: Leonardo Vinícius Monteiro de Assis, Maria Nathália Moraes, and Ana Maria de Lauro Castrucci designed the study. Leonardo Vinícius Monteiro de Assis, Maria Nathália Moraes, and Keila Karoline Magalhães-Marques acquired the data. Leonardo Vinícius Monteiro de Assis and Maria Nathália Moraes analyzed the data. Sanseray da Silveira Cruz-Machado extracted the SCN; Gabriela Sarti Kinker researched the bioinformatic data and together with Leonardo Vinícius Monteiro de Assis critically analyzed the data. Leonardo Vinícius Monteiro de Assis, Maria Nathália Moraes and Ana Maria de Lauro Castrucci drafted the manuscript. All authors critically revised the manuscript. All authors have approved the definitive version of the manuscript and agreed to be accountable for all aspects of the study in ensuring that questions related to the accuracy or integrity of any part of the study are appropriately investigated and resolved. All persons designated as authors qualify for authorship, and all those who qualify for authorship are listed.

Conflicts of Interest: The authors declare no conflict of interest.

References

1. Panda, S.; Sato, T.K.; Castrucci, A.M.; Rollag, M.D.; DeGrip, W.J.; Hogenesch, J.B.; Provencio, I.; Kay, S.A. Melanopsin (Opn4) requirement for normal light-induced circadian phase shifting. *Science* **2002**, *298*, 2213–2236. [CrossRef] [PubMed]
2. Provencio, I.; Rollag, M.D.; Castrucci, A.M. Photoreceptive net in the mammalian retina. This mesh of cells may explain how some blind mice can still tell day from night. *Nature* **2002**, *415*, 493. [CrossRef] [PubMed]
3. Reppert, S.M.; Weaver, D.R. Coordination of circadian timing in mammals. *Nature* **2002**, *418*, 935–941. [CrossRef] [PubMed]
4. Potter, G.D.; Skene, D.J.; Arendt, J.; Cade, J.E.; Grant, P.J.; Hardie, L.J. Circadian rhythm and sleep disruption: Causes, metabolic consequences, and countermeasures. *Endocr. Rev.* **2016**, *37*, 584–608. [CrossRef] [PubMed]
5. Roenneberg, T.; Merrow, M. The circadian clock and human health. *Curr. Biol.* **2016**, *26*, R432–R443. [CrossRef] [PubMed]
6. West, A.C.; Bechtold, D.A. The cost of circadian desynchrony: Evidence, insights and open questions. *Bioessays* **2015**, *37*, 777–788. [CrossRef] [PubMed]
7. Husse, J.; Eichele, G.; Oster, H. Synchronization of the mammalian circadian timing system: Light can control peripheral clocks independently of the SCN clock: Alternate routes of entrainment optimize the alignment of the body's circadian clock network with external time. *Bioessays* **2015**, *37*, 1119–1128. [CrossRef] [PubMed]
8. Takahashi, J.S. Transcriptional architecture of the mammalian circadian clock. *Nat. Rev. Genet.* **2017**, *18*, 164–179. [CrossRef] [PubMed]
9. Brown, S.A.; Azzi, A. Peripheral circadian oscillators in mammals. *Handb. Exp. Pharmacol.* **2013**, *217*, 45–66. [CrossRef]
10. Buhr, E.D.; Takahashi, J.S. Molecular components of the Mammalian circadian clock. *Handb. Exp. Pharmacol.* **2013**, *217*, 3–27. [CrossRef]
11. Dibner, C.; Schibler, U.; Albrecht, U. The mammalian circadian timing system: Organization and coordination of central and peripheral clocks. *Annu. Rev. Physiol.* **2010**, *72*, 517–549. [CrossRef] [PubMed]
12. Husse, J.; Leliavski, A.; Tsang, A.H.; Oster, H.; Eichele, G. The light-dark cycle controls peripheral rhythmicity in mice with a genetically ablated suprachiasmatic nucleus clock. *FASEB J.* **2014**, *28*, 4950–4960. [CrossRef] [PubMed]
13. Shostak, A. Circadian clock, cell division, and cancer: From molecules to organism. *Int. J. Mol. Sci.* **2017**, *18*, 873. [CrossRef] [PubMed]
14. Padmanabhan, K.; Billaud, M. Desynchronization of circadian clocks in cancer: A metabolic and epigenetic connection. *Front. Endocrinol.* **2017**, *8*, 136. [CrossRef] [PubMed]
15. Yang, S.L.; Ren, Q.G.; Wen, L.; Hu, J.L.; Wang, H.Y. Research progress on circadian clock genes in common abdominal malignant tumors. *Oncol. Lett.* **2017**, *14*, 5091–5098. [CrossRef] [PubMed]
16. De Assis, L.V.; Moraes, M.N.; da Silveira Cruz-Machado, S.; Castrucci, A.M. The effect of white light on normal and malignant murine melanocytes: A link between opsins, clock genes, and melanogenesis. *Biochim. Biophys. Acta* **2016**, *1863*, 1119–1133. [CrossRef] [PubMed]
17. Kettner, N.M.; Voicu, H.; Finegold, M.J.; Coarfa, C.; Sreekumar, A.; Putluri, N.; Katchy, C.A.; Lee, C.; Moore, D.D.; Fu, L. Circadian homeostasis of liver metabolism suppresses hepatocarcinogenesis. *Cancer Cell* **2016**, *30*, 909–924. [CrossRef] [PubMed]
18. Masri, S.; Kinouchi, K.; Sassone-Corsi, P. Circadian clocks, epigenetics, and cancer. *Curr. Opin. Oncol.* **2015**, *27*, 50–56. [CrossRef] [PubMed]
19. Fu, L.; Kettner, N.M. The circadian clock in cancer development and therapy. *Prog. Mol. Biol. Transl. Sci.* **2013**, *119*, 221–282. [CrossRef] [PubMed]
20. Bass, J.; Lazar, M.A. Circadian time signatures of fitness and disease. *Science* **2016**, *354*, 994–999. [CrossRef] [PubMed]
21. Johansson, A.S.; Owe-Larsson, B.; Hetta, J.; Lundkvist, G.B. Altered circadian clock gene expression in patients with schizophrenia. *Schizophr. Res.* **2016**, *174*, 17–23. [CrossRef] [PubMed]
22. Baron, K.G.; Reid, K.J. Circadian misalignment and health. *Int. Rev. Psychiatry* **2014**, *26*, 139–154. [CrossRef] [PubMed]
23. Rastrelli, M.; Tropea, S.; Rossi, C.R.; Alaibac, M. Melanoma: Epidemiology, risk factors, pathogenesis, diagnosis and classification. *In Vivo* **2014**, *28*, 1005–1011. [PubMed]

24. MacKie, R.M.; Hauschild, A.; Eggermont, A.M. Epidemiology of invasive cutaneous melanoma. *Ann. Oncol.* **2009**, *20* (Suppl. 6), vi1–vi7. [CrossRef] [PubMed]
25. Jemal, A.; Siegel, R.; Ward, E.; Hao, Y.; Xu, J.; Murray, T.; Thun, M.J. Cancer statistics, 2008. *CA Cancer J. Clin.* **2008**, *58*, 71–96. [CrossRef] [PubMed]
26. Duncan, L.M. The classification of cutaneous melanoma. *Hematol. Oncol. Clin. N. Am.* **2009**, *23*, 501–513. [CrossRef] [PubMed]
27. Song, X.; Zhao, Z.; Barber, B.; Farr, A.M.; Ivanov, B.; Novich, M. Overall survival in patients with metastatic melanoma. *Curr. Med. Res. Opin.* **2015**, *31*, 987–991. [CrossRef] [PubMed]
28. Hardeland, R. Chronobiology of melatonin beyond the feedback to the suprachiasmatic nucleus-Consequences to melatonin dysfunction. *Int. J. Mol. Sci.* **2013**, *14*, 5817–5841. [CrossRef] [PubMed]
29. Slominski, A.T.; Zmijewski, M.A.; Skobowiat, C.; Zbytek, B.; Slominski, R.M.; Steketee, J.D. Sensing the environment: Regulation of local and global homeostasis by the skin's neuroendocrine system. *Adv. Anat. Embryol. Cell Biol.* **2012**, *212*, 1–115. [CrossRef]
30. Slominski, A.T.; Kleszczynski, K.; Semak, I.; Janjetovic, Z.; Zmijewski, M.A.; Kim, T.K.; Slominski, R.M.; Reiter, R.J.; Fischer, T.W. Local melatoninergic system as the protector of skin integrity. *Int. J. Mol. Sci.* **2014**, *15*, 17705–17732. [CrossRef] [PubMed]
31. Shain, A.H.; Bastian, B.C. From melanocytes to melanomas. *Nat. Rev. Cancer* **2016**, *16*, 345–358. [CrossRef] [PubMed]
32. Redman, J.M.; Gibney, G.T.; Atkins, M.B. Advances in immunotherapy for melanoma. *BMC Med.* **2016**, *14*, 20. [CrossRef] [PubMed]
33. Long, G.V.; Stroyakovskiy, D.; Gogas, H.; Levchenko, E.; de Braud, F.; Larkin, J.; Garbe, C.; Jouary, T.; Hauschild, A.; Grob, J.J.; et al. Combined BRAF and MEK inhibition versus BRAF inhibition alone in melanoma. *N. Engl. J. Med.* **2014**, *371*, 1877–1888. [CrossRef] [PubMed]
34. Grimaldi, A.M.; Simeone, E.; Ascierto, P.A. The role of MEK inhibitors in the treatment of metastatic melanoma. *Curr. Opin. Oncol.* **2014**, *26*, 196–203. [CrossRef] [PubMed]
35. Chapman, P.B.; Hauschild, A.; Robert, C.; Haanen, J.B.; Ascierto, P.; Larkin, J.; Dummer, R.; Garbe, C.; Testori, A.; Maio, M.; et al. Improved survival with vemurafenib in melanoma with BRAF V600E mutation. *N. Engl. J. Med.* **2011**, *364*, 2507–2516. [CrossRef] [PubMed]
36. Poletini, M.O.; de Assis, L.V.; Moraes, M.N.; Castrucci, A.M. Estradiol differently affects melanin synthesis of malignant and normal melanocytes: A relationship with clock and clock-controlled genes. *Mol. Cell. Biochem.* **2016**, *421*, 29–39. [CrossRef] [PubMed]
37. De Assis, L.V.M.; Moraes, M.N.; Castrucci, A.M.L. Heat shock antagonizes UVA-induced responses in murine melanocytes and melanoma cells: An unexpected interaction. *Photochem. Photobiol. Sci.* **2017**, *16*, 633–648. [CrossRef] [PubMed]
38. Lengyel, Z.; Lovig, C.; Kommedal, S.; Keszthelyi, R.; Szekeres, G.; Battyani, Z.; Csernus, V.; Nagy, A.D. Altered expression patterns of clock gene mRNAs and clock proteins in human skin tumors. *Tumour Biol.* **2013**, *34*, 811–819. [CrossRef] [PubMed]
39. Kiessling, S.; Beaulieu-Laroche, L.; Blum, I.D.; Landgraf, D.; Welsh, D.K.; Storch, K.F.; Labrecque, N.; Cermakian, N. Enhancing circadian clock function in cancer cells inhibits tumor growth. *BMC Biol.* **2017**, *15*, 13. [CrossRef] [PubMed]
40. Spill, F.; Reynolds, D.S.; Kamm, R.D.; Zaman, M.H. Impact of the physical microenvironment on tumor progression and metastasis. *Curr. Opin. Biotechnol.* **2016**, *40*, 41–48. [CrossRef] [PubMed]
41. Balkwill, F.R.; Capasso, M.; Hagemann, T. The tumor microenvironment at a glance. *J. Cell Sci.* **2012**, *125*, 5591–5596. [CrossRef] [PubMed]
42. Wu, T.; Dai, Y. Tumor microenvironment and therapeutic response. *Cancer Lett.* **2017**, *387*, 61–68. [CrossRef] [PubMed]
43. Sun, Y. Tumor microenvironment and cancer therapy resistance. *Cancer Lett.* **2016**, *380*, 205–215. [CrossRef] [PubMed]
44. Fang, H.; Declerck, Y.A. Targeting the tumor microenvironment: From understanding pathways to effective clinical trials. *Cancer Res.* **2013**, *73*, 4965–4977. [CrossRef] [PubMed]

45. Alves, M.J.; Figueredo, R.G.; Azevedo, F.F.; Cavallaro, D.A.; Neto, N.I.; Lima, J.D.; Matos-Neto, E.; Radloff, K.; Riccardi, D.M.; Camargo, R.G.; et al. Adipose tissue fibrosis in human cancer cachexia: The role of TGFbeta pathway. *BMC Cancer* **2017**, *17*, 190. [CrossRef] [PubMed]
46. Silverio, R.; Lira, F.S.; Oyama, L.M.; Oller do Nascimento, C.M.; Otoch, J.P.; Alcantara, P.S.M.; Batista, M.L., Jr.; Seelaender, M. Lipases and lipid droplet-associated protein expression in subcutaneous white adipose tissue of cachectic patients with cancer. *Lipids Health Dis.* **2017**, *16*, 159. [CrossRef] [PubMed]
47. Al-Zoughbi, W.; Huang, J.; Paramasivan, G.S.; Till, H.; Pichler, M.; Guertl-Lackner, B.; Hoefler, G. Tumor macroenvironment and metabolism. *Semin. Oncol.* **2014**, *41*, 281–295. [CrossRef] [PubMed]
48. Egeblad, M.; Nakasone, E.S.; Werb, Z. Tumors as organs: Complex tissues that interface with the entire organism. *Dev. Cell* **2010**, *18*, 884–901. [CrossRef] [PubMed]
49. Masri, S.; Papagiannakopoulos, T.; Kinouchi, K.; Liu, Y.; Cervantes, M.; Baldi, P.; Jacks, T.; Sassone-Corsi, P. Lung adenocarcinoma distally rewires hepatic circadian homeostasis. *Cell* **2016**, *165*, 896–909. [CrossRef] [PubMed]
50. Hojo, H.; Enya, S.; Arai, M.; Suzuki, Y.; Nojiri, T.; Kangawa, K.; Koyama, S.; Kawaoka, S. Remote reprogramming of hepatic circadian transcriptome by breast cancer. *Oncotarget* **2017**, *8*, 34128–34140. [CrossRef] [PubMed]
51. Aran, D.; Camarda, R.; Odegaard, J.; Paik, H.; Oskotsky, B.; Krings, G.; Goga, A.; Sirota, M.; Butte, A.J. Comprehensive analysis of normal adjacent to tumor transcriptomes. *Nat. Commun.* **2017**, *8*, 1077. [CrossRef] [PubMed]
52. Slominski, A.T.; Hardeland, R.; Reiter, R.J. When the circadian clock meets the melanin pigmentarys system. *J. Investig. Dermatol.* **2015**, *135*, 943–945. [CrossRef] [PubMed]
53. Hardman, J.A.; Tobin, D.J.; Haslam, I.S.; Farjo, N.; Farjo, B.; Al-Nuaimi, Y.; Grimaldi, B.; Paus, R. The peripheral clock regulates human pigmentation. *J. Investig. Dermatol.* **2015**, *135*, 1053–1064. [CrossRef] [PubMed]
54. McLafferty, E.; Hendry, C.; Alistair, F. The integumentary system: Anatomy, physiology and function of skin. *Nurs. Stand.* **2012**, *27*, 35–42. [CrossRef] [PubMed]
55. Brozyna, A.A.; Jozwicki, W.; Roszkowski, K.; Filipiak, J.; Slominski, A.T. Melanin content in melanoma metastases affects the outcome of radiotherapy. *Oncotarget* **2016**, *7*, 17844–17853. [CrossRef] [PubMed]
56. Brozyna, A.A.; VanMiddlesworth, L.; Slominski, A.T. Inhibition of melanogenesis as a radiation sensitizer for melanoma therapy. *Int. J. Cancer* **2008**, *123*, 1448–1456. [CrossRef] [PubMed]
57. Freudlsperger, C.; Schumacher, U.; Reinert, S.; Hoffmann, J. The critical role of PPARgamma in human malignant melanoma. *PPAR Res.* **2008**, *2008*, 503797. [CrossRef] [PubMed]
58. Lee, J.S.; Choi, Y.M.; Kang, H.Y. PPAR-gamma agonist, ciglitazone, increases pigmentation and migration of human melanocytes. *Exp. Dermatol.* **2007**, *16*, 118–123. [CrossRef] [PubMed]
59. Moraes, M.N.; de Assis, L.V.M.; Magalhaes-Marques, K.K.; Poletini, M.O.; de Lima, L.; Castrucci, A.M.L. Melanopsin, a canonical light receptor, mediates thermal activation of clock genes. *Sci. Rep.* **2017**, *7*, 13977. [CrossRef] [PubMed]
60. Gaddameedhi, S.; Selby, C.P.; Kaufmann, W.K.; Smart, R.C.; Sancar, A. Control of skin cancer by the circadian rhythm. *Proc. Natl. Acad. Sci. USA* **2011**, *108*, 18790–18795. [CrossRef] [PubMed]
61. Oishi, K.; Amagai, N.; Shirai, H.; Kadota, K.; Ohkura, N.; Ishida, N. Genome-wide expression analysis reveals 100 adrenal gland-dependent circadian genes in the mouse liver. *DNA Res.* **2005**, *12*, 191–202. [CrossRef] [PubMed]
62. Hanahan, D.; Weinberg, R.A. Hallmarks of cancer: The next generation. *Cell* **2011**, *144*, 646–674. [CrossRef] [PubMed]
63. De Assis, L.V.; Moraes, M.N.; Magalhaes-Marques, K.K.; Castrucci, A.M. Melanopsin and rhodopsin mediate UVA-induced immediate pigment darkening: Unrevealing the photosensitive system of the skin. *Eur. J. Cell Biol.* **2018**, in press. [CrossRef] [PubMed]
64. Regazzetti, C.; Sormani, L.; Debayle, D.; Bernerd, F.; Tulic, M.K.; De Donatis, G.M.; Chignon-Sicard, B.; Rocchi, S.; Passeron, T. Melanocytes sense blue light and regulate pigmentation through opsin-3. *J. Investig. Dermatol.* **2018**, *138*, 171–178. [CrossRef] [PubMed]
65. Buscone, S.; Mardaryev, A.N.; Raafs, B.; Bikker, J.W.; Sticht, C.; Gretz, N.; Farjo, N.; Uzunbajakava, N.E.; Botchkareva, N.V. A new path in defining light parameters for hair growth: Discovery and modulation of photoreceptors in human hair follicle. *Lasers Surg. Med.* **2017**, *49*, 705–718. [CrossRef] [PubMed]

66. Wicks, N.L.; Chan, J.W.; Najera, J.A.; Ciriello, J.M.; Oancea, E. UVA phototransduction drives early melanin synthesis in human melanocytes. *Curr. Biol.* **2011**, *21*, 1906–1911. [CrossRef] [PubMed]
67. Kim, H.J.; Son, E.D.; Jung, J.Y.; Choi, H.; Lee, T.R.; Shin, D.W. Violet light down-regulates the expression of specific differentiation markers through Rhodopsin in normal human epidermal keratinocytes. *PLoS ONE* **2013**, *8*, e73678. [CrossRef] [PubMed]
68. Hughes, S.; Hankins, M.W.; Foster, R.G.; Peirson, S.N. Melanopsin phototransduction: Slowly emerging from the dark. *Prog. Brain Res.* **2012**, *199*, 19–40. [CrossRef] [PubMed]
69. Jiao, J.; Hong, S.; Zhang, J.; Ma, L.; Sun, Y.; Zhang, D.; Shen, B.; Zhu, C. Opsin3 sensitizes hepatocellular carcinoma cells to 5-fluorouracil treatment by regulating the apoptotic pathway. *Cancer Lett.* **2012**, *320*, 96–103. [CrossRef] [PubMed]
70. Yoshimoto, T.; Morine, Y.; Takasu, C.; Feng, R.; Ikemoto, T.; Yoshikawa, K.; Iwahashi, S.; Saito, Y.; Kashihara, H.; Akutagawa, M.; et al. Blue light-emitting diodes induce autophagy in colon cancer cells by Opsin 3. *Ann. Gastroenterol. Surg.* **2018**. [CrossRef]
71. Dakup, P.P.; Porter, K.I.; Little, A.A.; Gajula, R.P.; Zhang, H.; Skornyakov, E.; Kemp, M.G.; van Dongen, H.P.A.; Gaddameedhi, S. The circadian clock regulates cisplatin-induced toxicity and tumor regression in melanoma mouse and human models. *Oncotarget* **2018**, 1–15. [CrossRef] [PubMed]
72. Brozyna, A.A.; Jozwicki, W.; Carlson, J.A.; Slominski, A.T. Melanogenesis affects overall and disease-free survival in patients with stage III and IV melanoma. *Hum. Pathol.* **2013**, *44*, 2071–2074. [CrossRef] [PubMed]
73. Consortium, G.T. Human genomics. The Genotype-Tissue Expression (GTEx) pilot analysis: Multitissue gene regulation in humans. *Science* **2015**, *348*, 648–660. [CrossRef] [PubMed]
74. Akbani, R.; Akdemir, K.C.; Aksoy, B.A.; Albert, M.; Ally, A.; Amin, S.B.; Arachchi, H.; Arora, A.; Auman, J.T.; Ayala, B.; et al. Genomic classification of cutaneous melanoma. *Cell* **2015**, *161*, 1681–1696. [CrossRef] [PubMed]
75. Bland, C.L.; Byrne-Hoffman, C.N.; Fernandez, A.; Rellick, S.L.; Deng, W.; Klinke, D.J. Exosomes derived from B16F0 melanoma cells alter the transcriptome of cytotoxic T cells that impacts mitochondrial respiration. *FEBS J.* **2018**. [CrossRef] [PubMed]
76. Damsky, W.E.; Rosenbaum, L.E.; Bosenberg, M. Decoding melanoma metastasis. *Cancers* **2010**, *3*, 126–163. [CrossRef] [PubMed]
77. Yang, G.; Wright, C.J.; Hinson, M.D.; Fernando, A.P.; Sengupta, S.; Biswas, C.; La, P.; Dennery, P.A. Oxidative stress and inflammation modulate Rev-erbalpha signaling in the neonatal lung and affect circadian rhythmicity. *Antioxid. Redox Signal.* **2014**, *21*, 17–32. [CrossRef] [PubMed]
78. Yamazaki, S.; Numano, R.; Abe, M.; Hida, A.; Takahashi, R.; Ueda, M.; Block, G.D.; Sakaki, Y.; Menaker, M.; Tei, H. Resetting central and peripheral circadian oscillators in transgenic rats. *Science* **2000**, *288*, 682–685. [CrossRef] [PubMed]
79. Oishi, K.; Sakamoto, K.; Okada, T.; Nagase, T.; Ishida, N. Humoral signals mediate the circadian expression of rat period homologue (rPer2) mRNA in peripheral tissues. *Neurosci. Lett.* **1998**, *256*, 117–119. [CrossRef]
80. Oishi, K.; Sakamoto, K.; Okada, T.; Nagase, T.; Ishida, N. Antiphase circadian expression between BMAL1 and period homologue mRNA in the suprachiasmatic nucleus and peripheral tissues of rats. *Biochem. Biophys. Res. Commun.* **1998**, *253*, 199–203. [CrossRef] [PubMed]
81. Sundar, I.K.; Sellix, M.T.; Rahman, I. Redox regulation of circadian molecular clock in chronic airway diseases. *Free Radic. Biol. Med.* **2017**. [CrossRef] [PubMed]
82. Buchanan, G.F. Timing, sleep, and respiration in health and disease. *Prog. Mol. Biol. Transl. Sci.* **2013**, *119*, 191–219. [CrossRef] [PubMed]
83. Pekovic-Vaughan, V.; Gibbs, J.; Yoshitane, H.; Yang, N.; Pathiranage, D.; Guo, B.; Sagami, A.; Taguchi, K.; Bechtold, D.; Loudon, A.; et al. The circadian clock regulates rhythmic activation of the NRF2/glutathione-mediated antioxidant defense pathway to modulate pulmonary fibrosis. *Genes Dev.* **2014**, *28*, 548–560. [CrossRef] [PubMed]
84. Papagiannakopoulos, T.; Bauer, M.R.; Davidson, S.M.; Heimann, M.; Subbaraj, L.; Bhutkar, A.; Bartlebaugh, J.; Vander Heiden, M.G.; Jacks, T. Circadian rhythm disruption promotes lung tumorigenesis. *Cell Metab.* **2016**, *24*, 324–331. [CrossRef] [PubMed]
85. Panda, S.; Antoch, M.P.; Miller, B.H.; Su, A.I.; Schook, A.B.; Straume, M.; Schultz, P.G.; Kay, S.A.; Takahashi, J.S.; Hogenesch, J.B. Coordinated transcription of key pathways in the mouse by the circadian clock. *Cell* **2002**, *109*, 307–320. [CrossRef]

86. Hussain, M.M.; Pan, X. Clock genes, intestinal transport and plasma lipid homeostasis. *Trends Endocrinol. Metab.* **2009**, *20*, 177–185. [CrossRef] [PubMed]
87. Bugge, A.; Feng, D.; Everett, L.J.; Briggs, E.R.; Mullican, S.E.; Wang, F.; Jager, J.; Lazar, M.A. Rev-erbalpha and Rev-erbbeta coordinately protect the circadian clock and normal metabolic function. *Genes Dev.* **2012**, *26*, 657–667. [CrossRef] [PubMed]
88. Shimba, S.; Ogawa, T.; Hitosugi, S.; Ichihashi, Y.; Nakadaira, Y.; Kobayashi, M.; Tezuka, M.; Kosuge, Y.; Ishige, K.; Ito, Y.; et al. Deficient of a clock gene, brain and muscle Arnt-like protein-1 (BMAL1), induces dyslipidemia and ectopic fat formation. *PLoS ONE* **2011**, *6*, e25231. [CrossRef] [PubMed]
89. Grimaldi, B.; Bellet, M.M.; Katada, S.; Astarita, G.; Hirayama, J.; Amin, R.H.; Granneman, J.G.; Piomelli, D.; Leff, T.; Sassone-Corsi, P. PER2 controls lipid metabolism by direct regulation of PPARgamma. *Cell Metab.* **2010**, *12*, 509–520. [CrossRef] [PubMed]
90. Turek, F.W.; Joshu, C.; Kohsaka, A.; Lin, E.; Ivanova, G.; McDearmon, E.; Laposky, A.; Losee-Olson, S.; Easton, A.; Jensen, D.R.; et al. Obesity and metabolic syndrome in circadian Clock mutant mice. *Science* **2005**, *308*, 1043–1045. [CrossRef] [PubMed]
91. Ando, H.; Ushijima, K.; Shimba, S.; Fujimura, A. Daily fasting blood glucose rhythm in male mice: A role of the circadian clock in the liver. *Endocrinology* **2016**, *157*, 463–469. [CrossRef] [PubMed]
92. McGinnis, G.R.; Young, M.E. Circadian regulation of metabolic homeostasis: Causes and consequences. *Nat. Sci. Sleep* **2016**, *8*, 163–180. [CrossRef] [PubMed]
93. Moraes, M.N.; de Assis, L.V.M.; Henriques, F.D.S.; Batista, M.L., Jr.; Guler, A.D.; Castrucci, A.M.L. Cold-sensing TRPM8 channel participates in circadian control of the brown adipose tissue. *Biochim. Biophys. Acta* **2017**, *1864*, 2415–2427. [CrossRef] [PubMed]
94. Cho, H.; Zhao, X.; Hatori, M.; Yu, R.T.; Barish, G.D.; Lam, M.T.; Chong, L.W.; DiTacchio, L.; Atkins, A.R.; Glass, C.K.; et al. Regulation of circadian behaviour and metabolism by REV-ERB-alpha and REV-ERB-beta. *Nature* **2012**, *485*, 123–127. [CrossRef] [PubMed]
95. Pawlak, M.; Lefebvre, P.; Staels, B. Molecular mechanism of PPARalpha action and its impact on lipid metabolism, inflammation and fibrosis in non-alcoholic fatty liver disease. *J. Hepatol.* **2015**, *62*, 720–733. [CrossRef] [PubMed]
96. Tsytkin-Kirschenzweig, S.; Cohen, M.; Nahmias, Y. Tracking GLUT2 translocation by live-cell imaging. In *Glucose Transport: Methods and Protocols*; Lindkvist-Petersson, K., Hansen, J.S., Eds.; Springer: New York, NY, USA, 2018; pp. 241–254.
97. Leturque, A.; Brot-Laroche, E.; Le Gall, M. GLUT2 mutations, translocation, and receptor function in diet sugar managing. *Am. J. Physiol. Endocrinol. Metab.* **2009**, *296*, E985–E992. [CrossRef] [PubMed]
98. Chiang, J.Y. Bile acids: Regulation of synthesis. *J. Lipid Res.* **2009**, *50*, 1955–1966. [CrossRef] [PubMed]
99. Miyake, J.H.; Wang, S.L.; Davis, R.A. Bile acid induction of cytokine expression by macrophages correlates with repression of hepatic cholesterol 7alpha-hydroxylase. *J. Biol. Chem.* **2000**, *275*, 21805–21808. [CrossRef] [PubMed]
100. Zhang, T.; Zhao, M.; Lu, D.; Wang, S.; Yu, F.; Guo, L.; Wen, S.; Wu, B. REV-ERBa regulates CYP7A1 through repression of liver receptor homolog-1. *Drug Metab. Dispos.* **2017**. [CrossRef]
101. Golombek, D.A.; Rosenstein, R.E. Physiology of circadian entrainment. *Physiol. Rev.* **2010**, *90*, 1063–1102. [CrossRef] [PubMed]
102. Liu, A.C.; Welsh, D.K.; Ko, C.H.; Tran, H.G.; Zhang, E.E.; Priest, A.A.; Buhr, E.D.; Singer, O.; Meeker, K.; Verma, I.M.; et al. Intercellular coupling confers robustness against mutations in the SCN circadian clock network. *Cell* **2007**, *129*, 605–616. [CrossRef] [PubMed]
103. Labrecque, N.; Cermakian, N. Circadian clocks in the immune system. *J. Biol. Rhythm.* **2015**, *30*, 277–290. [CrossRef] [PubMed]
104. Scheiermann, C.; Kunisaki, Y.; Frenette, P.S. Circadian control of the immune system. *Nat. Rev. Immunol.* **2013**, *13*, 190–198. [CrossRef] [PubMed]
105. Brown, S.A. Circadian metabolism: From mechanisms to metabolomics and medicine. *Trends Endocrinol. Metab.* **2016**, *27*, 415–426. [CrossRef] [PubMed]
106. Albrecht, U. The circadian clock, metabolism and obesity. *Obes. Rev.* **2017**, *18* (Suppl. 1), 25–33. [CrossRef] [PubMed]
107. Gerhart-Hines, Z.; Lazar, M.A. Circadian metabolism in the light of evolution. *Endocr. Rev.* **2015**, *36*, 289–304. [CrossRef] [PubMed]

108. Tsang, A.H.; Astiz, M.; Friedrichs, M.; Oster, H. Endocrine regulation of circadian physiology. *J. Endocrinol.* **2016**, *230*, R1–R11. [CrossRef] [PubMed]
109. Gamble, K.L.; Berry, R.; Frank, S.J.; Young, M.E. Circadian clock control of endocrine factors. *Nat. Rev. Endocrinol.* **2014**, *10*, 466–475. [CrossRef] [PubMed]
110. Dakup, P.; Gaddameedhi, S. Impact of the circadian clock on UV-induced DNA damage response and photocarcinogenesis. *Photochem. Photobiol.* **2017**, *93*, 296–303. [CrossRef] [PubMed]
111. Izumo, M.; Pejchal, M.; Schook, A.C.; Lange, R.P.; Walisser, J.A.; Sato, T.R.; Wang, X.; Bradfield, C.A.; Takahashi, J.S. Differential effects of light and feeding on circadian organization of peripheral clocks in a forebrain Bmal1 mutant. *Elife* **2014**, *3*. [CrossRef] [PubMed]
112. Husse, J.; Zhou, X.; Shostak, A.; Oster, H.; Eichele, G. Synaptotagmin10-Cre, a driver to disrupt clock genes in the SCN. *J. Biol. Rhythm.* **2011**, *26*, 379–389. [CrossRef] [PubMed]
113. Tamaru, T.; Takamatsu, K. Circadian modification network of a core clock driver BMAL1 to harmonize physiology from brain to peripheral tissues. *Neurochem. Int.* **2018**. [CrossRef] [PubMed]
114. Kiessling, S.; Cermakian, N. The tumor circadian clock: A new target for cancer therapy? *Futur. Oncol.* **2017**, *13*, 2607–2610. [CrossRef] [PubMed]
115. Eberting, C.L.; Shrayer, D.P.; Butmarc, J.; Falanga, V. Histologic progression of B16 F10 metastatic melanoma in C57BL/6 mice over a six week time period: Distant metastases before local growth. *J. Dermatol.* **2004**, *31*, 299–304. [CrossRef] [PubMed]
116. Welsh, D.K.; Takahashi, J.S.; Kay, S.A. Suprachiasmatic nucleus: Cell autonomy and network properties. *Annu. Rev. Physiol.* **2010**, *72*, 551–577. [CrossRef] [PubMed]
117. Oancea, E.; Vriens, J.; Brauchi, S.; Jun, J.; Splawski, I.; Clapham, D.E. TRPM1 forms ion channels associated with melanin content in melanocytes. *Sci. Signal.* **2009**, *2*, ra21. [CrossRef] [PubMed]
118. Livak, K.J.; Schmittgen, T.D. Analysis of relative gene expression data using real-time quantitative PCR and the 2(-Delta Delta C(T)) Method. *Methods* **2001**, *25*, 402–408. [CrossRef] [PubMed]
119. Moraes, M.N.; Mezzalira, N.; de Assis, L.V.; Menaker, M.; Guler, A.; Castrucci, A.M. TRPV1 participates in the activation of clock molecular machinery in the brown adipose tissue in response to light-dark cycle. *Biochim. Biophys. Acta* **2017**, *1864*, 324–335. [CrossRef] [PubMed]

Chapter 7: Expression of the Circadian Clock Gene BMAL1 Positively Correlates with Antitumor Immunity and Patient Survival in Metastatic Melanoma

The content provided in this chapter has been published in Frontiers in Oncology 2018 12; 8:185. DOI: 10.3389/fonc.2018.00185.

Authors' names: de Assis LVM[*], Kinker GS[*], Moraes MN, Markus RP, Fernandes PA, Castrucci AML.

[*] Joint first authors

frontiers in Oncology

ORIGINAL RESEARCH
published: 12 June 2018
doi: 10.3389/fonc.2018.00185

Expression of the Circadian Clock Gene *BMAL1* Positively Correlates With Antitumor Immunity and Patient Survival in Metastatic Melanoma

Leonardo Vinícius Monteiro de Assis[1]†, Gabriela Sarti Kinker[2]*†, Maria Nathália Moraes[1], Regina P. Markus[2], Pedro Augusto Fernandes[2] and Ana Maria de Lauro Castrucci[1,3]*

[1] Laboratory of Comparative Physiology of Pigmentation, Department of Physiology, Institute of Biosciences, University of São Paulo, São Paulo, Brazil, [2] Laboratory of Neuroimmunemodulation, Department of Physiology, Institute of Biosciences, University of São Paulo, São Paulo, Brazil, [3] Department of Biology, University of Virginia, Charlottesville, VA, United States

OPEN ACCESS

Edited by:
Svetlana Karakhanova, Universität Heidelberg, Germany

Reviewed by:
Derre Laurent, Centre Hospitalier Universitaire Vaudois (CHUV), Switzerland
Zsuzsanna Lengyel, University of Pécs, Hungary

****Correspondence:***
Leonardo Vinícius Monteiro de Assis
deassis.leonardo@usp.br;
Gabriela Sarti Kinker
gabriela.kinker@usp.br

†These authors have contributed equally to this work.

Specialty section:
This article was submitted to Cancer Immunity and Immunotherapy, a section of the journal Frontiers in Oncology

Received: *10 February 2018*
Accepted: *10 May 2018*
Published: *12 June 2018*

Citation:
de Assis LVM, Kinker GS, Moraes MN, Markus RP, Fernandes PA and Castrucci AML (2018) Expression of the Circadian Clock Gene BMAL1 Positively Correlates With Antitumor Immunity and Patient Survival in Metastatic Melanoma. Front. Oncol. 8:185. doi: 10.3389/fonc.2018.00185

Introduction: Melanoma is the most lethal type of skin cancer, with increasing incidence and mortality rates worldwide. Multiple studies have demonstrated a link between cancer development/progression and circadian disruption; however, the complex role of tumor-autonomous molecular clocks remains poorly understood. With that in mind, we investigated the pathophysiological relevance of clock genes expression in metastatic melanoma.

Methods: We analyzed gene expression, somatic mutation, and clinical data from 340 metastatic melanomas from The Cancer Genome Atlas, as well as gene expression data from 234 normal skin samples from genotype-tissue expression. Findings were confirmed in independent datasets.

Results: In melanomas, the expression of most clock genes was remarkably reduced and displayed a disrupted pattern of co-expression compared to the normal skins, indicating a dysfunctional circadian clock. Importantly, we demonstrate that the expression of the clock gene aryl hydrocarbon receptor nuclear translocator-like protein 1 (*BMAL1*) positively correlates with patient overall survival and with the expression of T-cell activity and exhaustion markers in the tumor bulk. Accordingly, high *BMAL1* expression in pretreatment samples was significantly associated with clinical benefit from immune checkpoint inhibitors. The robust intratumoral T-cell infiltration/activation observed in patients with high *BMAL1* expression was associated with a decreased expression of key DNA-repair enzymes, and with an increased mutational/neoantigen load.

Conclusion: Overall, our data corroborate previous reports regarding the impact of *BMAL1* expression on the cellular DNA-repair capacity and indicate that alterations in the tumor-autonomous molecular clock could influence the cellular composition of the surrounding microenvironment. Moreover, we revealed the potential of *BMAL1* as a clinically relevant prognostic factor and biomarker for T-cell-based immunotherapies.

Keywords: skin cancer, melanoma, circadian rhythms, clock genes, ARNTL/BMAL1 immunotherapy

SIGNIFICANCE

Here, we provide a first glimpse regarding the impact of a disrupted tumor-autonomous molecular clock on the cellular composition of the tumor microenvironment through the modulation of DNA-repair capacity. Within this line, our data revealed the potential of *BMAL1* as a clinically relevant biomarker for immunotherapy response and overall survival of patients with metastatic melanoma.

INTRODUCTION

Melanoma is the most lethal type of skin cancer, with increasing incidence and mortality rates worldwide (1, 2). It represents only 4% of skin cancer but accounts for approximately 80% of skin cancer-related death (3). Although complete surgical resection is often curative for melanomas detected at initial stages, patients with metastatic disease have an overall survival of approximately 5 months (4). Therapeutic options for patients with metastatic melanoma have dramatically changed in the past years, with the introduction of more effective agents such as proto-oncogene, serine/theronine kinase (BRAF), mitogen activated protein kinase kinase (MAPK), and immunotherapeutic antibodies directed to cytotoxic T-lymphocyte-associated antigen 4 (CTLA-4), programmed cell-death protein 1 (PD-1) and its ligand (PD-L1) (5–8). Melanoma etiology is multifactorial and includes risk factors such as ultraviolet radiation exposure, genetic susceptibility, high nevus density, reduced skin pigmentation, and immunosuppression (9, 10).

Proper temporal control of physiological functions is crucial for maintaining the homeostasis of multi-cellular organisms (11–13). In mammals, the molecular machinery of timekeeping and circadian rhythm generation is based on interconnected positive and negative transcriptional–translational feedback loops. The central hypothalamic clock (suprachiasmatic nuclei, SCN) and clocks located in peripheral tissues share the same molecular architecture, engaging core genes such as aryl hydrocarbon receptor nuclear translocator-like protein 1 (*BMAL1* also known as *ARNTL*), cryptochrome 1 and 2 (*CRY1/2*), circadian locomotor output cycles kaput (*CLOCK*), period 1, 2, and 3 (*PER1/2/3*), receptor subfamily 1, group D, member 1/2 (*NRD1/2* also known as *REV-ERB*α/β), and RAR-related orphan receptor A and B (*RORA/B* also known as NR1F1/2). In healthy conditions, CLOCK–BMAL1 heterodimers translocate to the nucleus and induce the gene expression of their own inhibitors, PER and CRY proteins. This core oscillatory pathway is augmented and stabilized by a secondary loop involving *NRD1/2* and *RORA/B*, nuclear receptors that modulate *BMAL1* expression. Importantly, CLOCK–BMAL1 heterodimers also regulate the expression of several clock-controlled genes, which are tissue- and cell type-specific (11–13).

Many epidemiologic studies have demonstrated that the disturbance of biological rhythms through shift work, increased light exposure at night, and irregular feeding regimens (14–16) is associated with increased risk of developing several types of cancers (17–19). In fact, alterations in the cellular circadian machinery have been shown to affect cancer-related processes such as cell proliferation (20, 21), DNA damage response (22, 23), and metabolism (24–27) in a tumor-specific manner. Accordingly, the aberrant expression of clock core genes such as *CRY1*, *PER1*, and *PER2* has been shown to impact tumor progression in colorectal, prostate, and breast cancers, respectively (28–30).

In melanoma, mRNA levels and nuclear immunopositivity for CLOCK, CRY1, and PER1 are reduced compared to adjacent non-tumorous skin and present a significant association with clinicopathological features such as Breslow thickness (31). Moreover, the expression of RORA is lower in melanomas than in nevi, and positively correlates with overall survival and disease-free survival (32). Interestingly, enhancing the circadian clock function of melanoma cells impairs cell cycle progression and inhibits tumor growth *in vivo* (21). In this sense, we have previously demonstrated that the expression of clock core genes in murine melanoma cells can be activated by different stimulus, such as white light exposure (33), UVA radiation (34), estradiol (35), and thermal energy (36). Recently, we have demonstrated that a non-metastatic model of melanoma leads to a systemic chronodisruption in tumor-adjacent skin, lungs, liver, and SCN, as in these tissues the rhythmic expression of *Bmal1* was lost in tumor-bearing mice (37). These data reinforce that the modulation of tumor-autonomous clock might represent a novel and promising therapeutic strategy.

To further characterize the pathophysiological relevance of the molecular clock in skin cancer, we investigated the clinical value of clock core genes expression in metastatic melanoma, using public high-throughput molecular data. Overall, we revealed the robust prognostic power of *BMAL1* expression and provided evidence into its underlying biological processes.

MATERIALS AND METHODS

Datasets of Melanoma and Normal Skin Samples

Gene expression, somatic mutation, and clinical data from 340 metastatic melanomas from The Cancer Genome Atlas (TCGA) and gene expression data from 234 Genotype-Tissue Expression (GTEx) normal skin (not sun exposed) samples were downloaded from the UCSC XENA Browser (http://xena.ucsc.edu) in January of 2017. TCGA and GTEx gene expression data were originally generated by TCGA (38) and GTEx consortia (39), respectively, using the Illumina HiSeq 2000 RNA sequencing platform, quantified using RSEM, upper quartile normalized and $\log_2(x+1)$ transformed. TCGA somatic mutation data were generated using the Illumina GAIIx DNA sequencing platform and somatic variants (SNPs and small indels) were identified using MuTect2. Neoantigen load information for TCGA metastatic melanoma samples was obtained from Rooney et al. (40). Briefly, for each metastatic melanoma patient, all novel amino acid 9–10mers resulting from missense mutations in expressed genes (median > 10 TPM) were identified. Mutant peptides with a HLA-binding affinity <500 nM, predicted by NetMHCpan (v2.4), were considered antigenic (41). Clinical information and gene

expression data of pretreatment biopsies from 49 patients who received anti-PD1 immunotherapy (nivolumab) were obtained from Riaz et al. (42). Expression data were generated using the Illumina HiSeq 2000 RNA sequencing platform, counted using Rsamtools v3.2, upper quartile normalized and $\log_2(x + 1)$ transformed. Treatment response for patients was defined by RECIST v1.1.

Co-Expression Network Analysis

Undirected weighted co-expression networks were constructed based on the pairwise Spearman's correlation coefficients between the expression of clock core genes *BMAL1*, *CRY1*, *CRY2*, *NRD1*, *PER1*, *PER2*, *PER3*, and *RORA*. Using the CoGA R package (43), we compared the structural properties of co-expression networks from normal skin and metastatic melanomas by testing the equality in their spectral distributions (44, 45). The spectrum of a graph, defined as the set of eigenvalues of its adjacency matrix, describes several structural features and represents a comprehensive characterization of networks (44, 46). *P*-values were calculated based on 1,000 phenotype permutations and networks were visualized using the gplots R package.

Gene Set Enrichment Analysis (GSEA)

Genes in the TCGA expression dataset were ranked according to the Spearman's correlation coefficient between their expression and the expression of *BMAL1*. GSEA was performed using GSEA v3.0 and Reactome pathways (47, 48). Enrichment scores (ES) were calculated based on a weighted Kolmogorov–Smirnov-like statistic and normalized (NES) to account for the size of each gene set. *P*-values corresponding to each NES were calculated based on 1,000 phenotype permutations and corrected for multiple comparisons using the false discovery rate (FDR) procedure. Adjusted *P*-values < 0.05 were considered statistically significant.

Single Sample Gene Set Enrichment Analysis (ssGSEA)

Single sample gene set enrichment analysis, an extension of GSEA, was used to estimate the degree of enrichment of gene sets in individual samples within the TCGA gene expression dataset (49). For each sample, gene expression values were rank-normalized, and ESs were calculated based on the difference between weighted Empirical Cumulative Distribution Functions of genes inside and outside the gene sets. We performed ssGSEA using the GSVA R package (50) and DNA repair-related KEGG pathways (51), namely: base excision repair (hsa03410), nucleotide excision repair (hsa03420), mismatch repair (hsa03430), homologous recombination (hsa03440), and non-homologous end joining (hsa0345).

Statistical Analysis

We used the two-sided Wilcoxon–Mann–Whitney test to perform two-group comparisons, the Spearman's correlation test to assess ordinal associations, and the Chi-square test to analyze the relationship between two categorical variables. The impact of clock core genes expression on patient overall survival was evaluated using univariate Cox regressions. The prognostic power of *BMAL1* expression was further investigated using Kaplan–Meier curves, combined to the log-rank test, and multivariate Cox regressions. Hazard Ratios, including 95% confidence intervals, were calculated. Statistical analyses were performed with GraphPad Prism 6 and R (www.r-project.org). *P*-values < 0.05 were considered statistically significant. Where indicated, *P*-values were adjusted for multiple comparisons using the FDR procedure.

RESULTS

Clinical Relevance of Clock Core Genes Expression in Metastatic Melanomas

We first analyzed the expression of clock core genes in normal skin and in metastatic melanomas. Compared to normal skin, metastatic melanomas demonstrated a remarkably decreased expression of *BMAL1*, *CRY1*, *CRY2*, *NRD1*, *PER1*, *PER2*, *PER3*, and *RORA* and an increased expression of *CLOCK* (**Figure 1A**). In normal skin, we have found a classic pattern of clock gene expression: *PER*s and CRYs are concomitantly expressed (in phase) and are in antiphase with *BMAL1* and *CLOCK* expression, as expected; on the other hand, in metastatic melanomas such correlations are severely attenuated (**Figure 1B**), which further corroborates a dysfunctional circadian clock within the tumor. In metastatic melanomas, male presented increased percentage of tumor showing high expression of *NRD1*, *PER2,* and *PER3* ($P = 0.015$, $P = 0.028$, and $P < 0.001$, respectively; **Table 1**; Table S1 in Supplementary Material). Patients with high *PER3* expression were also significantly older and more frequently diagnosed with stage I–II tumors ($P = 0.002$ and $P = 0.037$, respectively; **Table 1**; Table S1 in Supplementary Material).

Next, using univariate Cox regressions we evaluated the clinical relevance of clock core genes in metastatic melanoma. Among all nine genes analyzed, only *BMAL1* showed a significant prognostic value: high *BMAL1* expression was associated with longer overall survival (HR = 0.678, $P = 0.002$; **Figures 1C,D**). Importantly, multivariate Cox regression adjusting for age, gender, tumor pathologic stage, ulceration status, mitotic count, and Breslow thickness revealed *BMAL1* expression as an independent prognostic factor (**Table 2**). Additionally, the prognostic value of *BMAL1* expression in metastatic melanomas was confirmed in two other independent datasets (GSE6590 and GSE54467; Figures S1A,B and Table S2 in Supplementary Material).

BMAL1 Expression and the Overall Biological Profile of Metastatic Melanoma

To investigate the biological mechanisms that likely underlie the impact of *BMAL1* expression on patient survival, we performed GSEA using genes ranked according to their Spearman's correlation with *BMAL1* expression. Significantly enriched pathways presented positive NES and were mainly involved in the activation of the immune system (**Figure 2A**). In fact, in metastatic

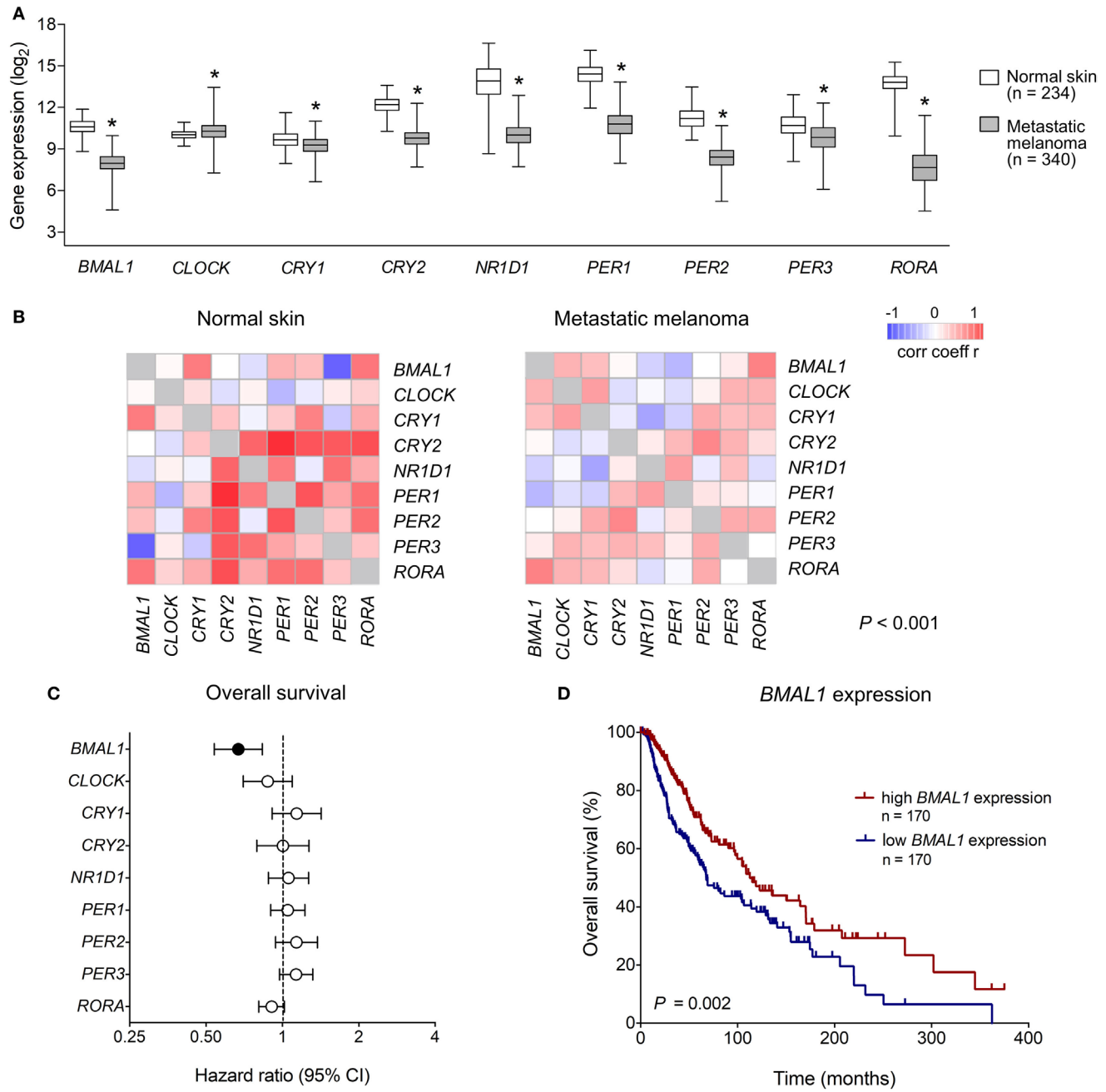

FIGURE 1 | Clinical relevance of clock genes expression in metastatic melanomas. **(A)** RNAseq analysis of clock genes expression in genotype-tissue expression (GTEx) normal skins (n = 234) and The Cancer Genome Atlas (TCGA) metastatic melanoma (n = 340). Expression values were estimated using RSEM and $\log_2(x + 1)$ transformed. The boxes extend from the 25th to the 75th percentile, the central bold line shows the median, and whiskers are drawn from minimum to maximum values. Comparisons were performed using the two-sided Wilcoxon–Mann–Whitney test. *Significantly different from normal skin ($P < 0.05$). **(B)** Co-expression matrix showing pairwise Spearman's correlation coefficients of clock core genes in GTEx normal skins (n = 234) and TCGA metastatic melanomas (n = 340). Networks were compared using the CoGA software. **(C)** Univariate Cox analysis of overall survival according to the expression of clock core genes in TCGA metastatic melanomas. Hazard Ratios including 95% confidence intervals are shown. Genes with a significant prognostic value ($P < 0.05$) are marked in black. **(D)** Kaplan–Meier survival curve according to the expression of aryl hydrocarbon receptor nuclear translocator-like protein 1 (*BMAL1*) in TCGA metastatic melanomas. The median expression of *BMAL1* was used as the cutoff to dichotomize the population. Comparisons were performed using the log-rank test.

melanomas, *BMAL1* expression exhibited a strong positive correlation with the expression of dendritic cell markers, T-cell markers *CD4* and *CD8A*, and T-cell activation/differentiation markers (**Figure 2B**). This robust intratumoral activation of leukocytes was accompanied by the expression of T-cells exhaustion markers (**Figure 2B**), such as *CTLA4*, *PD1*, and *PDL1*,

TABLE 1 | Clinicopathological features according to the expression of clock genes in The Cancer Genome Atlas metastatic melanomas.

	P-values*								
Variables	***BMAL1***	***CRY1***	***CRY2***	***CLOCK***	***NR1D1***	***PER1***	***PER2***	***PER3***	***RORA***
Age	0.59	0.592	0.998	0.151	0.057	0.19	0.754	**0.002**	0.286
Gender	0.659	0.271	0.269	0.269	**0.015**	0.06	**0.028**	**<0.001**	0.269
Pathologic stage	0.817	0.643	0.644	0.083	0.247	0.418	0.132	**0.037**	0.417
Ulceration status	1	0.404	0.094	0.889	1	0.78	0.267	0.889	1
Mitotic count	0.769	0.175	0.07	0.801	0.465	0.256	0.276	0.613	0.963
Breslow thickness	0.731	0.545	0.65	0.847	0.179	0.816	0.823	0.961	0.838

P-values in bold are statistically significant.

**Two-sided Wilcoxon–Mann–Whitney (continuous variables) or Chi-square exact test (categorical variable) comparing tumors with high vs. low expression.*

corroborating the fact that T-cell were chronically exposed to antigens (52, 53). Accordingly, patients with high *BMAL1* expression in pretreatment biopsies demonstrated improved response to anti-PD1 immunotherapy in comparison to patients expressing low *BMAL1* levels (**Figure 2C**).

The correlation between *BMAL1* expression and antitumor immune response was also confirmed in two additional independent datasets (GSE6590 and GSE54467; Figures S1C,D in Supplementary Material). Importantly, the expression of *BMAL1* was a prognostic factor independent of the percentage of leukocyte, monocyte, and neutrophil infiltration in TCGA melanomas (**Table 3**).

TABLE 2 | Multivariate Cox regression analysis of survival in The Cancer Genome Atlas metastatic melanomas.

	Overall survival	
Variables	**HR (95%CI)**	***P*-value**
Age	1.024 (1.007–1.041)	**0.006**
Gender		
Male vs. female	1.158 (0.655–2.051)	0.612
Pathologic stage		
III-IV vs. I–II	2.405 (1.427–4.053)	**<0.001**
Ulceration status		
Present vs. absent	0.994 (0.556–1.769)	0.985
Mitotic count	1.015 (0.986–1.045)	0.301
Breslow thickness	1.080 (1.004–1.161)	**0.038**
BMAL1 expression	0.525 (0.369–0.746)	**<0.001**

P-values in bold are statistically significant.

HR, hazard ratio; CI, confidence interval.

BMAL1 Expression and the Mutational Load in Metastatic Melanomas

Tumor somatic mutations can generate major histocompatibility complex Class I-associated neoantigens expression that plays a central role in inducing T-cell meditated antitumor cytolytic activity (54, 55). Interestingly, in metastatic melanomas, *BMAL1* expression positively correlated with the number of total somatic mutations and predicted neoantigens (**Figure 3A**). With that in mind, we investigated whether the expression of *BMAL1* was associated with the activation of different DNA-repair pathways. Using ssGSEA, we demonstrated that base excision repair is likely impaired in tumors expressing high *BMAL1* (**Figure 3B**). No significant differences were observed regarding the nucleotide excision repair, mismatch repair, homologous recombination, and non-homologous end joining DNA-repairing mechanisms. Importantly, the expression of base excision repair-related genes, such as *NTHL1*, *XRCC1*, and *SMUG1*, and the expression of general DNA repair-related genes, such as *POLD1*, *POLD2*, and *LIG1,* were downregulated in tumors expressing high *BMAL1* in all three datasets analyzed (**Figure 3C**; Figure S2 in Supplementary Material). High *BMAL1* expression was also associated with impaired DNA-repair capacity in human melanoma cell lines from the Cancer Cell Line Encyclopedia (Figure S3 in Supplementary Material).

DISCUSSION

Cancer onset, development, and progression have been linked to circadian disruption (17–19); however, the complex role of the tumor-autonomous molecular clock within these processes is yet poorly understood. Here, confirming previous reports in humans and in mice (32, 33, 35, 37), we showed that the expression of core components of the molecular clock machinery is severely repressed in melanomas. Moreover, we demonstrated that, for such tumors, high mRNA levels of *BMAL1* are associated with decreased gene expression of base excision repair enzymes and increased mutation load and predicted neoantigen presentation. The high incidence of antigenic peptides observed in metastatic melanomas with high *BMAL1* expression was accompanied by increased expression of cytotoxic T-cell activity markers in the tumor bulk and better prognosis. Even though our data do not provide a detailed mechanistic perspective, the present findings strongly support a role for *BMAL1* as a clinically relevant biomarker of DNA damage repair deficiency and intratumoral T-cell response. Thus, confirming such findings using common molecular techniques would be of great relevance for prognosis prediction and proposition of personalized therapeutic strategies.

Accumulating evidence implicates cell autonomous-circadian clocks in cancer development, as the disruption of peripheral systems of timekeeping seems to be a common event in malignant tissues (17, 18). As demonstrated here for metastatic melanomas, the expression of most clock core genes is downregulated in several types of cancers when compared to normal tissue (28, 32,

A

Reactome pathway	NES	Adjusted *P*-value
CYTOKINE SIGNALING IN IMMUNE SYSTEM	2.355	0.027
SIGNALING BY ILS	2.314	0.021
NUCLEOTIDE BINDING DOMAIN LEUCINE RICH REPEAT CONTAINING RECEPTOR NLR SIGNALING PATHWAYS	2.275	0.023
INNATE IMMUNE SYSTEM	2.256	0.024
NOD1 2 SIGNALING PATHWAY	2.212	0.035
IL1 SIGNALING	2.211	0.030
ADAPTIVE IMMUNE SYSTEM	2.210	0.025
TOLL RECEPTOR CASCADES	2.201	0.026
ACTIVATED TLR4 SIGNALLING	2.200	0.023
INTERFERON SIGNALING	2.194	0.023
MYD88 MAL CASCADE INITIATED ON PLASMA MEMBRANE	2.170	0.027
TCR SIGNALING	2.156	0.030
G ALPHA1213 SIGNALLING EVENTS	2.135	0.037
DOWNSTREAM TCR SIGNALING	2.135	0.034
REGULATION OF SIGNALING BY CBL	2.116	0.042
G ALPHA I SIGNALLING EVENTS	2.112	0.041
GASTRIN CREB SIGNALLING PATHWAY VIA PKC AND MAPK	2.105	0.041
TRAF6 MEDIATED INDUCTION OF NFKB AND MAP KINASES UPON TLR7 8 OR 9 ACTIVATION	2.093	0.045
INTERFERON GAMMA SIGNALING	2.080	0.049
IL 3 5 AND GM CSF SIGNALING	2.078	0.048
RIG I MDA5 MEDIATED INDUCTION OF IFN ALPHA BETA PATHWAYS	2.077	0.046
TRIF MEDIATED TLR3 SIGNALING	2.075	0.045

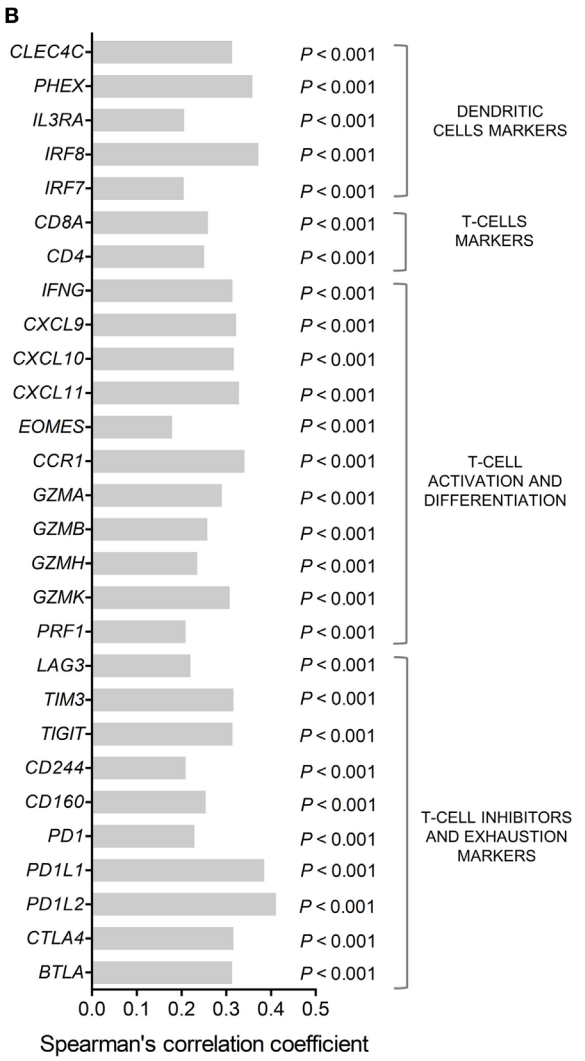

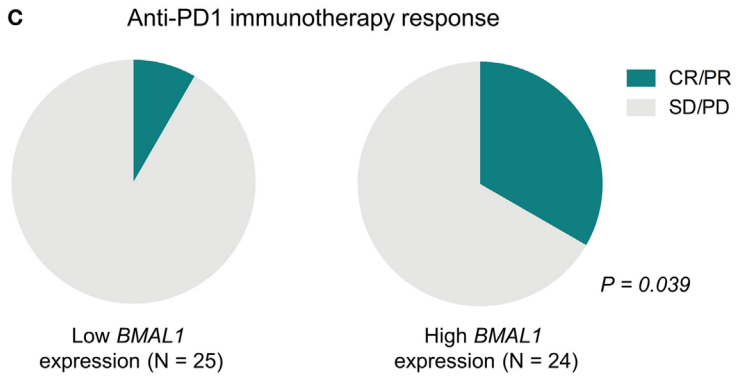

FIGURE 2 | Aryl hydrocarbon receptor nuclear translocator-like protein 1 (*BMAL1*) expression positively correlates with antitumor immunity in metastatic melanomas. **(A)** Gene Set Enrichment Analysis (GSEA) using genes ranked according to the Spearman's correlation coefficient between their expression and the expression of *BMAL1* in The Cancer Genome Atlas (TCGA) metastatic melanomas ($n = 340$). Normalized enrichment scores (NES) and *P*-values corrected by false discovery rate (FDR) were calculated using GSEA v3.0 and Reactome pathways. Only significantly enriched pathways (adjusted $P < 0.05$) are shown. **(B)** Spearman's correlation coefficient between the expression of *BMAL1* and immune cells markers in TCGA metastatic melanomas. *P*-values were corrected by FDR. **(C)** Association between *BMAL1* expression (pretreatment biopsies) and clinical benefit of melanoma patients from anti-PD1 immunotherapy (nivolumab). RNAseq data and treatment response information were obtained from Ref. (42). Comparisons were performed using the Chi-square test. CR, complete response; PR, partial response; SD, stable disease; PD, progressive disease.

TABLE 3 | Multivariate Cox regression analysis of overall survival in metastatic melanomas adjusted for the percentage of immune cell infiltration in The Cancer Genome Atlas metastatic melanomas.

	Overall survival	
Variables	**HR (95% CI)**	***P*-value**
% Lymphocyte infiltration	0.975 (0.932–1.019)	0.261
% Monocyte infiltration	1.001 (0.902–1.111)	0.974
% Neutrophil infiltration	0.956 (0.673–1.357)	0.901
BMAL1 expression	0.685 (0.550–0.854)	**<0.001**

P-values in bold are statistically significant.
HR, hazard ratio; CI, confidence interval.

56–61). Moreover, the overexpression of *PER1* and *PER2* has been shown to impair tumor proliferation and induce apoptosis in lung, prostate, and pancreatic cancer (29, 62, 63), reinforcing the idea that the molecular clock machinery may be considered as a new therapeutic target.

The protein encoded by *BMAL1* belongs to the family of the bHLH-PAS structural domain transcription factors and it is estimated to control the expression of more than 150 target genes, including the clock genes *CRY1*, *CRY2*, *NR1D1*, *PER1*, *PER2*, and *PER3* (64). *BMAL1* has also been revealed as a candidate gene for susceptibility to hypertension, diabetes, and obesity, and mutations in *BMAL1* have been linked to infertility and metabolic dysfunctions (65–70). Here, we demonstrated that, in metastatic melanomas, the expression of *BMAL1* is a robust positive prognostic factor of overall survival and has a negative association with the expression of key DNA-repair enzymes, such as *POLD1*, *POLD2*, and *LIG1*. Accordingly, in colorectal cancer, downregulation of *BMAL1* gene expression accelerates cell proliferation *in vitro*, promotes tumor growth in mice, and decreases DNA damage induced by cisplatin (71). Moreover, high *BMAL1* expression is associated with increased sensitivity of colorectal cancer cells to oxaliplatin *in vitro* and *in vivo*, and predicts favorable outcome for patients treated with oxaliplatin-based chemotherapy (72). *BMAL1* expression also positively correlates with patient survival in pancreatic ductal adenocarcinomas (61), causes growth inhibition in lymphoma/leukemia cells (58), negatively impacts DNA-repair capacity of mice fibroblast (73), but promotes proliferation in malignant pleura mesothelioma (74), suggesting that its role in tumorigenesis is complex and tissue-specific.

Although it has been shown that alterations in the tumor molecular clock impact some parameters of tumor progression (28–30, 62, 63), the influence of endogenous oscillatory systems on the cellular composition of the tumor microenvironment is largely unknown. In this sense, our data indicate that the prolonged survival of metastatic melanoma patients with high *BMAL1* bulk expression is associated with a robust intratumoral T-cell infiltration/activation, which can be partially explained by the increased neoantigen load that likely reflects the impaired DNA-repair capacity. Previous reports have also linked DNA-repair deficiency to increased mutational load and antitumor immune response in melanomas, lung, colorectal, and endometrial cancers (75–78). It is now clear that DNA repair and genomic instability have a pivotal role in the modulation of antitumor immune responses (79); thus, understanding their interplay with tumor-autonomous clocks may provide clinically relevant insights.

Immunotherapies that boost the ability of T lymphocytes to combat tumor cells have demonstrated therapeutic efficiency in a variety of solid tumors. Monoclonal antibodies against T-cell checkpoint proteins, such as CTLA-4, PD-1, and PD-L1, have now been approved for melanoma treatment and are associated with robust durable responses, but only in a subset of tumors (80–82). Thus, there is a need to identify biomarkers that will allow the selection of treatment-responsive patients, avoid unnecessary toxicity, and help personalize therapy regimens (83). Metastatic melanomas presenting high *BMAL1* expression have impaired DNA-repair capacity combined with increased mutation/neoantigen load, T-cell intratumoral infiltration, and T-cell expression of exhaustion markers, all of which have been shown to predict good clinical response to the treatment with immune checkpoint inhibitors (78, 84–87). In fact, we showed that high *BMAL1* expression in pretreatment melanoma samples is associated with clinical benefit from anti-PD1 immunotherapy. Considering that whole-genome and -transcriptome sequencing is expensive and time-consuming, profiling a smaller fraction of genes could serve as a useful tool to help translate those findings into routine clinical practices (88). Therefore, the present data indicate that *BMAL1* expression in melanoma patients must be considered as a relevant marker for immunotherapy efficacy. Nevertheless, larger clinical studies are necessary to validate the potential of *BMAL1* alone, or along with other biomarkers, in discriminating responders from non-responders in immunotherapy regiments.

CONCLUSION

The molecular characterization of melanomas using high-throughput approaches has the potential to generate insights into their biological heterogeneity, having important implications for prognosis and therapy. In this sense, our data highlight the relevance of further studies focusing on the biological and clinical relevance of the tumor-autonomous molecular clock machinery. Overall, we demonstrated that, in metastatic melanoma, a high bulk *BMAL1* expression seems to be associated with a "too tumorigenic" program and could be a marker for immunotherapy response.

ETHICS STATEMENT

All data presented in this manuscript are public and freely available. We did not perform any human or animal related experiments. All analyses and conclusions were drawn from the following public datasets: The Cancer Genome Atlas (TCGA), Genotype-Tissue Expression (GTEx), Gene Expression Omnibus, and datasets from Ref. (40, 42). In all mentioned

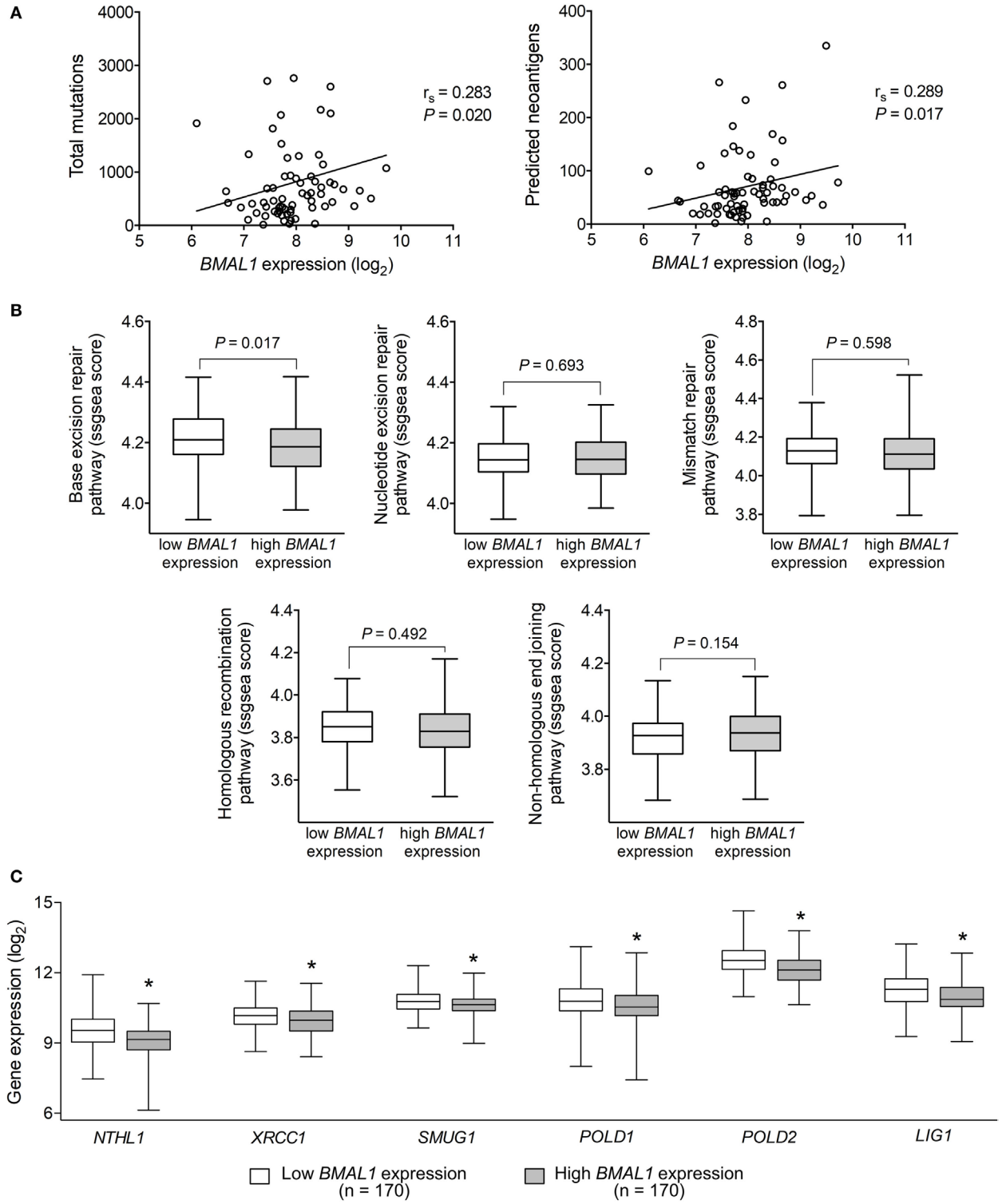

FIGURE 3 | Aryl hydrocarbon receptor nuclear translocator-like protein 1 (*BMAL1*) expression positively correlates with the mutational and neoantigen load in metastatic melanomas. **(A)** Spearman's correlation between the expression of *BMAL1* and the number of total mutations and predicted neoantigens in The Cancer Genome Atlas (TCGA) metastatic melanomas (n = 68). NetMHCpan-predicted neoantigens were obtained from Ref. (40). Gene expression of **(B)** DNA-repair programs and **(C)** selected base excision repair enzymes according to the expression of *BMAL1* in TCGA metastatic melanomas (n = 340). Pathway scores were calculated using single sample Gene Set Enrichment Analysis available in the GSVA R package. The median expression of *BMAL1* was used as the cutoff to dichotomize the population. The boxes extend from the 25th to the 75th percentile, the central bold line shows the median, and whiskers are drawn from minimum to maximum values. Comparisons were performed using the two-sided Wilcoxon–Mann–Whitney test. *Significantly different from the low *BMAL1* group.

papers, the authors stated that all procedures were carried out according ethical rules.

AUTHOR CONTRIBUTIONS

LA and GK designed the study, analyzed the data, and drafted the manuscript. All authors provided insightful discussion during data acquisition and aided in the writing process of the manuscript. All authors critically revised the manuscript. All authors have approved the definitive version of the manuscript and agreed to be accountable for all aspects of the study in ensuring that questions related to the accuracy or integrity of any part of the study are appropriately investigated and resolved. All persons designated as authors qualify for authorship, and all those who qualify for authorship are listed.

FUNDING

This work was partially supported by the Sao Paulo Research Foundation (FAPESP, grant 2012/50214-4) and by the National Council of Technological and Scientific Development (CNPq, grants 301293/2011-2 and 303070/2015-3). LA, GK, and MM are fellows of FAPESP (2013/24337-4; 2014/27287-0; and 2014/16412-9, respectively).

SUPPLEMENTARY MATERIAL

The Supplementary Material for this article can be found online at https://www.frontiersin.org/articles/10.3389/fonc.2018.00185/full#supplementary-material.

REFERENCES

1. Garbe C, Leiter U. Melanoma epidemiology and trends. *Clin Dermatol* (2009) 27:3–9. doi:10.1016/j.clindermatol.2008.09.001
2. Erdei E, Torres SM. A new understanding in the epidemiology of melanoma. *Expert Rev Anticancer Ther* (2010) 10:1811–23. doi:10.1586/era.10.170
3. Jemal A, Siegel R, Ward E, Hao Y, Xu J, Murray T, et al. Cancer statistics, 2008. *CA Cancer J Clin* (2008) 58:71–96. doi:10.3322/CA.2007.0010
4. Song X, Zhao Z, Barber B, Farr AM, Ivanov B, Novich M. Overall survival in patients with metastatic melanoma. *Curr Med Res Opin* (2015) 31:987–91. doi:10.1185/03007995.2015.1021904
5. Chapman PB, Hauschild A, Robert C, Haanen JB, Ascierto P, Larkin J, et al. Improved survival with vemurafenib in melanoma with BRAF V600E mutation. *N Engl J Med* (2011) 364:2507–16. doi:10.1056/NEJMoa1103782
6. Grimaldi AM, Simeone E, Ascierto PA. The role of MEK inhibitors in the treatment of metastatic melanoma. *Curr Opin Oncol* (2014) 26:196–203. doi:10.1097/CCO.0000000000000050
7. Long GV, Stroyakovskiy D, Gogas H, Levchenko E, De Braud F, Larkin J, et al. Combined BRAF and MEK inhibition versus BRAF inhibition alone in melanoma. *N Engl J Med* (2014) 371:1877–88. doi:10.1056/NEJMoa1406037
8. Redman JM, Gibney GT, Atkins MB. Advances in immunotherapy for melanoma. *BMC Med* (2016) 14:20. doi:10.1186/s12916-016-0571-0
9. Markovic SN, Erickson LA, Rao RD, Weenig RH, Pockaj BA, Bardia A, et al. Malignant melanoma in the 21st century, part 1: epidemiology, risk factors, screening, prevention, and diagnosis. *Mayo Clin Proc* (2007) 82:364–80. doi:10.1016/S0025-6196(11)61033-1
10. Vuong K, Armstrong BK, Weiderpass E, Lund E, Adami HO, Veierod MB, et al. Development and external validation of a melanoma risk prediction model based on self-assessed risk factors. *JAMA Dermatol* (2016) 152:889–96. doi:10.1001/jamadermatol.2016.0939
11. Brown SA, Azzi A. Peripheral circadian oscillators in mammals. *Handb Exp Pharmacol* (2013) 217:45–66. doi:10.1007/978-3-642-25950-0_3
12. Buhr ED, Takahashi JS. Molecular components of the mammalian circadian clock. *Handb Exp Pharmacol* (2013) 217:3–27. doi:10.1007/978-3-642-25950-0_1
13. Takahashi JS. Transcriptional architecture of the mammalian circadian clock. *Nat Rev Genet* (2017) 18:164–79. doi:10.1038/nrg.2016.150
14. Baron KG, Reid KJ. Circadian misalignment and health. *Int Rev Psychiatry* (2014) 26:139–54. doi:10.3109/09540261.2014.911149
15. West AC, Bechtold DA. The cost of circadian desynchrony: evidence, insights and open questions. *Bioessays* (2015) 37:777–88. doi:10.1002/bies.201400173
16. Potter GD, Skene DJ, Arendt J, Cade JE, Grant PJ, Hardie LJ. Circadian rhythm and sleep disruption: causes, metabolic consequences, and countermeasures. *Endocr Rev* (2016) 37:584–608. doi:10.1210/er.2016-1083
17. Savvidis C, Koutsilieris M. Circadian rhythm disruption in cancer biology. *Mol Med* (2012) 18:1249–60. doi:10.2119/molmed.2012.00077
18. Kelleher FC, Rao A, Maguire A. Circadian molecular clocks and cancer. *Cancer Lett* (2014) 342:9–18. doi:10.1016/j.canlet.2013.09.040
19. Masri S, Kinouchi K, Sassone-Corsi P. Circadian clocks, epigenetics, and cancer. *Curr Opin Oncol* (2015) 27:50–6. doi:10.1097/CCO.0000000000000153
20. Yang X, Wood PA, Ansell CM, Quiton DF, Oh EY, Du-Quiton J, et al. The circadian clock gene Per1 suppresses cancer cell proliferation and tumor growth at specific times of day. *Chronobiol Int* (2009) 26:1323–39. doi:10.3109/07420520903431301
21. Kiessling S, Beaulieu-Laroche L, Blum ID, Landgraf D, Welsh DK, Storch KF, et al. Enhancing circadian clock function in cancer cells inhibits tumor growth. *BMC Biol* (2017) 15:13. doi:10.1186/s12915-017-0349-7
22. Gaddameedhi S, Selby CP, Kaufmann WK, Smart RC, Sancar A. Control of skin cancer by the circadian rhythm. *Proc Natl Acad Sci U S A* (2011) 108:18790–5. doi:10.1073/pnas.1115249108
23. Gaddameedhi S, Selby CP, Kemp MG, Ye R, Sancar A. The circadian clock controls sunburn apoptosis and erythema in mouse skin. *J Invest Dermatol* (2015) 135:1119–27. doi:10.1038/jid.2014.508
24. Albrecht U. The circadian clock, metabolism and obesity. *Obes Rev* (2017) 18(Suppl 1):25–33. doi:10.1111/obr.12502
25. Krishnaiah SY, Wu G, Altman BJ, Growe J, Rhoades SD, Coldren F, et al. Clock regulation of metabolites reveals coupling between transcription and metabolism. *Cell Metab* (2017) 25(5):1206. doi:10.1016/j.cmet.2017.04.023
26. Moraes MN, De Assis LVM, Henriques FDS, Batista ML Jr., Guler AD, Castrucci AML. Cold-sensing TRPM8 channel participates in circadian control of the brown adipose tissue. *Biochim Biophys Acta* (2017) 1864:2415–27. doi:10.1016/j.bbamcr.2017.09.011
27. Moraes MN, Mezzalira N, De Assis LV, Menaker M, Guler A, Castrucci AM. TRPV1 participates in the activation of clock molecular machinery in the brown adipose tissue in response to light-dark cycle. *Biochim Biophys Acta* (2017) 1864:324–35. doi:10.1016/j.bbamcr.2016.11.010
28. Chen ST, Choo KB, Hou MF, Yeh KT, Kuo SJ, Chang JG. Deregulated expression of the PER1, PER2 and PER3 genes in breast cancers. *Carcinogenesis* (2005) 26:1241–6. doi:10.1093/carcin/bgi075
29. Cao Q, Gery S, Dashti A, Yin D, Zhou Y, Gu J, et al. A role for the clock gene per1 in prostate cancer. *Cancer Res* (2009) 69:7619–25. doi:10.1158/0008-5472.CAN-08-4199
30. Yu H, Meng X, Wu J, Pan C, Ying X, Zhou Y, et al. Cryptochrome 1 overexpression correlates with tumor progression and poor prognosis in patients with colorectal cancer. *PLoS One* (2013) 8:e61679. doi:10.1371/journal.pone.0061679
31. Lengyel Z, Lovig C, Kommedal S, Keszthelyi R, Szekeres G, Battyani Z, et al. Altered expression patterns of clock gene mRNAs and clock proteins in human skin tumors. *Tumour Biol* (2013) 34:811–9. doi:10.1007/s13277-012-0611-0
32. Brozyna AA, Jozwicki W, Skobowiat C, Jetten A, Slominski AT. RORalpha and RORgamma expression inversely correlates with human melanoma progression. *Oncotarget* (2016) 7(39):63261–82. doi:10.18632/oncotarget.11211
33. de Assis LV, Moraes MN, da Silveira Cruz-Machado S, Castrucci AM. The effect of white light on normal and malignant murine melanocytes: a link between opsins, clock genes, and melanogenesis. *Biochim Biophys Acta* (2016) 1863:1119–33. doi:10.1016/j.bbamcr.2016.03.001

34. de Assis LV, Moraes MN, Castrucci AM. Heat shock antagonizes UVA-induced responses in murine melanocytes and melanoma cells: an unexpected interaction. *Photochem Photobiol Sci* (2017) 16(5):633–48. doi:10.1039/c6pp00330c
35. Poletini MO, De Assis LV, Moraes MN, Castrucci AM. Estradiol differently affects melanin synthesis of malignant and normal melanocytes: a relationship with clock and clock-controlled genes. *Mol Cell Biochem* (2016) 421:29–39. doi:10.1007/s11010-016-2781-3
36. Moraes MN, De Assis LVM, Magalhaes-Marques KK, Poletini MO, De Lima L, Castrucci AML. Melanopsin, a canonical light receptor, mediates thermal activation of clock genes. *Sci Rep* (2017) 7:13977. doi:10.1038/s41598-017-13939-3
37. de Assis LVM, Moraes MN, Magalhães-Marques KK, Kinker GS, da Silveira Cruz-Machado S, Castrucci AM. Non-metastatic cutaneous melanoma induces chronodisruption in central and peripheral circadian clocks. *Int J Mol Sci* (2018) 19(4):E1065. doi:10.3390/ijms19041065
38. Cancer Genome Atlas Network. Genomic classification of cutaneous melanoma. *Cell* (2015) 161:1681–96. doi:10.1016/j.cell.2015.05.044
39. Consortium GT. Human genomics. The Genotype-Tissue Expression (GTEx) pilot analysis: multitissue gene regulation in humans. *Science* (2015) 348: 648–60. doi:10.1126/science.1262110
40. Rooney MS, Shukla SA, Wu CJ, Getz G, Hacohen N. Molecular and genetic properties of tumors associated with local immune cytolytic activity. *Cell* (2015) 160:48–61. doi:10.1016/j.cell.2014.12.033
41. Nielsen M, Lundegaard C, Blicher T, Lamberth K, Harndahl M, Justesen S, et al. NetMHCpan, a method for quantitative predictions of peptide binding to any HLA-A and -B locus protein of known sequence. *PLoS One* (2007) 2:e796. doi:10.1371/journal.pone.0000796
42. Riaz N, Havel JJ, Makarov V, Desrichard A, Urba WJ, Sims JS, et al. Tumor and microenvironment evolution during immunotherapy with nivolumab. *Cell* (2017) 171:934–49. doi:10.1016/j.cell.2017.09.028
43. Santos SDS, Galatro TFDA, Watanabe RA, Oba-Shinjo SM, Nagahashi Marie SK, Fujita A. CoGA: an R package to identify differentially co-expressed gene sets by analyzing the graph spectra. *PLoS One* (2015) 10:e0135831. doi:10.1371/journal.pone.0135831
44. Takahashi DY, Sato JR, Ferreira CE, Fujita A. Discriminating different classes of biological networks by analyzing the graphs spectra distribution. *PLoS One* (2012) 7:e49949. doi:10.1371/journal.pone.0049949
45. Kinker GS, Thomas AM, Carvalho VJ, Lima FP, Fujita A. Deletion and low expression of NFKBIA are associated with poor prognosis in lower-grade glioma patients. *Sci Rep* (2016) 6:24160. doi:10.1038/srep24160
46. Van Mieghem P. *Graph Spectra for Complex Networks*. Cambridge: Cambridge University Press (2010).
47. Subramanian A, Tamayo P, Mootha VK, Mukherjee S, Ebert BL, Gillette MA, et al. Gene set enrichment analysis: a knowledge-based approach for interpreting genome-wide expression profiles. *Proc Natl Acad Sci U S A* (2005) 102:15545–50. doi:10.1073/pnas.0506580102
48. Croft D, O'kelly G, Wu G, Haw R, Gillespie M, Matthews L, et al. Reactome: a database of reactions, pathways and biological processes. *Nucleic Acids Res* (2011) 39:D691–7. doi:10.1093/nar/gkq1018
49. Barbie DA, Tamayo P, Boehm JS, Kim SY, Moody SE, Dunn IF, et al. Systematic RNA interference reveals that oncogenic KRAS-driven cancers require TBK1. *Nature* (2009) 462:108–12. doi:10.1038/nature08460
50. Hänzelmann S, Castelo R, Guinney J. GSVA: gene set variation analysis for microarray and RNA-Seq data. *BMC Bioinformatics* (2013) 14:7. doi:10.1186/1471-2105-14-7
51. Kanehisa M, Goto S. KEGG: kyoto encyclopedia of genes and genomes. *Nucleic Acids Res* (2000) 28:27–30. doi:10.1093/nar/28.1.27
52. Wherry EJ, Kurachi M. Molecular and cellular insights into T cell exhaustion. *Nat Rev Immunol* (2015) 15:486–99. doi:10.1038/nri3862
53. Catakovic K, Klieser E, Neureiter D, Geisberger R. T cell exhaustion: from pathophysiological basics to tumor immunotherapy. *Cell Commun Signal* (2017) 15:1. doi:10.1186/s12964-016-0160-z
54. Gajewski TF, Schreiber H, Fu YX. Innate and adaptive immune cells in the tumor microenvironment. *Nat Immunol* (2013) 14:1014–22. doi:10.1038/ni.2703
55. Coulie PG, Van Den Eynde BJ, Van Der Bruggen P, Boon T. Tumour antigens recognized by T lymphocytes: at the core of cancer immunotherapy. *Nat Rev Cancer* (2014) 14:135–46. doi:10.1038/nrc3670
56. Yeh KT, Yang MY, Liu TC, Chen JC, Chan WL, Lin SF, et al. Abnormal expression of period 1 (PER1) in endometrial carcinoma. *J Pathol* (2005) 206:111–20. doi:10.1002/path.1756
57. Kuo SJ, Chen ST, Yeh KT, Hou MF, Chang YS, Hsu NC, et al. Disturbance of circadian gene expression in breast cancer. *Virchows Arch* (2009) 454:467–74. doi:10.1007/s00428-009-0761-7
58. Taniguchi H, Fernandez AF, Setien F, Ropero S, Ballestar E, Villanueva A, et al. Epigenetic inactivation of the circadian clock gene BMAL1 in hematologic malignancies. *Cancer Res* (2009) 69:8447–54. doi:10.1158/0008-5472.CAN-09-0551
59. Huisman SA, Ahmadi AR, Jn IJ, Verhoef C, Van Der Horst GT, De Bruin RW. Disruption of clock gene expression in human colorectal liver metastases. *Tumour Biol* (2016) 37(10):13973–81. doi:10.1007/s13277-016-5231-7
60. Jiang W, Zhao S, Jiang X, Zhang E, Hu G, Hu B, et al. The circadian clock gene Bmal1 acts as a potential anti-oncogene in pancreatic cancer by activating the p53 tumor suppressor pathway. *Cancer Lett* (2016) 371:314–25. doi:10.1016/j.canlet.2015.12.002
61. Li W, Liu L, Liu D, Jin S, Yang Y, Tang W, et al. Decreased circadian component Bmal1 predicts tumor progression and poor prognosis in human pancreatic ductal adenocarcinoma. *Biochem Biophys Res Commun* (2016) 472:156–62. doi:10.1016/j.bbrc.2016.02.087
62. Hua H, Wang Y, Wan C, Liu Y, Zhu B, Wang X, et al. Inhibition of tumorigenesis by intratumoral delivery of the circadian gene mPer2 in C57BL/6 mice. *Cancer Gene Ther* (2007) 14:815–8. doi:10.1038/sj.cgt.7701061
63. Oda A, Katayose Y, Yabuuchi S, Yamamoto K, Mizuma M, Shirasou S, et al. Clock gene mouse period2 overexpression inhibits growth of human pancreatic cancer cells and has synergistic effect with cisplatin. *Anticancer Res* (2009) 29:1201–9.
64. Hatanaka F, Matsubara C, Myung J, Yoritaka T, Kamimura N, Tsutsumi S, et al. Genome-wide profiling of the core clock protein BMAL1 targets reveals a strict relationship with metabolism. *Mol Cell Biol* (2010) 30:5636–48. doi:10.1128/MCB.00781-10
65. Rudic RD, Mcnamara P, Curtis AM, Boston RC, Panda S, Hogenesch JB, et al. BMAL1 and CLOCK, two essential components of the circadian clock, are involved in glucose homeostasis. *PLoS Biol* (2004) 2:e377. doi:10.1371/journal.pbio.0020377
66. Woon PY, Kaisaki PJ, Braganca J, Bihoreau MT, Levy JC, Farrall M, et al. Aryl hydrocarbon receptor nuclear translocator-like (BMAL1) is associated with susceptibility to hypertension and type 2 diabetes. *Proc Natl Acad Sci U S A* (2007) 104:14412–7. doi:10.1073/pnas.0703247104
67. Marcheva B, Ramsey KM, Buhr ED, Kobayashi Y, Su H, Ko CH, et al. Disruption of the clock components CLOCK and BMAL1 leads to hypoinsulinaemia and diabetes. *Nature* (2010) 466:627–31. doi:10.1038/nature09253
68. Milagro FI, Gomez-Abellan P, Campion J, Martinez JA, Ordovas JM, Garaulet M. CLOCK, PER2 and BMAL1 DNA methylation: association with obesity and metabolic syndrome characteristics and monounsaturated fat intake. *Chronobiol Int* (2012) 29:1180–94. doi:10.3109/07420528.2012.719967
69. Hodzic A, Ristanovic M, Zorn B, Tulic C, Maver A, Novakovic I, et al. Genetic variation in circadian rhythm genes CLOCK and ARNTL as risk factor for male infertility. *PLoS One* (2013) 8:e59220. doi:10.1371/journal.pone.0059220
70. Kettner NM, Katchy CA, Fu L. Circadian gene variants in cancer. *Ann Med* (2014) 46:208–20. doi:10.3109/07853890.2014.914808
71. Zeng ZL, Wu MW, Sun J, Sun YL, Cai YC, Huang YJ, et al. Effects of the biological clock gene Bmal1 on tumour growth and anti-cancer drug activity. *J Biochem* (2010) 148:319–26. doi:10.1093/jb/mvq069
72. Zeng ZL, Luo HY, Yang J, Wu WJ, Chen DL, Huang P, et al. Overexpression of the circadian clock gene Bmal1 increases sensitivity to oxaliplatin in colorectal cancer. *Clin Cancer Res* (2014) 20:1042–52. doi:10.1158/1078-0432.CCR-13-0171
73. Khapre RV, Kondratova AA, Susova O, Kondratov RV. Circadian clock protein BMAL1 regulates cellular senescence in vivo. *Cell Cycle* (2011) 10: 4162–9. doi:10.4161/cc.10.23.18381
74. Elshazley M, Sato M, Hase T, Yamashita R, Yoshida K, Toyokuni S, et al. The circadian clock gene BMAL1 is a novel therapeutic target for malignant pleural mesothelioma. *Int J Cancer* (2012) 131:2820–31. doi:10.1002/ijc.27598
75. Le DT, Uram JN, Wang H, Bartlett BR, Kemberling H, Eyring AD, et al. PD-1 blockade in tumors with mismatch-repair deficiency. *N Engl J Med* (2015) 372:2509–20. doi:10.1056/NEJMoa1500596
76. Rizvi NA, Hellmann MD, Snyder A, Kvistborg P, Makarov V, Havel JJ, et al. Cancer immunology. Mutational landscape determines sensitivity to PD-1

blockade in non-small cell lung cancer. *Science* (2015) 348:124–8. doi:10.1126/science.aaa1348

77. van Gool IC, Eggink FA, Freeman-Mills L, Stelloo E, Marchi E, De Bruyn M, et al. POLE proofreading mutations elicit an antitumor immune response in endometrial cancer. *Clin Cancer Res* (2015) 21:3347–55. doi:10.1158/1078-0432.CCR-15-0057
78. Hugo W, Zaretsky JM, Sun L, Song C, Moreno BH, Hu-Lieskovan S, et al. Genomic and transcriptomic features of response to anti-PD-1 therapy in metastatic melanoma. *Cell* (2016) 165:35–44. doi:10.1016/j.cell.2016.02.065
79. Mouw KW, Goldberg MS, Konstantinopoulos PA, D'andrea AD. DNA damage and repair biomarkers of immunotherapy response. *Cancer Discov* (2017) 7:675–93. doi:10.1158/2159-8290.CD-17-0226
80. Hodi FS, O'day SJ, Mcdermott DF, Weber RW, Sosman JA, Haanen JB, et al. Improved survival with ipilimumab in patients with metastatic melanoma. *N Engl J Med* (2010) 363:711–23. doi:10.1056/NEJMoa1003466
81. Topalian SL, Sznol M, Mcdermott DF, Kluger HM, Carvajal RD, Sharfman WH, et al. Survival, durable tumor remission, and long-term safety in patients with advanced melanoma receiving nivolumab. *J Clin Oncol* (2014) 32:1020–30. doi:10.1200/JCO.2013.53.0105
82. Schadendorf D, Hodi FS, Robert C, Weber JS, Margolin K, Hamid O, et al. Pooled analysis of long-term survival data from phase II and phase III trials of ipilimumab in unresectable or metastatic melanoma. *J Clin Oncol* (2015) 33:1889–94. doi:10.1200/JCO.2014.56.2736
83. Spencer KR, Wang J, Silk AW, Ganesan S, Kaufman HL, Mehnert JM. Biomarkers for immunotherapy: current developments and challenges. *Am Soc Clin Oncol Educ Book* (2016) 35:e493–503. doi:10.14694/EDBK_160766
84. Ji RR, Chasalow SD, Wang L, Hamid O, Schmidt H, Cogswell J, et al. An immune-active tumor microenvironment favors clinical response to ipilimumab. *Cancer Immunol Immunother* (2012) 61:1019–31. doi:10.1007/s00262-011-1172-6
85. Snyder A, Makarov V, Merghoub T, Yuan J, Zaretsky JM, Desrichard A, et al. Genetic basis for clinical response to CTLA-4 blockade in melanoma. *N Engl J Med* (2014) 371:2189–99. doi:10.1056/NEJMoa1406498
86. Taube JM, Klein A, Brahmer JR, Xu H, Pan X, Kim JH, et al. Association of PD-1, PD-1 ligands, and other features of the tumor immune microenvironment with response to anti-PD-1 therapy. *Clin Cancer Res* (2014) 20:5064–74. doi:10.1158/1078-0432.CCR-13-3271
87. Van Allen EM, Miao D, Schilling B, Shukla SA, Blank C, Zimmer L, et al. Genomic correlates of response to CTLA-4 blockade in metastatic melanoma. *Science* (2015) 350:207–11. doi:10.1126/science.aad0095
88. Johnson DB, Frampton GM, Rioth MJ, Yusko E, Xu Y, Guo X, et al. Targeted next generation sequencing identifies markers of response to PD-1 blockade. *Cancer Immunol Res* (2016) 4:959–67. doi:10.1158/2326-6066.CIR-16-0143

Conflict of Interest Statement: All authors state no conflict of interest that could have impacted the development of this study.

DISCUSSION

Photosensitive System of the Melanocytes and Melanoma Cells

In the beginning of this Ph.D. project, in 2014, only a handful of studies had evaluated the presence of opsins in skin cells (Miyashita et al., 2001; Lopes et al., 2009; Tsutsumi et al., 2009; Wicks et al., 2011; Kojima et al., 2011; Kim et al., 2013), and until 2011 no study had investigated the functionality of the system. This scenario changed with the pioneering research by Wicks and coworkers, who showed that OPN2 was responsible for the UV-induced IPD process in human melanocytes (Wicks et al., 2011). Two years later, Kim and coworkers reported a reduction in the levels of differentiation markers in response to overexpression of OPN2; in addition, OPN2 knockdown increased the violet light-induced differentiation markers in human keratinocytes (Kim et al., 2013). From 2014 to 2016, to our knowledge, no advancement in the field was reported in the literature.

Our first contribution to the literature was in 2016. We demonstrated that murine normal and malignant melanocytes express OPN2 and OPN4. In response to a visible light pulse, we reported that the molecular clock of malignant melanocytes was more responsive compared to normal cells (de Assis et al., 2016 – Chapter 1). These findings were the first in the literature to correlate the responsiveness of the molecular clock with the photosensitive system.

In light of these results, we raised two hypotheses to explain the increased sensitivity of malignant cells, as described in the following lines: 1) a severe downregulation of the components of the biological clock, i.e., chronodisruption, in malignant cells compared to normal cells; 2) a non-functional system in normal cells which would become functional in

association with the carcinogenic process (de Assis et al., 2016 – Chapter 1).

In the first hypothesis, we were not able to prove the cause-consequence relationship. By 2013, it was already known that several clock genes and proteins were less expressed in human melanoma compared to nevus and/or adjacent tissue (Lengyel et al., 2013). Accordingly, we have provided several layers of evidence that the molecular components of the biological clock are downregulated in *in vivo* tumors as well as in human primary and metastatic melanoma compared to healthy tissue (de Assis et al., 2018b; 2018c – Chapters 6 and 7, respectively). Thus, as in malignant melanocytes the basal expression of clock genes is severely reduced as compared to normal cells, one may suggest that the level of response to a similar light stimulus could lead to an augmented response in malignant cells. Therefore, chronodisruption could explain the increased responsiveness to visible light in malignant melanocytes.

The second hypothesis is based on the fact that OPN4 migrates to cell membrane in response to visible light only in malignant melanocytes, an event that does not take place in normal melanocytes (de Assis et al., 2016 – Chapter 1). Although we have observed a minor effect of visible light on the activation of the biological clock (de Assis et al., 2016 – Chapter 1), in 2017 we showed that UVA radiation in the absence of heat activated the biological clock of normal melanocytes; however, this response was still more evident in malignant melanocytes (de Assis et al., 2017 – Chapter 3). Subsequently, in 2018 we showed – for the first time – that both OPN2 and OPN4 are UVA sensors that activate a cGMP-dependent pathway that participates in the UVA-induced IPD in both normal and malignant melanocytes (de Assis et al., 2018a – Chapter 5).

Therefore, we have ruled out the non-functionality of the photosensitive system of normal melanocytes.

Although *Opn2* and *Opn4* are less expressed in malignant cells compared to melanocytes, the photosensitive system seems to be more sensitive to visible light (de Assis et al., 2016 – Chapter 1). In fact, these *in vitro* data are in line with transcriptome analysis as *OPN1SW* and *OPN3* are more expressed than *OPN1LW*, *OPN1MW*, *OPN2*, *OPN4*, and *OPN5* in human melanoma compared to healthy skin (de Assis et al., 2018b – Chapter 6). Thus, the reduced gene expression of opsins and the increased responsiveness shown by malignant cells are intriguing.

Another factor that could explain the increased response of malignant cells is related to coupling. We demonstrated that heat does not affect the molecular clock in free-running normal melanocytes but is able to activate the biological clock if the cells were first synchronized by medium change (Moraes et al., 2017 – Chapter 4). Interestingly, free-running malignant melanocytes respond to heat stimulus without previous synchronization (Moraes et al., 2017 – Chapter 4). As mentioned above, we have shown that free-running normal melanocytes respond to UVA radiation, but in a lesser extent, compared to malignant melanocytes (de Assis et al., 2017 – Chapter 3). Unpublished results acquired during this Ph.D. are also in line with previous data from our lab (Moraes et al., 2017 – Chapter 4) as we have shown that once synchronized, normal melanocytes respond to UVA radiation in a similar way as malignant cells (data not shown).

Therefore, taken together, our results suggest that coupling is an important factor when normal and malignant melanocytes are in culture – an event that should be considered when studying biological rhythms *in vitro*. However, a highlight needs to be made: We have used low irradiance protocols for both visible light and UVA radiation, and short time exposure

to heat stimulus. Therefore, whether higher doses and/or exposure time would affect the biological clock of free-running unsynchronized normal melanocytes needs to be further evaluated.

Lastly, our first study (de Assis et al., 2016 – Chapter 1) opened several fronts of investigation, which will be discussed in depth in the next pages.

In 2016, we assessed the role of estradiol in pigmentary responses and correlated its effects with the biological clock. Interestingly, we observed no effect of this hormone on pigmentary and biological clock responses of normal melanocytes, whereas a reduction of melanin content and activation of the biological clock was found in malignant cells (Poletini et al., 2016 – Chapter 2). Although we did not perform functional assays to evaluate the precise role of clock genes in melanin synthesis, our study corroborated a previous pioneering study (Hardman et al., 2015). The authors demonstrated that silencing the biological clock in human melanocytes induced an increase of melanin content. In terms of mechanism, when *BMAL1* is silenced, *PER1* transcription is reduced, which leads to the phosphorylation of microphthalmia-associated transcription factor (MITF) that ultimately stimulates melanogenesis. Therefore, Hardman and coworkers were the first to establish a negative cause-effect relationship between biological clock and melanogenesis (Hardman et al., 2015) – an event corroborated by our study (Poletini et al., 2016).

In the following year, we were the first to report a remarkable and yet neglected phenomenon. We were interested in evaluating the effects of UVA radiation *per se*, heat shock *per se*, and a combination of both stimuli on melanin content and the biological clock in normal and malignant melanocytes (de Assis et al., 2017 – Chapter 3). We found that just UVA radiation had a minor activating effect on the biological clock of normal

melanocytes while in malignant cells a more evident response was again reported –similar to what was observed in our previous study (de Assis et al., 2016 – Chapter 1). Heat shock *per se* showed no effect on the biological clock of either cell type. Interestingly, melanin content transiently increased in response to UVA radiation in both normal and malignant melanocytes, a process known as IPD. Remarkably, we have found unexpected results as most of the UVA-induced cell responses, described above, were lost when UVA radiation was applied concomitantly with heat stimulus (de Assis et al., 2017 – Chapter 3).

A significant portion of the researchers, unfortunately, does not consider the effect of temperature on UV-induced responses in the skin as criticized by some groups (Calapre et al., 2013; 2016; de Assis et al., 2017 – Chapters 1 and 3, respectively). Therefore, our findings are a warning to take in consideration a strict control of temperature in the design of UV-related experiments. We also suggested that these data could serve as basis for therapy improvement of despigmentary diseases, especially in vitiligo where UV-induced pigmentation is expected (de Assis et al., 2017 – Chapter 3). Still, further *in vivo* and human studies should be performed to evaluate the precise interaction between heat and UV radiation.

Still in 2017, our group reported that melanopsin, besides being a light sensor, also acts as thermosensor in normal and malignant melanocytes (Moraes et al., 2017 – Chapter 4). The first evidence of this non-canonical role of melanopsin was shown in *Drosophila* larvae, as rhodopsin knockout flies lose the ability to thermo-discriminate the comfortable temperature range (Shen et al., 2011). Surprisingly, temperature discrimination was restored when mouse melanopsin was introduced in rhodopsin knockout flies (Shen et al., 2011). In another study, the same group further demonstrated the role of two rhodopsins

(isoforms 5 and 6) as thermosensors in *Drosophila* larval stage (Sokabe et al., 2016).

In mammalian cells, the first study demonstrating the role of opsins as thermosensors was carried out by Pérez-Cerezales and coworkers (2015). The authors reported that melanopsin was localized in a region capping the nucleus of human sperm cells similarly to our findings in normal and malignant melanocytes (de Assis et al., 2016 – Chapter 1). Upon knockdown of OPN2 the spermatozoid thermotaxis became defective, thus demonstrating the role of rhodopsin as a thermosensor in mammalian cells (Pérez-Cerezales et al., 2015).

We have shown that the molecular clock of both normal and malignant melanocytes was activated after heat exposure (39^{o}C for 1 hour), and that upon pharmacological inhibition or gene silencing of OPN4, the heat-induced response was lost in both cell types (Moraes et al., 2017 – Chapter 4). Therefore, these findings corroborated previous reports in the literature, and helped pave a new and challenging field of investigation – the role of thermo-opsins in the regulation of biological processes.

In the following year, 2018, our group demonstrated that both OPN2 and OPN4 act as UVA-sensors in normal and malignant melanocytes (de Assis et al., 2018a – Chapter 5). This study was very important for the field as we have unraveled two main events: 1) OPN2 and OPN4 as UVA sensors, and 2) the signaling pathway involved in IPD. The first finding was in agreement with prior studies that have reported the functionality of the photosensitive system of the skin (Wicks et al., 2011; Bellono et al., 2013; Kim et al., 2013; Buscone et al., 2017; Regazzeti et al., 2018). The novelty of our data resides on the evidence that OPN2 and OPN4 may act as functional “dimers” as the removal of either one leads to complete loss of UVA-induced IPD. The second novel aspect regards the signaling pathway involved in UVA-induced IPD. Although IPD was discovered

several decades ago (Honigsmann et al., 1986), the signaling cascade involved in such process was completely ignored by the few studies present in the literature (Pathak et al., 1962; Pathak and Stratton, 1968; Jimbow et al., 1973; Lavker and Kaidbey, 1982; Beitner and Wennersten, 1985; Honigsmann et al., 1986)., Our study characterized – for the first time –that upon stimulation of OPN2 and OPN4 by UVA radiation a signaling pathway that involves cGMP (CAMK II/NOS/cGMP), and thus, results in a transient increase of melanin content, the IPD process is triggered (de Assis et al., 2018a – Chapter 5).

Based on the above-mentioned results obtained during this Ph.D. project, our group has acted on the frontier of knowledge and has brought significant advances to the understanding of the skin photosensitive system. In fact, our findings in addition to the ones reported in the literature undoubtedly show that the photosensitive system of the skin is a promising target for feasible clinical and therapeutic applications.

Still several questions remain to be answered such as: 1) Which biological processes are controlled by each opsin present in the skin? Are their functions redundant?; 2) What is the role of each opsin in each cell type of skin, and how this interaction takes place *in vivo*; 3) Are opsins protective or not against cancer development, i.e., does cancer recruits opsins to act as drivers of the carcinogenic process and, if so, could opsins be pharmacologically targeted with a new class of anticancer drugs? The list of questions can be exhausting, but it only affirms that the photosensitive system of the skin is a promising field of investigation.

The Molecular Clock of Melanocytes and Melanoma cells

From this point on, the results regarding the role of the biological clock in melanoma development both *in vivo* mouse and in human samples will be discussed in light of the current literature.

In 2018, the first *in vivo* study of this PhD project was published: We investigated the effects of the presence of an encapsulated and non-metastatic melanoma tumor on the biological clock of peripheral tissues. In this approach, B16-F10 melanoma cells were injected into the right flank of mice and tumor grew over the course of two weeks. At the end of this period, mice were euthanized every 6 hours along 24 h and several genes were evaluated by qPCR (de Assis et al., 2018b – Chapter 6).

Firstly, we analyzed the effect of tumor microenviroment (TME) on the adjacent skin. We demonstrated a chronodisruption scenario in the tumor adjacent skin compared to a healthy one, which showed a rhythmic clock gene expression, a fact supported by a previous study (Tanioka et al., 2009). The tumor adjacent skin displayed an intermediate profile of clock expression between healthy skin and the tumor itself, which corroborates a previous transcriptome analysis of several tumors, tumor-adjacent and healthy tissues (Aran et al., 2017). Although we have not assessed inflammatory and immunological parameters, the above-mentioned effects are likely to result from a pro-inflammatory condition induced by the tumor (Aran et al., 2017; Bland et al., 2018).

Therefore, our study further corroborates the fact that tumor-adjacent skin does not represent a healthy tissue, and thus, caution should be taken when tumor-adjacent tissue is used as the healthy control, as discussed in depth by Aran and colleagues (2017).

Using bioinformatics, we analyzed the behavior of the biological clock, opsins, *Pppar*, and *Xpa* genes on melanoma development. Based on

the expression profile of these gene families, we were able to cluster them in a pattern that clearly distinguishes primary melanoma and healthy skin; thus, demonstrating the importance of these genes in melanoma development, which warrants further investigation (de Assis et al., 2018b – Chapter 6).

In a pioneering fashion, this study was the first to show a 24 h clock gene expression and melanin content data in melanoma tumors. We detected a rhythmic, although profoundly reduced, clock gene expression in tumor cells compared to healthy and tumor-adjacent skins. Regarding melanin content, an ultradian rhythm of pigment concentration was observed – for the first time – in tumor cells, which may be associated to the rhythmic expression of the molecular clock. Nevertheless, it is now well established that the molecular clock of tumor cells is profoundly depressed, i.e., chronodisrupted. The low amplitude profile of the clock machinery suggests that this alteration may favor growth and survival of cancer cells (de Assis et al., 2018b – Chapter 6), and therefore, it becomes an interesting and promising pharmacological target (Kiessling et al., 2017; Kiessling and Cermakian, 2017).

Another translational application of these findings is that if an oscillatory profile of melanin content does also take place in human melanoma tumors, chronomodulated radiotherapy and chemotherapy regimens should be used, as it is known that melanotic melanomas are more resistant to radiotherapy than amelanotic ones (Brozyna et al., 2016).

In addition to tumor microenvironment, TME, we also evaluated the effects of tumor macroenviroment (TMaE), i.e., the effects of tumor-derived molecules such as secreted growth factor-, mRNA- and miRNA-containing micro-vesicles (Al-Zoughbi et al., 2014). In fact, it is widely accepted that TMaE effects are related to cancer-associated cachexia, systemic inflammation, immune system suppression, and altered

coagulation (Egeblad et al., 2010; Al-Zoughbi et al., 2014). Additionally, chronodisruption has been recently added as a new effect of TMaE as discussed below.

Masri and colleagues (2016) were the first to establish that a non-metastatic lung cancer rewires – through an inflammatory pathway – several clock-controlled hepatic metabolic processes, which ultimately impairs insulin, glucose, and lipid metabolism. Within this line, Hojo and colleagues (2017) demonstrated that a non-metastatic breast cancer alters the pattern of the molecular clock in the liver but not in the kidneys.

The results reported in our study (de Assis et al., 2018b – Chapter 6) are in agreement with all the above-mentioned data and increased our knowledge regarding the effects of TMaE. In fact, we demonstrated that a non-metastatic melanoma leads to severe chronodisruption in lungs and liver, both common sites of metastasis but, surprisingly, also causes chronodisruption in the central oscillator (SCN) – shown for the first time in the literature.

Our findings offer the view of an unexpected and still poorly comprehended process that could be linked to the metastatic process, and therefore, could be pharmacologically targeted. Interestingly, in all studied tissues, *Bmal1* expression was significantly affected by tumor presence, a fact that supports its role as "rheostat" of the biological clock (de Assis et al., 2018b – Chapter 6). In fact, *Bmal1* is the only clock gene that has no redundancy and it is, therefore knocked down to create a biological clock defective mouse (Husse et a., 2011; 2014). It is still an open question why *Bmal1* displays such an intriguing profile in cancer related processes. Therefore, we suggest that the systemic chronodisruption caused by the presence of a non-metastatic tumor may favor the progression of metastasis in the tissues where the molecular clock is disrupted, and

therefore, they may become more susceptible to tumoral cell establishment and growth.

Based on the above-mentioned data, we decided to explore the role of the biological clock in human melanoma using public transcriptomics database from The Cancer Genome Atlas – TCGA – (Cancer Genome Atlas Network, 2015). Initially, we noted that *BMAL1*, *CRY1*, *CRY2*, *REV-ERBα*, *PER1*, *PER2*, *PER3*, and *RORα* are less expressed in metastatic melanoma when compared to healthy skin. Only *CLOCK* is upregulated in metastatic melanoma. Despite the absence of temporal information of gene expression in TCGA database, we created a tool that provides a view of the biological clock status.

We used a correlation matrix for clock genes found in a classical antiphase relationship (for instance high *BMAL1* expression and low *PER1* expression) in healthy tissue. In a metastatic melanoma, such correlation matrix was severely attenuated, which confirmed a dysfunctional molecular clock (de Assis et al., 2018c – Chapter 7). In the beginning of this project only one article in the literature reported the biological clock expression through immunohystochemical and qPCR analysis in melanoma, nevus, and tumor-adjacent skin (Lengyel et al., 2013). In our Ph.D. project, we have consolidated the idea, through *in vitro*, *in vivo*, and bioinformatic analysis, that a chronodisruption does in fact take place in melanoma; however, whether chronodisruption is cause or consequence of cancer development is still an open question.

Next, looking into the putative role of each clock gene in prognostic, only *BMAL1* showed a significant association. We found that patients with highly *BMAL1* expressing tumors showed longer survival, and that this is an independent prognostic factor. Intrigued by such findings, we used several tools to discover the underlying biological processes that contributed to the increased survival.

We found that high *BMAL1* expressing melanomas correlate with immune system activation and with improved response to immunotherapy in pre-treatment biopsies compared to low levels expressing melanomas. In a subsequent analysis, we demonstrated that high *BMAL1* melanomas are defective in base excision DNA repair (BER), which is related to increased mutation load and neoantigen exposure, ultimately associated with immune system recognition and activation (de Assis et al., 2018c – Chapter 7). Taken these data together, we have, therefore, undoubtedly shown the chronodisruption scenario in melanoma cancer, as well as provided evidence of *BMAL1* role as a prognostic and a putative marker for immunotherapy success in metastatic melanoma.

The above-described studies have advanced our knowledge regarding the participation of the biological clock in melanoma, but some questions remain unanswered. For instance, what is the consequence of the systemic chronodisruption caused by tumor presence in the organism? Could peripheral tissues be pharmacologically targeted as therapy for treating and/or preventing tumor metastasis? Which other clock genes or clock-controlled genes participate in melanoma development, progression, and metastasis? Could they be pharmacological targets? Therefore, all the data found in this PhD project and those described in the literature clearly point the biological clock as a promising pharmacological candidate for cancer treatment.

CONCLUDING REMARKS

The results obtained during this project have advanced our frontier of knowledge in two fronts: the photosensitive system and the biological clock of the skin. In the former, we have provided evidence of the relevance and functionality of the photosensitive system of the skin as it is able to detect UVA radiation and temperature through common sensors – opsins – and that it participates in the biological clock activation and UV-induced pigmentary response.

Regarding the biological clock of the skin, we have demonstrated that this system is downregulated in primary and metastatic melanoma compared to healthy skin. We have also shown that tumor adjacent skin is chronodisrupted and displays an intermediary clock profile between healthy skin and tumor samples. We were the first to report that a systemic chronodisruption arises from the presence of a non-metastatic melanoma, which could favor the metastatic process, and thus, it could be pharmacologically targeted. Lastly, we also provided evidence that *BMAL1* may be used as a marker for survival and immunotherapy success in patients with metastatic melanoma.

METHODOLOGIES AND TECHNIQUES

RNA Extraction – Traditional Method

The culture medium was removed and 1 mL of Tri-Reagent-LS (Ambion, USA) was directly applied to the cells. Cell lysate was collected in a microcentrifuge tube and kept at room temperature (RT) for 5 min. Then, 200 µL of 1-bromo-3-chloropropane (BCP) were added, followed by vigorous agitation for 15 sec, then kept at RT for 10 min. After centrifugation at 12,000 x g for 15 min (4ºC), the aqueous phase (500 µL) containing RNA was collected. RNA was precipitated by adding 650 µL of isopropanol (Sigma-Aldrich, USA) during 10 min at RT, followed by centrifugation at 12,000 x g during 35 min (4ºC). Next, the supernatant was removed, the RNA was washed twice with 1.3 mL of ethanol (75%), air dried at RT, and resuspended in 20 µL of DEPC water (Ambion, USA).

Possible genomic DNA contamination was prevented by treating the samples with DNase (turboDNA-free™, Life Technologies, USA). To each sample, 2 µL of DNase Buffer (10x) and 1 µL of Turbo DNase enzyme were added. After incubation of the samples at 37ºC during 30 min, 3 µL of inactivation reagent was added to each sample, followed by 2 min incubation at RT, a period in which the samples were vortexed 2 to 3 times. Following centrifugation at 10,000 x g during 2 min (4ºC), the supernatant containing the RNA was transferred to a new tube. In this and the following procedure, RNA concentration was determined by absorbance in 260 nm and quality was assessed by total absorbance at 260/280 nm in a spectrophotometer (NanoDrop ND-1000, USA). Samples with 260/280 higher than 1.6 were processed and used to synthesize complementary DNA (cDNA).

RNA Extraction Colum Method

Tri-Reagent-LS (1 mL, Ambion, EUA) was added to cells or homogenized tissues and stored at -20ºC. Samples were purified using the Direct-zol™ miniprep kit accordingly to the manufacturer's instruction with minor adjustments as follows: RNA Wash Buffer was added to the columns (700 µL) and centrifuged at 15,000 g during 6 min instead of 1 min. Possible genomic contamination was addressed by treating the samples with DNAse. Then, RNA was eluted by adding 15 to 25 µL of DNA/RNAse free water (Zymo Research, USA).

Reverse Transcriptase Polymerase Chain Reaction (RT-PCR)

RT-PCR was used to synthesize cDNA as follows. Microcentrifuge tubes kept on ice received 1 µL of random primers (100 ng/µL), 1 µL of dNTPs (10 mM), and volume containing 1 to 4 µg RNA; final volume was completed to 13 µL with DEPC water. Samples were vortexed, centrifuged, and incubated in a thermocycler at 65°C during 5 min, and 1 min on ice. Next, 4 µL of buffer (PCR 5X buffer), 1 µL of DTT (0.1 mM), 1 µL of ribonuclease inhibitor (40 U/µL), and 0.25 to 1 µL of Superscript III (each 0.25 µL corresponding to each 1 µg of starting RNA; 200 U/µL) were added making a final volume of 20 µL. Samples were vortexed, centrifuged, and incubated in a thermocycler at 25°C during 5 min, 50°C during 50 min, and 70°C during 15 min. In case Superscript III (200 U/µL) was used in less volume than 1 µL, the remaining volume was completed with DEPC water.

Quantitative PCR (qPCR)

cDNA was used to perform qPCR; the target genes are described in each Chapter. In this Ph.D. project, we have used two methodologies: Sybr Green and TaqMan® for single and multiple gene detection (up to 4) per well, respectively. For more information about the protocols used, please refer to each Chapter. The mixes used in this project were acquired from BioRad Laboratories, USA, and Kapa Biosystems, USA.

Melanin Quantification *in vitro* samples (melanocytes)

After the experimental protocols, a 500 µL aliquot of the culture medium was collected and transferred to a 1.5 mL tube, and the same volume of 1 M NaOH in 10% DMSO was added. The remaining medium was discarded, and the cells were harvested with Tyrode/EDTA solution and centrifuged at 100 x g during 5 min. After cell counting, the supernatant was discarded and 1 mL of 1 M NaOH in10% DMSO was added. The melanin containing tubes were heated at 80ºC during 2 h, after which the samples were centrifuged at 1050 x g during 15 min, and the supernatant was collected.

Each sample (200 µL) was added to duplicate wells of a flat-bottom 96-well plate, and total absorbance was measured at 475 nm. The values were interpolated in a standard curve of synthetic melanin (Sigma-Aldrich, USA), ranging from 1.5625 µg/mL to 20 or 200 µg/mL. Total melanin content was shown as intracellular or total (intra- and extracellular) melanin normalized by the cell number.

Melanin Quantification *in vivo* samples (tumors)

A portion of the tumor was collected, lysed in 1% Triton X-100 in phosphate buffered saline, PBS, and kept at 4°C for 30 min to allow complete lysis. After vigorous agitation, the samples were centrifuged during 30 min at 14,000 x g (4°C) to separate soluble and insoluble fractions. The supernatant was used to quantify total protein by Lowry's method (BCA) according to the manufacturer's instruction (ThermoFisher Scientific, USA). The insoluble fraction containing the melanin pellet was resuspended in 1 mL of 1 M of NaOH in 10% DMSO and heated at 80 °C during 2 h. From now on the protocol followed the procedure for cell samples, described above, except that the melanin concentration for the standard curve ranged from 3.125 to 200 µg/mL, and the values (in µg/mL) were previously normalized by protein concentration.

Tyrosinase Activity

After the experimental protocol, the culture medium was discarded, the cells were harvested with Tyrode/EDTA solution, and the suspension was centrifuged at 100 x g during 5 min. The pellet was rinsed with PBS followed by a centrifugation at 1050 x g during 5 min. The pellet was incubated with 0.1 M Tris-HCL in 1% Triton X-100, pH 6.8, during 1 h at -20°C. After this period, the samples were thawed at RT and centrifuged at 14,000 x g during 10 min (4°C). The supernatant was transferred to a 1.5 mL tube and protein concentration was determined by the BCA method according to the manufacturer's instructions (ThermoFisher Scientific, USA). A volume containing 60 µg of protein and 20 µL of 10 mM L-DOPA (pH 6.8) was added to a 96-well flat bottom plate, completing with

Tris-HCL solution up to 200 µL. After incubation at 37°C during 1 h, total absorbance of each sample in duplicate was measured at 475 nm.

Fontana-Masson Staining

After the experimental protocol performed in specially coated 6- or 12-well plates, the culture medium was removed, and the cells were fixed in 4% paraformaldehyde (Electron Microscopy Sciences, USA) in PBS at 4°C for 30 min. Fontana-Masson staining was performed according the manufacturer's instructions (Easy Path, Brazil) with slight modifications as described below.

Each well was washed with 500 µL of ultrapure water, and received 500 µL of reagent A (prepared by adding one drop of reagent A to 1 mL of ultrapure water) followed by incubation during 35 min at 55°C. The wells were rinsed with 1 mL of ultrapure water, and 300 µL of reagent B were carefully added to each well and left for 15 seconds. After another rinse with 1 mL of ultrapure water, 300 µL of reagent C were added to each well for 3 min. After another rinse with ultrapure water, 300 µL of Reagent D were added during 1 min. After washing and adding 1 mL of ultrapure water, each sample was immediately analyzed in an inverted microscopy, Axiovert 40CFL (Zeiss, Germany) with a mercury lamp of 50 W. Bright field photo-micrographies were taken and, for a better visualization of the cells, cell autoflorescence was acquired using a Cy3 filter (excitation 549 and emission 562 nm). All images were processed in ZEN Lite software for Windows

Immunocytochemistry

After the experimental protocol performed in specially coated 8-well slide (ThermoFisher Scientific, USA), the culture medium was discarded, and the cells were fixed in 4% paraformaldehyde (Electron Microscopy Sciences, USA) in PBS at 4°C for 30 min. After blockade of non-specific sites with 6% normal goat serum containing 22.52 mg/mL of glycine (Sigma-Aldrich, USA) in PBS at 4°C for 1 h, the cells were incubated overnight at 4°C with the respective primary antibodies (for more information see the respective Chapters). A Cy3-labeled anti-rabbit secondary antibody at 1:500 was applied for 1 h at room temperature, to reveal the primary antibody binding. Primary and secondary antibodies were diluted in incubation buffer containing 1% bovine serum albumin (Calbiochem, USA), 0.25% carrageenan lambda and 0.3% Triton X-100 (both from Sigma-Aldrich, USA). The material was mounted with DAPI-Vectashield Hard aqueous medium (Vector Laboratories, USA) and cover slipped. Images were obtained in an inverted fluorescence microscope Axiovert 40CFL (Zeiss, Germany) with a mercury lamp of 50 W, and DAPI (excitation 358 and emission 463 nm) and Cy3 (excitation 549 and emission 562 nm) filters.

Flow Cytometry

After the experimental protocol, the culture medium was collected, and the cells harvested with a Tyrode/EDTA solution. Both the cell medium and cells were transferred to a tube, and centrifuged at 100 x g for 5 min. The pellet was resuspended in 70% cold ethanol, kept for at least 3 h at -20°C, washed twice with PBS, and resuspended in 200 µL of propidium iodide solution (PI, 200 µg/mL of RNase A, 20 µg/mL of

propidium iodide, and 0.1% of Triton X-100 in PBS). The cell suspension in PI solution was kept in the dark for 30 min, washed, resuspended in PBS, and centrifuged at 100 x g for 5 min. The fluorescence was measured in a flow cytometer (Guava GE Healthcare, USA), and a total of 10,000 events was captured per sample.

Image Flow Cytometry

After the experimental protocol, cells were collected using Tyrode/EDTA solution. After centrifugation and extensive washes, 2 x 10^6 cells in suspension were used for each staining. Briefly, after fixation and permeabilization (as described in Immunocytochemistry section), the cells were incubated with OPN2 or OPN4 polyclonal antibodies at 1:50 and 1:500 dilutions, respectively, followed by incubation with a sheep FITC-conjugated anti-rabbit antibody at 1:200 dilution (Sigma-Aldrich, USA). Results were collected as 50,000 cell counts per sample in FlowSight (Merck, USA) using a 488 nm laser. Negative controls were performed by the omission of the primary antibody and the incubation with FITC-conjugated anti-rabbit antibody. The data analysis was performed by IDEAS software (Merck, USA) based on scatter plot of bright field area versus aspect ratio. Putative single cells were selected by gating only the area consistent with single cells in the absence of doublets or debris-like dots. The expression and the percentage of OPN2- or OPN4-FITC positive cells was determined based on the frequency of the counts over negative controls.

Gene Silencing by esiRNAs

To specifically target *Opn2* and *Opn4* mRNAs, we used esiRNAs (Merck, USA) which silence mouse *Opn2* (Access Number NM_145383) and mouse *Opn4* variants 1 and 2 (Access Numbers NM_001128599.1 and NM_013887.2, respectively). EsiRNAs result from the cleavage of long double-stranded RNAs (dsRNAs), that generates a heterogeneous mixture of siRNAs, which targets the same mRNA. We used an esiRNA that targets enhanced Green Fluorescent Protein (*Egfp*), as a negative control.

Cells were transfected with 10 nM esiRNA against *Opn2*, *Opn4*, or *Egfp* using Lipofectamine 3000 transfection kit (ThermoFisher Scientific, USA). In brief, in one tube 50 µL of Optimen media and 3 µL of Lipofectamine 3000 were added. In a second tube, 50 µL of Optimen and 1.48 µL of esiRNA (corresponding to 0.3 µg or 2.025 x 10^{-11} moles) were added. Then, the content of tube 1 was added to tube 2, followed by incubation at RT for 15 minutes. Next, the tube content was added to each well containing 2 mL of 2% fetal bovine serum medium. Forty-eight hours after transfection, protein reduction was confirmed by immunocytochemistry.

Bioinformatics

Gene expression and clinical data of 104 primary and 340 metastatic melanomas from The Cancer Genoma Atlas (TCGA) and 557 normal skins (sun and non-sun exposed) from Genotype-Tissue Expression (GTEx) were downloaded from the UCSC XENA Browser (http://xena.ucsc.edu) TCGA and GTEx gene expression data were generated using the Illumina HiSeq 2000 RNA sequencing platform, quantified using RSEM, upper quartile normalized and log2(x + 1) transformed, according to the

platform. Unsupervised hierarchical clustering was performed using the Euclidean distance and complete linkage. Gene expression data were checked for normality using the D'Agostino & Pearson test. Comparisons between normal skin samples and primary melanomas were performed using the Mann-Whitney test. Analyses were conducted in the R statistical environment (https://www.r-project.org).

REFERENCES

Al-Zoughbi W, Huang J, Paramasivan GS, Till H, Pichler M, Guertl-Lackner B, Hoefler G. Tumor macroenvironment and metabolism. Semin Oncol. 2014;41(2):281-95.

Aran D, Camarda R, Odegaard J, Paik H, Oskotsky B, Krings G, Goga A, Sirota M, Butte AJ. Comprehensive analysis of normal adjacent to tumor transcriptomes. Nat Commun. 2017;8(1):1077.

Aspberg S, Dahlquist G, Kahan T, Kallen B. Confirmed association between neonatal phototherapy or neonatal icterus and risk of childhood asthma. Pediatr Allergy Immunol. 2010;21(4 Pt 2):e733-9.

Bae K, Jin X, Maywood ES, Hastings MH, Reppert SM, Weaver DR. Differential functions of mPer1, mPer2, and mPer3 in the SCN circadian clock. Neuron. 2001;30(2):525-36.

Baggs JE, Price TS, DiTacchio L, Panda S, Fitzgerald GA, Hogenesch JB. Network features of the mammalian circadian clock. PLoS Biol. 2009;7(3):e52.

Baron KG, Reid KJ. Circadian misalignment and health. Int Rev Psychiatry. 2014;26(2):139-54.

Beitner H, Wennersten G. A qualitative and quantitative transmission electronmicroscopic study of the immediate pigment darkening reaction. Photodermatol. 1985;2(5):273-8.

Bellono NW, Kammel LG, Zimmerman AL, Oancea E. UV light phototransduction activates transient receptor potential A1 ion channels in human melanocytes. Proc Natl Acad Sci U S A. 2013;110(6):2383-8.

Bjarnason GA, Jordan RC, Wood PA, Li Q, Lincoln DW, Sothern RB, Hrushesky WJ, Ben-David Y. Circadian expression of clock genes

in human oral mucosa and skin: association with specific cell-cycle phases. Am J Pathol. 2001;158(5):1793-801.

Bland CL, Byrne-Hoffman CN, Fernandez A, Rellick SL, Deng W, Klinke DJ. Exosomes derived from B16F0 melanoma cells alter the transcriptome of cytotoxic T cells that impacts mitochondrial respiration. FEBS J. 2018;285(6):1033-50.

Boivin DB, Boudreau P. Impacts of shift work on sleep and circadian rhythms. Pathol Biol (Paris). 2014;62(5):292-301.

Brenner M, Hearing VJ. The protective role of melanin against UV damage in human skin. Photochem Photobiol. 2008;84(3):539-49.

Brown SA, Azzi A. Peripheral circadian oscillators in mammals. Handb Exp Pharmacol. 2013; 217:45-66.

Brozyna AA, Jozwicki W, Roszkowski K, Filipiak J, Slominski AT. Melanin content in melanoma metastases affects the outcome of radiotherapy. Oncotarget. 2016;7(14):17844-53.

Buhr ED, Takahashi JS. Molecular components of the Mammalian circadian clock. Handb Exp Pharmacol. 2013(217):3-27.

Buijs R, Salgado R, Sabath E, Escobar C. Peripheral circadian oscillators: time and food. Prog Mol Biol Transl Sci. 2013;119:83-103.

Bunger MK, Wilsbacher LD, Moran SM, Clendenin C, Radcliffe LA, Hogenesch JB, Simon MC, Takahashi JS, Bradfield CA. Mop3 is an essential component of the master circadian pacemaker in mammals. Cell. 2000;103(7):1009-17.

Buscone S, Mardaryev AN, Raafs B, Bikker JW, Sticht C, Gretz N, Farjo N, Uzunbajakava NE, Botchkareva NV. A new path in defining light parameters for hair growth: Discovery and modulation of photoreceptors in human hair follicle. Lasers Surg Med. 2017;49(7):705-18.

Cadet J, Berger M, Douki T, Morin B, Raoul S, Ravanat JL, Spinelli S.

Effects of UV and visible radiation on DNA-final base damage. Biol Chem. 1997;378(11):1275-86.

Calapre L, Gray ES, Kurdykowski S, David A, Hart P, Descargues P, Ziman M. Heat-mediated reduction of apoptosis in UVB-damaged keratinocytes in vitro and in human skin ex vivo. BMC Dermatology. 2016;16(1):6.

Calapre L, Gray ES, Ziman M. Heat stress: a risk factor for skin carcinogenesis. Cancer Lett. 2013;337(1):35-40.

Cancer Genome Atlas N. Genomic Classification of Cutaneous Melanoma. Cell. 2015;161(7):1681-96.

Castellano-Pellicena I, Uzunbajakava NE, Mignon C, Raafs B, Botchkarev VA, Thornton MJ. Does blue light restore human epidermal barrier function via activation of Opsin during cutaneous wound healing? Lasers Surg Med. 2018. DOI: 10.1002/lsm.23015

Chiarelli-Neto O, Ferreira AS, Martins WK, Pavani C, Severino D, Faiao-Flores F, Maria-Engler SS, Aliprandini E, Martinez GR, Di Mascio P, Medeiros MH, Baptista MS. Melanin photosensitization and the effect of visible light on epithelial cells. PLoS One. 2014;9(11):e113266.

Crosio C, Cermakian N, Allis CD, Sassone-Corsi P. Light induces chromatin modification in cells of the mammalian circadian clock. Nat Neurosci. 2000;3(12):1241-7.

de Assis LV, Moraes MN, da Silveira Cruz-Machado S, Castrucci AM. The effect of white light on normal and malignant murine melanocytes: A link between opsins, clock genes, and melanogenesis. Biochim Biophys Acta. 2016;1863(6 Pt A):1119-33.

de Assis LVM, Kinker GS, Moraes MN, Markus RP, Fernandes PA, Castrucci AML. Expression of the Circadian Clock Gene BMAL1

Positively Correlates With Antitumor Immunity and Patient Survival in Metastatic Melanoma. Front Oncol. 2018;8:185.

de Assis LVM, Moraes MN, Castrucci AML. Heat shock antagonizes UVA-induced responses in murine melanocytes and melanoma cells: an unexpected interaction. Photochem Photobiol Sci. 2017;16(5):633-48.

de Assis LVM, Moraes MN, Magalhaes-Marques KK, Castrucci AML. Melanopsin and rhodopsin mediate UVA-induced immediate pigment darkening: Unravelling the photosensitive system of the skin. Eur J Cell Biol. 2018;97(3):150-62.

de Assis LVM, Moraes MN, Magalhaes-Marques KK, Kinker GS, da Silveira Cruz-Machado S, Castrucci AML. Non-Metastatic Cutaneous Melanoma Induces Chronodisruption in Central and Peripheral Circadian Clocks. Int J Mol Sci. 2018;19(4).

DeBruyne JP, Weaver DR, Reppert SM. CLOCK and NPAS2 have overlapping roles in the suprachiasmatic circadian clock. Nat Neurosci. 2007a;10(5):543-5.

DeBruyne JP, Weaver DR, Reppert SM. Peripheral circadian oscillators require CLOCK. Curr Biol. 2007b;17(14):R538-9.

Desotelle JA, Wilking MJ, Ahmad N. The circadian control of skin and cutaneous photodamage. Photochem Photobiol. 2012;88(5):1037-47.

Dibner C, Schibler U, Albrecht U. The mammalian circadian timing system: organization and coordination of central and peripheral clocks. Annu Rev Physiol. 2010;72:517-49.

Dupont E, Gomez J, Bilodeau D. Beyond UV radiation: a skin under challenge. Int J Cosmet Sci. 2013;35(3):224-32.

Egeblad M, Nakasone ES, Werb Z. Tumors as organs: complex tissues that interface with the entire organism. Dev Cell. 2010;18(6):884-901.

Eller MS, Ostrom K, Gilchrest BA. DNA damage enhances melanogenesis. Proc Natl Acad Sci U S A. 1996;93(3):1087-92.

Eller MS, Yaar M, Gilchrest BA. DNA damage and melanogenesis. Nature. 1994;372(6505):413-4.

Fortini P, Pascucci B, Parlanti E, D'Errico M, Simonelli V, Dogliotti E. 8-Oxoguanine DNA damage: at the crossroad of alternative repair pathways. Mutat Res. 2003;531(1-2):127-39.

Froy O. Metabolism and circadian rhythms--implications for obesity. Endocr Rev. 2010;31(1):1-24.

Gaddameedhi S, Selby CP, Kaufmann WK, Smart RC, Sancar A. Control of skin cancer by the circadian rhythm. Proc Natl Acad Sci U S A. 2011;108(46):18790-5.

Gathwala G, Sharma S. Phototherapy induces oxidative stress in premature neonates. Indian J Gastroenterol. 2002;21(4):153-4.

Gerstner JR, Yin JC. Circadian rhythms and memory formation. Nat Rev Neurosci. 2010;11(8):577-88.

Gilchrest BA, Eller MS. DNA photodamage stimulates melanogenesis and other photoprotective responses. J Investig Dermatol Symp Proc. 1999;4(1):35-40.

Gilchrest BA, Zhai S, Eller MS, Yarosh DB, Yaar M. Treatment of human melanocytes and S91 melanoma cells with the DNA repair enzyme T4 endonuclease V enhances melanogenesis after ultraviolet irradiation. J Invest Dermatol. 1993;101(5):666-72.

Ginty DD, Kornhauser JM, Thompson MA, Bading H, Mayo KE, Takahashi JS, Greenberg ME. Regulation of CREB phosphorylation in the suprachiasmatic nucleus by light and a circadian clock. Science. 1993;260(5105):238-41.

Golombek DA, Rosenstein RE. Physiology of circadian entrainment. Physiol Rev. 2010;90(3):1063-102.

Gordijn MCM, t Mannetje D, Meesters Y. The effects of blue-enriched light treatment compared to standard light treatment in Seasonal Affective Disorder. J Affect Disord. 2012;136(1-2):72-80.

Green CB, Takahashi JS, Bass J. The meter of metabolism. Cell. 2008;134(5):728-42.

Haltaufderhyde K, Ozdeslik RN, Wicks NL, Najera JA, Oancea E. Opsin expression in human epidermal skin. Photochem Photobiol. 2015;91(1):117-23.

Hannibal J. Roles of PACAP-containing retinal ganglion cells in circadian timing. Int Rev Cytol. 2006;251:1-39.

Hardman JA, Tobin DJ, Haslam IS, Farjo N, Farjo B, Al-Nuaimi Y, Grimaldi B, Paus R. The peripheral clock regulates human pigmentation. J Invest Dermatol. 2015;135(4):1053-64.

Herzog ED. Neurons and networks in daily rhythms. Nat Rev Neurosci. 2007;8(10):790-802.

Hogenesch JB, Ueda HR. Understanding systems-level properties: timely stories from the study of clocks. Nat Rev Genet. 2011;12(6):407-16.

Hojo H, Enya S, Arai M, Suzuki Y, Nojiri T, Kangawa K, Koyama S, Kawaoka S. Remote reprogramming of hepatic circadian transcriptome by breast cancer. Oncotarget. 2017;8(21):34128-40.

Honigsmann H, Schuler G, Aberer W, Romani N, Wolff K. Immediate pigment darkening phenomenon. A reevaluation of its mechanisms. J Invest Dermatol. 1986;87(5):648-52.

Husse J, Eichele G, Oster H. Synchronization of the mammalian circadian timing system: Light can control peripheral clocks independently of the SCN clock: alternate routes of entrainment optimize the alignment of the body's circadian clock network with external time. Bioessays. 2015;37(10):1119-28.

Husse J, Leliavski A, Tsang AH, Oster H, Eichele G. The light-dark cycle controls peripheral rhythmicity in mice with a genetically ablated suprachiasmatic nucleus clock. FASEB J. 2014;28(11):4950-60.

Husse J, Zhou X, Shostak A, Oster H, Eichele G. Synaptotagmin10-Cre, a driver to disrupt clock genes in the SCN. J Biol Rhythms. 2011;26(5):379-89.

Izumo M, Pejchal M, Schook AC, Lange RP, Walisser JA, Sato TR, Wang X, Bradfield CA, Takahashi JS. Differential effects of light and feeding on circadian organization of peripheral clocks in a forebrain Bmal1 mutant. Elife. 2014;3.

Jimbow K, Pathak MA, Fitzpatrick TB. Effect of ultraviolet on the distribution pattern of microfilaments and microtubules and on the nucleus in human melanocytes. Yale J Biol Med. 1973;46(5):411-26.

Kawara S, Mydlarski R, Mamelak AJ, Freed I, Wang B, Watanabe H, Shivji G, Tavadia SK, Suzuki H, Bjarnason GA, Jordan RC, Sauder DN. Low-dose ultraviolet B rays alter the mRNA expression of the circadian clock genes in cultured human keratinocytes. J Invest Dermatol. 2002;119(6):1220-3.

Kelleher FC, Rao A, Maguire A. Circadian molecular clocks and cancer. Cancer Lett. 2014;342(1):9-18.

Kiessling S, Beaulieu-Laroche L, Blum ID, Landgraf D, Welsh DK, Storch KF, Labrecque N, Cermakian N. Enhancing circadian clock function in cancer cells inhibits tumor growth. BMC Biol. 2017;15(1):13.

Kiessling S, Cermakian N. The tumor circadian clock: a new target for cancer therapy? Future Oncol. 2017;13(29):2607-10.

Kim HJ, Son ED, Jung JY, Choi H, Lee TR, Shin DW. Violet light down-regulates the expression of specific differentiation markers through

Rhodopsin in normal human epidermal keratinocytes. PLoS One. 2013;8(9):e73678.

Kojima D, Mori S, Torii M, Wada A, Morishita R, Fukada Y. UV-sensitive photoreceptor protein OPN5 in humans and mice. PLoS One. 2011;6(10):e26388.

Kornhauser JM, Mayo KE, Takahashi JS. Light, immediate-early genes, and circadian rhythms. Behav Genet. 1996;26(3):221-40.

Korytowski W, Pilas B, Sarna T, Kalyanaraman B. Photoinduced generation of hydrogen peroxide and hydroxyl radicals in melanins. Photochem Photobiol. 1987;45(2):185-90.

Kovac J, Husse J, Oster H. A time to fast, a time to feast: the crosstalk between metabolism and the circadian clock. Mol Cells. 2009;28(2):75-80.

Kowalska E, Brown SA. Peripheral clocks: keeping up with the master clock. Cold Spring Harb Symp Quant Biol. 2007;72:301-5.

Krutmann J, Bouloc A, Sore G, Bernard BA, Passeron T. The skin aging exposome. J Dermatol Sci. 2017;85(3):152-61.

Kuse Y, Ogawa K, Tsuruma K, Shimazawa M, Hara H. Damage of photoreceptor-derived cells in culture induced by light emitting diode-derived blue light. Sci Rep. 2014;4:5223.

Kvam E, Tyrrell RM. The role of melanin in the induction of oxidative DNA base damage by ultraviolet A irradiation of DNA or melanoma cells. J Invest Dermatol. 1999;113(2):209-13.

Kyriacou CP, Hastings MH. Circadian clocks: genes, sleep, and cognition. Trends Cogn Sci. 2010;14(6):259-67.

Lavker RM, Kaidbey KH. Redistribution of melanosomal complexes within keratinocytes following UV-A irradiation: a possible mechanism for cutaneous darkening in man. Arch Dermatol Res. 1982;272(3-4):215-28.

Le Fur I, Reinberg A, Lopez S, Morizot F, Mechkouri M, Tschachler E. Analysis of circadian and ultradian rhythms of skin surface properties of face and forearm of healthy women. J Invest Dermatol. 2001;117(3):718-24.

Lengyel Z, Lovig C, Kommedal S, Keszthelyi R, Szekeres G, Battyani Z, Csernus V, Nagy AD. Altered expression patterns of clock gene mRNAs and clock proteins in human skin tumors. Tumour Biol. 2013;34(2):811-9.

Leung NY, Montell C. Unconventional roles of opsins. Annu Rev Cell Dev Biol. 2017;33:241-64.

Liebel F, Kaur S, Ruvolo E, Kollias N, Southall MD. Irradiation of skin with visible light induces reactive oxygen species and matrix-degrading enzymes. J Invest Dermatol. 2012;132(7):1901-7.

Lopes GJ, Gois CC, Lima LH, Castrucci AM. Modulation of rhodopsin gene expression and signaling mechanisms evoked by endothelins in goldfish and murine pigment cell lines. Braz J Med Biol Res. 2010;43(9):828-36.

Luber AJ, Ensanyat SH, Zeichner JA. Therapeutic implications of the circadian clock on skin function. J Drugs Dermatol. 2014;13(2):130-4.

Mahmoud BH, Hexsel CL, Hamzavi IH, Lim HW. Effects of visible light on the skin. Photochem Photobiol. 2008;84(2):450-62.

Masri S, Papagiannakopoulos T, Kinouchi K, Liu Y, Cervantes M, Baldi P, Jacks T, Sassone-Corsi P. Lung adenocarcinoma distally rewires hepatic circadian homeostasis. Cell. 2016;165(4):896-909.

Matsumi Y, Kawasaki M. Photolysis of atmospheric ozone in the ultraviolet region. Chem Rev. 2003;103(12):4767-82.

Matsunaga N, Itcho K, Hamamura K, Ikeda E, Ikeyama H, Furuichi Y, Watanabe M, Koyanagi S, Ohdo S. 24-hour rhythm of aquaporin-

3 function in the epidermis is regulated by molecular clocks. J Invest Dermatol. 2014;134(6):1636-44.

Menck CFM, Munford V. DNA repair diseases: What do they tell us about cancer and aging? Genet Mol Biol. 2014;37(1 Suppl):220-33.

Mieda M, Sakurai T. Bmal1 in the nervous system is essential for normal adaptation of circadian locomotor activity and food intake to periodic feeding. J Neurosci. 2011;31(43):15391-6.

Miyamura Y, Coelho SG, Schlenz K, Batzer J, Smuda C, Choi W, Brenner M, Passeron T, Zhang G, Kolbe L, Wolber R, Hearing VJ. The deceptive nature of UVA tanning versus the modest protective effects of UVB tanning on human skin. Pigment Cell Melanoma Res. 2011;24(1):136-47.

Miyashita Y, Moriya T, Kubota T, Yamada K, Asami K. Expression of opsin molecule in cultured murine melanocyte. J Investig Dermatol Symp Proc. 2001;6(1):54-7.

Moraes MN, de Assis LVM, Magalhaes-Marques KK, Poletini MO, de Lima L, Castrucci AML. Melanopsin, a Canonical Light Receptor, Mediates Thermal Activation of Clock Genes. Sci Rep. 2017;7(1):13977.

Mouret S, Baudouin C, Charveron M, Favier A, Cadet J, Douki T. Cyclobutane pyrimidine dimers are predominant DNA lesions in whole human skin exposed to UVA radiation. Proc Natl Acad Sci U S A. 2006;103(37):13765-70.

Musio C, Santillo S. Nonvisual photosensitivity and circadian vision. CRC Handbook of Organic Photochem and Photobiol. 2012;Chapter 50:1195-1210

Obrietan K, Impey S, Storm DR. Light and circadian rhythmicity regulate MAP kinase activation in the suprachiasmatic nuclei. Nat Neurosci. 1998;1(8):693-700.

Olah J, Toth-Molnar E, Kemeny L, Csoma Z. Long-term hazards of neonatal blue-light phototherapy. Br J Dermatol. 2013;169(2):243-9.

Panda S, Provencio I, Tu DC, Pires SS, Rollag MD, Castrucci AM, Pletcher MT, Sato TK, Wiltshire T, Andahazy M, Kay SA, Van Gelder RN, Hogenesch JB. Melanopsin is required for non-image-forming photic responses in blind mice. Science. 2003;301(5632):525-7.

Panda S, Sato TK, Castrucci AM, Rollag MD, DeGrip WJ, Hogenesch JB, Provencio I, Kay SA. Melanopsin (Opn4) requirement for normal light-induced circadian phase shifting. Science. 2002;298(5601):2213-6.

Park S, Kim K, Bae IH, Lee SH, Jung J, Lee TR, Cho EG. TIMP3 is a CLOCK-dependent diurnal gene that inhibits the expression of UVB-induced inflammatory cytokines in human keratinocytes. FASEB J. 2018;32(3):1510-23.

Pathak MA, Riley FJ, Fitzpatrick TB, Curwen WL. Melanin formation in human skin induced by long-wave ultra-violet and visible light. Nature. 1962;193:148-50.

Pathak MA, Stratton K. Free radicals in human skin before and after exposure to light. Arch Biochem Biophys. 1968;123(3):468-76.

Pereira DS, van der Veen DR, Gonçalves BSB, Tufik S, von Schantz M, Archer SN, Pedrazzoli M. The effect of different photoperiods in circadian rhythms of Per3 knockout mice. BioMed Res Intl. 2014;2014:5.

Perez-Cerezales S, Boryshpolets S, Afanzar O, Brandis A, Nevo R, Kiss V, Eisenbach M. Involvement of opsins in mammalian sperm thermotaxis. Sci Rep. 2015;5:16146.

Pfeifer GP, Besaratinia A. UV wavelength-dependent DNA damage and

human non-melanoma and melanoma skin cancer. Photochem Photobiol Sci. 2012;11(1):90-7.

Pittendrigh CS, Daan S. A functional analysis of circadian pacemakers in nocturnal rodents. J Comp Physiol.1976;106(3):333-55.

Poletini MO, de Assis LV, Moraes MN, Castrucci AM. Estradiol differently affects melanin synthesis of malignant and normal melanocytes: a relationship with clock and clock-controlled genes. Mol Cell Biochem. 2016;421(1-2):29-39.

Potter GD, Skene DJ, Arendt J, Cade JE, Grant PJ, Hardie LJ. Circadian rhythm and sleep disruption: Causes, metabolic consequences, and countermeasures. Endocr Rev. 2016;37(6):584-608.

Provencio I, Jiang G, De Grip WJ, Hayes WP, Rollag MD. Melanopsin: An opsin in melanophores, brain, and eye. Proc Natl Acad Sci U S A. 1998;95(1):340-5.

Provencio I, Rollag MD, Castrucci AM. Photoreceptive net in the mammalian retina. This mesh of cells may explain how some blind mice can still tell day from night. Nature. 2002;415(6871):493.

Ralph MR, Foster RG, Davis FC, Menaker M. Transplanted suprachiasmatic nucleus determines circadian period. Science. 1990;247(4945):975-8.

Ralph MR, Menaker M. A mutation of the circadian system in golden hamsters. Science. 1988;241(4870):1225-7.

Regazzetti C, Sormani L, Debayle D, Bernerd F, Tulic MK, De Donatis GM, Chignon-Sicard B, Rocchi S, Passeron T. Melanocytes sense blue light and regulate pigmentation through Opsin-3. J Invest Dermatol. 2018;138(1):171-8.

Richards J, Gumz ML. Advances in understanding the peripheral circadian clocks. FASEB J. 2012;26(9):3602-13.

Ridley AJ, Whiteside JR, McMillan TJ, Allinson SL. Cellular and sub-

cellular responses to UVA in relation to carcinogenesis. Int J Radiat Biol. 2009;85(3):177-95.

Roecklein KA, Rohan KJ, Duncan WC, Rollag MD, Rosenthal NE, Lipsky RH, Provencio I. A missense variant (P10L) of the melanopsin (OPN4) gene in seasonal affective disorder. J Affect Disord. 2009;114(1-3):279-85.

Roenneberg T, Merrow M. The circadian clock and human health. Curr Biol. 2016;26(10):R432-43.

Rosen CF, Seki Y, Farinelli W, Stern RS, Fitzpatrick TB, Pathak MA, Gange RW. A comparison of the melanocyte response to narrow band UVA and UVB exposure in vivo. J Invest Dermatol. 1987;88(6):774-9.

Runger TM, Kappes UP. Mechanisms of mutation formation with long-wave ultraviolet light (UVA). Photodermatol Photoimmunol Photomed. 2008;24(1):2-10.

Sandu C, Dumas M, Malan A, Sambakhe D, Marteau C, Nizard C, Schnebert S, Perrier E, Challet E, Pevet P, Felder-Schmittbuhl MP. Human skin keratinocytes, melanocytes, and fibroblasts contain distinct circadian clock machineries. Cell Mol Life Sci. 2012;69(19):3329-39.

Sandu C, Liu T, Malan A, Challet E, Pevet P, Felder-Schmittbuhl MP. Circadian clocks in rat skin and dermal fibroblasts: differential effects of aging, temperature and melatonin. Cell Mol Life Sci. 2015;72(11):2237-48.

Savvidis C, Koutsilieris M. Circadian rhythm disruption in cancer biology. Mol Med. 2012;18(1):1249-60.

Shearman LP, Jin X, Lee C, Reppert SM, Weaver DR. Targeted disruption of the mPer3 gene: subtle effects on circadian clock function. Mol Cell Biol. 2000;20(17):6269-75.

Shen WL, Kwon Y, Adegbola AA, Luo J, Chess A, Montell C. Function of rhodopsin in temperature discrimination in Drosophila. Science. 2011;331(6022):1333-6.

Sklar LR, Almutawa F, Lim HW, Hamzavi I. Effects of ultraviolet radiation, visible light, and infrared radiation on erythema and pigmentation: a review. Photochem Photobiol Sci. 2013;12(1):54-64.

Smolensky MH, Hermida RC, Reinberg A, Sackett-Lundeen L, Portaluppi F. Circadian disruption: New clinical perspective of disease pathology and basis for chronotherapeutic intervention. Chronobiol Int. 2016;33(8):1101-19.

Sokabe T, Chen HC, Luo J, Montell C. A Switch in thermal preference in Drosophila larvae depends on multiple rhodopsins. Cell Rep. 2016;17(2):336-44.

Solano F. Melanins: Skin pigments and much more - types, structural models, biological functions, and formation routes. N J Sci. 2014;2014:28.

Solomon SG, Lennie P. The machinery of colour vision. Nat Rev Neurosci. 2007;8(4):276-86.

Sparsa A, Faucher K, Sol V, Durox H, Boulinguez S, Doffoel-Hantz V, Calliste CA, Cook-Moreau J, Krausz P, Sturtz FG, Bedane C, Jauberteau-Marchan MO, Ratinaud MH, Bonnetblanc JM. Blue light is phototoxic for B16F10 murine melanoma and bovine endothelial cell lines by direct cytocidal effect. Anticancer Res. 2010;30(1):143-7.

Sporl F, Schellenberg K, Blatt T, Wenck H, Wittern KP, Schrader A, Kramer A. A circadian clock in HaCaT keratinocytes. J Invest Dermatol. 2011;131(2):338-48.

Strong RE, Marchant BK, Reimherr FW, Williams E, Soni P, Mestas R.

Narrow-band blue-light treatment of seasonal affective disorder in adults and the influence of additional nonseasonal symptoms. Depress Anxiety. 2009;26(3):273-8.

Svobodova AR, Galandakova A, Sianska J, Dolezal D, Lichnovska R, Ulrichova J, Vostalova J. DNA damage after acute exposure of mice skin to physiological doses of UVB and UVA light. Arch Dermatol Res. 2012;304(5):407-12.

Takahashi JS. Transcriptional architecture of the mammalian circadian clock. Nat Rev Genet. 2017;18(3):164-79.

Takeuchi S, Zhang W, Wakamatsu K, Ito S, Hearing VJ, Kraemer KH, Brash DE. Melanin acts as a potent UVB photosensitizer to cause an atypical mode of cell death in murine skin. Proc Natl Acad Sci U S A. 2004;101(42):15076-81.

Tanioka M, Yamada H, Doi M, Bando H, Yamaguchi Y, Nishigori C, Okamura H. Molecular clocks in mouse skin. J Invest Dermatol. 2009;129(5):1225-31.

Thody AJ, Higgins EM, Wakamatsu K, Ito S, Burchill SA, Marks JM. Pheomelanin as well as eumelanin is present in human epidermis. J Invest Dermatol. 1991;97(2):340-4.

Toh PP, Bigliardi-Qi M, Yap AM, Sriram G, Bigliardi P. Expression of peropsin in human skin is related to phototransduction of violet light in keratinocytes. Exp Dermatol. 2016;25(12):1002-5.

Tsutsumi M, Ikeyama K, Denda S, Nakanishi J, Fuziwara S, Aoki H, Denda M. Expressions of rod and cone photoreceptor-like proteins in human epidermis. Exp Dermatol. 2009;18(6):567-70.

van der Horst GT, Muijtjens M, Kobayashi K, Takano R, Kanno S, Takao M, de Wit J, Verkerk A, Eker AP, van Leenen D, Buijs R, Bootsma D, Hoeijmakers JH, Yasui A. Mammalian Cry1 and Cry2 are essential for maintenance of circadian rhythms. Nature.

1999;398(6728):627-30.

Vitaterna MH, Selby CP, Todo T, Niwa H, Thompson C, Fruechte EM, Hitomi K, Thresher RJ, Ishikawa T, Miyazaki J, Takahashi JS, Sancar A. Differential regulation of mammalian period genes and circadian rhythmicity by cryptochromes 1 and 2. Proc Natl Acad Sci U S A. 1999;96(21):12114-9.

Welsh DK, Yoo SH, Liu AC, Takahashi JS, Kay SA. Bioluminescence imaging of individual fibroblasts reveals persistent, independently phased circadian rhythms of clock gene expression. Curr Biol. 2004;14(24):2289-95.

West AC, Bechtold DA. The cost of circadian desynchrony: Evidence, insights and open questions. Bioessays. 2015;37(7):777-88.

Wicks NL, Chan JW, Najera JA, Ciriello JM, Oancea E. UVA phototransduction drives early melanin synthesis in human melanocytes. Curr Biol. 2011;21(22):1906-11.

Wikonkal NM, Brash DE. Ultraviolet radiation induced signature mutations in photocarcinogenesis. J Investig Dermatol Symp Proc. 1999;4(1):6-10.

Yosipovitch G, Sackett-Lundeen L, Goon A, Yiong Huak C, Leok Goh C, Haus E. Circadian and ultradian (12 h) variations of skin blood flow and barrier function in non-irritated and irritated skin-effect of topical corticosteroids. J Invest Dermatol. 2004;122(3):824-9.

Yosipovitch G, Xiong GL, Haus E, Sackett-Lundeen L, Ashkenazi I, Maibach HI. Time-dependent variations of the skin barrier function in humans: transepidermal water loss, stratum corneum hydration, skin surface pH, and skin temperature. J Invest Dermatol. 1998;110(1):20-3.

Zanello SB, Jackson DM, Holick MF. Expression of the circadian clock genes clock and period1 in human skin. J Invest Dermatol.

2000;115(4):757-60.

Zastrow L, Groth N, Klein F, Kockott D, Lademann J, Renneberg R, Ferrero L. The missing link--light-induced (280-1,600 nm) free radical formation in human skin. Skin Pharmacol Physiol. 2009;22(1):31-44.

Zheng B, Albrecht U, Kaasik K, Sage M, Lu W, Vaishnav S, Li Q, Sun ZS, Eichele G, Bradley A, Lee CC. Nonredundant roles of the mPer1 and mPer2 genes in the mammalian circadian clock. Cell. 2001;105(5):683-94.